Neural circuit architecture and evolutionary adaptations in the *Drosophila* olfactory system

Dissertation

To Fulfill the Requirements for the Degree of

„doctor rerum naturalium“ (Dr. rer. nat.)

Submitted to the Council of the Faculty of Biological Sciences

of Friedrich Schiller University Jena

by Lydia Gruber (M.Sc.)

born on February 4, 1988 in Freital, Germany

REVIEWERS

1. Prof. Dr. Bill S. Hansson
2. Prof. Dr. Manuela Nowotny
3. Prof. Dr. Martin P. Nawrot

Date of public defense

Jena, 06.07.2023

Dedicated to

the person who opened my eyes to the magic of nature.

Albrecht Demmig

the two people who always encouraged me.

Heiderose and Jürgen Gruber

TABLE OF CONTENTS

INTRODUCTION

"*For the sense of smell, almost more than any other, has the power to recall memories and it is a pity that you use it so little*." – Rachel Carson

General Introduction

The sense of smell, olfaction, allows the detection and perception of volatile chemicals which enables animals to interpret their olfactory environment. We as humans often forget the power of our sense of smell and its ecological importance. We do not blindly trust our olfactory judgment to evaluate food conditions and we hardly recognize food or people by their smell. We often cover our natural fragrance with perfume and in a way "paralyze" our sense of smell by constantly facing it with strong volatile molecules (odorants). However, at the same time, we are still highly manipulated by odors subconsciously, a strategy used by industries to influence our behavior (Minsky, 2018). One odorant exhibiting this phenomenon is geosmin[1]. The fruit fly, *Drosophila melanogaster*, sense geosmin at concentrations down to picomolar (10^{-12}) (Stensmyr *et al.*, 2012). Geosmin for us humans is an earthy-smelling chemical, produced by microbes (Gerber *et al.*, 1965), which we perceive especially after rain near meadows or the forest. In contrast to most insects, for most humans, geosmin is associated with positive feelings (Stensmyr *et al.*, 2012).

One reason why olfaction, more than any other sensory modality, is highly potent to induce immediate positive (appetitive) or negative (aversive) emotions, is that odors take a direct route to the limbic system, a brain region related to emotions and memories (Mori, 2014; Soudry *et al.*, 2011; Wilson *et al.*, 2006). Only two synapses separate the olfactory periphery from the limbic system in vertebrates or, in insects, from the central brain (mushroom body, lateral horn), a pathway initializing odor-guided behavior (de Belle *et al.*, 1994; Dolan *et al.*, 2018; Liang *et al.*, 2010; Owald *et al.*, 2015; Shepherd, 2011; Su *et al.*, 2009).

From an evolutionary perspective, olfaction is one of the "firstborn" senses and is common from bacteria to mammals (Zou *et al.*, 2009). Insects, which include over five million species, have successfully colonized in over 400 million years numerous niches and have

[1] Greek: gê - "earth", osmḗ - "odor"

evolved a highly sophisticated sensory system adjusted to their environmental conditions, food sources, hazards and conspecifics (Hansson *et al.*, 2011; Stork, 2018). Their survival and reproductive success depend to a high degree on the insect's olfactory capability.

The insect olfactory system is highly efficient in extracting relevant signals from many background signals while walking or flying. One cannot understand the success of evolutionary adaptations of insects to diverse olfactory environments without understanding the processing of complex olfactory information. In order to understand olfactory processing, it is indispensable to understand the principles of the olfactory pathway (neural architecture) and map neuronal networks of the nervous system (Luo, 2021; Milo *et al.*, 2002).

The focus of my thesis lies on the neural architecture, in particular neuronal synaptic circuits, of the primary olfactory center, the antennal lobe, in the fruit fly, *Drosophila melanogaster*, and how the circuitries changes with distinct computational demands or on the macroscale level how the olfactory system adapts to evolutionary changes. The small size of *Drosopholids* should not fool one into thinking that the neuronal architecture of the olfactory system is rather simple and easy to understand. Scientists are just beginning to build up a comprehensive picture of the olfactory neuronal network.

Why studying olfaction in *Drosophila* species?

Unraveling the structure of neuronal circuits is not an easy task without setting landmarks for orientation in the "wild forest" of entangled neuronal fibers. Thanks to Thomas H. Morgan and his group, the pioneers in *Drosophila* genetic research, *Drosophila* became the foremost model for genetics (Jennings, 2011), and provided the basics to mark cells of interest in the *Drosophila* brain. In the early decade of the 20th century, Morgan and colleagues identified for the first time associative factors (genes) located in *Drosophila (Morgan, 1910)* and received the Nobel Prize in 1933 in Physiology or Medicine for their investigations. Their work laid the foundation for a long successful relationship between scientists and *Drosophila* (Jennings, 2011).

The *Drosophila* genome (~180 Mb) was one of the first genomes mapped in March 2000 (Adams, 2000; Myers *et al.*, 2000). The rather small genome of *Drosophila,* compared to humans (3 billion base pairs), is 60% homologous to the human genome (Ugur *et al.*, 2016). The development of genetic tools, such as the binary expression system (e.g.: GAL4/UAS system), expressing transgenes in cells of interest (Duffy, 2002; Elliott *et al.*, 2008; Lai *et al.*,

2006; Potter *et al.*, 2010), was unstoppable. In combination, with the discovery of the green fluorescent protein (GFP), a reporter to mark proteins and thus cells of interest in vitro or in vivo, and awarded with the Nobel Prize in Chemistry 2008, *Drosophila* provides almost infinite opportunities for understanding brain and body function (Chalfie *et al.*, 1994). Along with the advantages of early genome sequencing and genetic tractability, *Drosophila* has a short generation period (12 days life cycle), and is easy to rear in the laboratory. Many mutants and transgenic flies are available from stock centers[2], and all the information on previous experiments and discoveries is well documented (Matthews *et al.*, 2005).

These groundbreaking discoveries have motivated research in almost every field of biology, ranging from molecular to evolutionary studies (Yamaguchi *et al.*, 2018). One of the scientific fields with vivid interest in *Drosophila* research is neuroscience (Bellen *et al.*, 2010; Venken *et al.*, 2005). Particularly in olfaction, *Drosophila* has proven to be a great model to study molecular mechanisms of olfaction e.g. (Carlson, 1991; Ernst *et al.*, 1977; Grabe *et al.*, 2018; Sass, 1976; Stocker *et al.*, 1983; Vareschi, 1971; Wicher, 2018; Wicher *et al.*, 2021) olfaction driven-behaviors (Bartelt et al., 1985; Becher et al., 2010; Van Breugel & Dickinson, 2014), olfactory learning (Mohamed et al., 2019) and evolution of host specialization (Auer et al., 2020; Stensmyr et al., 2003) as well as evolutionary aspects (Ache *et al.*, 2005; Auer *et al.*, 2020; Hansson *et al.*, 2011).

The *Drosophila* brain comprises 150,000-200,000 neurons (Davie *et al.*, 2018; Raji *et al.*, 2021) in contrast to the human or mouse brain, with around 100 billion neurons and 70 million neurons, respectively (Erö *et al.*, 2018; Herculano-Houzel, 2009; Herculano-Houzel *et al.*, 2006). As a consequence of reduced complexity, with perspective to the low number of neurons, *Drosophila* nervous system attracted massive attention for the study of neuronal networks and whole brain connectomes (see last paragraph below) (Meinertzhagen, 2016; Meinertzhagen, 2018).

In the last two decades, the genus *Drosophila* gained further attention in the perspective of the scientific field of “evolutionary neuroecology” (Auer *et al.*, 2020; Prieto-Godino *et al.*, 2017; Singh *et al.*, 2019; Zhao *et al.*, 2020), encouraged by novel genetic techniques, such as CRISAPR-CAS9 genome editing (Fandino *et al.*, 2019), and the growing global interest in our fragile ecological equilibrium. The genus *Drosophila* comprises 1,200 to

[2] https://flybase.org/

1,500 species, spanning through nearly every imaginable ecological niche and host choice, from deserts to forests, from islands to mountains (Dekker *et al.*, 2006; Jezovit *et al.*, 2017; Markow *et al.*, 2005; Stensmyr *et al.*, 2008). It provides, therefore, the opportunity to study closely related species and their diversity of specialization to distinct habitats and food sources from an evolutionary perspective.

Odor perception at the peripheral olfactory organs

Volatile molecules are detected by receptors located on the insect "nose", which is comprised of the olfactory appendages present at the *Drosophila* head, the distal antennae (the funiculi) and the maxillary palps. There several porous hair-like structures are located, which house dendrites of 1-4 olfactory sensory neurons (OSNs) (Couto *et al.*, 2005; de Bruyne *et al.*, 2001; Shanbhag *et al.*, 2000; Shanbhag *et al.*, 1995). Around 400 sensilla at the funiculus and the palps are categorized by shape and length into four groups, the club-shaped basiconic, long pointed shaped trichoid, intermediate sensilla with an in-between morphology and the short peg-like coeloconic sensilla (Nava Gonzales *et al.*, 2021; Shanbhag *et al.*, 1999) **(**Figure 1**)**. *Drosophila* species revealed a high diversity of different sensilla types, ranging from 400 -1200 (**Chapter III**). The palps contain around 60 basiconic sensilla housing two OSNs each and mediate short- *and* long-range attraction (de Bruyne *et al.*, 1999; Dweck *et al.*, 2016; Singh *et al.*, 1985).

Once an olfactory molecule has passed the pore of a sensillum it encounters the aqueous sensillum lymph surrounding the OSN dendritic branches (Nava Gonzales *et al.*, 2021; Shanbhag *et al.*, 2000). Olfactory support cells (tecogen, trichogen and tormogen cells) surround the OSN dendrites and separate the inner from the outer dendritic region (Keil, 1999; Nava Gonzales *et al.*, 2021; Shanbhag *et al.*, 2000). Different protein types, such as the odor binding proteins (OBPs), or sensory membrane protein I (SNMP1) facilitate the odorant transport and binding of olfactory molecules to the chemoreceptors, located in the OSN dendritic membrane (Benton *et al.*, 2007; Fan *et al.*, 2011; Gomez-Diaz *et al.*, 2016; Rihani *et al.*, 2021; Wicher *et al.*, 2021).

Three types of chemoreceptors in *Drosophila* are involved in olfaction. The most abundant type are odorant receptors (Ors) (Clyne *et al.*, 1999; Getahun *et al.*, 2013; Missbach *et al.*, 2014; Vosshall *et al.*, 1999). Some receptors are ionotropic receptors family (Irs) (Benton *et al.*, 2009). Gustatory receptors (Grs) are mainly involved in gustation (taste), and some GRs

mediate the detection of carbon dioxide (Jones *et al.*, 2007; Kwon *et al.*, 2007) or pheromones (Kohl *et al.*, 2015).

ORs in insects form a ligand gated cation channel with its ubiquitously expressed co-receptor protein, Orco (Benton *et al.*, 2006; Butterwick *et al.*, 2018; Larsson *et al.*, 2004; Vosshall *et al.*, 2011) permeable to Na^+; K^+ and CA^{2+} (Sato *et al.*, 2008; Wicher, 2010; Wicher, 2018). In addition to the ionotropic pathway, insect Ors have a complementary metabotropic pathway (Chatterjee *et al.*, 2009; Deng *et al.*, 2011; Getahun *et al.*, 2013; Kain *et al.*, 2008; Miazzi *et al.*, 2016). Therefore, Ors could be characterized as metabotropically regulated ionotropic receptors, enabling a double strategy for odor detection (Wicher, 2010; Wicher *et al.*, 2021), different from the vertebrate ORs, which are GPCRs (Breer *et al.*, 2019). This duality, in combination with sensitization, described in insects ORs, might be extremely important for tracking odor plumes encountered during flight (Getahun *et al.*, 2013; Halty-deLeon *et al.*, 2018; Halty-deLeon *et al.*, 2021). In general, one receptor type is expressed in one OSN type (Malnic *et al.*, 1999; Serizawa *et al.*, 2000), but also polymodal expression of two types of receptors in the same OSN has been recently described in the fruit fly and the mosquito (Task *et al.*, 2022; Younger *et al.*, 2022).

The chemoreceptors show a continuum of odor tuning, ranging from being highly specific or broadly tuned to many odorants. Examples for specialized receptors, as investigated in **manuscript I**, are the pheromone receptor (Or47b) that binds the pheromone methyl laurate (Dweck, H. K. M. *et al.*, 2015) or the receptor Or56a binding exclusively geosmin, an earthy smelling odorant (for humans), which is an aversive signal for *Drosophila* (Stensmyr *et al.*, 2012). An example of a broadly tuned receptor is the Or7a activated by amines, acids, ammonia and other odorants (Hallem *et al.*, 2006; Münch *et al.*, 2016; Pelz *et al.*, 2006).

OSNs, receive an olfactory signal (perception), convert it into an electrical signal, and convey therefore olfactory information to second-order neurons in the primary olfactory relay station, the antennal lobe (AL). The AL is an analog to the olfactory lobe in crustaceans or the olfactory bulb in vertebrates (Ache *et al.*, 2005; Harzsch *et al.*, 2018; Homberg *et al.*, 1989; Shepherd, 2011; Wilson *et al.*, 2006).

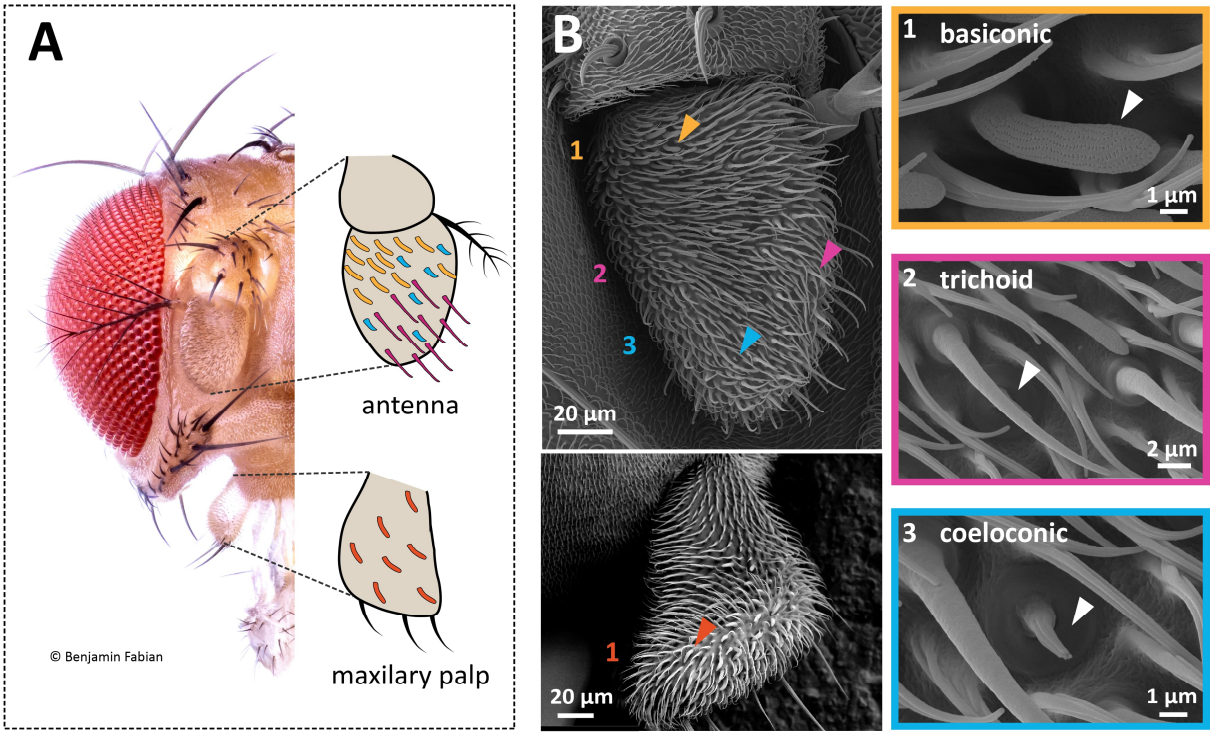

Figure 1 The sensory organs of *Drosophila.* The olfactory appendages at the *Drosophila* head are one pair of antennae and maxillary palps (**A**). They are covered with many hair-like structures, the sensilla (**A** and **B**), which have different shapes, classified in basiconic (orange), trichoid sensilla (magenta) and coeloconic (blue) sensilla. **B**: Scanning electron microscopic images of the third antenna segment, the funiculus, and a maxillary pulp with diverse sensilla types, the basiconic (1), trichoid (2) and coeloconic (3) sensilla.

The olfactory pathway

In most insects, OSNs expressing the same receptor converge onto the same glomeruli, spherical structures in the AL (Couto *et al.*, 2005; Gao *et al.*, 2000; Silbering *et al.*, 2008; Vosshall *et al.*, 2000; Wilson, 2013). The number of OSN axon terminals projecting to each glomerulus varies from 8-60 and correlates with the glomerular volume (Grabe *et al.*, 2016). The 58 glomeruli, including 51 olfactory and 7 thermo- and hygrosensitive glomeruli (Bates *et al.*, 2020; Rodrigues, 1988), are different in their stereotypic location, size and form. These criteria can be used to easily identify the same glomerulus across different individuals (Couto *et al.*, 2005; Grabe *et al.*, 2015; Laissue *et al.*, 2008).

In *Drosophila,* most glomeruli are innervated by OSNs originating at the ipsilateral and contralateral antenna, which cross via the AL commissure (Gaudry *et al.*, 2013; Stocker *et al.*, 1990; Tanaka *et al.*, 2012) (Figure 2). In total around 1300 OSNs converge in the *Drosophila* AL onto around 300 projection neurons (PNs)(convergence: 1:6; (Bates *et al.*, 2020; Bhandawat *et al.*, 2007; Kazama *et al.*, 2009; Masse *et al.*, 2009; Stocker, 2001; Stocker *et al.*, 1990)).

Two morphologically distinct types of PNs exist in the AL: the uniglomerular PNs (uPNs) that innervate one glomerulus and the multiglomerular projection neuron (mPNs) that innervate many glomeruli (Bates *et al.*, 2020; Liang *et al.*, 2013; Strutz *et al.*, 2014; Tanaka *et al.*, 2012; Yu *et al.*, 2010). OSNs and the majority of uPNs are excitatory (ePNs), forming cholinergic synapses (Croset *et al.*, 2018; Davie *et al.*, 2018; Stocker, 1994; Wilson *et al.*, 2006; Yasuyama *et al.*, 2003). mPNs, were previously described to be composed of mainly inhibitory PNs (iPNs) (Jefferis *et al.*, 2007; Liang *et al.*, 2013; Okada *et al.*, 2009). However, new mPNs have been disclosed recently and now the group of mPNs can be split equally into iPNs and ePNs (Bates *et al.*, 2020).

From the AL, iPNs and ePNs project via three separate tracts (Schultzhaus *et al.*, 2017; Tanaka *et al.*, 2012) (**Figure 2**), to higher brain centers of the protocerebrum, the lateral horn (LH) and the mushroom body (MB) calyx (Bates *et al.*, 2020; Dolan *et al.*, 2019; Gruntman *et al.*, 2013; Heimbeck *et al.*, 2001; Heisenberg, 2003; Marin *et al.*, 2002; Schultzhaus *et al.*, 2017; Wong *et al.*, 2002). The LH, innervated by iPNS and ePNs (**Figure 2**) (Ito *et al.*, 1997), is described to be involved in the odor valance, intensity coding and implementation of innate behavior (Badel *et al.*, 2016; Das Chakraborty *et al.*, 2021; Li, J. *et al.*, 2020; Schultzhaus *et al.*, 2017; Strutz *et al.*, 2014). The stereotypic arborization and zonal clustering of the PN axon terminals in the LH provide a spatially segregated projection map and characterize the activity of these zones to distinct odor information (Das Chakraborty *et al.*, 2021; Dolan *et al.*, 2019; Fisek *et al.*, 2014; Frechter *et al.*, 2019; Grabe *et al.*, 2018; Liang *et al.*, 2013; Parnas *et al.*, 2013). Two types of iPN in the LH convey separately the information about either positive valence or odor intensity and project to distinct LH regions (Sachse, Silke *et al.*, 2016; Schultzhaus *et al.*, 2017; Strutz *et al.*, 2014).

The MB, the center of associative learning and memory formation (Busto *et al.*, 2010; Fiala, 2007; Heisenberg, 2003; Yu *et al.*, 2004), receives input from the PNs in the area called calyx, where the PNs project randomly to the 2,000 -2,500 Kenyon cells (Aso *et al.*, 2009; Caron *et al.*, 2013; Eichler *et al.*, 2017; Ito *et al.*, 1997; Li, F. *et al.*, 2020). However, the degree of complexity increases at the axonal terminals of the PNs, where an extensive multimodal integration of olfactory and visual sensory information takes place (Badel *et al.*, 2016; Barth *et al.*, 1997; Das Chakraborty *et al.*, 2021; Li, J. *et al.*, 2020; Vogt *et al.*, 2016; Vogt *et al.*, 2014; Wong *et al.*, 2002).

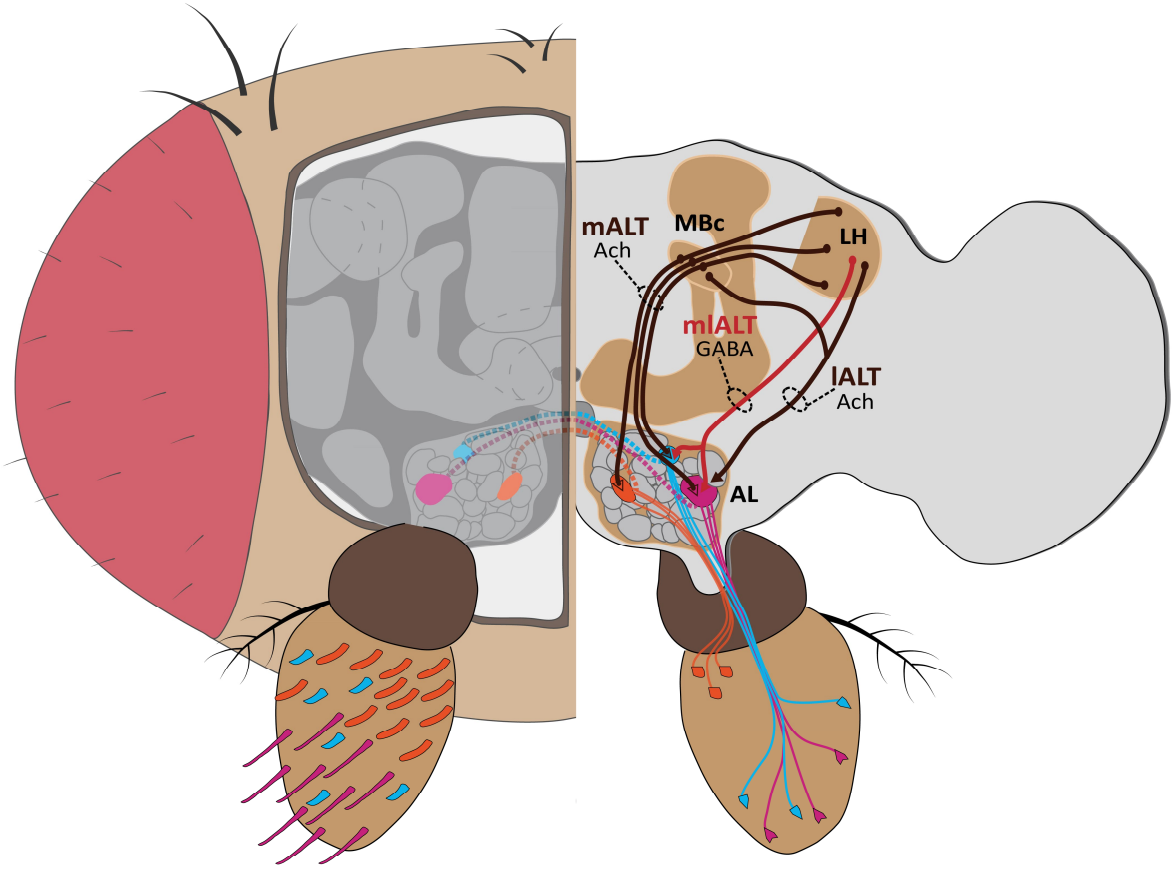

Figure 2 The olfactory pathways in *Drosophila*. Olfactory sensory neurons (OSNs) expressing a specific receptor repertoire (orange, blue, magenta) convey information to projection neurons (PNs) in the antennal lobe (AL). Most of the OSNs project bilaterally to the ipsilateral and contralateral AL. From the AL excitatory uniglomerular PNs project via the medial antennal lobe tract (mALT) to the mushroom body calyx (MBc) and the lateral horn (LH). Multiglomerular inhibitory PNs project via the medio-lateral ALT (mlALT) to the LH and excitatory multiglomerular or uniglomerular PNs project via the lateral ALT (lALT) to the LH and MBc.

The third main neuronal class within the AL are modulatory local interneurons (LNs), which form inhibitory or excitatory synapses with OSNs, PNs and with each other intra- and inter-glomerular (Chou *et al.*, 2010; Liu *et al.*, 2013; Okada *et al.*, 2009; Seki *et al.*, 2010). Around 200 LNs, which are mainly unilateral, branch exclusively within the AL (Chou *et al.*, 2010; Schlegel *et al.*, 2021). LNs are a morphologically versatile neuron class and their individual contribution to distinct coding mechanisms is poorly understood (Wilson, 2013; Wilson *et al.*, 2006). Most abundant LN fibers are from broadly arborizing LNs (pan-glomerular LNs), which are mainly inhibitory (Schlegel *et al.*, 2021). LNs synapse reciprocally with each other (disinhibition) or with OSN presynaptic boutons, performing presynaptic inhibition

(Olsen *et al.*, 2008; Root *et al.*, 2008). This inter-glomerular inhibitory regulation (gain control) is balancing OSN activity throughout the AL and is therefore playing an important role in the combinatorial coding of olfactory cues in the AL (Galizia, 2014; Sachse *et al.*, 2021; Szyszka *et al.*, 2015); see next paragraph below). Smaller LNs, innervating sub-regions of the AL, the patchy, sparse or regional LNs, differ greatly in their morphology, performing selective inter- or intra-glomerular modulation (Laurent, 2002; Olsen *et al.*, 2010; Schlegel *et al.*, 2021; Wilson *et al.*, 2005). Some of these LNs form excitatory chemical synapses and electrical connections mainly with other LNs and PNs (Das *et al.*, 2017; Huang *et al.*, 2010; Seki *et al.*, 2010; Shang *et al.*, 2007; Yaksi *et al.*, 2010). The cooperative action of excitatory and inhibitory LNs is important for coding odor mixtures (Mohamed *et al.*, 2019b; Silbering *et al.*, 2007), a synergistic effect of odorants (Das *et al.*, 2017) or the fine-tuning of PN responses (Fusca *et al.*, 2021; Nagel *et al.*, 2015; Ng *et al.*, 2002; Root *et al.*, 2007; Shang *et al.*, 2007). Recent circuit studies showed that these neuronal classes, OSNs, PNs and LNs, form synapses with each other and form generic circuit motifs in olfactory glomeruli (**Figure 3**) (Berck *et al.*, 2016; Horne *et al.*, 2018; Martin *et al.*, 2011; Rybak *et al.*, 2018; Rybak *et al.*, 2016; Schlegel *et al.*, 2021; Shepherd *et al.*, 2021; Tobin *et al.*, 2017).

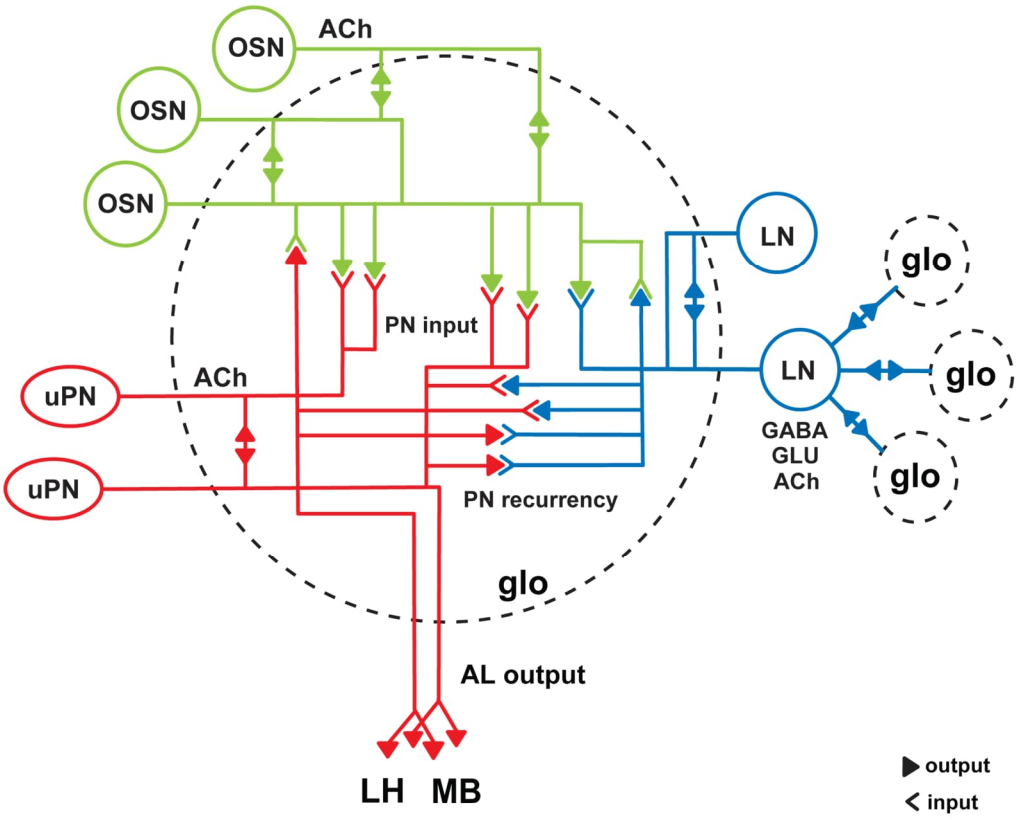

Figure 3 Circuit motifs in the olfactory glomeruli of *Drosophila*. Scheme (modified after: (Rybak *et al.*, 2018)) shows the principle neuronal connections in olfactory glomeruli (glo). In the glomeruli the olfactory sensory neurons (OSNs) convey the olfactory signal to uniglomerular projection neurons (uPNs) (PN input), which in turn convey this signal further to the lateral horn (LH) or the mushroom body (MB), representing the antennal lobe (AL) output. The excitatory OSNs releasing acetylcholine (ACh), excitatory uPNs releasing ACh and inhibitory or excitatory local interneurons (LNs) releasing either γ-aminobutyric (GABA), ACh or glutamate (GLU) all synapse onto each other. LNs provide an important modulation in the glomerular circuitry, such as presynaptic inhibition at LN-to-OSN feedback synapses, lateral inhibition through inter-glomerular connections between different glomeruli or uPN response tuning through intra-glomerular modulation by OSN-LN-uPN or uPN-LN-uPN connection motifs (PN recurrency).

Besides classical neurotransmitters, such as acetylcholine, γ-aminobutyric acid (GABA) and glutamate, other neuromodulators act in the AL. Neuropeptides and amines are released by LNs, peptidergic neurons or descending neurons (Carlsson *et al.*, 2010; Coates *et al.*, 2020; Dacks *et al.*, 2005; Dacks *et al.*, 2009; Distler, 1990; Ignell *et al.*, 2009; Lizbinski *et al.*, 2018; Nässel *et al.*, 2006). The wide spectra of neuronal modulation is still not well understood including missing knowledge about the neuronal sites of modulation (Bokil *et al.*, 2001; Collmann *et al.*, 2004; Vroman *et al.*, 2013); **chapter II**).

Olfactory glomeruli have been shown to be versatile in their shape, neuronal composition and their sensitivity to inhibition by LNs (Carlsson *et al.*, 2010; Grabe *et al.*, 2016;

Grabe *et al.*, 2018; Grabe *et al.*, 2020; Grabe *et al.*, 2015; Hong *et al.*, 2015; Laissue *et al.*, 1999). Recent studies showed that glomeruli, innervated by OSNs that express narrowly tuned receptors dedicated to 1-3 odorants, have more outgoing uPNs and fewer LNs, whereas glomeruli innervated by broadly tuned OSNs, have 1-2 uPNs and are innervated by more LNs (Grabe *et al.*, 2016) (**Figure 4**).

Complexity of odor coding and glomerular microcircuits

The odor coding is the transformation of external olfactory cues from the environment (olfactory space) into an internal representation (neuronal code) readable in the brain as electrical signals, and eventually inducing a behavior (motor output) ensuring the animal's survival (Pannunzi *et al.*, 2019). Odor plumes are a complex collection of almost infinite information, composed of the molecules identity (Couto *et al.*, 2005; Galizia, 2014; Silbering *et al.*, 2008), the dynamically varying concentration, and its gradient (rate of change) (Asahina *et al.*, 2009; Kim *et al.*, 2011, 2015; Murlis J *et al.*, 1992; Pannunzi *et al.*, 2019), as well as the source location (Gaudry *et al.*, 2013; Mohamed *et al.*, 2019a; Taisz *et al.*, 2022), the odor valence (Bell *et al.*, 2016; Grabe *et al.*, 2018; Knaden *et al.*, 2014; Knaden *et al.*, 2012) and the mixture conditions (Mohamed *et al.*, 2019b; Silbering *et al.*, 2007).

Drosophila as a flying insect has evolved coding strategies at all levels of olfactory processing to improve transduction speed. In fact, in *Drosophila,* olfactory behavior initiation was observed within 100 ms after OSN activity onset (Bhandawat *et al.*, 2010; Gaudry *et al.*, 2013). In addition, at the peripheral level of odor perception, ephaptic communication between OSNs in the same sensillum (Su *et al.*, 2012; Zhang *et al.*, 2019) and distinct dynamics of OSN response influence signal transmission. This is considered the first "filter" for olfactory information (French *et al.*, 2011; Getahun *et al.*, 2012; Halty-deLeon *et al.*, 2021; Kim *et al.*, 2011; Nagel *et al.*, 2011; Prelic *et al.*, 2021; Schuckel *et al.*, 2008).

At the level of the AL, raw information of odor plumes, as mentioned above, are encoded (Gaudry *et al.*, 2013; Grabe *et al.*, 2018; Kim *et al.*, 2015; Knaden *et al.*, 2014; Knaden *et al.*, 2012; Menini, 2010; Tobin *et al.*, 2017). A major task of the AL is thereby odor signal amplification, which happens in a non-linear way (i.e. strongest amplification at odor onset), normalization and noise reduction (Bhandawat *et al.*, 2007; Kazama *et al.*, 2008; Masse *et al.*, 2009). This is important for balancing all incoming electrical potentials, with diverse intensities, for better discrimination, to enhance the contrast, and reduce background noise.

Thus, the odor perception of flies stays reliable and prices over a wide range of fluctuating concentrations of different odors (Masse *et al.*, 2009; Nagel *et al.*, 2015; Wilson, 2013). Flies have an impressive capability to find the odor source over long distances, detecting concentrations down to picomolar concentrations, and coding these concentration fluctuations that are up to ten times per second (Halty-deLeon *et al.*, 2021; Nagel *et al.*, 2011; Olsen *et al.*, 2010).

How does an olfactory system, which is limited in its size and number of coding units (58 glomeruli), encodes almost an infinite number of different olfactory cues? The number of glomeruli is rather limited in *Drosophila* species (~60); compared to other insects, such as honey bees, (~170), ants (~400) or (~2000) and humans (>5500) olfactory glomeruli (Chen *et al.*, 2005; Galizia *et al.*, 2001; Maresh *et al.*, 2008; Stieb *et al.*, 2011). To encode the high amount of olfactory molecules flies encode most of the odor molecule via combinatorial coding, i.e. several receptors are sensitive to one odorant and the stereotypic activation of OSNs and their targets. Glomerular circuits create thus a spatially segregated activity “odotopic” map at the AL, which is specific for each odorant (Galizia, 2014; Grabe *et al.*, 2018; Malnic *et al.*, 1999; Sachse, S. *et al.*, 2016; Seki *et al.*, 2017; Szyszka *et al.*, 2015).

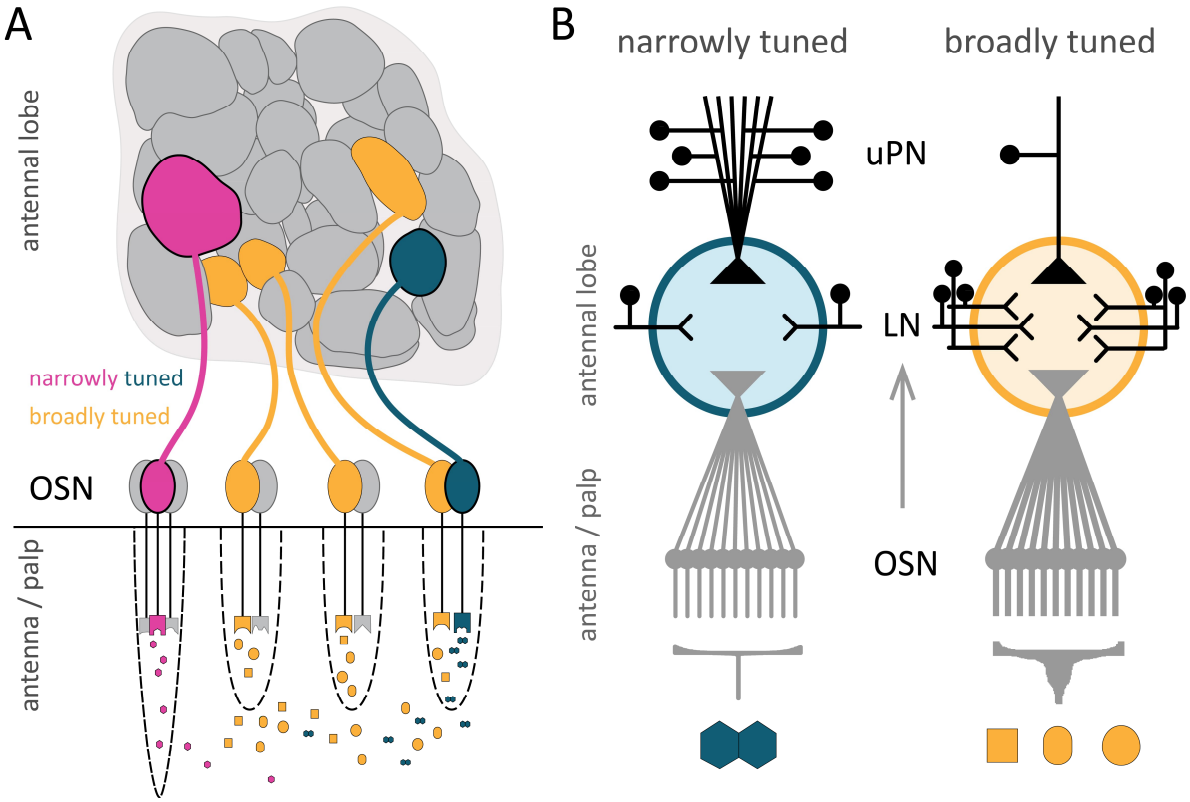

Figure 4 Specialized and broadly tuned olfactory glomerular circuits. A: OSNs in the *Drosophila* brain have different response dynamics. Some are narrowly tuned, activated by a single or few odorant(s) (magenta, blue). Different shapes of small forms (magenta, orange or blue) illustrate different odorants. Most of the OSN receptors are broadly tuned, activated by many different odorants (orange). **B**: Glomerular circuits that are specialized (blue), in which OSNs and uPNs activation is narrowly tuned to few odorants, have more uPNs and are innervated by less LNs (modified after (Grabe *et al.*, 2016).

Survival and reproduction of the fly depend on the specificity of ecological relevant odorants. These odorants bind one or two receptors that have evolved a high specificity to 1-2 chemicals and are narrowly tuned, as well as their activated glomerular circuit (Andersson *et al.*, 2015; Haverkamp *et al.*, 2018; Keesey *et al.*, 2021) (Figure 4). These narrowly tuned glomerular circuits belong often to dedicated olfactory pathways ("labeled lines"), which process single odorants that encode information of particular importance for reproduction and survival (Datta *et al.*, 2008; Dweck, H. K. M. *et al.*, 2015; Ebrahim *et al.*, 2015; Gao *et al.*, 2015; Kurtovic *et al.*, 2007; Stensmyr *et al.*, 2012).

The odorant geosmin, bounding to the Or56a receptor, is an example which is highly sensitive to geosmin (Halty-deLeon *et al.*, 2021), and exclusively activating the glomerular circuit of DA2, which is in turn only activated by geosmin (Stensmyr *et al.*, 2012). This dedicated olfactory pathway, is conserved throughout the *Drosophila* genus and also found in

mosquitos (Melo *et al.*, 2020; Stensmyr *et al.*, 2012). Geosmin is an alcohol, which has for humans an earthy smell (Gerber *et al.*, 1965; Liato *et al.*, 2017). It is a non-toxic odorant that, however, can be produced by for drosophila potentially toxic microorganisms (Gerber *et al.*, 1965; Jüttner *et al.*, 2007; Mattheis *et al.*, 1992) and functions as alarm molecule for some organisms (Scarano *et al.*, 2021; Stensmyr *et al.*, 2012; Zaroubi *et al.*, 2022), but is attractive for others (Becher *et al.*, 2020; Melo *et al.*, 2020). Another example of a dedicated pathway is glomerulus VA1v, responding to methyl laurate, a pheromone which induces a strongly attractive response in female flies leading to aggregation behavior (Dweck, H. K. M. *et al.*, 2015). In the contrary, broadly tuned glomerular circuits, such as the DL5, participate at the combinatorial coding of aversive odorants, like E2-hexanal or benzaldehyde (Knaden *et al.*, 2012; Mohamed *et al.*, 2019b; Münch *et al.*, 2016; Seki *et al.*, 2017). This functional diversity suggests the existence of differences in neuronal composition and synaptic connectivity between broadly and narrowly tuned glomeruli.

The question arises why in an insect olfactory system two coding strategies exist and how odorant information is implemented differently in narrowly tuned versus broadly tuned glomerular circuits (Andersson *et al.*, 2015; Haverkamp *et al.*, 2018; Keesey *et al.*, 2021). In order to help to find answers to this question, a comprehensive understanding of the neuronal microarchitecture and circuit motifs (the building blocks of the nervous system) is necessary (Alon, 2007; Luo, 2021; Milo *et al.*, 2002) (**Figure 3**) (Rybak *et al.*, 2018; Rybak *et al.*, 2016; Shepherd *et al.*, 2021) (**chapter I and II**).

How to unravel the apparently invisible?

The missing link to a mechanistic understanding of neural computation is a comprehensive knowledge of neuronal networks (Denk *et al.*, 2012; Luo, 2021). There has always been a desire to resolve the structure of neuronal networks in the brain in order to understand neuronal communication and processing (DeFelipe, 2010; Rybak, 2013). One of the greatest advocate of this doctrine was the Spanish artist and pathologist Santiago Ramón y Cajal, who produced in the late nineteenth and early twentieth century the first drawings of neurons and their organization in the brain (Cajal, 1894; Jones, 2006). Cajal´s drawings are still missing the single synaptic connections of neurons and it is therefore not a connectome, i.e. comprehensive description of the neuronal network with all is synaptic connections. A term

that was coined in the beginning of the 21st century spurred by innovations in microscopy neuronal tracing techniques (Rybak, 2013; Sporns *et al.*, 2005).

The story of connectomics started before the word was coined. In the early 70th Sydney Brenner, then a biologist at Cambridge University, decided to identify the connections of every cell in the nervous system of a small nematode worm called *Caenorhabditis elegans* (Emmons, 2015; White, J. G. *et al.*, 1986). With the methods used at that time, a complete connectome of a *Drosophila* brain would not have been accomplished (Lichtman *et al.*, 2008; Meinertzhagen, 2016; Meinertzhagen, 2018). The reason for this is the need of high-resolution imaging, resolving single synapses and finest neuronal fibers (20 nm) throughout the full brain volume. Recent innovation that overcome the pitfall of the diffraction limit of light microscopy (~250 nm) (Hell *et al.*, 1994), such as STED (Stimulated emission depletion) or STORM (Stochastic optical reconstruction microscopy) (Betzig *et al.*, 2006; Schermelleh *et al.*, 2010; Willig *et al.*, 2007) in combination with synaptic markers, such as MARCM (mosaic analysis with a repressible cell marker) and GRASP (GFP reconstitution across synaptic partners) (Feinberg *et al.*, 2008; Lee *et al.*, 1999; Mishchenko, 2011) enabled new insights into the synaptic composition (Mosca *et al.*, 2014; Pech *et al.*, 2013).

However, to establish a complete mapping of all fine neurites and synapses of a neuropil or the full brain, novel electron microscopy (EM) techniques are indispensable (resolution down to 1 nm). In particular, in insects brain housing polyadic synapses, i.e. one presynaptic site is connecting to several postsynaptic profiles. Resolving each neuronal profile at these entangled specialized regions needs high resolution microscopy minimum down to 20 nm. Automated serial sectioning in combination with multi-beam transmission EM techniques (ssTEM) (resolution down to 1 x 1 x 20 nm) or tissue milling with scanning EM techniques (FIB-SEM) (resolution down to 1 x 1 x 1, depending on the volume and time) have been developed (Briggman *et al.*, 2012; Cardona *et al.*, 2010; Denk *et al.*, 2004a, 2004b; Hanslovsky *et al.*, 2017; Knott *et al.*, 2008; Lichtman *et al.*, 2008; Saalfeld, 2012; Xu *et al.*, 2017). Innovative neuronal reconstruction tools, like the web-based reconstruction software CATMAID[3] or the semi-automated “flood filling” approach contributed furthermore to reduce the time of mapping complete neuronal networks (Li, P. H. *et al.*, 2020; Saalfeld *et al.*, 2009; Schneider-Mizell *et al.*, 2016).

[3] http://www.catmaid.org/

After the first connectome of *Caenorhabditis elegans (White, J.G. et al., 1986)*, *Drosophila melanogaster* full brain connectome was the goal of many cooperating scientists. The optic lobe in the adult brain was the first connectome published, followed by insights into the AL and the full larvae brain network (Berck *et al.*, 2016; Horne *et al.*, 2018; Rybak *et al.*, 2016; Takemura *et al.*, 2008; Tobin *et al.*, 2017). During the time of data acquisition for this thesis, the complete connectome of the *Drosophila* full brain using ssTEM[4] or FIB-SEM[5] was accomplished (Scheffer *et al.*, 2020; Zheng *et al.*, 2018). The focus of this thesis has been on local circuits in a restrict relay, the olfactory glomeruli, with the aim to produce a dense connectome of identified olfactory glomeruli, and to resolve fine neuronal structures (**chapter I and II**).

[4] https://v2.virtualflybrain.org
[5] https://neuprint.janelia.org/

OBJECTIVE OF THE DISSERTATION

Insects have evolved throughout evolution sophisticated sensory systems to orientate, to survive and to communicate within their own ecological niche. In order to understand the functional adaptation of the olfactory nervous system, it is indispensable to understand the differences in the neuroanatomy, neuronal ultrastructure and circuits. To enhance our knowledge on that topic the aims of the thesis were the following.

First, insects olfactory glomeruli circuits perform computational tasks in processing either multiple odorants, that is thus involved in combinatorial coding of odorants, or such as are dedicated in the processing of 1-3 odorants. The purpose of this mechanism is still not clear. To find answers to how olfactory information are processed in glomeruli with different specialization, we provided, in **manuscript I,** comprehensive knowledge about the dense neuronal structure and synaptic connections of each of these two types of glomerular circuits.

Second, the classical concept of neuronal communication by chemical synapses throughout neurotransmitters that are binding receptors at the postsynaptic density is well described. However, the spectra of mutual neuronal modulation are still unknown. In **manuscript II**, we discovered a, so far, unknown neuronal structures in the olfactory glomerular neuropil, synaptic spinules, and discussed their putative function in neuronal modulation and communication.

Third, I contributed to a study in which my colleagues and I considered the following question: How evolutionary pressure in concert with developmental mechanisms across closely related species shapes the neural assembly of sensory systems and the fly behavior? We examined, in **manuscript III,** 62 related *Drosophila* species and explored their diversity in phenotypes, sensory organs and behavior. We provide evidence of a developmental genetic constraint accompanying evolutionary specialization of either the olfactory or the visual system. Behavioral experiments provide evidence for the impact of this sensory bias in host-navigation and courtship.

OVERVIEW OF MANUSCRIPTS

Manuscript 1

Diversification of neuropil organization in specialized and broadly tuned olfactory glomerular circuits in *Drosophila melanogaster*

Lydia Gruber, Rafael Cantera, Markus Pleijzier, Bill S. Hansson and Jürgen Rybak

BioRxiv

Uploaded as preprint on October 2 2022

In this study, I established a novel approach combining genetic tools in *Drosophila melanogaster* to mark the glomeruli of interest with 2-photon laser branding and state-of-the-art volume-based electron microscopy, Focused Ion Beam Electron Microscopy (FIB-SEM). With this method I disclosed the neuronal architecture and synaptic circuitry in a narrowly tuned glomerulus, processing the single aversive odorant geosmin (DA2) and compared it with the neuronal composition of the broadly tuned glomerulus processing multiple aversive odorants (DL5). By comparing the novel data with a previously mapped narrowly tuned glomerular circuit (VA1v), putative generic features of narrowly tuned glomerular circuits could be extracted. Furthermore, I disclosed a substantial amount of autapses, self-activating synaptic feedback loops, in the large dendrite of the PN of the DL5 glomerulus potentially inducing increased projection neuron spiking after OSN activation.

Author contributions:

Conceived and designed study:	J. Rybak and L. Gruber (70%), B.S. Hansson
Performed experiments:	L. Gruber (100%)
Analyzed data:	L. Gruber (90%), J. Rybak, M. Pleijzier
Wrote the manuscript:	J. Rybak; R. Cantera, L. Gruber (80%), B. S. Hansson

Manuscript 2

Synaptic Spinules in the Olfactory Circuit of *Drosophila melanogaster*

Lydia Gruber, Jürgen Rybak, Bill S. Hansson and Rafael Cantera

Frontiers in Cellular Neurosacience

Published online on March 27, 2018

In this study, I report neuronal protruding cellular structures that frequently and predominantly invaginate presynaptic terminals of olfactory sensory neurons in the *Drosophila* antennal lobe emanating from neighboring postsynaptic neurons. These structures, so-called spinules, were previously studied in the central brain of vertebrates and are accompanied with double membrane vesicles, putative pinched off from the spinules. They are likely playing a key role in the synaptic tagging, synaptic remodeling and neuronal plasticity.

Author contributions:

Conceived and designed study:	J, Rybak, L. Gruber (70%)
Performed experiments:	L. Gruber (100%)
Analyzed data:	L. Gruber (90%), J. Rybak
Wrote the manuscript:	J. Rybak; R. Cantera, L. Gruber (60%), B. S. Hansson

Manuscript 3

Inverse resource allocation between vision and olfaction across the genus *Drosophila*

Ian W. Keesey, Veit Grabe, Lydia Grube, Sarah Koerte, George F. Obiero, Grant Bolton, Mohammed A. Khallaf, Grit Kunert, Sofia Lavista-Llanos, Dario Riccardo Valenzano, Jürgen Rybak, Bruce A. Barrett, Markus Knaden and Bill S. Hansson

Nature Communication

Published online on March 11, 2019

In this study, my colleagues and I used a wide array of techniques to study 62 closely related species within the genus of *Drosophila* with a focus on their phenotypic diversity, sensory specialization and behavior differences. Our study identified an inverse resource allocation between vision and olfaction that we observed at the periphery (eye size vs. antennal size), within the brain (visual vs. olfactory first relay station), as well as during larval development (antennal vs. imaginal disc). We investigate this sensory bias across the entire genus, consistently favoring one sensory modality over the other one, which appears to represent repeated, independent evolutionary events.

Author contributions:

Conceived and designed study:	I.W. Keesey, V. Grabe, M. Knaden, B.S. Hansson, L. Gruber (10%), S. Koerte
Performed experiments:	I.W. Keesey, V. Grabe, L. Gruber (15%), S. Koerte, G. Bolton, B. A. Barrett
Analyzed data:	I.W. Keesey, V. Grabe, L. Gruber (10%), S. Koerte, J. Rybak, S. Lavista-Llanos, G. Bolton, B. A. Barrett, D.R. Valenzano and G. Kunert, G.F. Obiero, M. Knaden
Wrote the manuscript:	I.W. Keesey, M. Knaden, B.S. Hansson

CHAPTER 1

Diversification of neuropil organization in specialized and broadly tuned olfactory glomeruli

Lydia Gruber, Rafael Cantera, Markus Pleijzier, Bill S. Hansson and Jürgen Rybak

Preprint on bioRxiv

Posted on October 2, 2022

FORM 1

Manuscript No. Manuscript I

Manuscript title:

Diversification of neuropil organization in specialized and broadly tuned olfactory glomerular circuits in Drosophila melanogaster

Authors: Lydia Gruber, Rafael Cantera, Markus Pleijzier, Bill S. Hansson, Jürgen Rybak

Bibliographic information:

Gruber, L., Cantera, R., Pleijzier, M. W., Hansson, B. S., & Rybak, J. (2022). Diversification of neuropil organization in specialized and broadly tuned olfactory glomerular circuits in *Drosophila* melanogaster. *bioRxiv*, 2022.2009.2030.510181. doi:10.1101/2022.09.30.510181

The candidate is (Please tick the appropriate box.)

☒ First author, ☐ Co-first author, ☐ Corresponding author, ☐ Co-author.

Status: in preparation"

Authors' contributions (in %) to the given categories of the publication

Author	Conceptual	Data analysis	Experimental	Writing the manuscript	Provision of material
Gruber, L.	**70%**	**90%**	**100%**	**80%**	-
Cantera, R.	-	-	-	5%	-
Pleijzier, M.	-	5%	-	-	-
Hansson, B.S.	10%	-	-	5%	100%
Rybak, J.	20%	5%	-	10%	-
Total:	100%	100%	100%	100%	100%

_____ _____

Signature candidate Signature supervisor (member of the Faculty)

Diversification of neuropil organization in specialized and broadly tuned olfactory glomerular circuits in *Drosophila melanogaster*

Lydia Gruber[1], Rafael Cantera[2], Markus William Pleijzier[3], Bill S. Hansson[1#], Jürgen Rybak [1#]

1 Max Planck Institute for Chemical Ecology, Department of Evolutionary Neuroethology, 07745 Jena, Germany
2 Instituto de Investigaciones Biológicas Clemente Estable, Departamento de Biología del Neurodesarrollo, 11600 Montevideo, Uruguay
3 Neurobiology Division, MRC Laboratory of Molecular Biology, Cambridge, CB2 0QH, England, United Kingdom

# contributed equally

*Correspondence: Jürgen Rybak, jrybak@ice.mpg.de

Keywords: olfactory circuitry, DA2, DL5, connectome, *Drosophila melanogaster*, FIB-SEM, synapses, sensory lateralization

ABSTRACT

To manage the great complexity of detecting and identifying olfactory cues, the insect olfactory system has evolved two main strategies: combinatorial coding and specialized, narrowly tuned olfactory pathways. In combinatorial coding, odorants are encoded by activation of multiple, broadly tuned olfactory sensory neurons that innervate distinct sets of glomeruli. In specialized olfactory pathways, information regarding a single or a few odorants is processed in a discrete, narrowly tuned circuit within a dedicated glomerulus. Here, we compared the narrowly tuned glomerulus DA2 with the broadly tuned glomerulus DL5 at the ultrastructural level, by using volume based focused ion beam scanning electron microscopy. We provide a detailed analysis of neuronal innervation, synaptic composition as well as a circuit diagram of the major glomerular cell types: olfactory sensory neurons (OSNs), uniglomerular projection neurons (uPNs) and multiglomerular neurons (MGNs). By comparing our data with a previously mapped narrowly tuned glomerulus (VA1v), we disclose putative generic features of narrowly tuned glomerular circuits: a high density of neuronal fibers and synapses, a low degree of sensory lateralization, strong axo-axonic connections between OSNs as well as dendro-dendritic connections between uPNs, and a low degree of presynaptic inhibition at the OSN axons. We also show a unique property of the large uPN dendrite in DL5, which forms substantial amount of autapses.

INTRODUCTION

Olfaction is an anatomically shallow sensory system. In mammals and invertebrates just one synapse separates the sensory periphery from the central brain (Su et al., 2009;Liang and Luo, 2010;Shepherd, 2011;Owald and Waddell, 2015;Dolan et al., 2018). In the olfactory system of *Drosophila melanogaster*, the first relay station of synaptic transmission is the antennal lobe (AL) which has a circuit architecture homologous to that of the vertebrate olfactory bulb (Boeckh et al., 1990;Sachse and Manzini, 2021;Shepherd et al., 2021). The fly AL consists of approximately 58 spherical compartments, called glomeruli, which can be distinguished by size, shape and location (Laissue et al., 1999;Gao et al., 2000;Vosshall et al., 2000;Grabe et al., 2015;Bates et al., 2020). Each glomerulus receives stereotypic input from axon terminals of olfactory sensory neurons (OSNs), which have their cell bodies and dendrites located in the antennae or maxillary palps (de Bruyne et al., 1999;Shanbhag et al., 1999;de Bruyne et al., 2001;Hallem et al., 2004;Benton et al., 2006). All the OSNs innervating a given glomerulus express a typical repertoire of ligand-gated chemoreceptors (Couto et al., 2005;Fishilevich and Vosshall, 2005;Benton et al., 2006), which represent a wide range of specifications, binding either a single, few, or many distinct chemicals (Hallem et al., 2004;Hallem and Carlson, 2006;Knaden et al., 2012;Münch and Galizia, 2016;Seki et al., 2017;Wicher and Miazzi, 2021).

Most OSNs project bilaterally to the corresponding glomeruli in the left and right AL (Gaudry et al., 2013;Tobin et al., 2017). In the AL, OSNs convey odor signals to excitatory uniglomerular projection neurons (uPNs), which branch only within a single glomerulus, or to inhibitory multiglomerular PNs (mPNs) and (inhibitory or excitatory) interglomerular local interneurons (LNs) (Ng et al., 2002;Cuntz et al., 2007;Kazama and Wilson, 2008;Kreher et al., 2008;Kazama and Wilson, 2009;Masse et al., 2009;Tanaka et al., 2012;Ai and Hagio, 2013;Wilson, 2013;Bates et al., 2020). LNs innervate several glomeruli and are the key modulatory neurons in the AL (Chou et al., 2010;Seki et al., 2010). The highly converging OSNs-to-PN signal transmission (Chen and Shepherd, 2005;Masse et al., 2009;Jeanne and Wilson, 2015) is lateralized, activating ipsilateral uPNs more strongly than contralateral ones (Agarwal and Isacoff, 2011;Gaudry et al., 2013;Tobin et al., 2017). From the AL, uPNs and mPNs relay processed signal information to higher brain centers (Norgate et al., 2006;Fiala, 2007;Jefferis et al., 2007;Keene and Waddell, 2007;Galizia, 2014;Guven-Ozkan and Davis, 2014;Strutz et al., 2014;Bates et al., 2020).

The stereotypic activity pattern of the olfactory glomeruli by distinct odorants encodes the odor space, represented in a so-called odotopic map of the AL according to the glomerular activation by distinct chemical classes. (Couto et al., 2005;Laissue and Vosshall, 2008;Knaden and Hansson, 2014;Grabe et al., 2015;Grabe and Sachse, 2018). Some odorants induce a fixed innate behavior (aversion or attraction), activating characteristically specific glomeruli (Semmelhack and Wang, 2009;Knaden et al., 2012;Knaden and Hansson, 2014;Gao et al., 2015;Grabe and Sachse, 2018). The encoding of hedonic valence already at the level of the AL is important for a fast odor

coding. Most odorants are encoded in a combinatorial manner in the fly AL by activating multiple OSNs types expressing broadly tuned receptors and their glomerular circuits, including broadly tuned uPNs (de Bruyne et al., 2001;Silbering and Galizia, 2007;Silbering et al., 2008;Masse et al., 2009;Galizia, 2014;Szyszka and Galizia, 2015;Sachse and Hansson, 2016;Seki et al., 2017). Certain chemoreceptors and their downstream glomerular circuit, however, have evolved a very high specificity and sensitivity to single or very few chemicals (Andersson et al., 2015;Haverkamp et al., 2018;Keesey and Hansson, 2021). These narrowly tuned glomerular circuits often belong to dedicated olfactory pathways, called "labeled lines", which process information regarding single odorants of particular importance for reproduction and survival (Kurtovic et al., 2007;Datta et al., 2008;Stensmyr et al., 2012;Dweck et al., 2015;Gao et al., 2015). An extreme example is the DA2 glomerulus, which responds exclusively to geosmin, an ecologically relevant chemical that alerts flies to the presence of harmful microbes, causing the fly to avoid laying eggs at these locations (Stensmyr et al., 2012). This dedicated olfactory pathway and its receptor sequence is conserved throughout evolution (Keesey et al., 2019;Keesey and Hansson, 2021). Another example is glomerulus VA1v, which responds to methyl laurate, a pheromone that induces a strongly attractive response in female flies leading to aggregation behavior (Dweck et al., 2015). DL5, on the other hand, is an example of a broadly tuned glomerulus, innervated by OSNs activated by several aversive odorants, like E2-hexenal or benzaldehyde (Knaden et al., 2012;Münch and Galizia, 2016;Seki et al., 2017;Mohamed et al., 2019b). This functional diversity suggests differences in neuronal composition and synaptic connectivity between broadly and narrowly tuned glomeruli.

A survey of neuronal composition across glomeruli revealed great variation in the numbers of the different types of neurons innervating narrowly and broadly tuned glomeruli (Grabe et al., 2016). In general, narrowly tuned glomeruli were found to be innervated by more uPNs and fewer LNs compared to more broadly tuned glomeruli (Chou et al., 2010;Grabe et al., 2016). In addition, narrowly tuned OSNs received less global interglomerular LN inhibition than broadly tuned ones (Hong and Wilson, 2015;Grabe et al., 2020;Schlegel et al., 2021). For example, in female flies, the narrowly tuned glomerulus DA2 contains dendrites of 6-8 uPNs, whereas the broadly tuned glomerulus DL5 houses only 1 or 2 uPNs and has a higher number of innervating LNs. Interestingly, both glomeruli are innervated by the same number of OSNs (Grabe et al., 2016).

Little is known, however, about the microarchitecture of the synaptic circuitry in distinct glomeruli and, in particular, about principal ultrastructural differences between narrowly vs. broadly tuned glomerular circuits. Electron microscopy (EM) allows volume imaging with dense reconstruction of fine neurite branches and synapses in brain tissue at nanometer resolution, necessary to map synapses (Briggman and Denk, 2006;Cardona et al., 2009;Helmstaedter, 2013;Rybak, 2013;Meinertzhagen, 2018). The first ultrastructural insights into the synaptic connectivity of *Drosophila* olfactory glomeruli were obtained by studies based on serial

section transmission EM (ssTEM) (Rybak, 2016;Tobin et al., 2017). In these studies, Rybak *et al*. (2016) showed that all 3 basic classes of AL neurons make synapses with each other, while Tobin *et al*. (2017) revealed that the differences in number of innervating uPNs between the left and right DM6 glomeruli are compensated by differences in synaptic strength. With focused ion beam-scanning electron microscopy (FIB-SEM; (Knott et al., 2008)) a complete reconstruction of all neurons in the narrowly tuned, pheromone processing glomerulus VA1v was obtained (Horne et al., 2018). Recent technological innovations in ssTEM, FIB-SEM and automated neuron reconstruction have made connectome datasets of the adult *Drosophila* central nervous system available (Saalfeld et al., 2009;Zheng et al., 2018;Li et al., 2020b;Scheffer et al., 2020) and provided complete circuit descriptions of several brain centres (Felsenberg et al., 2018;Dolan et al., 2019;Auer et al., 2020;Bates et al., 2020;Coates et al., 2020;Huoviala et al., 2020;Li et al., 2020a;Marin et al., 2020;Otto et al., 2020;Hulse et al., 2021;Schlegel et al., 2021).

In an attempt to find answers to how highly specialized olfactory glomerular circuits of dedicated olfactory pathways differ in their signal integration from broadly tuned glomerular circuits, we compared the microarchitecture and synaptic circuitry of a narrowly and a broadly tuned glomerulus (DA2 and DL5). By using a correlative workflow combining transgenic markers with FIB-SEM, in order to identify our glomeruli of interest, we reconstructed OSNs, uPNs and multiglomerular neurons (MGNs) and mapped all associated synapses and compared the circuit organization of both glomeruli.

RESULTS

Volume-based electron microscopy of two different olfactory glomeruli

To compare the synaptic circuitries of two olfactory glomeruli known to belong to either narrowly or broadly tuned glomerular types in *Drosophila melanogaster*, we mapped all synapses of glomeruli DA2 (right AL) and DL5 (left AL) in one female fly (**Figure 1A-B**) with the aid of focused ion beam scanning electron microscopy (FIB-SEM). A partial reconstruction of a second DA2 in another fly was used for neuronal volume measurements (see Methods). The reconstructions were based on high resolution (4x4x20 nm) datasets (**Figure 1**; **Figure 1 – video 1),** thus allowing reconstruction of fine neuronal branches (~20 nm diameter; **Figure 1C-D**) as well as mapping chemical synapses (example in **Figure 1E**) in the two volumes of interest (VOI). To restrict the imaging volume to the target VOIs, we employed a correlative approach for the first time for a *Drosophila* EM volume reconstruction. The glomeruli of interest were identified by their size, shape and location in brains of transgenic flies (*Orco-GAL4; UAS-GCaMP6s*) using the glomerular map of (Grabe et al., 2015). The flies expressed the protein GCaMP6, a green fluorescent protein coupled with calmodulin and M13 (a peptide sequence from myosin light-chain kinase; **Figure 1A-B**). Subsequently, the identified glomeruli were marked by laser branding using a two-photon laser (Bishop et al., 2011). These fiducial marks were apparent under both light (Figure 1A-B) and electron microscopy **(Figure 1C-D)** and facilitated the delimitation of the VOIs during FIB-SEM scanning. We produced two complete FIB-SEM datasets: one for glomerulus DA2 and one for DL5 (pure imaging time for both glomeruli: ~60 h) and a partial dataset for DA2 in a second fly.

Skeleton based neuron reconstruction and synapse identification

We reconstructed all neurons within the two VOIs (example neuron: **Figure 1F**) and mapped all their synaptic connections using an iterative skeleton-based reconstruction approach, similar to previously reported procedures (Berck et al., 2016;Schneider-Mizell et al., 2016;Zheng et al., 2017) with the aid of the web-based neuron reconstruction software CATMAID (http://www.catmaid.org; RRID:SCR_006278; (Cardona et al., 2009;Schneider-Mizell et al., 2016); **Figure 1 – video 1**). Synapses were identified by their presynaptic transmitter release site, which in *Drosophila* is composed of a presynaptic density called a T-bar, surrounded by synaptic vesicles and apposed postsynaptic elements (**Figure 1E**), as previously described (Trujillo-Cenoz, 1969;Fröhlich, 1985;Rybak et al., 2016;Huang et al., 2018;Li et al., 2020b). All synapses observed in our FIB-SEM data sets were polyadic, i.e. each presynaptic site connected to multiple postsynaptic sites (See example in **Figure 1E**), a feature of insect brain synapses (Meinertzhagen and O'Neil, 1991;Malun et al., 1993;Prokop and Meinertzhagen, 2006;Hartenstein, 2016;Rybak et al., 2016). Some synaptic complexes had up to 16 postsynaptic sites (**Figure 2 – figure supplement 1B**),

i.e. one T-bar to 16 single synaptic profiles (i.e. 1:1 single output-input connections). Short neuronal fragments (<10 µm), which could not be connected to any neuronal fiber were designated as "orphans". These fragments represented 4% of the total length of all traced neuronal fibers in DA2 and 6% in DL5 and contained about ~12% of all synaptic contacts in both glomeruli.

Glomerular neurons: classification, description and inventory

Previous descriptions of the ultrastructural characteristics of the AL in *Drosophila* helped to classify AL neurons into 3 main classes (**Figure 2A**) Olfactory sensory neurons (OSNs), uniglomerular projection neurons (uPNs) and multiglomerular neurons (MGNs; cells that interconnect multiple glomeruli). MGNs are further subdivided into multiglomerular projection neurons (mPNs) and local interneurons (LNs) (Berck et al., 2016;Rybak et al., 2016;Zheng et al., 2017;Gruber et al., 2018;Horne et al., 2018;Li et al., 2020b;Schlegel et al., 2021). Most of the neuronal profiles within the MGN neuron class are probably inhibitory local neurons, as this cell type is the most numerous and broadly arborizing of the multiglomerular cell types in the antennal lobe (Chou et al., 2010;Lin et al., 2012). In addition, we observed a few neuronal fibers with an electron-dense and vesicle-rich cytosol, which we interpreted to be either peptidergic neurons (Nässel and Homberg, 2006;Eckstein et al., 2020) or the contralaterally projecting, serotonin-immunoreactive deutocerebral (CSD) neuron, (Dacks et al., 2006;Goyal and Chaudhury, 2013;Zheng et al., 2017;Coates et al., 2020;Eckstein et al., 2020). Except for these neuronal fibers containing abundant electron-dense vesicles, all other neuronal fibers were assigned to either OSNs, uPNs or MGNs based on their morphologies (**Figure 2A, B;** see Methods).

OSNs formed large, elongated synaptic boutons (**Figure 2A**), had the largest volume/length ratio of all three neuron classes (**Figure 2 – figure supplement 1A**) and displayed the lowest degree of branching intensity of all neurons in both glomeruli (**Figure 2B**). In agreement with what had been observed in other glomeruli (Rybak et al., 2016), the majority of output synapses made by OSN terminals were triads (1:3) and tetrads (1:4). The T-bars of OSN synapses exhibited a large variation in length: some were large enough to accommodate 16 postsynaptic contacts (**Figure 2 – figure supplement 1B**). The frequency of large T-bars was much higher in OSNs than in other neuron classes with an average polyadicity (average number of postsynaptic sites at each T-bar) of 6 (1:6; (**Table 1,** row 14). As OSNs had the greatest T-bar and output density along their axons (**Table 1**, row 10-11) they also displayed the largest synaptic ratios (both for the T-bars/input sites and output sites/input sites) of all neuron classes (**Table 1,** row 12-13), which was in line with previous observations (Rybak et al., 2016).

The uPNs exhibited the highest degree of branching intensity of the three neuron classes in both glomeruli (**Figure 2A-B**). They showed numerous very fine apical branches that frequently connected multiple times via spines to the same presynaptic site, leading to an entangled 3D shape typical of uPNs (**Figure 2A**) (Rybak et al.,

2016;Tobin et al., 2017;Schlegel et al., 2021). uPNs had the smallest volume/length ratio of all neuron classes (for the DA2: **Figure 2 - supplement 1A**). In addition to having many fine branches, uPN dendrites also had enlarged regions with almost no cytosol that were packed with large mitochondrial profiles extending over considerable distances. These enlarged profiles showed a larger degree of mitochondria fission (dividing and segregating mitochondrion organelles; personal observation) than the other neuron classes with rather round and compact mitochondria (**Figure 2A**; FIB-SEM image; see data availability). In glomerulus DA2 we found 7 uPNs, consistent with previous reports (Grabe et al., 2016). Two of them (PN#1, PN#2; see data availability) branched broadly and innervated the full glomerulus, receiving more synaptic input than the other 5 uPNs (PN#3-#7; **see Table S3**), which branched exclusively in sub-regions of the glomerulus, with partial overlap. In addition to abundant clear small vesicles (~20 nm in diameter) (Yasuyama et al., 2003;Strutz et al., 2014;Bates et al., 2020), uPN dendrites also displayed small electron-dense vesicles, as previously reported for PN axon terminals in the mushroom body calyx (Butcher et al., 2012;Yang et al., 2022). These electron-dense vesicles are packed with different types of neuropeptides that act as neuromodulators or co-transmitters (Gondré-Lewis et al., 2012;Li et al., 2017;Croset et al., 2018;Eckstein et al., 2020). In both glomeruli, uPNs had the highest neuronal synaptic input density and the lowest T-bar and output density of the three neuron classes (**Table 1,** row 9-11; DA2 and DL5 differences: see next section). The synaptic ratios (T-bars/input sites and output sites/input sites) were much lower for uPNs than for the other neuron classes (**Table 1,** row 12-13). The majority of uPN dendritic output synapses (feedback synapses) were tetrads in both glomeruli, with an average polyadicity of around 5 (lower than in OSNs; (**Figure 2 – supplement 1; Table 1,** row 14).

The majority of the neuronal fibers in both glomeruli belonged to MGNs (**Figure 2A**). MGNs exhibited variable morphology and ultrastructure, as expected, but shared also some ultrastructural features. Their synaptic boutons were formed by thin fibers, thus the volume/length ratio of MGNs was lower than that of OSNs but greater than that of uPNs (**Figure 2 – figure supplement 1A**). A similar relationship was found for the number of output sites and the T-bar density along MGN fibers, which were smaller than in OSNs but larger than in uPNs (**Table 1,** row 10-11). In contrast, branching intensity in MGNs was larger than in OSNs but smaller than in uPNs (**Figure 2B**). The synaptic ratio of output-to-input sites was around one (**Table 1**, row 12-13). MGNs had the lowest polyadicity (~3) of the three neuron classes (**Table 1**, row 14) and their synapses were mainly triads (**Figure 2 – supplement 1D**). Interestingly, besides the abundant clear small vesicles (~20 nm in diameter), some MGNs had small electron-dense vesicles, most likely housing the neuropeptide sNPF (Nässel et al., 2008).

DA2 is more densely innervated and has a higher synapse density than DL5

In our FIB-SEM datasets the volume of glomerulus DA2 was 45% smaller than that of glomerulus DL5 (1500 µm³ vs. 2700 µm³), which is in agreement with measurements based on light microscopy (DA2 = 1600 µm³, DL5 = 2900 µm³ (Grabe et al., 2016). We also confirmed that a similar number of OSNs (44-46 OSNs) innervated both glomeruli (**Figure 2C**), and that each glomerulus received OSN innervation from both the ipsilateral and contralateral antennae (Vosshall et al., 2000;Grabe et al., 2016). Also in agreement with (Grabe et al., 2016), the DA2 glomerulus was innervated by 7 uPNs whereas DL5 had a single uPN (**Figure 2C**). MGN cell numbers could not be counted in our study due to their multiglomerular morphology, which also prevented us from tracing MGN fibers to their soma due to our partial volume acquisition (see Methods).

To further investigate differences in neuronal populations we now turned our attention to the glomerular innervation and synaptic composition of DA2 and DL5 neuronal fibers (Grabe et al., 2016). We measured the total length (sum in µm) of all neuronal fibers of each neuron class within the DA2 and DL5 (**Figure 2C; Table 1**, row 1). In addition, we counted all T-bars and their output sites (1:1 synaptic contacts) as well as all postsynaptic sites (input sites) for all neuron fibers together and of each neuron class individually (**Table 1, row 2-4**). We counted in total ~ 14 000 synaptic contacts and 2648 T-bars in DA2 and ~ 17 000 contacts and 3387 T-bars in DL5 (**Figure 2C, Table 1, row 4**). Most of these synapses were triads and tetrads (**Figure 2 – figure supplement 1B-D**). In order to compare DA2 and DL5 we normalized neuronal length and synaptic counts to glomerular volume. We then analyzed (**1**) the innervation density, i.e., the length of neurons per glomerular volume (µm/µm³) and (**2**) the glomerular synaptic density (T-bar #, output site or input site #/µm³). Data are reported in total for all neuronal fibers of each neuron class (**Table 1, row 5-8**) and as an average for neuronal fibers of the respective neuron class **(Figure 3)**. In addition, we compared (**3**) the average polyadicity for each neuron class **(Figure 3)** and **(4)** the average neuronal synaptic density (T-bar, output and input site density along each neuronal fiber) (#/µm) (**Figure 3 – figure supplement 1B**).

We observed that the average neuron innervation density of OSNs was significantly higher in DA2 than in DL5, with a total innervation density that was 20% higher in DA2 (**Figure 3A**), **Table S1**). The glomerular synaptic density of input sites, output sites and T-bars along OSNs was significantly higher in DA2 than in DL5 (**Figure 3A**). OSNs in DA2 formed therefore more input sites, and much more T-bars and output sites per glomerular volume than in DL5 (**Table 1**, row 7-8; relative differences: **Table S1**). In contrast, the density of input sites distributed along the length of OSN fibers was similar in DA2 and DL5, whereas T-bar and output site density along the OSN axons was significantly higher in DA2 (**Figure 3 – figure supplement 1A**).

We then asked if the DA2 glomerulus, due to its higher number of uPNs, also had a higher uPN innervation density and synaptic density of its postsynaptic sites and/or presynaptic sites compared to the DL5 glomerulus, which contains a single uPN. In the DA2, the fibers of the 7 uPNs had almost the same total length as the fibers

of the single uPN in the more voluminous DL5 (4652 µm in DA2 vs. 5015 µm in DL5; **Table 1**, row 1). The DA2 uPNs had in addition a similar total number of input sites as the single uPN in the DL5 (3887 vs. 3955; **Table 1**, row 2). As such, in DA2 the total innervation density of its 7 uPNs was higher as compared to the innervation density of the single uPN in DL5 (**Table 1**, row 5), even though the average innervation density of DA2-uPNs was lower (**Figure 3B**). The total glomerular input density of all uPNs was higher in DA2 as compared to DL5 (**Table 1**, row 6). On the other hand, the total glomerular synaptic density of the T-bars and output sites was similar in DA2 and DL5 (**Table 1**, rows 7-8). In line with these results, the neuronal density of T-bars and output sites was less in the DA2 uPNs as compared to the DL5 uPN, whereas the neuronal density of input sites was similar (**Figure 3 – figure supplement 1B; Table 1**, row 9-10). This caused almost twice as high synaptic ratios (T-bars-to-inputs and outputs-to-inputs) in the DL5 uPN relative to DA2 uPNs (**Table 1**; row 12-13).

We then hypothesized that DA2 will have a lower innervation density of MGNs (mainly LNs) than DL5 as it had been reported that DL5 is innervated by fewer LNs (Chou et al., 2010;Grabe et al., 2016). However, we observed the opposite: the innervation density of MGNs was significantly higher in DA2 than in DL5 (**Figure 3C**), with slightly higher total innervation density (**Table 1,** row 5**).** Interestingly, only the glomerular input density was significantly higher for DA2 MGNs compared to that found in DL5, not the glomerular synaptic density of output sites or of the T-bars (**Figure 3C**). However, the total glomerular synaptic density of input sites, output sites and T-bars were still higher in DA2 than in DL5 **(Table 1,** rows 6-8**).** Synaptic densities along the MGN fibers were similar in DA2 and DL5 (**Figure 3 – supplement 1**).

In summary, the DA2 glomerulus is more densely innervated than DL5 with neuronal fibers, which results in a more densely packed DA2 neuropil with more synaptic contacts. The DA2 has a significantly higher innervation density and higher density of T-bars, output and input sites per volume (**Figure 3D**, **Table 1,** row 5-8). The degree of synapse polyadicity is also significantly higher in DA2 than in DL5 (**Figure 3D, Table 1,** row 14) due to a shift to higher polyadicity among OSN (**Figure 3A**) and MGN synapses (**Figure 3C**). OSNs show the strongest shift in polyadicity, with tetrads being the most abundant synapse type in DA2 whereas triads are the most abundant in DL5 OSNs (**Figure 2 – figure supplement 1B).**

Lateralization of OSN glomerular connectivity

In *Drosophila melanogaster*, the majority of olfactory glomeruli receive bilateral OSN input (Stocker et al., 1983;Stocker et al., 1990;Vosshall et al., 2000;Silbering et al., 2011) see scheme in **Figure 4A**). Recent studies have shown that ipsi- and contralateral OSNs are asymmetric in their synaptic connectivity to other neurons in the majority of the glomeruli (Tobin et al., 2017;Schlegel et al., 2021) and that ipsi- and contralateral OSNs activate uPNs in an asymmetric way (Gaudry et al., 2013;Tobin et al., 2017). However, not all glomeruli appear to have the same degree of lateralized OSN connectivity (Schlegel et al., 2021). At least for one narrowly tuned glomerulus (DA1),

there is functional evidence that in female flies its uPNs are evenly activated by either ipsi- or contralateral antennal stimulation (Agarwal and Isacoff, 2011). We hypothesized that this lack of lateralization could be a feature of other narrowly tuned glomeruli.

Ipsi- and contralateral OSNs in DA2 and DL5 were identified based on the location and trajectory of their axons (**Figure 4B**). In both glomeruli, ipsilateral OSN terminals were longer than their contralateral counterparts within the VOI, while polyadicity was stronger in contralateral axons. Synaptic density was not consistently higher or lower in ipsilateral OSNs compared to contralateral ones in DA2 and DL5 (**Figure 4 – figure supplement 1**).

We observed that the synaptic output of ipsi- vs. contralateral OSNs was asymmetric, with significant differences in the ipsi- and contralateral OSN output to either uPNs, OSNs or MGNs (**Figure 4C**, DA2 and DL5). In agreement with previous observations in other glomeruli (Schlegel et al., 2021), the output fraction to uPNs and OSNs was greater in ipsilateral OSNs than in contralateral ones (**Figure 4C**, DA2 and DL5). Vice versa, the OSN output to MGNs was greater in the contralateral glomerulus than the ipsilateral side (**Figure 4C**, DA2 and DL5). However, the differences between the medians and means were smaller in DA2 than in DL5 (**Figure 4C**; differences between means: see data availability).

Our finding of less lateralized connections in the DA2 (**Figure 4C**, DA2 and DL5) was also observed in another narrowly tuned glomerulus (VA1v; Dweck et al., 2015) for which connectome data is available (Horne et al., 2018). In VA1v, the OSN output to uPNs and MGNs was significantly asymmetric in the same manner as in DA2 and DL5, i.e. with greater ipsilateral OSN output fractions to uPNs and OSNs and greater contralateral OSN output fraction to MGNs (**Figure 4C**). Asymmetry in the VA1v OSN output fractions was even less distinct than in DA2 (regarding both the difference between the median and the mean; **Figure 4C** and data availability). In VA1v, the OSN output fraction to OSNs was similar in ipsi- and contralateral OSNs (**Figure 4C**). In addition, the OSN input, from either sister OSNs or MGNs, was asymmetric in DL5 but not in the narrowly tuned glomeruli (**Figure 4D**). The inputs from uPNs to ipsi- or contralateral OSNs were not compared due to their low numbers.

In summary, our data add to the knowledge of lateralized connectivity within olfactory glomeruli and supports the hypothesis that narrowly tuned glomeruli have a lower degree of lateralization of OSN connectivity compared to broadly tuned glomeruli.

Glomeruli DA2 and DL5 differ in several features of their circuitry

Next, we asked whether the synaptic circuitries of DA2 and DL5 differ from each other. We counted each synaptic contact (**Table S2 and S3**) and categorized the distinct connection motifs according to the neuron class the output and input neuron belonged to (**Figure 5A; Table S2).** Each connection motif (for example OSN>uPN, i.e., the OSN-to-uPN feedforward connection) was then assessed for its relative synaptic

strength, i.e. how many synaptic contacts of this particular connection motif were found compared to the total number of synaptic contacts within the respective circuitry (**Figure 5A-D**; see Methods).

We found that neurons from each class made synaptic contacts with each other in DA2 and DL5, as previously reported for other glomeruli (Berck et al., 2016;Rybak et al., 2016;Tobin et al., 2017;Horne et al., 2018;Schlegel et al., 2021). In both DA2 and DL5, OSNs provided the strongest relative synaptic output, i.e. 49% of all synaptic connections in DA2 and 43% in DL5 were formed by OSNs (**Figure 5B-C**). Thus, even though DA2 and DL5 had similar numbers of OSNs (44 and 46, respectively), those in DA2 provided a stronger circuit output (14% stronger; **Table S2**) than those in DL5 (**Figure 5B-C**). In both glomeruli the main OSN output partners were MGNs and uPNs, i.e. 27% of all circuitry connections in DA2 and 24% in DL5 were OSN>MGN connections and 20% in DA2 and 18% in DL5 were OSN>uPN connections (**Figure 5B-C**). In DA2, interestingly, each of the 7 uPNs received input from almost all OSNs and so could maintain a high degree of convergent signal transmission (**Table S3**). In contrast, OSNs received the lowest relative input of all neuron classes in DA2 and DL5 (7% and 8% respectively; **Figure 5B-C**). In line with previous observations in other glomeruli (Horne et al., 2018;Schlegel et al., 2021), OSNs also made abundant axo-axonic synapses with sister OSNs (2.6% in DA2 and 1.5% in DL5; **Figure 5B-C**). Thus, the relative synaptic strength of the OSN>OSN connection was 70% stronger in DA2 than in DL5 (**Figure 5B-C; Table S2**).

The uPNs in both glomeruli had the weakest relative output of all neuron classes within their circuitry, and this was even weaker (38%) in DA2 (**Figure 5B-C; Table S2**). In contrast, the relative synaptic input onto uPNs was greater in DA2 than in DL5 (33% vs. 28%, respectively; **Figure 5B-C;** 16% stronger in DA2; **Table S2**), which is in line with our finding that in DA2, the uPNs provide more input sites per unit of glomerular volume than in the DL5 (**Figure 3B-C**). In both glomeruli, the feedback connections from uPNs (depicted in **Figure 5A**), were almost exclusively directed towards MGNs, as previously reported for the broadly tuned DM6 and the narrowly tuned glomerulus VA1v (Tobin et al., 2017;Horne et al., 2018). However, the relative synaptic strength of the uPN>MGN connection was 40% weaker in DA2 than in DL5 (uPN>MGN: 10% in DA2 and 17% in DL5). Only a few cases of uPN>OSN synaptic connections were observed (a total of 16 in DA2 and 26 in DL5) representing a synaptic strength of 0.1% in DA2 and 0.2% in DL5 (**Table S2**). Finally, uPNs in DA2 also made 71 reciprocal synaptic connections (representing a synaptic strength of 0.6%; **Table S2**; **Figure 5B**), consistent with electrophysiological evidence for reciprocal synaptic interactions between sister uPNs (Kazama and Wilson, 2009). The single uPN of the DL5 had 54 dendro-dendritic synapses (representing 0.4% of all DL5 synaptic contacts; **Figure 5C**), which were exclusively autapses, i.e. synapses formed by a neuron onto itself. Dendritic uPN autapses exist also in DA2-uPNs, but they were few: we observed only 14 autaptic uPN-uPN connections in DA2, which were mainly located at the two longest uPN dendrites (for further analysis of autapses see next section).

MGNs received the strongest input in both glomeruli (60% of the total input in DA2 and 64% in DL5; **Figure 5B-C**). This is in line with the observation that MGNs provided the majority of all traced neuronal fibers in each glomerulus and had the highest innervation density of all neuron classes; **Table 1**). The relative output strength of MGNs was similar in both glomerular circuits (~40% of the total output in each glomerulus; **Figure 5B-C**). MGNs made many reciprocal synapses to each other, accounting for 23% of all synapses in both glomeruli (**Figure 5B-C)**. The relative synaptic strength between MGN>uPN was stronger in DA2 (12%) than DL5 (10%) (**Figure 5B**-C; **Table S2**). The MGN>OSN feedback connection was relatively weak in both glomeruli (5% in DA2 vs. 6% in DL5; **Figure 5B-C**) but weaker (25%) in DA2 than in DL5 (**Table S2**).

We then looked at the fractional output and input of each neuron class (Figure 5E', E''). In both glomeruli OSNs had a similar proportion of their synaptic output onto uPNs (40%-41%), onto MGNs (55% in both) and onto sister OSNs (4%-5%) (**Figure 5E'**). From the uPNs perspective, over 93%-96% of their recurrent synaptic output was directed to MGNs in both DA2 and DL5, and few synapses were directed onto OSNs (~1% of the uPN output; **Figure 5E'**). The uPN>uPN output fraction of the 7 uPNs in DA2 (reciprocal synapses) was twice the uPN output fraction (autaptic) of the single uPN dendrite in DL5 (6% vs. 3%; **Figure 5E'**). MGNs formed synaptic output mainly to other MGNs (58%-59% of the total MGN output in DA2 and DL5). Among MGNs we found also rare cases of autapses. The MGN>uPN output fraction was greater in DA2 (30%) than in DL5 (25%), whereas the MGN>OSN output fraction was smaller in DA2 (12%) than in DL5 (16%; **Figure 5E'**).

Turning to the input fractions of each neuron class, we found that in both glomeruli, OSNs received most of their input from MGNs (>50%). In DA2 the input fraction onto OSNs (MGN>OSN) was smaller than in DL5 (63% vs. 78%; **Figure 5E''**). In contrast, the OSN input fraction from sister OSNs was greater in DA2 (35% vs. 20%; **Figure 5E''**). In both glomeruli, the OSNs received only weak uPN input (2%) (**Figure 5E''**). The input fractions onto the 7 uPNs, formed by uPNs, MGNs and OSNs, in the DA2 and the single uPN in DL5 were similar (**Figure 5E''**). Most uPN input was delivered by OSNs (~62% in both glomeruli) and less from MGNs (~36%). The uPN input fraction from other uPNs in DA2 or the autaptic input from the single uPN in DL5 was small (2%; **Figure 5E''**). The MGNs in DA2 received a smaller fraction of uPN feedback input than in DL5 (17% vs. 26%; **Figure 5E''**) but a greater OSN input fraction (45% vs. 38%; **Figure 5E''**). The MGN input from other MGNs was similar in both glomeruli.

To further explore whether differences in circuitry between DA2 and DL5 might represent characteristic features of broad vs. narrowly tuned glomeruli, we analyzed connectome data from another narrowly tuned glomerulus (VA1v; (Horne et al., 2018). We calculated the relative synaptic strength between OSNs (n=107), uPNs (n=5) and MGNs (n=74) in the VA1v (**Figure 5D; Table S2**) (**Figure 5E**). We found that the two narrowly tuned glomeruli shared five circuit features that were different from the broadly tuned glomerulus DL5: (**1**), OSNs in VA1v, as reported above for DA2,

displayed a stronger relative feedforward output to uPNs (22%) and to MGNs (32%) (**Figure 5D**). The uPNs and MGNs in VA1v, received a larger fraction of OSN input than in DL5 (**Figure 5E''**). (**2**), the OSN>OSN synaptic output was four times stronger (6%) than in DL5 (1.5%; **Figure 5B-D, Table S1**). This was also reflected in the OSN output fraction to sister OSNs (10%), which in VA1v was more than twice that of DL5 (4%; **Figure 5E'**) and in the much greater OSN input fraction (38%) to OSNs in the VA1v than in DL5 (20%; **Figure 5E''**). (**3**), in the VA1v the uPN>uPN relative synaptic output was more than twice that of DL5 (1% vs. 0.4% in DL5; **Figure 5D**), which is in accordance with a much greater uPN output fraction to uPNs (14%) in VA1v than in DL5 (3%) (**Figure 5E'**). (**4**), as observed before in DA2, VA1v uPNs had fewer feedback synapses onto MGNs than in DL5 (relative synaptic strength of uPN>MGN connection: 6% vs. 17%; **Figure 5C-D**), also reflected in a smaller output fraction from uPNs to MGNs in VA1v than in DL5 (81% vs. 96%; **Figure 5E'**). In agreement, the MGN input fraction from uPNs in VA1v was much smaller than in DL5 (10% vs. 26%; **Figure 5E''**). (**5**), OSNs in VA1v received a smaller MGN input fraction than DL5 OSNs (60% vs. 78%; **Figure 5E''**).

Besides relative differences (stronger or weaker) in DA2 and VA1v connection motifs compared to DL5, two connection motifs were stronger in DA2 and DL5 but weaker in VA1v: **(1)** the MGN>uPN connection, showing a synaptic strength of 12% and 10% in DA2 and DL5 vs. 8% in VA1v (**Figure 5B-D, Table S2**). In agreement with this, the MGN output fraction to uPNs (**Figure 5E'**, MGN output) and the MGN input fraction in uPNs was greater in DA2 and DL5 than in VA1v (**Figure 5E''**, uPN input). **(2)**, the relative synaptic strength in MGN>MGN motifs was similar between DA2 and DL5 (23%; **Figure 5B-C**), but weaker in VA1v (17%; **Figure 5D, Table S2**). This was also reflected in a smaller MGN output and input fraction from or to MGNs (**Figure 5E' and E''**).

In summary, the two narrowly tuned glomerular circuits studied here shared several circuit features when compared with the broadly tuned glomerular circuit (all glomerular circuit features in DA2, DL5 and VA1v are shown in **Figure 6A**). These features were (1) a stronger OSN>uPN and OSN>MGN connection, (2) a much stronger axo-axonic communication between sister OSNs, (3) a stronger dendro-dendritic connection between uPN dendrites, (4) less feedback from uPNs to MGNs and (5) less feedback from MGNs to OSNs (**Figure 6B**).

Autapses in the large DL5 uPN connect distant regions of its dendritic tree

Autapses (synapses made by a neuron upon itself) have seldomly been reported in the *Drosophila* central nervous system (Takemura et al., 2015;Horne et al., 2018). In the DA2 glomerulus we found few autapses in uPNs and MGNs but more in the single DL5 uPN (**Figure 5C; Figure 7A**). In the dendritic tree of the single DL5 uPN, on the other hand, three observers registered 54 autaptic connections independently (see Methods). This represents 3% of the output connections of this neuron and 0.4% of all synaptic contacts in the whole glomerulus (**Figure 7A**; **Figure**

525 **5C; E'**). We hypothesized that these autapses could be important for connecting
526 distant parts of this very large dendritic tree. We thus analyzed the exact location and
527 distribution of autaptic presynaptic and postsynaptic sites in this neuron (**Figure 7A**)
528 and found that the autapses along the dendrites of the DL5 uPN were not distributed
529 evenly. Some dendritic branches received several autaptic inputs, whereas other had
530 no autaptic input (**Figure 7A**). We also discovered a difference in the distribution of
531 the pre- and postsynaptic elements of DL5 autapses. Whilst their presynaptic T-bars
532 were evenly distributed at basal (strahler order: 5) and distal regions (strahler order:
533 1-4), 95% of their postsynaptic sites were located at the most distal region (strahler
534 order 2-1; **Figure 7B-C**). We also calculated the geodesic distance (i.e., along-the-arbor
535 distance) from pre- and post-synaptic sites to the basal root node, which is the node
536 point where the uPN enters the glomerulus and is equivalent to the closest point to
537 the soma in our reconstruction. The geodesic distance from the presynaptic site to the
538 basal root node was significantly shorter than the geodesic distance from postsynaptic
539 sites to the basal root node (**Figure 7 – figure supplement 1B**). The pre- and
540 postsynaptic sites of each autapse were either close to each other along the dendritic
541 tree, or distant from each other (see examples in the dendrogram depicted in **Figure**
542 **7D**). Thus, the geodesic distance between pre- and postsynaptic sites, (see scheme in
543 **Figure 7E**), as well as the number of branching points between pre- and postsynaptic
544 partners, were bimodally distributed (**Figure 7F-G**). Autapses that connected distant
545 dendritic subunits were more frequent than those that connected close subunits of the
546 dendrite (**Figure 7E-G**). In summary, we found abundant autapses within the uPN
547 dendrite of DL5. These autapses were unevenly distributed, with many output sites
548 located in a few sub-branches connecting distal dendritic regions.
549

DISCUSSION

We hypothesized that specialized, narrowly tuned glomerular circuits differ in their ultrastructure and microcircuitry from broadly tuned glomerular circuits. By comparing the connectomes of two narrowly tuned olfactory glomeruli with that of a broadly tuned glomerulus, in *Drosophila melanogaster,* we found prominent features of narrowly tuned glomeruli involving synaptic composition, lateralization of sensory input and synaptic circuitry.

Glomerular circuit analysis: a correlative approach

The small size of olfactory glomeruli in *Drosophila* gave us the opportunity to reconstruct and analyze the dense connectome of entire glomeruli with volume-based electron microscopy in a reasonable time period. Here we developed a correlative workflow that combines transgenic neuron labeling with near-infra-red-laser-branding for precise volume targeting. We then used FIB-SEM (Bishop et al., 2011) to resolve glomerular networks at the synaptic level. A similar procedure was used recently to investigate single cellular organelles (Ronchi et al., 2021). An advantage of this approach is that it facilitates localization of the volume of interest with high precision and consequently limits the image volume to a minimum and reduces scanning time. At the same time, the limitation in volume is a drawback of our workflow, as it was impossible to reconstruct neurons back to their soma. This fact prevented the identification of individual neurons as in other connectome studies (Berck et al., 2016;Eichler et al., 2017;Horne et al., 2018;Zheng et al., 2018;Bates et al., 2020;Scheffer et al., 2020;Xu et al., 2020;Schlegel et al., 2021).

We provide data on innervation and synapse density of olfactory sensory neurons (OSNs), uniglomerular projection neurons (uPNs) and multiglomerular neurons (MGNs) in the *Drosophila* antennal lobe (AL). We observed a higher innervation density of all neuron types but mainly by uPNs and MGNs and in parallel higher density of synaptic contacts along OSN terminals in the narrowly tuned DA2 compared with DL5. These results suggest that narrowly tuned glomeruli have a more densely packed neuropil, forming more numerous synaptic connections in the feedforward motifs OSN>uPN and OSN>MGN. Overall, our observations on synapse density were comparable with previous reports (Mosca and Luo, 2014;Rybak et al., 2016;Horne et al., 2018).

Specific features of narrowly tuned glomerular circuits

Our analysis revealed circuit features in the narrowly tuned glomerulus DA2 and VA1v that might be adaptations specific of such dedicated glomerular circuits. Nevertheless, future studies, analyzing precise numbers of synaptic connections in more individuals, combined with physiological studies and computational models are required to test this hypothesis.

The OSN>uPN feedforward connection is stronger in DA2 and VA1v

OSN presynaptic terminals provide the major input to uPNs in insect olfactory glomeruli (Hansson and Anton, 2000;Chen and Shepherd, 2005;Kazama and Wilson, 2008;Lei et al., 2010;Tobin et al., 2017;Horne et al., 2018;Rybak and Hansson, 2018;Schlegel et al., 2021). Here we showed that this connection is stronger in DA2 and VA1v than in DL5 (**Figure 5 and 6**). A strong OSNs>uPN synaptic connection will drive non-linear signal amplification, which improves signal detection at low odor concentrations (Ng et al., 2002;Bhandawat et al., 2007;Kazama and Wilson, 2008;Masse et al., 2009). Increasing the number of synapses of this type could have the potential to improve this amplification effect, as shown by artificial increase of synaptic sites in the AL (Acebes and Ferrus, 2001) and in lateral horn dendrites (Liu et al., 2022).

Each of the 7 uPNs in DA2 received convergent synaptic input from almost all DA2-OSNs. This is in agreement with reports on the narrowly tuned glomeruli DA1 and VA1v (Agarwal and Isacoff, 2011;Jeanne and Wilson, 2015;Horne et al., 2018) and for broadly tuned glomeruli (Vosshall et al., 2000;Chen and Shepherd, 2005;Kazama and Wilson, 2009;Masse et al., 2009;Tobin et al., 2017). High OSN>uPN convergence is the main driver of highly correlated activity among uPNs in pheromone coding glomeruli in flies as well as moths (Kazama and Wilson, 2009;Rospars et al., 2014). High convergence in the lateral horn improves signal transmission from uPNs to lateral horn neurons without sacrificing speed (Jeanne and Wilson, 2015;Huoviala et al., 2020). In the mushroom body calyces, however, the high degree of convergence is only pursued for DA2 uPNs, which converge onto few Kenyon cells, whereas VA1v uPNs randomly synapse onto many dispersed Kenyon cells (Caron 2013; Zheng 2020; Li 2020), indicating diverse signal integration in the mushroom body.

From our study, we hypothesize that narrowly tuned glomerular circuits have more uPNs, which have strong convergence onto downstream partners, to improve signal transmission accuracy within a single glomerular circuit. Secondly, a stronger OSN-uPN connection might compensate for the lack of OSN signal transmission sites distributed across glomeruli that are activated by odorants activating multiple broadly tuned OSNs.

Reciprocal connections between sister OSNs and sister uPNs are stronger in narrowly tuned glomeruli

The reciprocal OSN-OSN synapse is generally stronger in narrowly tuned glomeruli DA1, DL3 and DL4, compared to broadly tuned glomeruli DL5, DM6, DM3 and DM4 (Suh et al., 2004;Knaden et al., 2012;Dweck et al., 2015;Ebrahim et al., 2015;Grabe et al., 2016;Seki et al., 2017;Tobin et al., 2017;Schlegel et al., 2021). A high degree of axo-axonic synapses between sister OSNs was also found in VA1v (Horne et al., 2018;Schlegel et al., 2021)and DA2 but not in the DL5 (this study). Hence, we suggest that a strong OSN-OSN connection is a characteristic feature of the synaptic circuitry of narrowly tuned olfactory glomeruli. Axo-axonic connections have also

been reported between gustatory and mechanosensory neurons in *Drosophila* larvae (Miroschnikow et al., 2018) and in the olfactory epithelium and the olfactory bulb of vertebrates (Hirata, 1964;Shepherd et al., 2021). In vertebrates axo-axonic synapses between excitatory sensory neurons are involved in correlated transmitter release (Cover and Mathur, 2021), reminiscent of correlated uPN activity due to reciprocal synaptic and electric coupling in the *Drosophila* AL and LH (Kazama and Wilson, 2009;Huoviala et al., 2020). A strong OSN-OSN connection also has the potential to increase the correlation of OSN spiking events and therefore facilitate a robust OSN signal (de la Rocha et al., 2007).

Reciprocal dendro-dendritic synapses between sister uPNs of the DA2 have been reported previously also for glomeruli DM6, DM4, VA7 and VA1v (Kazama and Wilson, 2009;Rybak et al., 2016;Tobin et al., 2017;Horne et al., 2018). These types of synapses enhance uPN signal correlation (Kazama and Wilson, 2009), as reported for mitral and tufted cells of the vertebrate olfactory bulb, the circuit equivalent to PNs of insect ALs (Christie et al., 2005;McTavish et al., 2012;Shepherd et al., 2021). In *Drosophila* multiple uPNs could induce correlated PN depolarization events, which improve the signal-to-noise-ratio of PN signal transmission (Chen and Shepherd, 2005;Kazama and Wilson, 2009;Jeanne and Wilson, 2015).

In summary, our data give evidence that reciprocal OSN-OSN and uPN-uPN connections are a prominent feature of the synaptic circuit of narrowly tuned glomeruli. With stronger OSN>uPN output, we think that reciprocal dendro-dendritic synapses boost signal amplification and neuronal correlation and that this will in turn enhance the signal-to-noise ratio (accuracy) and transmission probability of weak and/or irregular odorant input, increasing processing speed.

Less lateralization in the OSN bilateral connectivity in narrowly tuned glomeruli

In *Drosophila*, most OSN axons project bilaterally and form synapses in their corresponding glomerulus on both the left and right brain hemispheres (Stocker et al., 1990;Vosshall et al., 2000;Couto et al., 2005;Kazama and Wilson, 2009;Silbering et al., 2011;Tobin et al., 2017;Schlegel et al., 2021). This is rarely observed in other insects and absent in vertebrates (Stocker et al., 1983;Masson and Mustaparta, 1990;Galizia et al., 1998;Hansson and Anton, 2000;Anton et al., 2003;Parthasarathy and Bhalla, 2013;Dalal et al., 2020). In the mammalian olfactory system, bilateral comparison of olfactory input only occurs in higher brain centers (Dalal et al., 2020). In flies, bilateral sensory input enables them to discriminate odor sources of different spatial origin through bilateral comparison of olfactory stimulation (Borst and Heisenberg, 1982;Duistermars et al., 2009;Gaudry et al., 2013;Mohamed et al., 2019a;Taisz et al., 2022). Asymmetric OSN connectivity, shown for many olfactory OSNs (Tobin et al., 2017;Schlegel et al., 2021) seems to be the origin of a bilateral contrast in the uPN response (Agarwal and Isacoff, 2011;Gaudry et al., 2013;Tobin et al., 2017;Taisz et al., 2022), and is most likely the key to precise odor source localization (Taisz et al., 2022). Bilateral comparison is also used in the lateral horn (a higher olfactory brain center in

Drosophila) for odorant position coding (Mohamed et al., 2019a). However, not all glomeruli are similar in the magnitude of bilateral asymmetry with respect to their OSN connectivity (Schlegel et al., 2021) or their uPN responses (Agarwal and Isacoff, 2011).

We found, in agreement with observations in other olfactory glomeruli (Tobin et al., 2017;Schlegel et al., 2021), that glomeruli DL5, DA2 and VA1v (data from: (Horne et al., 2018) have ipsilaterally asymmetric OSN synaptic output to excitatory uPNs and sister OSNs and contralaterally an enhanced OSN>MGN output (**Figure 4**). We believe that, in agreement with a recent study, these asymmetric connections determine a strong left-right-contrast in the uPN response, akin to a "winner-takes-all" principle (Taisz et al., 2022).

We also observed that the degree of bilateral OSN asymmetry in DA2 and VA1v was much weaker than in DL5 (**Figure 4**). Weakly lateralized OSN connectivity is perhaps insufficient to induce an adequate bilateral contrast necessary for odor source localization. Recent work supports this idea by showing the importance of the interplay of asymmetric OSN signaling and LN inhibition to enhance the bilateral contrast of uPN activity and to facilitate navigation (Taisz et al., 2022).

Why do these narrowly tuned glomeruli have weaker bilateral contrast than broadly tuned glomeruli? The answer could lie in the ecological significance of the individual odorants. Geosmin, encoded by glomerulus DA2 (Stensmyr et al., 2012), and the pheromone methyl laurate, encoded by glomerulus VA1v (Dweck et al., 2015), act at short distances, mainly when the fly is walking and not flying, influencing either oviposition or aggregation behavior in females. Perhaps, the decision between avoiding and staying when geosmin or methyl laurate are detected does not need a precise odor source location, as is the case for food odorants. Food odor detection, which happens mainly at flying conditions, needs continuous processing of odor position and body alignment to navigate towards the odor source (Thoma et al., 2015;Demir et al., 2020). The bilateral OSN projection onto uPNs in DA2 and VA1v potentially has a distinct function other than odor position coding and could, via the enhancement of the effect of convergence of OSN>uPN signal transmission, enhance odor signal amplification (Bhandawat et al., 2007;Kazama and Wilson, 2009;Masse et al., 2009;Jeanne and Wilson, 2015)

Distinct synaptic integration of local modulatory neurons in narrowly tuned glomeruli

MGNs are composed of multiglomerular projection neurons (mPNs) that project directly to the LH (Jefferis et al., 2007;Strutz et al., 2014;Bates et al., 2020) and inhibitory and excitatory local interneurons (LNs) that interconnect the AL glomeruli (Masse et al., 2009;Okada et al., 2009;Chou et al., 2010;Seki et al., 2010;Liu and Wilson, 2013). Since LNs are the most numerous and broadly arborizing of the multiglomerular cell types in the AL (Chou et al., 2010;Lin et al., 2012), we focus our discussion on these. Multiglomerular LNs are crucial in modulation of the OSN>uPN

signal transmission (Masse et al., 2009;Chou et al., 2010;Seki et al., 2010;Galizia, 2014;Szyszka and Galizia, 2015).

Previous observations have shown that glomeruli DA2 and VA1v have a lower number of innervating LNs (Chou et al., 2010;Grabe et al., 2016) and receive less global interglomerular LN inhibition than broadly tuned glomeruli (Hong and Wilson, 2015). We therefore assumed that DA2 or VA1v would have a lower LN innervation density and less LN synaptic integration in their circuitry. However, we did not observe a general lower synaptic integration in DA2 **(Figure 5**) and found a greater MGN innervation density, and a higher density of input sites than in DL5. VA1v MGNs on the other hand received less synaptic input and provided less output in its glomerular circuit than MGNs in DL5.

Taking a closer look at particular synaptic connection motifs of MGNs we saw that narrowly tuned glomeruli had a weak uPN>MGN feedback (**Figure 6**). uPN feedback onto LNs and their reciprocal connection (LN>uPN) was reported in *Drosophila* and other insects, such as honey bees, cockroaches and moths, but its function is still poorly understood (Boeckh and Tolbert, 1993;Sun et al., 1997;Sachse and Galizia, 2002). In *Apis mellifera* reciprocal dendro-dendritic synapses between excitatory and inhibitory neurons enhance signal contrast and the reliability of true signal representations throughout the AL (Yokoi et al., 1995;Sachse and Galizia, 2002). Here we could not differentiate the LN types involved in the uPN>MGN synaptic motif. However, the prevailing uPN>LN synapses involve mainly widespread pan-glomerular LNs in the adult (Horne et al., 2018) and larval AL (Berck et al., 2016), which are important for combinatorial coding (Galizia, 2014;Sachse and Hansson, 2016). Thus, weaker uPN>MGN feedback in the narrowly tuned DA2 and VA1v circuits might be a compensatory mechanism to lower the computational demand of interglomerular communication for odor identity coding.

We also observed that OSNs in the narrowly tuned DA2 and VA1v received less MGN input than the OSNs of the DL5, suggesting that the OSNs in DA2 and VA1v receive relatively weak presynaptic inhibition. Pan-glomerular GABAergic LNs induce presynaptic inhibition at OSN presynaptic site (Berck et al., 2016;Schlegel et al., 2021). These inhibitory LNs are drivers of balanced glomerular gain control and are a key player for odor identity coding, balancing incoming and alternating odor intensities (Olsen and Wilson, 2008;Root et al., 2008;Silbering et al., 2008;Asahina et al., 2009;Wang, 2012;Galizia, 2014;Hong and Wilson, 2015;Szyszka and Galizia, 2015;Sachse and Hansson, 2016). Our data support these observations and provide an argument for why narrowly tuned OSNs receive much lower inhibition during AL stimulation with odorants activating other OSN populations (Hong and Wilson, 2015). Even though DA2 and VA1v might receive less interglomerular inhibition, their OSN>MGN output is still strong, in agreement with studies showing that throughout the AL, global lateral inhibition, mediated by LNs, scales with general OSN activation (Olsen and Wilson, 2008;Hong and Wilson, 2015).

In summary, narrowly tuned circuits are probably influenced more strongly by intraglomerular than by interglomerular modulation. Narrowly tuned circuits

perhaps have greater computational capacities in intraglomerular modulation of signal transmission, which could be important for example for PN fine-tuning and response adjustment (Ng et al., 2002;Assisi et al., 2012).

Above we discussed putative generic features of narrowly tuned glomerular circuits. Besides these circuit features, we found a strong MGN>MGN connection in the aversive glomerular circuits DA2 and DL5 in contrast to a much weaker MGN>MGN connection in the attractive glomerulus VA1v (Knaden et al., 2012;Stensmyr et al., 2012;Knaden and Hansson, 2014;Dweck et al., 2015;Mohamed et al., 2019b). Why do aversive olfactory circuits have a stronger MGN-MGN connection than attractive circuits? In the larval *Drosophila* AL, reciprocal LN-LN synapses induce disinhibition induced by a strong connection between the pan-glomerular LNs and a bilateral projecting LN, the Keystone LN, which synapses strongly onto pan-glomerular LNs and selectively onto OSNs, which are activated by attractive food odors. This is thought to be a key feature to switch from homogenous to heterogeneous presynaptic inhibition and therefore to a selective gain control enhancing contrast between attractive and aversive odor activation (Berck et al., 2016). Such balanced inhibitory systems could also be present in the adult *Drosophila* AL, reflected in the strong LN-LN connection in DA2 and DL5. Disinhibition of interglomerular presynaptic inhibition in aversive glomeruli circuits might be important for the fly to stay vigilant to aversive odors, while perceiving attractive cues, for example during feeding conditions so that a fast switch in behavior can be initiated.

Autaptic connection within the dendritic tree of a single uPN

We observed autapses along the large dendritic tree of the single DL5-uPN. To our knowledge, this is the first report of bulk dendro-dendritic autapses in the *Drosophila* olfactory system, indicating a cell-type specific occurrence of autapses in the DL5-uPN as reported for certain cell types of the optic lobe (Takemura et al., 2015). Autapses are also reported to be present at different frequencies in different types of neurons in the mammalian brain (Van der Loos and Glaser, 1972;Tamás et al., 1997;Bekkers, 1998;Bacci and Huguenard, 2006;Ikeda and Bekkers, 2006;Bekkers, 2009;Saada et al., 2009). In *Drosophila,* most uPNs are cholinergic (Yasuyama and Salvaterra, 1999;Yasuyama et al., 2003;Kazama and Wilson, 2008;Tanaka et al., 2012;Croset et al., 2018) and DL5-uPN autapses might activate either nicotinic or muscarinic acetylcholine postsynaptic receptors. Muscarinic acetylcholine receptors have an inhibitory effect in the Kenyon cells of the mushroom body (Bielopolski et al., 2019), but mediate excitation in the AL (Rozenfeld et al., 2019).

What is the function of these autaptic feedback loops within a DL5-uPN dendrite? Recent studies in vertebrates show that excitatory autapses enhance neuron bursting and excitability (Guo et al., 2016;Wiles et al., 2017;Yin et al., 2018). Autaptic inhibitory connections have been implicated in circuit synchronization, spike-timing precision, self-stabilization of neuronal circuits and feedback inhibition (Ikeda and

Bekkers;Van der Loos and Glaser, 1972;Tamás et al., 1997;Bekkers, 1998;Bacci and Huguenard, 2006;Saada et al., 2009).

Autapses in the DL5 uPN form mainly long-distance feedback loops, connecting distinct dendritic subtrees and the basal dendrite region (closer to the soma) with distal branches. This spatial segregation is similar to the distribution of non-autaptic pre- and postsynaptic sites in *Drosophila* uPNs, where presynapses are located more frequently at basal dendrites than postsynapses (Rybak et al., 2016) and other insects, such as *Periplaneta americana* and moths (Malun, 1991;Sun et al., 1997;Lei et al., 2010). Dendro-dendritic autaptic feedback loops connecting basal to distal branches and distinct dendritic subtrees of a large dendritic tree might facilitate activity correlation between distant dendritic subunits, as described for non-autaptic, reciprocal uPN-uPN connections (Kazama and Wilson, 2009). This could be important in a large compartmentalized dendrite that receives inhomogeneous excitation by several OSNs at distinct dendritic sites, in order to enhance synchronized depolarization events along the dendrite, supporting signal integration (Graubard et al., 1980;Tran-Van-Minh et al., 2015). Clustered autapses could mediate local signal input amplification for distinct dendritic subunits (Kumar et al., 2018;Liu et al., 2022). Autaptic contacts, finally, could be able to shift the uPN membrane depolarization towards the spiking threshold, and enhance the firing probability during activation.

In conclusion, we provide a comprehensive comparative analysis of the ultrastructure and synaptic circuitry of two functionally diverse olfactory glomeruli with distinct computational demands, processing either single odorant information in a dedicated olfactory pathway (DA2) or input regarding several odorants and taking part in combinatory coding across distributed glomeruli (DL5). Our work provides an opportunity to gain insight into variations in network architecture and provides fundamental knowledge for future understanding of glomerular processing. By comparing our data with those from another narrowly tuned glomerulus (VA1v), we distilled prominent circuit features that suggest that narrowly tuned glomerular circuits encode odor signals with a weaker left-right-contrast, improved accuracy, stronger signal amplification and stronger intraglomerular signal modulation relative to broadly tuned glomeruli. Our findings reveal the existence of autapses in olfactory glomeruli and indicate that dendro-dendritic autapses play an important role in dendritic signal integration.

Acknowledgments

The authors are most grateful to Michael Steinert and Thomas Pertsch for their support and advice of the FIB-SEM imaging, Katrin Buder for the support with electron microscopy, and Veit Grabe for advice on two-photon imaging. Great thanks also to Albert Cardona for discussion on synaptic networks, him, and Tom Kazimiers (Kazmos GmbH) for the instruction of CATMAID. The neuronal reconstructions were conducted with the outstanding support of Damilola E. Akinyemi, Eckard E. Schumann, and Michael Adewoye. We thank Martin Nawrot

839 and Magdalena Springer for constructive comments and discussions about autapses.
840 The work was supported by Roland Kilper and Ute Müller, (aura optics, Jena),
841 the European Regional Development Fund, by funds from the DFG (grant no.
842 430592330), in the Priority Program 'Evolutionary Optimisation of Neuronal
843 Processing' (DFG-SPP 2205) and by the Max Planck Society.

MATERIAL AND METHODS

Fly line and fly rearing

Flies of the genotype *Orco-GAL4; UAS-GCaMP6s* were obtained from the Bloomington *Drosophila* Stock Center (https://bdsc.indiana.edu) and reared on standard *Drosophila* food at 25°C and 70% humidity on a 12 h:12 h day:night cycle. Seven-days old female flies were used. In these flies, Orco-positive olfactory sensory cells emit green fluorescence, making possible to identify individual glomeruli.

Brain dissection and fixation for Focus Ion Beam microscopy

Two 7-day old female flies were anesthetized with nitric oxide (with Sleeper TAS; INJECT+MATIC, Switzerland) and decapitated with forceps. Heads were dipped for one minute in 0.05% Triton X-100 in 0.1M Sorensen's phosphate buffer, pH 7.3 and transferred to a droplet of freshly prepared ice-cooled fixative (2.5% glutaraldehyde and 2.0% paraformaldehyde in 0.1M Sørensen's phosphate buffer, pH 7.3; as in (Karnovsky, 1965). The proboscis was removed and the back of the head was opened to improve fixative penetration. After 5-10 minutes, the brain was dissected out of the head capsule and post-fixed for two hours on ice. Fixation was stopped by rinsing the brain several times in ice-cooled 0.1M Sørensen's phosphate buffer, pH 7.3 (after (Rybak et al., 2016)).

Laser branding of glomeruli for identification during FIB microscopy

To identify the glomeruli of interest at the ultrastructural level and to limit to a minimum the volume of tissue to be scanned with FIB, near-infrared laser branding (NIRB, (Bishop et al., 2011)). Glomeruli of interest were first located with light microscopy in brains of *Orco-GAL4; UAS-GCaMP6s* flies using a confocal microscope (ZEISS LSM 710 NLO, Carl Zeiss, Germany), a 40x water immersion objective (W Plan-Apochromat 40x/1.0 DIC VIS-IR, Carl Zeiss, Jena, Germany), a laser wavelength of 925 nm at 30% laser power and ZEN software (Carl Zeiss, Germany). Once glomeruli DA2 or DL5 were identified by means of location, shape and size the volume of interest (VOI) was tagged with fiducial marks ("laser-branded") close to the borders of the glomerulus (**Figure 1A-B**), using an infrared Chameleon Ultra diode-pumped laser (Coherent, Santa Clara, USA) at wavelength 800 nm and at 75-90% of laser power).Two laser scan rounds were performed for each induced fiducial brand. DA2 (right AL) and DL5 (left AL) were laser-branded in the same fly. A second glomerulus DA2 was marked in the right AL of another fly.

Transmission Electron Microscopy

Brains were rinsed with 2.5% sodium-cacodylate buffer and incubated in 1% uranyl acetate in 50% acetone for 30 minutes in the dark for *en bloc* staining. They were then dehydrated with a graded ascending acetone series (30%-100%) and gradually infiltrated with Araldites (glycerol-based aromatic epoxy resins; Serva, Germany). In the final step, the tissue was embedded in pure resin and left in a 60°C incubator to

polymerize for 48h. Resin blocks were trimmed with a Reichert UltraTrim microtome (Leica, USA) and the fiducial laser marks were then located in semi-thin sections. To check tissue quality before performing high-resolution volume based electron microscopy, serial sections 50 nm in thickness were cut with a diamond knife (Ultra 45°, Diatome, Switzerland) on a Reichert Ultracut S ultramicrotome (Leica, Germany), collected on single slot grids (2 x 1 mm), and imaged with a JEM 1400 electron microscope (Jeol, Germany) operated at 80 kV. Digital micrographs were obtained with a Gatan Orius SC 1000 CCD camera (Gatan Orius SC 1000; Gatan, USA) controlled with the Gatan Microscopy Suite software Vers. 2.31.734.0.

Focused Ion Beam-Scanning Electron Microscopy (FIB-SEM)

Before serial Focused Ion Beam Scanning Electron Microscopy imaging (FIB-SEM; (Knott et al., 2008;Xu et al., 2017), the surface of the trimmed block was coated with a conductive layer of carbon to prevent charging artifacts. The VOIs were imaged using a FEI Helios NanoLab G3 UC equipment (FEI, USA). The laser marks used to landmark the VOI were visible across the surface of the block. The VOI surface was protected via a local electron beam and subsequently, an ion beam deposition of platinum was applied using a gas injection system to remove surrounding material and to reduce re-deposition. Serial images across the entire VOI were generated by repeated cycles of milling and imaging, orthogonal to the block surface. The tissue was milled with a focused beam of gallium ions using FEI's Tomahawk ion column (accelerating voltage: 30 kV, beam current: 790 pA, milling steps: 20 nm). After each milling cycle, the back-scattering electrons were detected with an in-column detector (FEI's Elstar electron column operating at 3kV accelerating voltage; 1.6 nA beam current; 10 µs dwell time) used to create an image of the newly exposed surface during each scan cycle. The DA2 and DL5 volumes (DA2: 769 slices; DL5: 976 slices) in the first fly were imaged with a pixel resolution of 4.9 x 4.9 x 20 nm/pix (pixel field: 4096 x 3536 (DA2) and 5218 x 3303 (DL5). The dataset of the DA2 volume (571 slices) in a second fly was imaged with a pixel resolution of 4.4 x 4.4 x 20 nm/pix (pixel field: 4096 x 3536). The milling/imaging cycles were controlled with the FEI Auto Slice and View operating 4.0 software (FEI).

Image alignment, 3D reconstruction and segmentation

FIB-SEM image stacks were aligned by maximizing the Pearson correlation coefficient of the central part of two consecutive images using template matching from the openCV library (https://opencv.org). Dense reconstruction of the glomeruli were produced by manually tracing all neuronal fibers and by annotating all synapses within the two glomeruli, using a skeleton-based reconstruction procedure similar to previous approaches (Berck et al., 2016;Schneider-Mizell et al., 2016;Zheng et al., 2017). Up to five independent tracers and two reviewers participated in an iterative reconstruction process using the web-based reconstruction software CATMAID (http://www.catmaid.org; RRID:SCR_006278; (Saalfeld et al., 2009;Schneider-Mizell et al., 2016); **Figure 1D, Figure 1 -- video 1**), performing a dense reconstruction of a

synaptic neuropil. In a another fly, neurons of a DA2 glomerulus were manually reconstructed with the volume-based reconstruction method TrakEM2 (Cardona et al., 2012), an ImageJ (Fiji) plugin (https://imagej.net/TrakEM2).

Glomerular border definition

The definition of the boundary between olfactory glomeruli was based on the combination of several structural features: the spatial position of pre- and postsynaptic elements along OSN axons, the position of the majority of uPN postsynaptic sites, the faint glial leaflets scattered at the periphery of the glomerulus, and the fiducial laser marks (**Figure 1B, D**).

Neuron identification

Neuronal fibers were assigned to one of three pre-defined neuron classes: OSNs, uPNs, and MGNs. The classification was based on their 3D shape (**Figure 2A**), their branching intensity (**Figure 2B**), the average diameter of their fibers (neuronal profiles: **Figure 2A** - FIB-SEM image; exemplary volume based reconstruction), the ratio of T-bars-to-input sites and the size of their T-bars, which were either "small" (few postsynaptic connections) or "large" (many postsynaptic connections **Figure 2 – supplement 1B-D)**. In addition, several intracellular features helped to classify neuron classes: the shape and appearance of mitochondria, the size and electron density of vesicles and the amount of spinules (small filopodia-like invaginations of neighboring cells (**Figure 2A** - FIB-SEM image; (Gruber et al., 2018). OSNs and uPNs could be counted, due to their uniglomerular character, by means of the identification of the axons (OSNs) or main dendrites (uPNs) entering the glomerulus. The number of MGNs could not be counted because of their pan-glomerular projection patterns in the AL. Ipsi- and contralateral OSNs in DA2 and DL5 were identified based on the trajectory of axonal fibers and their entry location in each glomerulus, (example neurons: **Figure 4B).** Ipsilateral OSNs reach the glomerulus from the ipsilateral antennal nerve and leave the glomerulus towards the antennal lobe commissure (ALC: (Tanaka et al., 2012)). Contralateral OSNs reach the glomerulus projecting from the ALC.

Data analysis

With the aid of the web-based software CATMAID (http://www.catmaid.org), we traced neurons in each VOI and the following properties were quantified: the glomerular volume, neuronal fiber length (in µm), number of fiber branching points, number of synaptic input and output sites and T-bars (see data availability). In a second fly, the volume of neurons in DA2 was measured with the aid of TrakEM2 (Cardona et al., 2012), an ImageJ (Fiji) plugin (https://imagej.net/TrakEM2). The following calculations were performed:

1. $Innervation\ density = \frac{total\ neuron\ length\ (\mu m)}{glomerular\ volume\ (\mu m^3)}$,

   a. calculated as a ratio: (1)the sum of all neuronal fibers of each neuron class or (2) all together (**Table 1**) or (3) for each neuron individually (**Figure 3**)

2. $Glomerular\ synaptic\ density = \frac{\#\ of\ synaptic\ inputs,-\ outputs\ or\ T-bars}{glomerular\ volume\ (\mu m^3)}$,
   a. calculated as a ratio: (1) the sum of all neuronal fibers of each neuron class or (2) all together (**Table 1**) or (3) for each neuron individually (**Figure 3**)
3. $Neuronal\ synaptic\ density = \frac{\#\ of\ synaptic\ inputs-,outputs\ or\ T-bars}{neuronal\ fiber\ length\ (\mu m)}$ (**Table 1; Figure 3 – figure supplement 1**)
4. $Synaptic\ ratios = \frac{\#\ of\ T-bars\ or\ outputs}{inputs}$ (represents the average for each neuron class; **Table 1**)
5. $Polyadicity = \frac{\#\ of\ outputs}{T-bars}$ (represents the average number of postsynaptic sites at a T-bar of each neuron class; **Table 1 and Figure 1E**)
6. Relative differences $= \frac{respective\ value\ target\ glomerulus-value\ \ source\ \ glomerulus}{source\ glomerulus} \times 100$ (**Table S1; Table S2**)
7. Relative synaptic strength $= \frac{\#\ of\ synaptic\ contacts\ from\ neuron\ class\ A\ to\ B}{\#\ all\ synaptic\ contacts\ in\ corresponding\ glomerulus}$ (**Table S1; Table S2**)
8. Fraction of output $= \frac{\#\ of\ outputs\ of\ neuron\ class\ A\ directed\ to\ neuron\ class\ B}{total\ \#\ of outputs\ of\ neuron\ class\ A} \times 100$
9. Fraction of input $= \frac{\#\ of\ \ inputs\ from\ neuron\ class\ A\ from\ class\ B}{total\ \#\ of\ inputs\ of\ neuron\ class\ A} \times 100$

Graphs were made with the programming language R and RStudio (R Core Team, 2018) using the packages 'ggplot2' and 'reshape' (see data availability) or with Python (see data availability). All figures were compiled with Adobe Illustrator CS5 software (Adobe Inc.).

Statistical analysis was performed with R Studio (R Studio Team, 2016) using the packages 'ggsignif'. Differences between samples DA2 and DL5 or between ipsilateral and contralateral OSNs were tested for significance with a two-sided student's t-test if sample size was normally distributed, or with Wilcoxon two sample test if the data was not normally distributed (noted in figure legend). Data is in all cases represented as mean + standard deviation.

Analysis of autapses

The location of autapses, the measurement of their geodesic (distance along the neuronal dendrite) and the number of branching points from point A (presynaptic site) to B (postsynaptic profile) was analyzed with Python using the package 'neuroboom' https://github.com/markuspleijzier/neuroboom (see also data availability).

Data availability

1008 Datasets will be available through the public CATMAID instance:
1009 https://catmaid.ice.mpg.de/catmaid_2020.02.15/#. Neurons are named according to
1010 their neuron classification. All data and source code packages used in this study are
1011 hosted on GitHub: https://github.com/. The neuroboom Python package was used for
1012 dendrogram analysis, available at https://github.com/markuspleijzier/neuroboom
1013 and https://pypi.org/project/neuroboom/.

REFERENCES

Acebes, A., and Ferrus, A. (2001). Increasing the Number of Synapses Modifies Olfactory Perception in Drosophila. *Journal of Neuroscience* 21, 6264–6273.

Agarwal, G., and Isacoff, E. (2011). Specializations of a pheromonal glomerulus in the Drosophila olfactory system. *Journal of Neurophysiology* 105, 1711-1721.

Ai, H., and Hagio, H. (2013). Morphological analysis of the primary center receiving spatial information transferred by the waggle dance of honeybees. *Journal of Comparative Neurology* 521, 2570-2584.

Andersson, M.N., Löfstedt, C., and Newcomb, R.D. (2015). Insect olfaction and the evolution of receptor tuning. *Frontiers in Ecology and Evolution* 3.

Anton, S., Van Loon, J.J., Meijerink, J., Smid, H.M., Takken, W., and Rospars, J.P. (2003). Central projections of olfactory receptor neurons from single antennal and palpal sensilla in mosquitoes. *Arthropod Struct Dev* 32, 319-327.

Asahina, K., Louis, M., Piccinotti, S., and Vosshall, L.B. (2009). A circuit supporting concentration-invariant odor perception in Drosophila. *J Biol* 8, 9.

Assisi, C., Stopfer, M., and Bazhenov, M. (2012). Excitatory Local Interneurons Enhance Tuning of Sensory Information. *PLOS Computational Biology* 8, e1002563.

Auer, T.O., Khallaf, M.A., Silbering, A.F., Zappia, G., Ellis, K., Álvarez-Ocaña, R., Arguello, J.R., Hansson, B.S., Jefferis, G.S.X.E., Caron, S.J.C., Knaden, M., and Benton, R. (2020). Olfactory receptor and circuit evolution promote host specialization. *Nature*.

Bacci, A., and Huguenard, J.R. (2006). Enhancement of spike-timing precision by autaptic transmission in neocortical inhibitory interneurons. *Neuron* 49, 119-130.

Bates, A.S., Schlegel, P., Roberts, R.J.V., Drummond, N., Tamimi, I.F.M., Turnbull, R., Zhao, X., Marin, E.C., Popovici, P.D., Dhawan, S., Jamasb, A., Javier, A., Serratosa Capdevila, L., Li, F., Rubin, G.M., Waddell, S., Bock, D.D., Costa, M., and Jefferis, G. (2020). Complete Connectomic Reconstruction of Olfactory Projection Neurons in the Fly Brain. *Curr Biol* 30, 3183-3199 e3186.

Bekkers, J.M. (1998). Neurophysiology: are autapses prodigal synapses? *Curr Biol* 8, R52-55.

Bekkers, J.M. (2009). Synaptic Transmission: Excitatory Autapses Find a Function? *Current Biology* 19, R296-R298.

Benton, R., Sachse, S., Michnick, S.W., and Vosshall, L.B. (2006). Atypical Membrane Topology and Heteromeric Function of *Drosophila* Odorant Receptors In Vivo. *PLoS Biol* 4, 240-257.

Berck, M.E., Khandelwal, A., Claus, L., Hernandez-Nunez, L., Si, G., Tabone, C.J., Li, F., Truman, J.W., Fetter, R.D., Louis, M., Samuel, A.D.T., and Cardona, A. (2016). The wiring diagram of a glomerular olfactory system. *eLife* 5, e14859.

Bhandawat, V., Olsen, S.R., Gouwens, N.W., Schlief, M.L., and Wilson, R.I. (2007). Sensory processing in the *Drosophila* antennal lobe increases reliability and

1056 separability of ensemble odor representations. *Nature neuroscience* 10, 1474-
1057 1482.
1058 Bielopolski, N., Amin, H., Apostolopoulou, A.A., Rozenfeld, E., Lerner, H.,
1059 Huetteroth, W., Lin, A.C., and Parnas, M. (2019). Inhibitory muscarinic
1060 acetylcholine receptors enhance aversive olfactory learning in adult
1061 Drosophila. *Elife* 8.
1062 Bishop, D., Nikic, I., Brinkoetter, M., Knecht, S., Potz, S., Kerschensteiner, M., and
1063 Misgeld, T. (2011). Near-infrared branding efficiently correlates light and
1064 electron microscopy. *Nat Meth* 8, 568-570.
1065 Boeckh, J., Distler, P., Ernst, K.D., Hösl, M., and Malun, D. (1990). "Olfactory bulb
1066 and antennal lobe," in *NATO ASI Series, Vol. H39: Chemosensory Information
1067 Processing*, ed. D. Schild. (Berlin, Heidelberg: Springer Verl), 201-227.
1068 Boeckh, J., and Tolbert, L.P. (1993). Synaptic organization and development of the
1069 antennal lobe in insects. *Microscopy research and technique* 24, 260-280.
1070 Borst, A., and Heisenberg, M. (1982). Osmotropotaxis inDrosophila melanogaster.
1071 *Journal of comparative physiology* 147, 479-484.
1072 Briggman, K.L., and Denk, W. (2006). Towards neural circuit reconstruction with
1073 volume electron microscopy techniques. *Curr Opin Neurobiol* 16, 562-570.
1074 Butcher, N.J., Friedrich, A.B., Lu, Z., Tanimoto, H., and Meinertzhagen, I.A. (2012).
1075 Different classes of input and output neurons reveal new features in
1076 microglomeruli of the adult *Drosophila* mushroom body calyx. *J Comp Neurol*
1077 520, 2185-2201.
1078 Cardona, A., Saalfeld, S., Schindelin, J., Arganda-Carreras, I., Preibisch, S., Longair,
1079 M., Tomancak, P., Hartenstein, V., and Douglas, R.J. (2012). TrakEM2
1080 Software for Neural Circuit Reconstruction. *PLoS One* 7, e38011.
1081 Cardona, A., Saalfeld, S., Tomancak, P., and Hartenstein, V. (2009). *Drosophila* brain
1082 development: closing the gap between a macroarchitectural and
1083 microarchitectural approach. *Cold Spring Harb Symp Quant Biol* 74, 235-248.
1084 Chen, W.R., and Shepherd, G.M. (2005). The olfactory glomerulus: A cortical module
1085 with specific functions. *Journal of Neurocytology* 34, 353–360.
1086 Chou, Y.H., Spletter, M.L., Yaksi, E., Leong, J.C., Wilson, R.I., and Luo, L. (2010).
1087 Diversity and wiring variability of olfactory local interneurons in the
1088 *Drosophila* antennal lobe. *Nature neuroscience* 13, 439-449.
1089 Christie, J.M., Bark, C., Hormuzdi, S.G., Helbig, I., Monyer, H., and Westbrook, G.L.
1090 (2005). Connexin36 mediates spike synchrony in olfactory bulb glomeruli.
1091 *Neuron* 46, 761-772.
1092 Coates, K.E., Calle-Schuler, S.A., Helmick, L.M., Knotts, V.L., Martik, B.N., Salman,
1093 F., Warner, L.T., Valla, S.V., Bock, D.D., and Dacks, A.M. (2020). The Wiring
1094 Logic of an Identified Serotonergic Neuron That Spans Sensory Networks. *The
1095 Journal of Neuroscience* 40, 6309-6327.
1096 Couto, A., Alenius, M., and Dickson, B.J. (2005). Molecular, anatomical, and
1097 functional organization of the *Drosophila* olfactory system. *Current biology* 15,
1098 1535-1547.

1099 Cover, K.K., and Mathur, B.N. (2021). Axo-axonic synapses: Diversity in neural
1100 circuit function. *J Comp Neurol* 529, 2391-2401.
1101 Croset, V., Treiber, C.D., and Waddell, S. (2018). Cellular diversity in the Drosophila
1102 midbrain revealed by single-cell transcriptomics. *Elife* 7.
1103 Cuntz, H., Borst, A., and Segev, I. (2007). Optimization principles of dendritic
1104 structure. *Theor Biol Med Model* 4, 21.
1105 Dacks, A.M., Christensen, T.A., and Hildebrand, J.G. (2006). Phylogeny of a
1106 serotonin-immunoreactive neuron in the primary olfactory center of the insect
1107 brain. *J Comp Neurol* 498, 727-746.
1108 Dalal, T., Gupta, N., and Haddad, R. (2020). Bilateral and unilateral odor processing
1109 and odor perception. *Commun Biol* 3, 150.
1110 Datta, S.R., Vasconcelos, M.L., Ruta, V., Luo, S., Wong, A., Demir, E., Flores, J.,
1111 Balonze, K., Dickson, B.J., and Axel, R. (2008). The *Drosophila* pheromone cVA
1112 activates a sexually dimorphic neural circuit. *Nature* 452, 473-477.
1113 De Bruyne, M., Clyne, P.J., and Carlson, J.R. (1999). Odor coding in a model olfactory
1114 organ: the *Drosophila* maxillary palp. *Journal of Neuroscience* 19, 4520-4532.
1115 De Bruyne, M., Foster, K., and Carlson, J.R. (2001). Odor Coding in the *Drosophila*
1116 Antenna. *Neuron* 30, 537-552.
1117 De La Rocha, J., Doiron, B., Shea-Brown, E., Josić, K., and Reyes, A. (2007).
1118 Correlation between neural spike trains increases with firing rate. *Nature* 448,
1119 802-806.
1120 Demir, M., Kadakia, N., Anderson, H.D., Clark, D.A., and Emonet, T. (2020).
1121 Walking Drosophila navigate complex plumes using stochastic decisions
1122 biased by the timing of odor encounters. *Elife* 9.
1123 Dolan, M.-J., Frechter, S., Bates, A.S., Dan, C., Huoviala, P., Roberts, R.J.V., Schlegel,
1124 P., Dhawan, S., Tabano, R., Dionne, H., Christoforou, C., Close, K., Sutcliffe,
1125 B., Giuliani, B., Li, F., Costa, M., Ihrke, G., Meissner, G.W., Bock, D.D., Aso, Y.,
1126 Rubin, G.M., and Jefferis, G.S.X.E. (2019). Neurogenetic dissection of the
1127 Drosophila lateral horn reveals major outputs, diverse behavioural functions,
1128 and interactions with the mushroom body. *eLife* 8, e43079.
1129 Dolan, M.J., Belliart-Guérin, G., Bates, A.S., Frechter, S., Lampin-Saint-Amaux, A.,
1130 Aso, Y., Roberts, R.J.V., Schlegel, P., Wong, A., Hammad, A., Bock, D., Rubin,
1131 G.M., Preat, T., Plaçais, P.Y., and Jefferis, G. (2018). Communication from
1132 Learned to Innate Olfactory Processing Centers Is Required for Memory
1133 Retrieval in Drosophila. *Neuron* 100, 651-668.e658.
1134 Duistermars, B.J., Chow, D.M., and Frye, M.A. (2009). Flies require bilateral sensory
1135 input to track odor gradients in flight. *Current Biology* 19, 1301-1307.
1136 Dweck, H.K.M., Ebrahim, S.a.M., Thoma, M., Mohamed, A.a.M., Keesey, I.W., Trona,
1137 F., Lavista-Llanos, S., Svatoš, A., Sachse, S., Knaden, M., and Hansson, B.S.
1138 (2015). Pheromones mediating copulation and attraction in *Drosophila*.
1139 *Proceedings of the National Academy of Sciences* 112, E2829-E2835.
1140 Ebrahim, S.a.M., Dweck, H.K.M., Stökl, J., Hofferberth, J.E., Trona, F., Weniger, K.,
1141 Rybak, J., Seki, Y., Stensmyr, M.C., Sachse, S., Hansson, B.S., and Knaden, M.

(2015). *Drosophila* Avoids Parasitoids by Sensing Their Semiochemicals via a Dedicated Olfactory Circuit. *PLoS Biol* 13, e1002318.

Eckstein, N., Bates, A.S., Du, M., Hartenstein, V., Jefferis, G.S.X.E., and Funke, J. (2020). Neurotransmitter Classification from Electron Microscopy Images at Synaptic Sites in Drosophila. *bioRxiv*, 2020.2006.2012.148775.

Eichler, K., Litwin-Kumar, A., Li, F., Park, Y., Andrade, I., Schneider-Mizell, C.M., Saumweber, T., Huser, A., Eschbach, C., Gerber, B., Fetter, R.D., Truman, J.W., Priebe, C.E., Abbott, L.F., Thum, A.S., Zlatic, M., and Cardona, A. (2017). The Complete Connectome Of A Learning And Memory Center In An Insect Brain. *bioRxiv*.

Felsenberg, J., Jacob, P.F., Walker, T., Barnstedt, O., Edmondson-Stait, A.J., Pleijzier, M.W., Otto, N., Schlegel, P., Sharifi, N., Perisse, E., Smith, C.S., Lauritzen, J.S., Costa, M., Jefferis, G.S.X.E., Bock, D.D., and Waddell, S. (2018). Integration of Parallel Opposing Memories Underlies Memory Extinction. *Cell* 175, 709-722.e715.

Fiala, A. (2007). Olfaction and olfactory learning in Drosophila: recent progress. *Curr Opin Neurobiol* 17, 720-726.

Fishilevich, E., and Vosshall, L.B. (2005). Genetic and functional subdivision of the *Drosophila* antennal lobe. *Current biology* 15, 1548-1553.

Fröhlich, A. (1985). Freeze-Fracture Study of an Invertebrate Multiple-Contact Synapse: The Fly Photoreceptor Tetrad. *Journal of Comparative Neurology* 241, 311-326.

Galizia, C.G. (2014). Olfactory coding in the insect brain: data and conjectures. *European Journal of Neuroscience* 39, n/a-n/a.

Galizia, C.G., Nagler, K., Holldobler, B., and Menzel, R. (1998). Odour coding is bilaterally symmetrical in the antennal lobes of honeybees (Apis mellifera). *European Journal of Neuroscience* 10, 2964-2974.

Gao, Q., Yuan, B., and Chess, A. (2000). Convergent projections of Drosophila olfactory neurons to specific glomeruli in the antennal lobe. *Nature*.

Gao, X.J., Clandinin, T.R., and Luo, L. (2015). Extremely Sparse Olfactory Inputs Are Sufficient to Mediate Innate Aversion in *Drosophila PLoS ONE* 10, e0125986.

Gaudry, Q., Hong, E.J., Kain, J., De Bivort, B.L., and Wilson, R.I. (2013). Asymmetric neurotransmitter release enables rapid odour lateralization in *Drosophila*. *Nature* 493, 424-428.

Gondré-Lewis, M.C., Park, J.J., and Loh, Y.P. (2012). "Chapter Two - Cellular Mechanisms for the Biogenesis and Transport of Synaptic and Dense-Core Vesicles," in *International Review of Cell and Molecular Biology,* ed. K.W. Jeon. Academic Press), 27-115.

Goyal, R.K., and Chaudhury, A. (2013). Structure activity relationship of synaptic and junctional neurotransmission. *Autonomic Neuroscience: Basic and Clinical* 176, 11-31.

1183 Grabe, V., Baschwitz, A., Dweck, Hany k.M., Lavista-Llanos, S., Hansson, Bill s., and
1184 Sachse, S. (2016). Elucidating the Neuronal Architecture of Olfactory
1185 Glomeruli in the *Drosophila* Antennal Lobe. *Cell Reports* 16, 3401-3413.
1186 Grabe, V., and Sachse, S. (2018). Fundamental principles of the olfactory code.
1187 *Biosystems* 164, 94-101.
1188 Grabe, V., Schubert, M., Strube-Bloss, M., Reinert, A., Trautheim, S., Lavista-Llanos,
1189 S., Fiala, A., Hansson, B.S., and Sachse, S. (2020). Odor-Induced Multi-Level
1190 Inhibitory Maps in Drosophila. *eNeuro* 7.
1191 Grabe, V., Strutz, A., Baschwitz, A., Hansson, B.S., and Sachse, S. (2015). Digital in
1192 vivo 3D atlas of the antennal lobe of *Drosophila melanogaster*. *Journal of*
1193 *Comparative Neurology* 523, 530-544.
1194 Graubard, K., Raper, J.A., and Hartline, D.K. (1980). Graded synaptic transmission
1195 between spiking neurons. *Proc Natl Acad Sci U S A* 77, 3733-3735.
1196 Gruber, L., Rybak, J., Hansson, B.S., and Cantera, R. (2018). Synaptic Spinules in the
1197 Olfactory Circuit of Drosophila melanogaster. *Front Cell Neurosci* 12, 86.
1198 Guo, D., Wu, S., Chen, M., Perc, M., Zhang, Y., Ma, J., Cui, Y., Xu, P., Xia, Y., and
1199 Yao, D. (2016). Regulation of Irregular Neuronal Firing by Autaptic
1200 Transmission. *Sci Rep* 6, 26096.
1201 Guven-Ozkan, T., and Davis, R.L. (2014). Functional neuroanatomy of *Drosophila*
1202 olfactory memory formation. *Learning & Memory* 21, 519-526.
1203 Hallem, E.A., and Carlson, J.R. (2006). Coding of odors by a receptor repertoire. *Cell*
1204 125, 143-160.
1205 Hallem, E.A., Ho, M.G., and Carlson, J.R. (2004). The molecular basis of odor coding
1206 in the Drosophila antenna. *Cell* 117, 965-979.
1207 Hansson, B.S., and Anton, S. (2000). Function and morphology of the antennal lobe:
1208 new developments. *Annu Rev Entomol* 45, 203-231.
1209 Hartenstein, V. (2016). "The Central Nervous System of Invertebrates," in *The Wiley*
1210 *Handbook of Evolutionary Neuroscience,* ed. S.V. Shepherd.), 173-235.
1211 Haverkamp, A., Hansson, B.S., and Knaden, M. (2018). Combinatorial Codes and
1212 Labeled Lines: How Insects Use Olfactory Cues to Find and Judge Food,
1213 Mates, and Oviposition Sites in Complex Environments. *Front Physiol* 9, 49.
1214 Helmstaedter, M. (2013). Cellular-resolution connectomics: challenges of dense
1215 neural circuit reconstruction. *Nature Methods* 10, 501-507.
1216 Hirata, Y. (1964). Some observations on the fine structure of the synapses in the
1217 olfactory bulb of the mouse, with particular reference to the atypical synaptic
1218 configurations. *Archivum histologicum japonicum* 24, 293-302.
1219 Hong, E.J., and Wilson, R.I. (2015). Simultaneous encoding of odors by channels with
1220 diverse sensitivity to inhibition. *Neuron* 85, 573-589.
1221 Horne, J.A., Langille, C., Mclin, S., Wiederman, M., Lu, Z., Xu, C.S., Plaza, S.M.,
1222 Scheffer, L.K., Hess, H.F., and Meinertzhagen, I.A. (2018). A resource for the
1223 *Drosophila* antennal lobe provided by the connectome of glomerulus VA1v.
1224 *Elife* 7, e37550.

1225 Huang, G.B., Scheffer, L.K., and Plaza, S.M. (2018). Fully-Automatic Synapse
1226 Prediction and Validation on a Large Data Set. *Frontiers in Neural Circuits* 12.
1227 Hulse, B.K., Haberkern, H., Franconville, R., Turner-Evans, D.B., Takemura, S.-Y.,
1228 Wolff, T., Noorman, M., Dreher, M., Dan, C., Parekh, R., Hermundstad, A.M.,
1229 Rubin, G.M., and Jayaraman, V. (2021). A connectome of the Drosophila
1230 central complex reveals network motifs suitable for flexible navigation and
1231 context-dependent action selection. *eLife* 10, e66039.
1232 Huoviala, P., Dolan, M.-J., Love, F.M., Myers, P., Frechter, S., Namiki, S., Pettersson,
1233 L., Roberts, R.J.V., Turnbull, R., Mitrevica, Z., Breads, P., Schlegel, P., Bates,
1234 A.S., Rodrigues, T., Aso, Y., Bock, D., Rubin, G.M., Stensmyr, M., Card, G.,
1235 Costa, M., and Jefferis, G.S.X.E. (2020). Neural circuit basis of aversive odour
1236 processing in Drosophila from sensory input to descending
1237 output. 394403.
1238 Ikeda, K., and Bekkers, J.M. Autapses. *Current Biology* 16, R308.
1239 Ikeda, K., and Bekkers, J.M. (2006). Autapses. *Curr Biol* 16, R308.
1240 Jeanne, James m., and Wilson, Rachel i. (2015). Convergence, Divergence, and
1241 Reconvergence in a Feedforward Network Improves Neural Speed and
1242 Accuracy. *Neuron* 88, 1014-1026.
1243 Jefferis, G.S., Potter, C.J., Chan, A.M., Marin, E.C., Rohlfing, T., Maurer, C.R., Jr., and
1244 Luo, L. (2007). Comprehensive maps of *Drosophila* higher olfactory centers:
1245 spatially segregated fruit and pheromone representation. *Cell* 128, 1187-1203.
1246 Karnovsky, M.J. (1965). A formaldehyde-glutaraldehyde fixative of high osmolarity
1247 for use in electron microscopy. *Journal of Cellular Biology* 27, 137.
1248 Kazama, H., and Wilson, R.I. (2008). Homeostatic Matching and Nonlinear
1249 Amplification at Identified Central Synapses. *Neuron* 58, 401-413.
1250 Kazama, H., and Wilson, R.I. (2009). Origins of correlated activity in an olfactory
1251 circuit. *Nat Neurosci* 12, 1136-1144.
1252 Keene, A.C., and Waddell, S. (2007). Drosophila olfactory memory: single genes to
1253 complex neural circuits. *Nat Rev Neurosci* 8, 341-354.
1254 Keesey, I.W., and Hansson, B.S. (2021). "10 - The neuroethology of labeled lines in
1255 insect olfactory systems," in *Insect Pheromone Biochemistry and Molecular*
1256 *Biology (Second Edition),* eds. G.J. Blomquist & R.G. Vogt. (London: Academic
1257 Press), 285-327.
1258 Keesey, I.W., Zhang, J., Depetris-Chauvin, A., Obiero, G.F., Knaden, M., and
1259 Hansson, B.S. (2019). Evolution of a pest: towards the complete neuroethology
1260 of Drosophila suzukii and the subgenus Sophophora.
1261 *bioRxiv*, 717322.
1262 Knaden, M., and Hansson, B.S. (2014). Mapping odor valence in the brain of flies and
1263 mice. *Curr Opin Neurobiol* 24, 34-38.
1264 Knaden, M., Strutz, A., Ahsan, J., Sachse, S., and Hansson, B.S. (2012). Spatial
1265 representation of odorant valence in an insect brain. *Cell Reports* 1, 392-399.

1266 Knott, G., Marchman, H., and Lich, B. (2008). Serial Section Scanning Electron
1267 Microscopy of Adult Brain Tissue Using Focused Ion Beam Milling. *Journal of*
1268 *Neuroscience* 28, 2964-2959.
1269 Kreher, S.A., Mathew, D., Kim, J., and Carlson, J.R. (2008). Translation of sensory
1270 input into behavioral output via an olfactory system. *Neuron* 59, 110-124.
1271 Kumar, A., Schiff, O., Barkai, E., Mel, B.W., Poleg-Polsky, A., and Schiller, J. (2018).
1272 NMDA spikes mediate amplification of inputs in the rat piriform cortex. *eLife*
1273 7, e38446.
1274 Kurtovic, A., Widmer, A., and Dickson, B.J. (2007). A single class of olfactory
1275 neurons mediates behavioural responses to a Drosophila sex pheromone.
1276 *Nature* 446, 542-546.
1277 Laissue, P.P., Reiter, C., Hiesinger, P.R., Halter, S., Fischbach, K.F., and Stocker, R.F.
1278 (1999). Three-dimensional reconstruction of the antennal lobe in *Drosophila*
1279 *melanogaster*. *The Journal of Comparative Neurology* 405, 543-552.
1280 Laissue, P.P., and Vosshall, L.B. (2008). "The Olfactory Sensory Map in *Drosophila*," in
1281 *Brain Development in Drosophila melanogaster,* ed. G.M. Technau. (New York:
1282 Springer), 102-114
1283 Lei, H., Oland, L.A., Riffell, J.A., Beyerlein, A., and Hildebrand, J.G. (2010).
1284 "Microcircuits for Olfactory Information Processing in the Antennal Lobe of
1285 *Manduca sexta*," in *Handbook of Brain Microcircuits,* eds. G.M. Shepherd & S.
1286 Grillner. (New York: Oxford University Press), 417-426.
1287 Li, F., Lindsey, J.W., Marin, E.C., Otto, N., Dreher, M., Dempsey, G., Stark, I., Bates,
1288 A.S., Pleijzier, M.W., Schlegel, P., Nern, A., Takemura, S.Y., Eckstein, N.,
1289 Yang, T., Francis, A., Braun, A., Parekh, R., Costa, M., Scheffer, L.K., Aso, Y.,
1290 Jefferis, G.S., Abbott, L.F., Litwin-Kumar, A., Waddell, S., and Rubin, G.M.
1291 (2020a). The connectome of the adult Drosophila mushroom body provides
1292 insights into function. *Elife* 9.
1293 Li, H., Horns, F., Wu, B., Xie, Q., Li, J., Li, T., Luginbuhl, D.J., Quake, S.R., and Luo,
1294 L. (2017). Classifying Drosophila Olfactory Projection Neuron Subtypes by
1295 Single-Cell RNA Sequencing. *Cell* 171, 1206-1220.e1222.
1296 Li, P.H., Lindsey, L.F., Januszewski, M., Zheng, Z., Bates, A.S., Taisz, I., Tyka, M.,
1297 Nichols, M., Li, F., Perlman, E., Maitin-Shepard, J., Blakely, T., Leavitt, L.,
1298 Jefferis, G.S.X.E., Bock, D., and Jain, V. (2020b). Automated Reconstruction of
1299 a Serial-Section EM *Drosophila* Brain with Flood-Filling Networks and Local
1300 Realignment. *bioRxiv*, 605634.
1301 Liang, L., and Luo, L. (2010). The olfactory circuit of the fruit fly *Drosophila*
1302 *melanogaster*. *Sci China Life Sci* 53, 472-484.
1303 Lin, S., Kao, C.-F., Yu, H.-H., Huang, Y., and Lee, T. (2012). Lineage analysis of
1304 Drosophila lateral antennal lobe neurons reveals notch-dependent binary
1305 temporal fate decisions. *PLoS biology* 10, e1001425-e1001425.
1306 Liu, T.X., Davoudian, P.A., Lizbinski, K.M., and Jeanne, J.M. (2022). Connectomic
1307 features underlying diverse synaptic connection strengths and subcellular
1308 computation. *Current Biology* 32, 559-569.e555.

1309 Liu, W.W., and Wilson, R.I. (2013). Glutamate is an inhibitory neurotransmitter in
1310 the *Drosophila* olfactory system. *Proceedings of the National Academy of Sciences*
1311 110, 10294–10299.
1312 Malun, D. (1991). Inventory and distribution of synapses of identified uniglomerular
1313 projection neurons in the antennal lobe of Periplaneta americana. *Journal of*
1314 *comparative neurology* 305, 348-360.
1315 Malun, D., Waldow, U., Kraus, D., and Boeckh, J. (1993). Connections between the
1316 Deutocerebrum and the Protocerebrum, and Neuroanatomy of Several
1317 Classes of Deutocerebral Projection Neurons in the Brain of Male Periplaneta-
1318 Americana. *Journal of Comparative Neurology* 329, 143-162.
1319 Marin, E.C., Büld, L., Theiss, M., Sarkissian, T., Roberts, R.J.V., Turnbull, R., Tamimi,
1320 I.F.M., Pleijzier, M.W., Laursen, W.J., Drummond, N., Schlegel, P., Bates, A.S.,
1321 Li, F., Landgraf, M., Costa, M., Bock, D.D., Garrity, P.A., and Jefferis, G.
1322 (2020). Connectomics Analysis Reveals First-, Second-, and Third-Order
1323 Thermosensory and Hygrosensory Neurons in the Adult Drosophila Brain.
1324 *Curr Biol* 30, 3167-3182.e3164.
1325 Masse, N.Y., Turner, G.C., and Jefferis, G.S. (2009). Olfactory information processing
1326 in Drosophila. *Curr Biol* 19, R700-713.
1327 Masson, C., and Mustaparta, H. (1990). Chemical information processing in the
1328 olfactory system of insects. *Physiological Review* 70(1), 199-245.
1329 Mctavish, T., Migliore, M., Shepherd, G., and Hines, M. (2012). Mitral cell spike
1330 synchrony modulated by dendrodendritic synapse location. *Frontiers in*
1331 *Computational Neuroscience* 6.
1332 Meinertzhagen, I.A. (2018). Of what use is connectomics? A personal perspective on
1333 the *Drosophila* connectome. *Journal of Experimental Biology* 221, jeb164954.
1334 Meinertzhagen, I.A., and O'neil, S.D. (1991). Synaptic organization of columnar
1335 elements in the lamina of the wild type in Drosophila melanogaster. *Journal of*
1336 *Comparative Neurology* 305, 232-263.
1337 Miroschnikow, A., Schlegel, P., Schoofs, A., Hueckesfeld, S., Li, F., Schneider-Mizell,
1338 C.M., Fetter, R.D., Truman, J.W., Cardona, A., and Pankratz, M.J. (2018).
1339 Convergence of monosynaptic and polysynaptic sensory paths onto common
1340 motor outputs in a Drosophila feeding connectome. *eLife* 7, e40247.
1341 Mohamed, A.a.M., Hansson, B.S., and Sachse, S. (2019a). Third-Order Neurons in the
1342 Lateral Horn Enhance Bilateral Contrast of Odor Inputs Through
1343 Contralateral Inhibition in Drosophila. *Front Physiol* 10, 851.
1344 Mohamed, A.a.M., Retzke, T., Das Chakraborty, S., Fabian, B., Hansson, B.S.,
1345 Knaden, M., and Sachse, S. (2019b). Odor mixtures of opposing valence unveil
1346 inter-glomerular crosstalk in the Drosophila antennal lobe. *Nat Commun* 10,
1347 1201.
1348 Mosca, T.J., and Luo, L. (2014). Synaptic organization of the *Drosophila* antennal lobe
1349 and its regulation by the Teneurins. *elife* 3, e03726.
1350 Münch, D., and Galizia, C.G. (2016). DoOR 2.0 - Comprehensive Mapping of
1351 Drosophila melanogaster Odorant Responses. *Scientific Reports* 6, 21841.

1352 Nässel, D.R., Enell, L.E., Santos, J.G., Wegener, C., and Johard, H.A. (2008). A large
1353 population of diverse neurons in the Drosophila central nervous system
1354 expresses short neuropeptide F, suggesting multiple distributed peptide
1355 functions. *BMC Neurosci* 9, 90.
1356 Nässel, D.R., and Homberg, U. (2006). Neuropeptides in interneurons of the insect
1357 brain. *Cell Tissue Res* 326, 1-24.
1358 Ng, M., Roorda, R.D., Lima, S.Q., Zemelman, B.V., Morcillo, P., and Miesenböck, G.
1359 (2002). Transmission of Olfactory Information between Three Populations of
1360 Neurons in the Antennal Lobe of the Fly. *Neuron* 36, 463-474.
1361 Norgate, M., Lee, E., Southon, A., Farlow, A., Batterham, P., Camakaris, J., and
1362 Burke, R. (2006). Essential Roles in Development and Pigmentation for the
1363 *Drosophila* Copper Transporter DmATP7. *Molecular Biology of the Cell* 17, 475-
1364 484.
1365 Okada, R., Awasaki, T., and Ito, K. (2009). Gamma-aminobutyric acid (GABA)-
1366 mediated neural connections in the *Drosophila* antennal lobe. *Journal of*
1367 *Comparative Neurology* 514, 74-91.
1368 Olsen, S.R., and Wilson, R.I. (2008). Lateral presynaptic inhibition mediates gain
1369 control in an olfactory circuit. *Nature* 452, 956-960.
1370 Otto, N., Pleijzier, M.W., Morgan, I.C., Edmondson-Stait, A.J., Heinz, K.J., Stark, I.,
1371 Dempsey, G., Ito, M., Kapoor, I., Hsu, J., Schlegel, P.M., Bates, A.S., Feng, L.,
1372 Costa, M., Ito, K., Bock, D.D., Rubin, G.M., Jefferis, G.S.X.E., and Waddell, S.
1373 (2020). Input Connectivity Reveals Additional Heterogeneity of Dopaminergic
1374 Reinforcement in Drosophila. *Current Biology* 30, 3200-3211.e3208.
1375 Owald, D., and Waddell, S. (2015). Olfactory learning skews mushroom body output
1376 pathways to steer behavioral choice in Drosophila. *Current Opinion in*
1377 *Neurobiology* 35, 178-184.
1378 Parthasarathy, K., and Bhalla, U.S. (2013). Laterality and symmetry in rat olfactory
1379 behavior and in physiology of olfactory input. *J Neurosci* 33, 5750-5760.
1380 Prokop, A., and Meinertzhagen, I.A. (2006). Development and structure of synaptic
1381 contacts in Drosophila. *Semin Cell Dev Biol* 17, 20-30.
1382 Ronchi, P., Mizzon, G., Machado, P., D'imprima, E., Best, B.T., Cassella, L.,
1383 Schnorrenberg, S., Montero, M.G., Jechlinger, M., Ephrussi, A., Leptin, M.,
1384 Mahamid, J., and Schwab, Y. (2021). High-precision targeting workflow for
1385 volume electron microscopy. *J Cell Biol* 220.
1386 Root, C.M., Masuyama, K., Green, D.S., Enell, L.E., Nassel, D.R., Lee, C.H., and
1387 Wang, J.W. (2008). A presynaptic gain control mechanism fine-tunes olfactory
1388 behavior. *Neuron* 59, 311-321.
1389 Rospars, J.-P., Grémiaux, A., Jarriault, D., Chaffiol, A., Monsempes, C., Deisig, N.,
1390 Anton, S., Lucas, P., and Martinez, D. (2014). Heterogeneity and Convergence
1391 of Olfactory First-Order Neurons Account for the High Speed and Sensitivity
1392 of Second-Order Neurons. *PLOS Computational Biology* 10, e1003975.

1393 Rozenfeld, E., Lerner, H., and Parnas, M. (2019). Muscarinic Modulation of Antennal
1394 Lobe GABAergic Local Neurons Shapes Odor Coding and Behavior. *Cell Rep*
1395 29, 3253-3265.e3254.
1396 Rybak, J. (2013). "Exploring Brain Connectivity in Insect Model Systems of Learning
1397 and Memory," in *Invertebrate Learning and Memory,* eds. R. Menzel & P.
1398 Benjamin. (San Diego: Academic Press), 26-40.
1399 Rybak, J. (2016). "Perspective-Brain atlases for studying neuronal circuitry in
1400 arthropods," in *Structure and Evolution of Invertebrate Nervous Systems,* eds. A.
1401 Schmidt-Rhaesa, S. Harzsch & G. Purschke. (New York: Oxford University
1402 Press).
1403 Rybak, J., and Hansson, B.S. (2018). "Olfactory Microcircuits in *Drosophila*
1404 *Melanogaster*," in *Handbook of Brain Microcircuits,* eds. G.M. Shepherd & S.
1405 Grillner. 2nd ed (Oxford, UK: Oxford University Press), 361-367.
1406 Rybak, J., Talarico, G., Ruiz, S., Arnold, C., Cantera, R., and Hansson, B.S. (2016).
1407 Synaptic circuitry of identified neurons in the antennal lobe of *Drosophila*
1408 *melanogaster*. *J Comp Neurol* 524, 1920-1956.
1409 Saada, R., Miller, N., Hurwitz, I., and Susswein, A.J. (2009). Autaptic excitation elicits
1410 persistent activity and a plateau potential in a neuron of known behavioral
1411 function. *Curr Biol* 19, 479-484.
1412 Saalfeld, S., Cardona, A., Hartenstein, V., and Tomančák, P. (2009). CATMAID:
1413 collaborative annotation toolkit for massive amounts of image data.
1414 *Bioinformatics* 25, 1984-1986.
1415 Sachse, S., and Galizia, C.G. (2002). Role of inhibition for temporal and spatial odor
1416 representation in olfactory output neurons: a calcium imaging study. *Journal*
1417 *of neurophysiology* 87, 1106-1117.
1418 Sachse, S., and Hansson, B.S. (2016). "Research spotlight: Olfactory coding in
1419 *Drosophila melanogaster*," in *Structure and Evolution of Invertebrate Nervous*
1420 *Systems,* eds. A. Schmidt-Rhaesa, S. Harzsch & G. Purschke. (Oxford: Oxford
1421 University Press), 640-645.
1422 Sachse, S., and Manzini, I. (2021). Editorial for the special issue "Olfactory Coding
1423 and Circuitries". *Cell Tissue Res* 383, 1-6.
1424 Scheffer, L.K., Xu, C.S., Januszewski, M., Lu, Z., Takemura, S.-Y., Hayworth, K.J.,
1425 Huang, G.B., Shinomiya, K., Maitlin-Shepard, J., Berg, S., Clements, J.,
1426 Hubbard, P.M., Katz, W.T., Umayam, L., Zhao, T., Ackerman, D., Blakely, T.,
1427 Bogovic, J., Dolafi, T., Kainmueller, D., Kawase, T., Khairy, K.A., Leavitt, L.,
1428 Li, P.H., Lindsey, L., Neubarth, N., Olbris, D.J., Otsuna, H., Trautman, E.T.,
1429 Ito, M., Bates, A.S., Goldammer, J., Wolff, T., Svirskas, R., Schlegel, P., Neace,
1430 E., Knecht, C.J., Alvarado, C.X., Bailey, D.A., Ballinger, S., Borycz, J.A.,
1431 Canino, B.S., Cheatham, N., Cook, M., Dreher, M., Duclos, O., Eubanks, B.,
1432 Fairbanks, K., Finley, S., Forknall, N., Francis, A., Hopkins, G.P., Joyce, E.M.,
1433 Kim, S., Kirk, N.A., Kovalyak, J., Lauchie, S.A., Lohff, A., Maldonado, C.,
1434 Manley, E.A., Mclin, S., Mooney, C., Ndama, M., Ogundeyi, O., Okeoma, N.,
1435 Ordish, C., Padilla, N., Patrick, C.M., Paterson, T., Phillips, E.E., Phillips, E.M.,

1436 Rampally, N., Ribeiro, C., Robertson, M.K., Rymer, J.T., Ryan, S.M., Sammons,
1437 M., Scott, A.K., Scott, A.L., Shinomiya, A., Smith, C., Smith, K., Smith, N.L.,
1438 Sobeski, M.A., Suleiman, A., Swift, J., Takemura, S., Talebi, I., Tarnogorska,
1439 D., Tenshaw, E., Tokhi, T., Walsh, J.J., Yang, T., Horne, J.A., Li, F., Parekh, R.,
1440 Rivlin, P.K., Jayaraman, V., Costa, M., Jefferis, G.S.X.E., et al. (2020). A
1441 connectome and analysis of the adult Drosophila central brain. *eLife* 9, e57443.
1442 Schlegel, P., Bates, A.S., Stürner, T., Jagannathan, S.R., Drummond, N., Hsu, J.,
1443 Serratosa Capdevila, L., Javier, A., Marin, E.C., Barth-Maron, A., Tamimi,
1444 I.F.M., Li, F., Rubin, G.M., Plaza, S.M., Costa, M., and Jefferis, G.S.X.E. (2021).
1445 Information flow, cell types and stereotypy in a full olfactory connectome.
1446 *eLife* 10, e66018.
1447 Schneider-Mizell, C.M., Gerhard, S., Longair, M., Kazimiers, T., Li, F., Zwart, M.F.,
1448 Champion, A., Midgley, F.M., Fetter, R.D., Saalfeld, S., and Cardona, A.
1449 (2016). Quantitative neuroanatomy for connectomics in *Drosophila*. *eLife* 5,
1450 e12059.
1451 Seki, Y., Dweck, H.K.M., Rybak, J., Wicher, D., Sachse, S., and Hansson, B.S. (2017).
1452 Olfactory coding from the periphery to higher brain centers in the Drosophila
1453 brain. *BMC Biol* 15, 56.
1454 Seki, Y., Rybak, J., Wicher, D., Sachse, S., and Hansson, B.S. (2010). Physiological and
1455 morphological characterization of local interneurons in the *Drosophila*
1456 antennal lobe. *Journal of Neurophysiology* 104, 1007-1019.
1457 Semmelhack, J.L., and Wang, J.W. (2009). Select Drosophila glomeruli mediate innate
1458 olfactory attraction and aversion. *Nature* 459, 218-223.
1459 Shanbhag, S.R., Muller, B., and Steinbrecht, R.A. (1999). Atlas of olfactory organs of
1460 *Drosophila melanogaster* - 1. Types, external organization, innervation and
1461 distribution of olfactory sensilla. *International Journal of Insect Morphology &*
1462 *Embryology* 28, 377-397.
1463 Shepherd, G.M. (2011). "The Olfactory Bulb: A Simple System in the Mammalian
1464 Brain," in *Comprehensive Physiology*. John Wiley & Sons, Inc.).
1465 Shepherd, G.M., Rowe, T.B., and Greer, C.A. (2021). An Evolutionary Microcircuit
1466 Approach to the Neural Basis of High Dimensional Sensory Processing in
1467 Olfaction. *Frontiers in Cellular Neuroscience* 15.
1468 Silbering, A.F., and Galizia, C.G. (2007). Processing of odor mixtures in the
1469 Drosophila antennal lobe reveals both global inhibition and glomerulus-
1470 specific interactions. *J Neurosci* 27, 11966-11977.
1471 Silbering, A.F., Okada, R., Ito, K., and Galizia, C.G. (2008). Olfactory information
1472 processing in the *Drosophila* antennal lobe: anything goes? *Journal of*
1473 *Neuroscience* 28, 13075-13087.
1474 Silbering, A.F., Rytz, R., Grosjean, Y., Abuin, L., Ramdya, P., Jefferis, G.S., and
1475 Benton, R. (2011). Complementary Function and Integrated Wiring of the
1476 Evolutionarily Distinct *Drosophila* Olfactory Subsystems. *Journal of neuroscience*
1477 31, 13357-13375.

1478 Stensmyr, M.C., Dweck, H.K., Farhan, A., Ibba, I., Strutz, A., Mukunda, L., Linz, J.,
1479 Grabe, V., Steck, K., Lavista-Llanos, S., Wicher, D., Sachse, S., Knaden, M.,
1480 Becher, P.G., Seki, Y., and Hansson, B.S. (2012). A conserved dedicated
1481 olfactory circuit for detecting harmful microbes in *Drosophila*. *Cell* 151, 1345-
1482 1357.
1483 Stocker, R.F., Lienhard, M.C., Borst, A., and Fischbach, K.F. (1990). Neuronal
1484 architecture of the antennal lobe in Drosophila melanogaster. *Cell and tissue*
1485 *research* 262, 9-34.
1486 Stocker, R.F., Singh, R.N., Schorderet, M., and Siddiqi, O. (1983). Projection patterns
1487 of different types of antennal sensilla in the antennal glomeruli of Drosophila
1488 melanogaster. *Cell and Tissue Research* 232, 237-248.
1489 Strutz, A., Soelter, J., Baschwitz, A., Farhan, A., Grabe, V., Rybak, J., Knaden, M.,
1490 Schmuker, M., Hansson, B.S., and Sachse, S. (2014). Decoding odor quality
1491 and intensity in the *Drosophila* brain. *eLife* 3, e04147.
1492 Su, C.-Y., Menuz, K., and Carlson, J.R. (2009). Olfactory Perception: Receptors, Cells,
1493 and Circuits. *Cell* 139, 45-59.
1494 Suh, G.S.B., Wong, A.M., Hergarden, A.C., Wang, J.W., Simon, A.F., Benzer, S., Axel,
1495 R., and Anderson, D.J. (2004). A single population of olfactory sensory
1496 neurons mediates an innate avoidance behaviour in *Drosophila*. *Nature* 431,
1497 854-859.
1498 Sun, X.J., Tolbert, L.P., and Hildebrand, J.G. (1997). Synaptic organization of the
1499 uniglomerular projection neurons of the antennal lobe of the moth *Manduca*
1500 *sexta*: a laser scanning confocal and electron microscopic study. *Journal of*
1501 *Comparative Neurology* 379, 2-20.
1502 Szyszka, P., and Galizia, C.G. (2015). "Olfaction in Insects," in *Handbook of Olfaction*
1503 *and Gustation,* ed. R.L. Doty. 3 ed: John Wiley & Sons, Inc), 531-546.
1504 Taisz, I., Donà, E., Münch, D., Bailey, S.N., Morris, W.J., Meechan, K.I., Stevens,
1505 K.M., Varela, I., Gkantia, M., Schlegel, P., Ribeiro, C., Jefferis, G.S.X.E., and
1506 Galili, D.S. (2022). Generating parallel representations of position and identity
1507 in the olfactory system. *bioRxiv*, 2022.2005.2013.491877.
1508 Takemura, S.-Y., Xu, C.S., Lu, Z., Rivlin, P.K., Parag, T., Olbris, D.J., Plaza, S., Zhao,
1509 T., Katz, W.T., Umayam, L., Weaver, C., Hess, H.F., Horne, J.A., Nunez-
1510 Iglesias, J., Aniceto, R., Chang, L.-A., Lauchie, S., Nasca, A., Ogundeyi, O.,
1511 Sigmund, C., Takemura, S., Tran, J., Langille, C., Le Lacheur, K., Mclin, S.,
1512 Shinomiya, A., Chklovskii, D.B., Meinertzhagen, I.A., and Scheffer, L.K.
1513 (2015). Synaptic circuits and their variations within different columns in the
1514 visual system of Drosophila. *Proceedings of the National Academy of Sciences* 112,
1515 13711-13716.
1516 Tamás, G., Buhl, E.H., and Somogyi, P. (1997). Massive Autaptic Self-Innervation of
1517 GABAergic Neurons in Cat Visual Cortex. *The Journal of Neuroscience* 17, 6352-
1518 6364.

1519 Tanaka, N.K., Endo, K., and Ito, K. (2012). The organization of antennal lobe-
1520 associated neurons in the adult *Drosophila* melanogaster brain. *Journal of*
1521 *Comparative Neurology* 520, 4067-4130.
1522 Thoma, M., Hansson, B.S., and Knaden, M. (2015). High-resolution Quantification of
1523 Odor-guided Behavior in Drosophila melanogaster Using the Flywalk
1524 Paradigm. *J Vis Exp*, e53394.
1525 Tobin, W.F., Wilson, R.I., and Lee, W.-C.A. (2017). Wiring variations that enable and
1526 constrain neural computation in a sensory microcircuit. *eLife* 6, e24838.
1527 Tran-Van-Minh, A., Cazé, R.D., Abrahamsson, T., Cathala, L., Gutkin, B.S., and
1528 Digregorio, D.A. (2015). Contribution of sublinear and supralinear dendritic
1529 integration to neuronal computations. *Frontiers in Cellular Neuroscience* 9.
1530 Trujillo-Cenoz, O. (1969). Some Aspects of the Structural Organization of the
1531 Medulla in Muscoid Flies I. *J Ultrastructural Research* 27, 533-553.
1532 Van Der Loos, H., and Glaser, E.M. (1972). Autapses in neocortex cerebri: synapses
1533 between a pyramidal cell's axon and its own dendrites. *Brain Res* 48, 355-360.
1534 Vosshall, L.B., Wong, A.M., and Axel, R. (2000). An olfactory sensory map in the fly
1535 brain. *Cell* 102, 147-159.
1536 Wang, J.W. (2012). Presynaptic modulation of early olfactory processing in
1537 *Drosophila*. *Developmental neurobiology* 72, 87-99.
1538 Wicher, D., and Miazzi, F. (2021). Functional properties of insect olfactory receptors:
1539 ionotropic receptors and odorant receptors. *Cell Tissue Res* 383, 7-19.
1540 Wiles, L., Gu, S., Pasqualetti, F., Parvesse, B., Gabrieli, D., Bassett, D.S., and Meaney,
1541 D.F. (2017). Autaptic Connections Shift Network Excitability and Bursting. *Sci*
1542 *Rep* 7, 44006.
1543 Wilson, R.I. (2013). Early Olfactory Processing in Drosophila: Mechanisms and
1544 Principles. *Annual review of neuroscience* 36, 217-241.
1545 Xu, C.S., Hayworth, K.J., Lu, Z., Grob, P., Hassan, A.M., García-Cerdán, J.G., Niyogi,
1546 K.K., Nogales, E., Weinberg, R.J., and Hess, H.F. (2017). Enhanced FIB-SEM
1547 systems for large-volume 3D imaging. *eLife* 6, e25916.
1548 Xu, C.S., Januszewski, M., Lu, Z., Takemura, S.-Y., Hayworth, K.J., Huang, G.,
1549 Shinomiya, K., Maitin-Shepard, J., Ackerman, D., Berg, S., Blakely, T.,
1550 Bogovic, J., Clements, J., Dolafi, T., Hubbard, P., Kainmueller, D., Katz, W.,
1551 Kawase, T., Khairy, K.A., Leavitt, L., Li, P.H., Lindsey, L., Neubarth, N.,
1552 Olbris, D.J., Otsuna, H., Troutman, E.T., Umayam, L., Zhao, T., Ito, M.,
1553 Goldammer, J., Wolff, T., Svirskas, R., Schlegel, P., Neace, E.R., Knecht, C.J.,
1554 Alvarado, C.X., Bailey, D.A., Ballinger, S., Borycz, J.A., Canino, B.S.,
1555 Cheatham, N., Cook, M., Dreher, M., Duclos, O., Eubanks, B., Fairbanks, K.,
1556 Finley, S., Forknall, N., Francis, A., Hopkins, G.P., Joyce, E.M., Kim, S., Kirk,
1557 N.A., Kovalyak, J., Lauchie, S.A., Lohff, A., Maldonado, C., Manley, E.A.,
1558 Mclin, S., Mooney, C., Ndama, M., Ogundeyi, O., Okeoma, N., Ordish, C.,
1559 Padilla, N., Patrick, C., Paterson, T., Phillips, E.E., Phillips, E.M., Rampally,
1560 N., Ribeiro, C., Robertson, M.K., Rymer, J.T., Ryan, S.M., Sammons, M., Scott,
1561 A.K., Scott, A.L., Shinomiya, A., Smith, C., Smith, K., Smith, N.L., Sobeski,

M.A., Suleiman, A., Swift, J., Takemura, S., Talebi, I., Tarnogorska, D., Tenshaw, E., Tokhi, T., Walsh, J.J., Yang, T., Horne, J.A., Li, F., Parekh, R., Rivlin, P.K., Jayaraman, V., Ito, K., Saalfeld, S., George, R., Meinertzhagen, I., et al. (2020). A Connectome of the Adult *Drosophila* Central Brain. 2020.2001.2021.911859.

Yang, K., Liu, T., Wang, Z., Liu, J., Shen, Y., Pan, X., Wen, R., Xie, H., Ruan, Z., Tan, Z., Chen, Y., Guo, A., Liu, H., Han, H., Di, Z., and Zhang, K. (2022). Classifying Drosophila olfactory projection neuron boutons by quantitative analysis of electron microscopic reconstruction. *iScience* 25, 104180.

Yasuyama, K., Meinertzhagen, I.A., and Schurmann, F.W. (2003). Synaptic connections of cholinergic antennal lobe relay neurons innervating the lateral horn neuropile in the brain of *Drosophila melanogaster*. *J Comp Neurol* 466, 299-315.

Yasuyama, K., and Salvaterra, P.M. (1999). Localization of choline acetyltransferase-expressing neurons in *Drosophila* nervous system. *Microscopy Research and Technique* 45, 65-79.

Yin, L., Zheng, R., Ke, W., He, Q., Zhang, Y., Li, J., Wang, B., Mi, Z., Long, Y.-S., Rasch, M.J., Li, T., Luan, G., and Shu, Y. (2018). Autapses enhance bursting and coincidence detection in neocortical pyramidal cells. *Nature Communications* 9, 4890.

Yokoi, M., Mori, K., and Nakanishi, S. (1995). Refinement of odor molecule tuning by dendrodendritic synaptic inhibition in the olfactory bulb. *Proceedings of the National Academy of Sciences* 92, 3371-3375.

Zheng, Z., Lauritzen, J.S., Perlman, E., Robinson, C.G., Nichols, M., Milkie, D., Torrens, O., Price, J., Fisher, C.B., Sharifi, N., Calle-Schuler, S.A., Kmecova, L., Ali, I.J., Karsh, B., Trautman, E.T., Bogovic, J., Hanslovsky, P., Jefferis, G.S.X.E., Kazhdan, M., Khairy, K., Saalfeld, S., Fetter, R.D., and Bock, D.D. (2017). A Complete Electron Microscopy Volume Of The Brain Of Adult Drosophila melanogaster. *bioRxiv*.

Zheng, Z., Lauritzen, J.S., Perlman, E., Robinson, C.G., Nichols, M., Milkie, D., Torrens, O., Price, J., Fisher, C.B., Sharifi, N., Calle-Schuler, S.A., Kmecova, L., Ali, I.J., Karsh, B., Trautman, E.T., Bogovic, J.A., Hanslovsky, P., Jefferis, G.S.X.E., Kazhdan, M., Khairy, K., Saalfeld, S., Fetter, R.D., and Bock, D.D. (2018). A Complete Electron Microscopy Volume of the Brain of Adult Drosophila melanogaster. *Cell* 174, 730-743.e722.

FIGURES

Figure 1: A correlative approach to analyze the ultrastructure of identified olfactory glomeruli

A-B: Two-photon laser scans of the antennal lobes in *Orco-Gal4; UAS-GCaMP6s* flies where Orco-positive olfactory sensory neurons (OSNs) in the glomerular neuropils were labeled by GCaMP (green fluorescence). Glomeruli DA2 (A) and DL5 (B) are encircled. Schematics show their relative position in the antennal lobe. Once the glomeruli of interest were identified, glomerular borders were marked with fiducial marks (arrowheads) via laser branding, which enabled their identification at the ultrastructural level. **C-D**: Representative images of the same glomeruli (DA2 in **C** and DL5 in **D**) obtained with focused-ion-beam electron microscopy (FIB-SEM), showing their ultrastructure. Asterisks indicate the main neurite of uniglomerular projection neurons entering the glomerulus. White arrowhead shows a 2-photon laser mark (see also **A** and **B**). **E**: FIB-SEM image of a polyadic synapse: the presynaptic site (red arrowhead) is composed of a T-bar shaped presynaptic density surrounded by small vesicles and is opposed by several postsynaptic profiles (cyan dots). Scheme of a tetrad synapse: a presynaptic site with its T-bar (red arrowhead) forms four output connections (arrows) with four postsynaptic input sites (cyan dots). **F:** A skeleton-based reconstruction of an OSN axon terminal (green line) with presynaptic (red dots) and postsynaptic sites (cyan dots). The dark grey shading surrounding the OSN trace represents the volume-based reconstruction of the same neuron. Tracing and reconstruction were performed within the FIB-SEM dataset (light grey area).

Figure 2: Neuron classification and neuronal composition of the DA2 and DL5 glomeruli

A: Example FIB-SEM images (left column), volumetric neuronal reconstructions (middle column), and skeleton-based neuron traces (right column) of a representative example of each neuron class: OSNs (green), uniglomerular projection neurons (uPNs, red) and multiglomerular neurons (MGNs, blue). The ultrastructure of neurons, including T-bars (black arrowheads), mitochondria (asterisks) and spinules (white arrowhead) are indicated. Exemplar volumetric reconstructions (middle column) show the general morphology of each neuron class. Presynapses and postsynapses are indicated with red and cyan dots on the skeleton traces (right column). **B:** Average branching intensity (branching points per µm of neuronal-fiber length) of each neuron class OSNs, uPNs and MGNs in DA2 and DL5. Data represent mean+ standard deviation (error bars). Data points represent single values. Means were compared using Wilcoxon two-sample test. No significant differences of branching points/µm in OSNs or MGNs between glomeruli were found (significance was not tested for uPNs due to the presence of a single uPN in DL5). **C**: Schematic summary indicating, for each glomerulus, its volume (in μm^3), the number of

neurons of each class (MGNs were not counted), the total fiber length of all neurons for each neuron class and the total number of single synaptic contacts for each glomerulus.

Table 1. Glomerular innervation and synaptic composition

Quantitative neuronal data comparing glomeruli DA2 and DL5, detailing glomerular innervation and synaptic properties for each neuronal class: OSNs (green), uPNs (red) and MGNs (blue) and the sum of all of them. **Row 1**: Total length of all neurons of each neuron class and total length for all neurons in each glomerulus. **Row 2-4**: Synaptic counts: input sites (inputs), output sites (outputs) and T-bars (T-bars). **Row 5**: Innervation density: total neuron length (μm; row 1)/glomerular volume (μm³); glomerular volume: DA2=1500 μm³ and DL5=2700 μm³ (see Figure 1C). **Row 6-8**: Total synaptic density per unit of glomerular volume (μm³): sum of all input sites (inputs), output sites (outputs) and T-bars of each neuron class or of all neurons/glomerular volume. **Row 9-11**: Average synaptic density along neuronal fibers (illustrated also in Figure 3 – supplement 1): number of inputs, outputs or T-bars/neuron length (μm). **Row 12-13:** Average synaptic ratios: the ratio of T-bars-to-inputs or outputs-to-inputs. **Row 14:** Polyadicity: the average number of postsynaptic sites at each T-bar in DA2 and DL5. The ratios in rows 12-14 were calculated based on synaptic counts normalized to neuron length (rows 9-11). The color shading highlights values that have a relative difference greater than 20% (see relative differences Table S1) between DA2 and DL5. Dark shades highlights values that are greater in DA2 than in DL5 (green (OSNs), red (uPNs), blue (MGNs)) and light colors highlight values that are less in DA2 than in DL5.

Figure 3: Innervation density and synaptic density in DA2 and DL5

A-E: The average glomerular innervation density of OSNs (**A**), uPNs (**B**), MGNs (**C**) and collectively of all glomerular neurons (**D**); the average synaptic density of input sites (inputs), output sites (outputs) and T-bars and the average polyadicity. Innervation density: length (μm) of each neuronal fiber normalized to one μm³ of glomerular (glom.) volume. Synaptic density: number of input sites, output sites or T-bars of each neuronal fiber normalized to one μm³ of glomerular volume. Polyadicity: average number of single output sites per T-bar in each neuronal fiber. Data for DA2 shown in dark colors and for DL5 in light colors. Number of neurons in DA2: OSNs (green) n= 44; uPNs (red) n= 7; MGNs (blue) n=180; all neurons n=231, in DL5: OSNs n=46; uPN n=1; MGNs n=221; all neurons n=268. Data represent mean + standard deviation (error bars). Data points represent single values. Means were compared using either Student's t-test (OSNs) or Wilcoxon two-sample test (MGNs and all neurons). uPNs were not compared, since the DL5 has only one. Significance value: $p>0.05$ (not significant, no star), $p\leq0.05$ (*), $p\leq0.01$ (**), $p\leq0.001$ (***). Values are provided at data availability; polyadicity values are listed in Table 1, row 14.

Figure 4: Lateralization of OSN terminals in the antennal lobe

A: Illustration of an ipsilateral (dark green) and a contralateral (light green) OSN with dendrites in the corresponding antennae and their axonal projections to the ipsilateral olfactory glomerulus in the antennal lobe (AL) (dashed rectangle). **B**: Exemplary skeleton traces of an ipsilateral (dark green) and a contralateral (light green) OSN terminal inside glomerulus DA2. The ipsilateral OSN axons reach the glomerulus via the ipsilateral antennal nerve (arrow down) and leave the glomerulus towards the AL commissure (arrow up) while OSN axons originating at the contralateral antenna reach the glomerulus via the AL commissure. Red dots: presynapses; blue dots: postsynapses. **C**: Boxplots showing the fraction of synaptic output to uPNs (in red), - to OSNs (in green) or - toMGNs (in blue), , for the ipsilateral OSNs (dark green boxplot) and contralateral OSNs (light green), respectively, in the DA2, DL5 and VA1v glomeruli (VA1v data obtained from Horne et al., 2018). **D**: Boxplots showing the fraction of synaptic input of the same ipsilateral and contralateral OSNs that they receive from OSNs and MGNs. Connection polarity is indicated by arrows in the schematic neuronal drawings on the left of each plot. Dots represent single values. Means were compared using either Student's T-test. Significance value: $p>0.05$ (not significant, no star)), $p\leq0.05$ (*), $p\leq0.01$ (**), $p\leq0.001$ (***). Mean and Median values are provided at data availability.

Figure 5: Strength of synaptic connection between neuron classes in the circuitry of DA2, DL5 and VA1v.

A: Schematic representation of principal connection motifs between the neuron classes OSNs (green), uPNs (red) and MGNs (blue). The synaptic flow directed towards uPNs is a feedforward and that directed towards OSNs or from uPNs to MGNs defined as a feedback connection (arrows). **B-D**: Alluvial diagrams of the glomerular circuitry in DA2 (**B**), DL5 (**C**) and VA1v (**D**). Each diagram shows the relative synaptic strength calculated as the proportion of 1:1 single synaptic contacts between each neuron class in relation to the total number of synaptic contacts in their respective glomerulus. The synaptic strength between each neuron class, given as percentage, is indicated by the thickness of the lines. The proportions (as percentage) of output (left side) or input (right side) are illustrated by colored rectangles to the left or right of each alluvial diagram. The total number of synaptic contacts is indicated below the diagrams. Percentages of the relative synaptic strength and synaptic counts are listed in the supplementary Table S1. **E:** Stacked bar charts depict output (E') and input (E'') fractions (given as percentages) of each neuron class: OSNs (green), uPNs (red), MGNs (blue), schematically illustrated next to the bar charts respectively, to each of the other neuron classes for glomeruli DA2, DL5 and VA1v. Fractions are color-coded according to the neuron class of the respective connecting partner.

Figure 6: Differences in connectivity strength in glomeruli DA2, DL5 and VA1v
A: Schematic representation of synaptic connection motifs (arrows) between OSNs (green), uPNs (red), and MGNs (blue) in glomeruli DA2, DL5 and VA1v. The number of neurons of each class or truncated neuronal fibers (in brackets) is noted in the corresponding circle. **B**: Schematics of connection motifs (left) that are jointly stronger or weaker in DA2 and VA1v than in DL5. The relative differences (as percentage) between DA2 and DL5 as well as VA1v and DL5 are illustrated as arrows up (stronger) or arrows down (weaker) according to their intensity (see legend at the bottom) from the perspective of the target glomerulus (defined in the table header). The values of relative differences are listed in the Table S2.

Figure 7: Distribution of pre- and postsynaptic partners of autapses in the uPN dendrite of the DL5
A: Distribution of autaptic presynaptic (red dots) and postsynaptic sites (cyan dots) mapped in a dendrogram of the dendrite of the single uPN in glomerulus DL5. The basal root node (black dot) represents the entry site of the uPN dendrite into the glomerulus (closest point to its soma). Clustering of autaptic input sites along some branches are encircled. **B**: Simplified representation of the uPN's dendrogram illustrating the distinct strahler orders, at distal branches (1-4) and at basal branches (5-8); see legend on the right). **C**: Distribution of autaptic presynaptic (left) and postsynaptic input sites (right) along the dendrite, as proportions at each corresponding strahler order (color coded). Note that autaptic postsynaptic sites are located almost exclusively at the most distal dendritic branches. **D**: Dendrogram of the DL5-uPN showing the distribution of presynaptic sites (triangles) and postsynaptic sites (circles) of selected autapses (indicated by same color). Distant pairs of pre- and postsynapses (long geodesic distance) are indicated by numbers whereas closely attached synaptic sites (short geodesic distance) are encircled and labelled with letters. **E**: Schematic of the dendrogram illustrating the location of the presynaptic (red dot) and postsynaptic (cyan dot) sites of a single autapse, the geodesic distance between them, i.e. the distance along the dendrite (μm), and the number of branching points (orange dots) between the pre- and postsynaptic components of the same autapse. **F**: Number of autapses with distinct geodesic distances between their pre- and postsynapses (illustrated in E). **G**: Number of autapses with the number of branch points between their pre- and postsynapses counted along the uPN dendrite (illustrated in E).

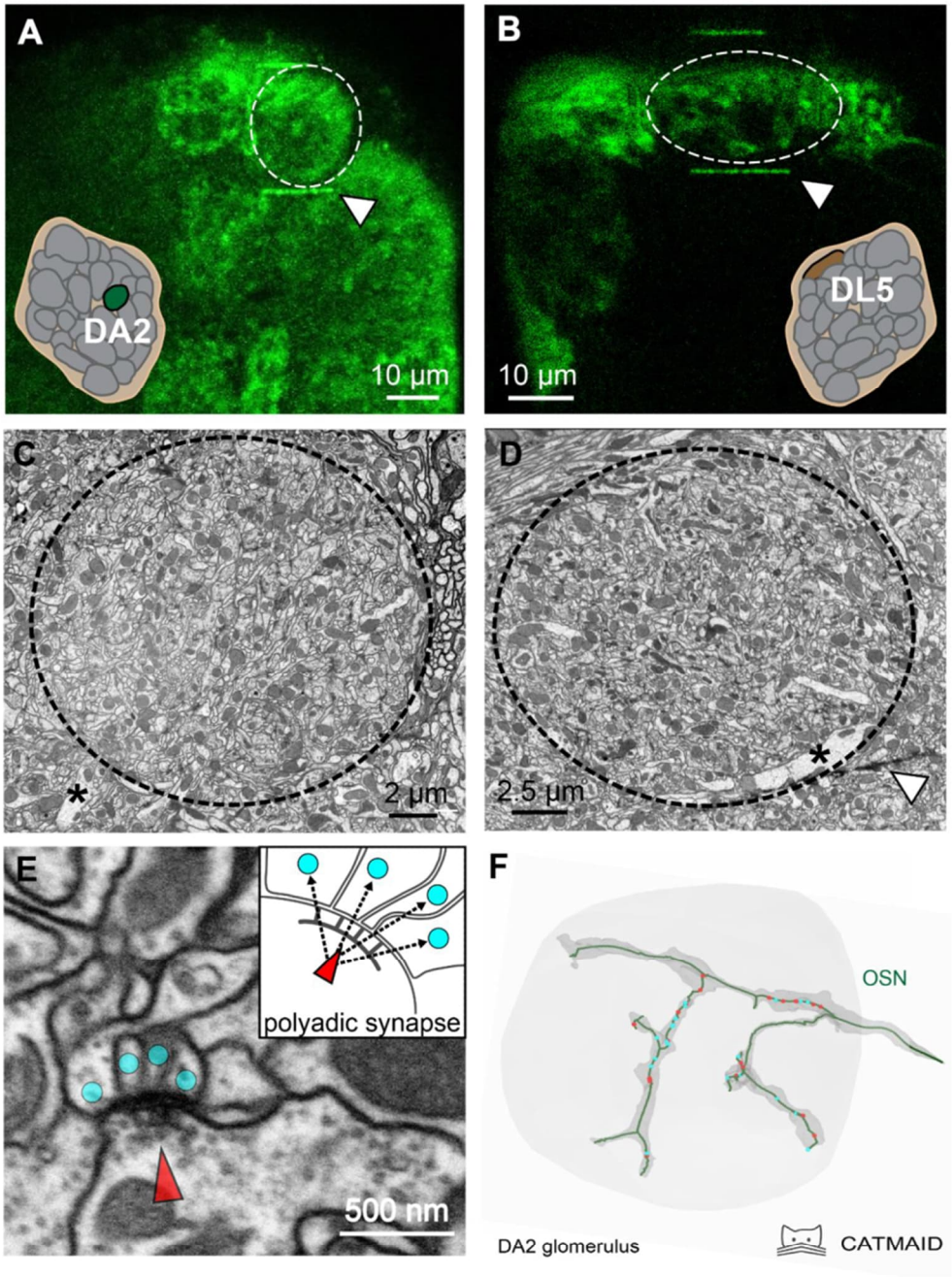
A
DA2
10 µm
B
DL5
10 µm
C
2 µm
D
2.5 µm
E
polyadic synapse
500 nm
F
OSN
DA2 glomerulus
CATMAID

Figure 1

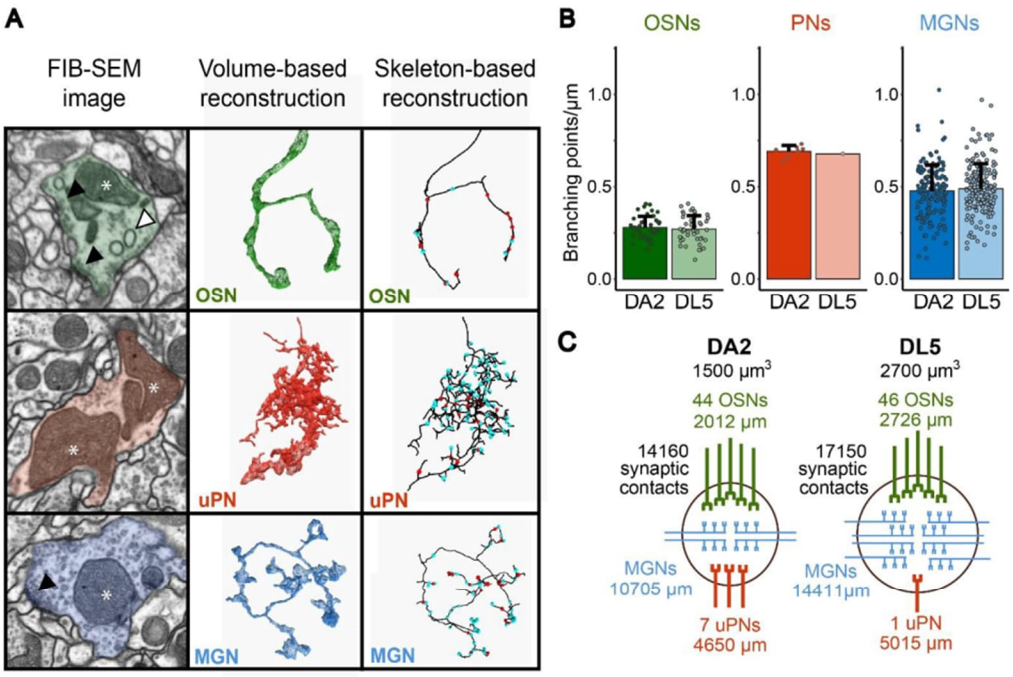
A
FIB-SEM image
Volume-based reconstruction
Skeleton-based reconstruction
OSN
OSN
uPN
uPN
MGN
MGN
B
OSNs
PNs
MGNs
Branching points/µm
1.0
0.5
0.0
DA2 DL5
C
DA2
1500 µm3
44 OSNs
2012 µm
14160 synaptic contacts
MGNs
10705 µm
7 uPNs
4650 µm
DL5
2700 µm3
46 OSNs
2726 µm
17150 synaptic contacts
MGNs
14411µm
1 uPN
5015 µm

Figure 2

Row	Values	Unit	OSNs		uPNs		MGNs		all neurons	
			DA2	DL5	DA2	DL5	DA2	DL5	DA2	DL5
1	Total neuronal length	µm	2012	2727	4652	5015	10705	14411	17370	22153
2	Total synaptic counts	input	868	1083	3887	3955	7229	9018	11984	14056
3		output	6671	6828	1624	3108	5659	6749	13954	16685
4		T-bars	1063	1213	322	602	1263	1572	2648	3387
5	Total innervation density (sum of length of all neuronal fibers/glom. volume)	µm/µm³	1.26	1.05	2.91	1.93	6.69	5.54	10.86	8.52
6	Total glomerular synaptic density (total synaptic counts/glomerular volume)	inputs/µm³	0.54	0.42	2.43	1.52	4.52	3.47	7.49	5.41
7		outputs/µm³	4.17	2.63	1.02	1.20	3.54	2.60	8.72	6.42
8		T-bars/µm³	0.66	0.47	0.20	0.23	0.79	0.60	1.66	1.30
9	Neuronal synaptic density (synaptic counts/neuronal length)	inputs/µm	0.42	0.39	0.83	0.79	0.62	0.59	0.59	0.56
10		outputs/µm	3.37	2.62	0.33	0.62	0.52	0.51	1.06	0.87
11		T-bars/µm	0.53	0.46	0.07	0.12	0.12	0.12	0.19	0.18
12	Synaptic ratio	T-bars/inputs	1.31	1.27	0.08	0.15	0.23	0.24	0.43	0.42
13		outputs/inputs	8.29	7.29	0.40	0.79	1.04	1.11	2.40	2.17
14	Polyadicity	outputs/T-bars	6.35	5.70	4.95	5.16	3.22	2.64	3.88	3.17

Table 1

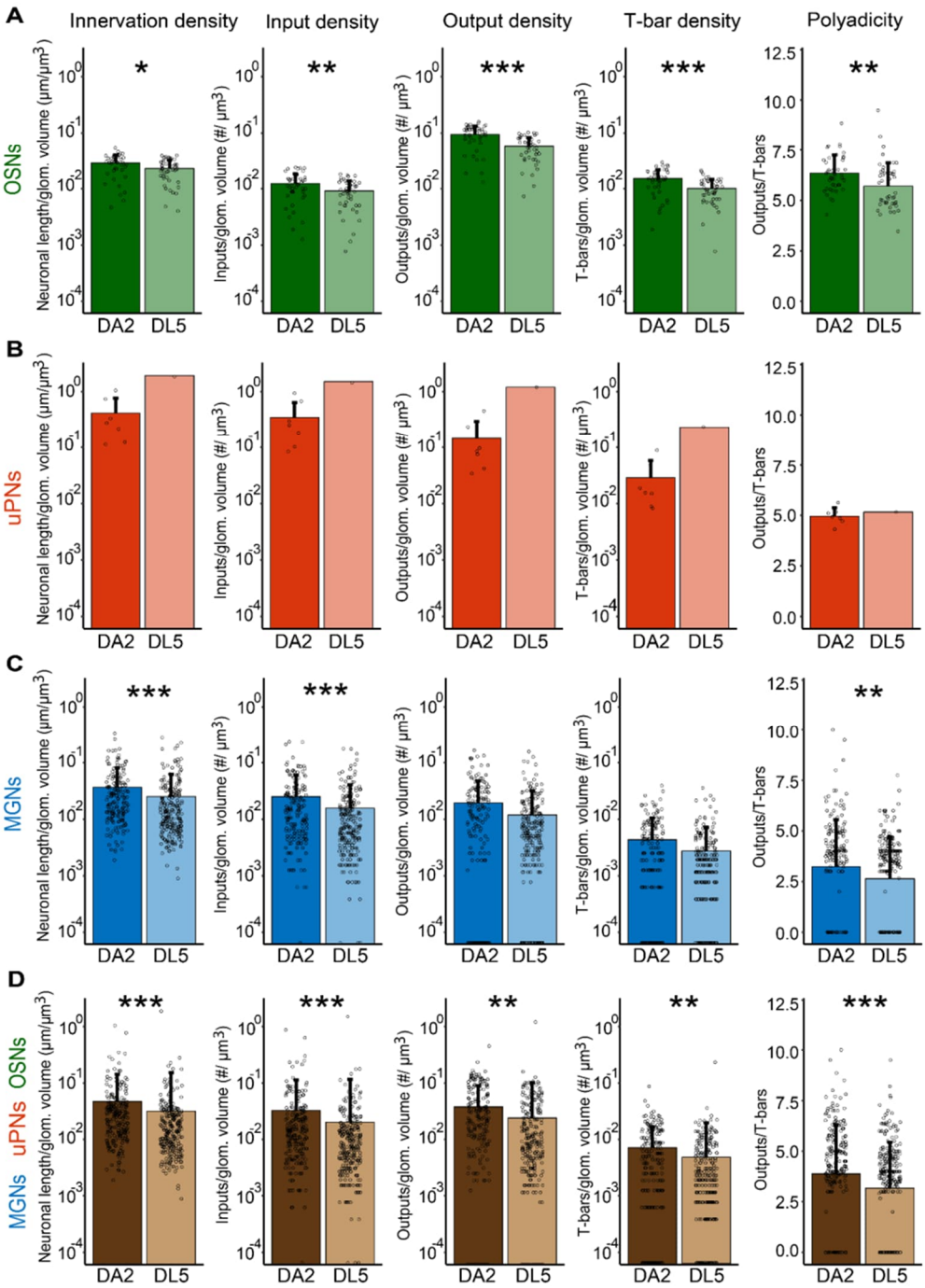

Figure 3

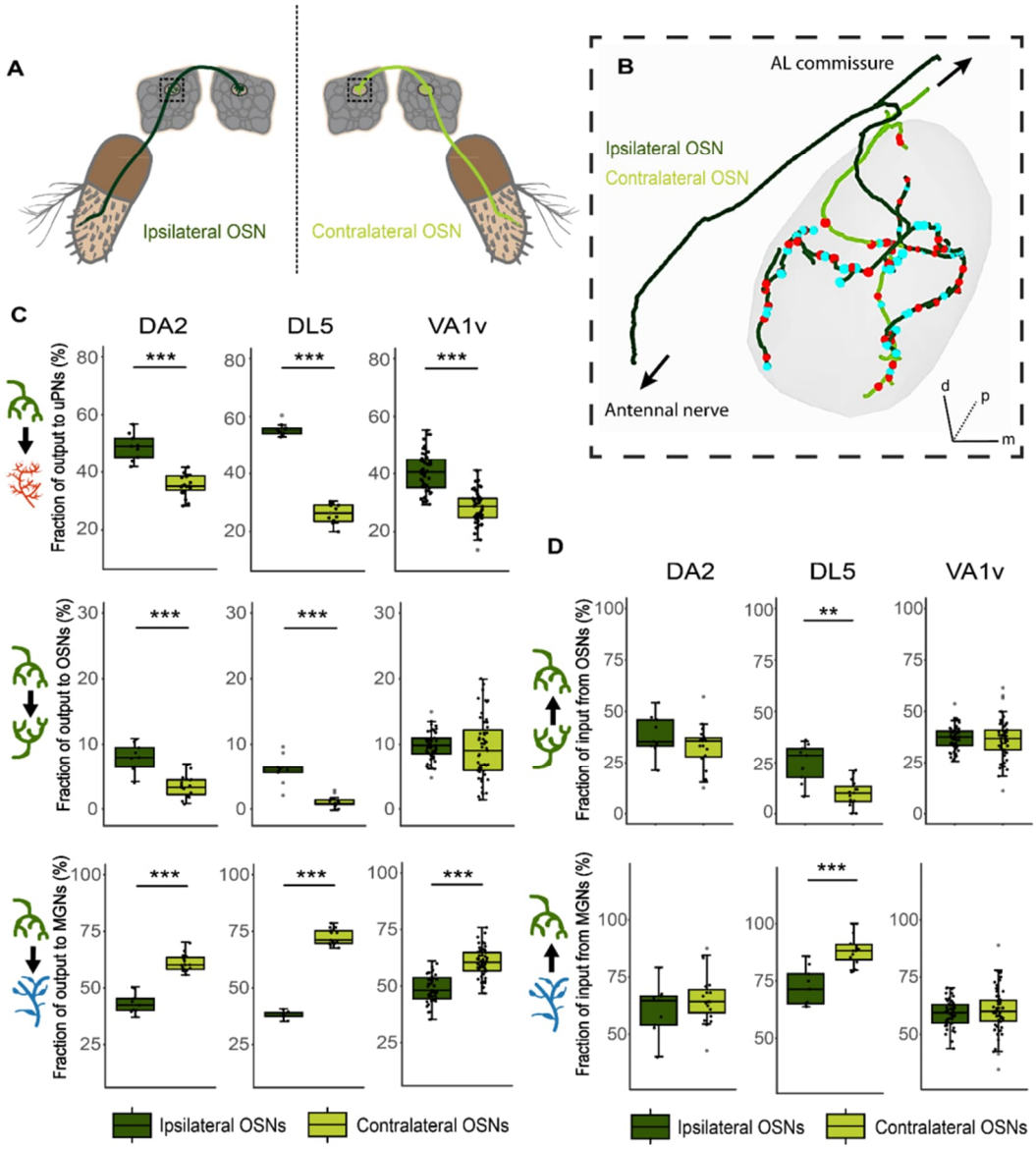

Figure 4

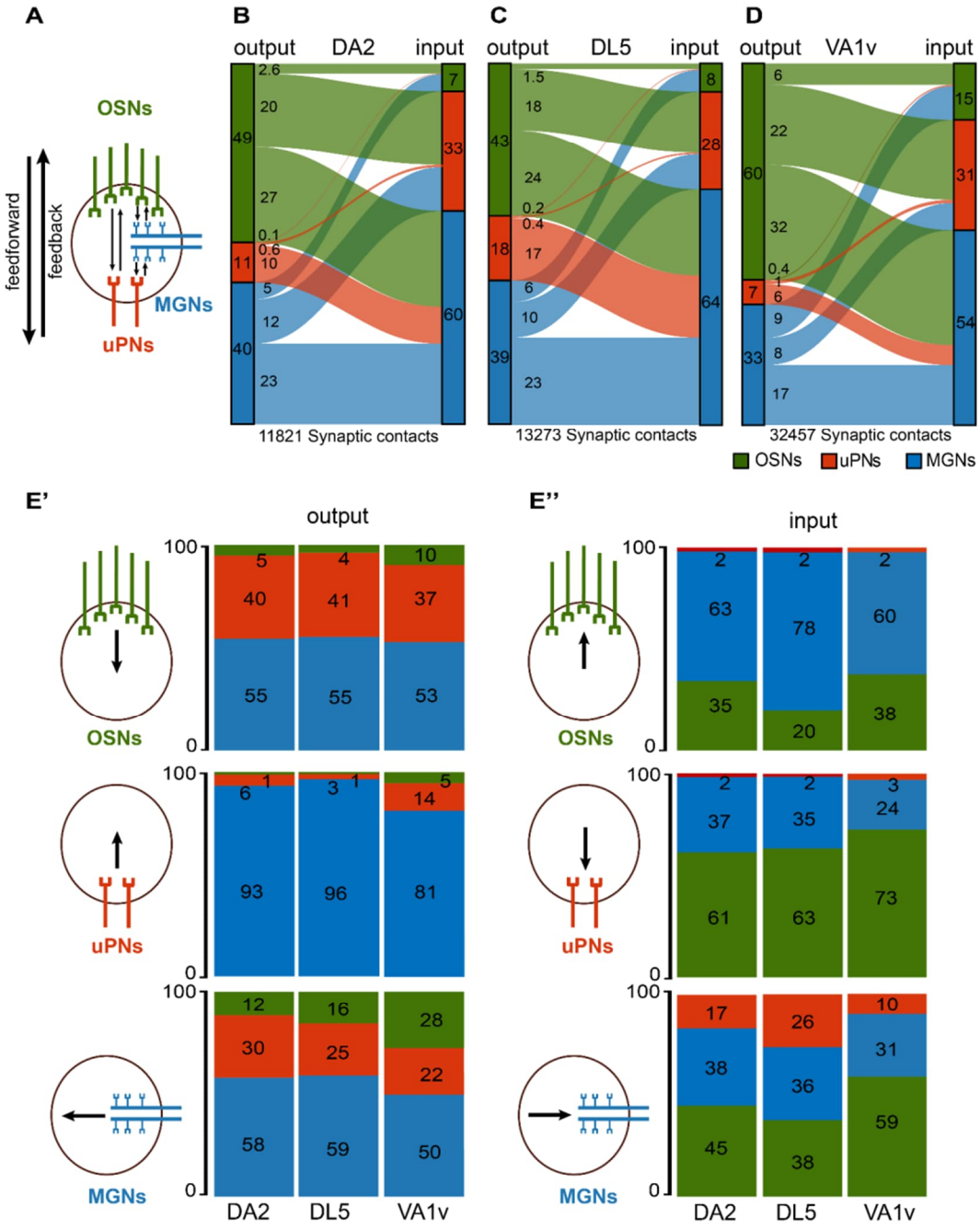

Figure 5

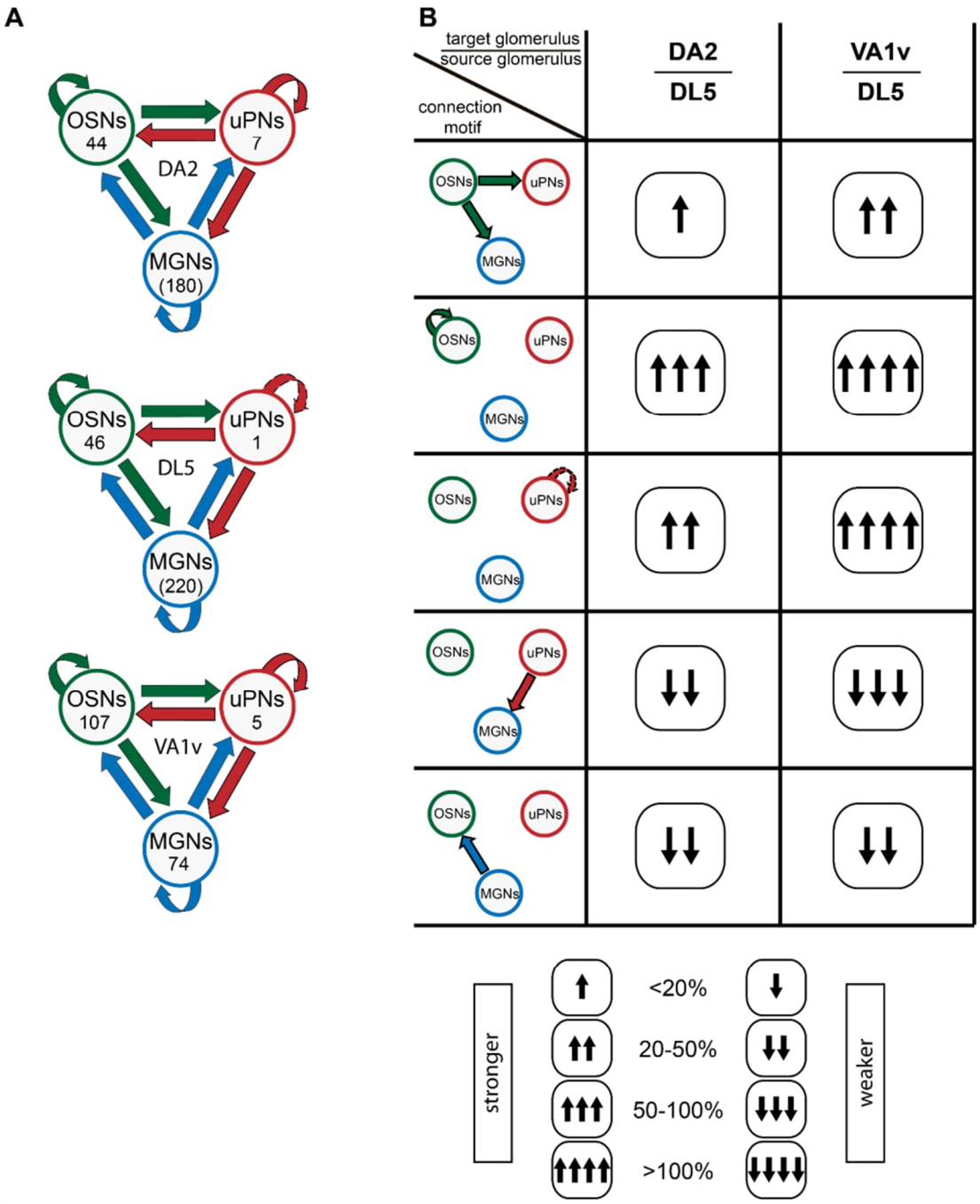

Figure 6

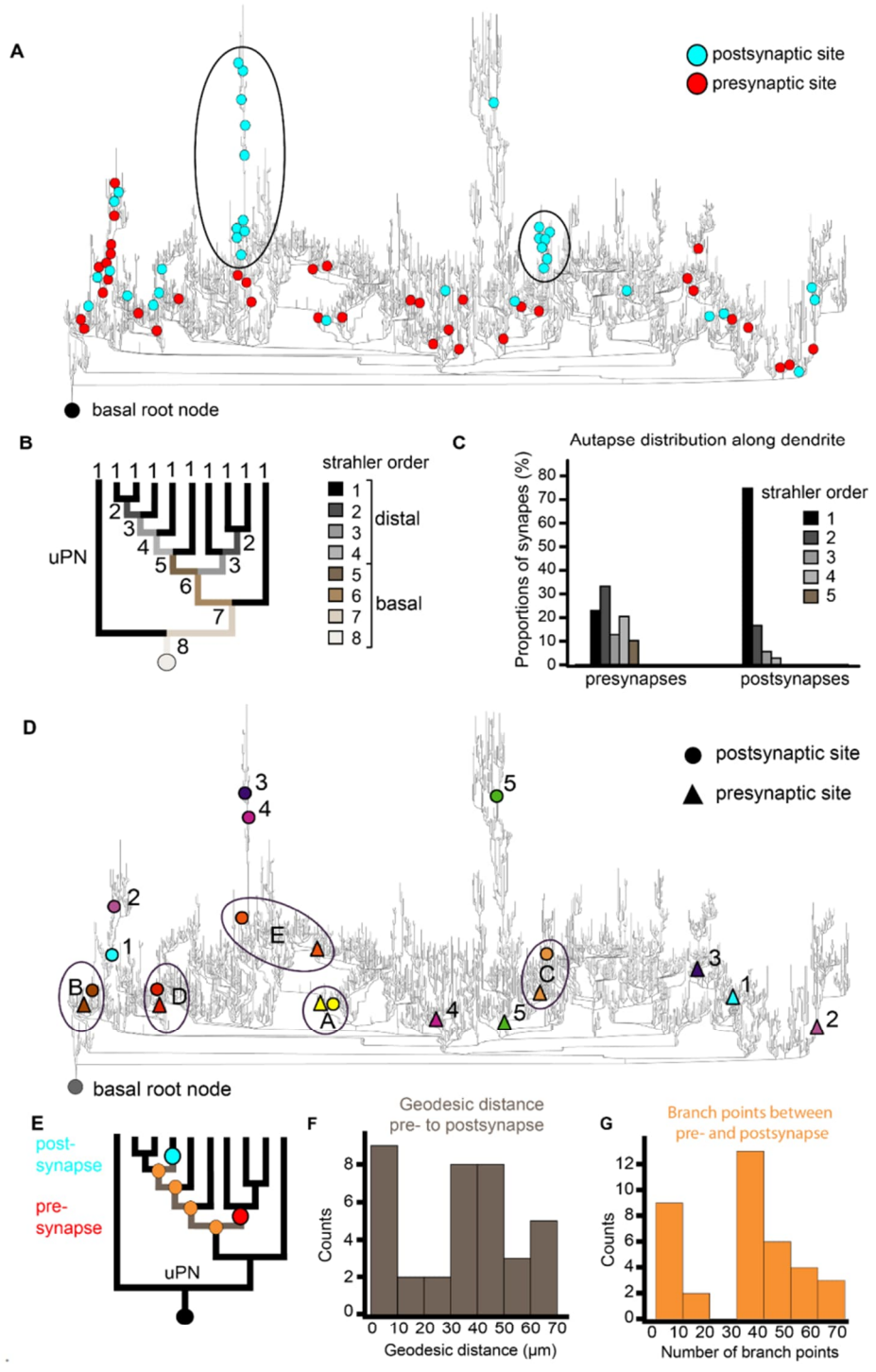

Figure 7

SUPPLEMENTARY FIGURES

Figure 1 – Video 1: FIB-SEM scan of a DA2 dataset with highlighted uPN reconstruction (see extra file)

The video shows a full FIB-SEM scan of a DA2 glomerulus at pixel resolution 4x4x20 nm, with the neuron trace of a single uniglomerular projection neuron (uPN#2) highlighted in yellow.

Figure 2 – figure supplement 1: Neuronal volume and polyadicity

A: Ratio between neuronal fiber volume and length in OSNs (30 neurons were measured), uPNs (n =5) and MGNs (n = 16) in glomerulus DA2. Data represent mean + standard deviation (error bars). **B-D**: Frequency of T-bars associated with a number of postsynaptic contacts (Polyadicity) in OSNs (**B**), uPNs (**C**) and MGNs (**D**) in DA2 (dark shade) and DL5 (light shade)

Supplementary Table S1: Relative differences of glomerular innervation and synaptic composition between DA2 and DL5

The Table lists the relative differences between DA2 and DL5 (see Methods for calculations). Relative differences above 20% in both directions are highlighted. Dark shades highlights values that are greater in DA2 than in DL5 and light colors highlight values that are less in DA2 than in DL5.

Figure 3 – figure supplement 1: Synaptic density along neuronal fibers in DA2 and DL5

Counts of synaptic inputs, synaptic outputs and T-bars normalized to 1 µm of neuronal length along OSN, uPN or MGN fibers and collectively for all neurons within glomeruli DA2 (dark colors) and DL5 (light colors). DA2: OSNs (green) n= 44; uPNs (red) n= 7; MGNs (blue) n=180; all neurons n=231. DL5: OSNs n=46; uPN n=1; MGNs n=221; all neurons n=268. Data represent mean + standard deviation (error bars). Data points represent single values. Means are compared using either Student's T-test (in OSNs) or Wilcoxon two-sample test (in MGNs and all neurons). The uPNs of the DA2 are not compared to the single uPN of the DL5. Significance value: $p>0.05$ (not significant, no star), $p\leq0.05$ (*), $p\leq0.01$ (**), $p\leq0.001$ (***). Values are listed in Table 1, row 9-11.

Figure 4 – figure supplement 1: Properties of ipsi- and contralateral OSNs.

A: Boxplots for total neuronal-fiber length and synaptic density (inputs, outputs, T-bars per unit of neuronal fiber length) of ipsilateral (dark green) and contralateral OSN terminals (light green). Dots represent single values. Means were compared using Student's T-test. Significance value: $p\leq0.05$ (*), $p\leq0.01$ (**), $p\leq0.001$ (***).

Supplementary Table S2: **Synaptic connectivity and relative differences between DA2, DL5 and VA1v**

Synapse counts and synaptic strength of each connection type in DA2, DL5 and VA1v. Three comparisons are shown: DA2 compared with DL5 (top table), VA1v with DL5 (middle) and VA1v with DA2 (bottom). The relative synaptic strength (rel syn strength) of each connection type is listed on the left side and the relative differences (rel differences) is listed on the right side.

Supplementary Table S3: Connectivity of single neurons in DA2 (see extra file)

Supplementary Table S4: Connectivity of single neurons in DL5 (see extra file)

Figure 7 – figure supplement 1: Distribution of synapses and autapses along the DL5 uPN dendrite in DL5

A: 3D-reconstruction of the uPN dendrite (skeleton trace) in the DL5 glomerulus showing the presynaptic (red dots) and postsynaptic sites (cyan dots) of all its autapses. **B**: Number of autaptic presynaptic (red) and postsynaptic sites (cyan) according to their geodesic distance to the basal root node point (indicated with a black circle in A). **C**: Proportional distribution of all presynapses and postsynapses (excluding autaptic connections) in the DL5 uPN at each strahler order (see legend inset). Note the high proportion of postsynaptic sites on most distal dendritic branches.

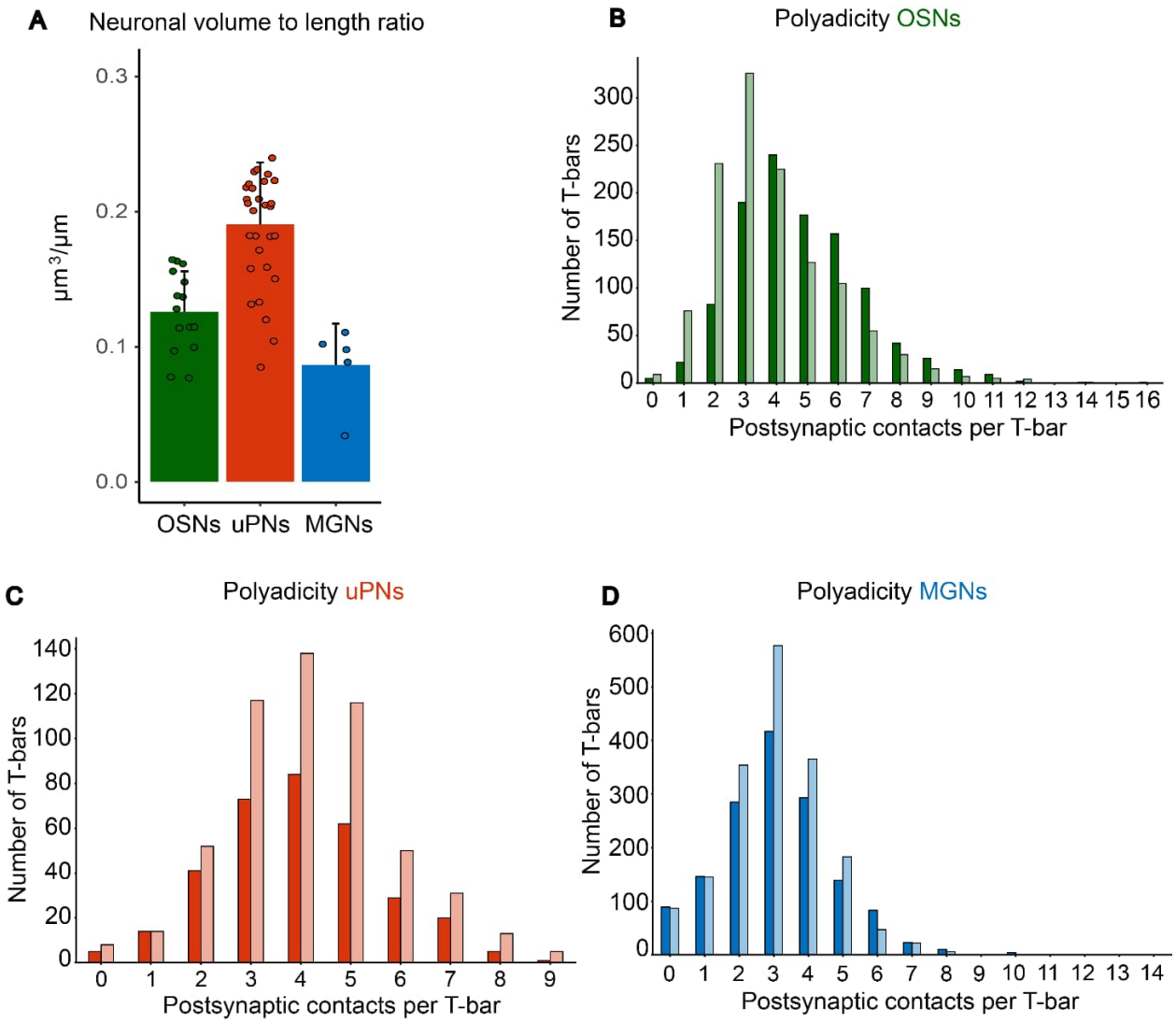

Figure 2 – figure supplement 1

Supplementary Table S1

Row	Values	Unit	OSNs	uPNs	MGNs	all neuron
			Relative differences between DA2 and DL5			
1	Total neuronal length	µm	-26	-7	-26	-22
2	Total synaptic counts	input	-20	-2	-20	-15
3		output	-2	-48	-16	-16
4		T-bars	-12	-47	-20	-22
5	Total innervation density (sum of length of all neuronal fibers/glom. volume)	µm/µm^3	20	51	21	27
6	Total glomerular synaptic density (total synaptic counts/glomerular volume)	inputs/µm^3	30	60	30	39
7		outputs/µm^3	59	-15	36	36
8		T-bars/µm^3	42	-13	31	27
9	Neuronal synaptic density (synaptic counts/neuronal length)	inputs/µm	8	5	5	6
10		outputs/µm	29	-47	2	21
11		T-bars/µm	16	-45	-5	7
12	Synaptic ratio	T-bars/inputs	3	-47	-6	2
13		outputs/inputs	14	-50	-6	11
14	Polyadicity	outputs/T-bars	11	-4	22	22

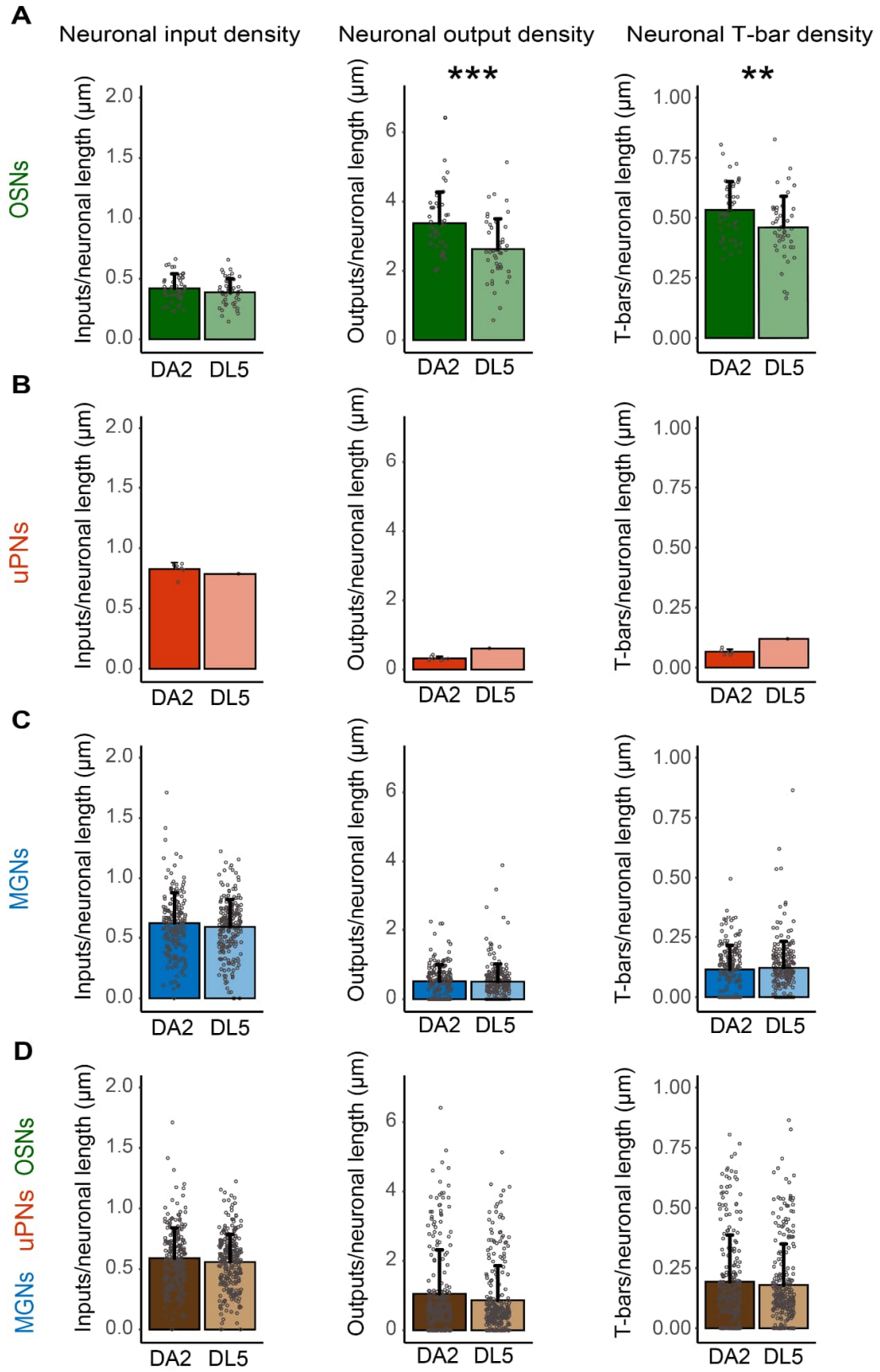

Figure 3 – figure supplement 1

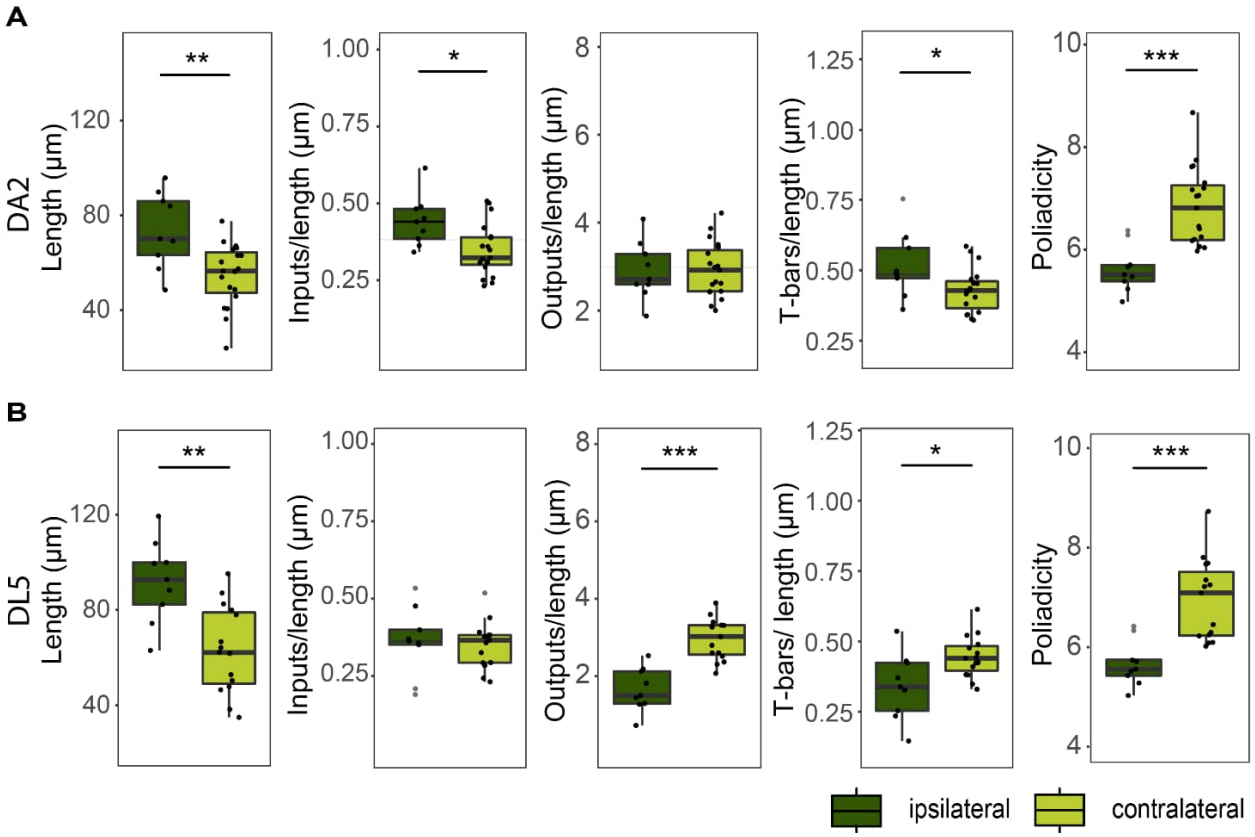

Figure 4 – figure supplement 1

neuron class	connection motif	DA2	rel syn strength (%)	rel out classes (%)	rel in classes (%)	DL5	rel syn strength (%)	rel out classes (%)	rel in classes (%)	rel difference (%)	rel out difference (%)	rel in difference (%)
OSNs	OSNs>uPNs	2365	19.99	49.48	7.37	2354	17.76	43.44	7.89	12.52	13.93	-6.63
	OSNs>MGNs	3186	26.92			3201	24.15			11.47		
	OSNs>OSNs	305	2.58			202	1.52			69.11		
uPNs	uPNs>OSNs	16	0.14	10.92	32.62	26	0.20	17.50	28.07	-31.08	-37.63	16.18
	uPNs>MGNs	1205	10.18			2240	16.90			-39.75		
	uPNs>uPNs	71	0.60			54	0.41			47.26		
MGNs	MGNs>OSNs	551	4.66	39.60	60.01	818	6.17	39.06	64.03	-24.56	1.38	-6.28
	MGNs>uPNs	1424	12.03			1313	9.91			21.47		
	MGNs>MGNs	2711	22.91			3046	22.98			-0.32		
	SUM	11833	100	100	100	13254	100	100	100			

Supplementary Table S2

neuron class	connection motif	VA1v	rel syn strength (%)	rel out classes (%)	rel in classes (%)	DL5	rel syn strength (%)	rel out classes (%)	rel in classes (%)	rel difference (%)	rel out difference (%)	rel in difference (%)
OSNs	OSNs>uPNs	7226	22.26	59.84	15.51	2354	17.76	43.44	7.89	25.35	37.76	96.53
	OSNs>MGNs	10295	31.72			3201	24.15			31.33		
	OSNs>OSNs	1901	5.86			202	1.52			284.30		
uPNs	uPNs>OSNs	117	0.36	6.83	30.67	26	0.20	17.50	28.07	83.76	-60.96	9.26
	uPNs>MGNs	1801	5.55			2240	16.90			-67.17		
	uPNs>uPNs	300	0.92			54	0.41			126.86		
MGNs	MGNs>OSNs	3016	9.29	33.33	53.82	818	6.17	39.06	64.03	50.56	-14.68	-15.96
	MGNs>uPNs	2430	7.49			1313	9.91			-24.42		
	MGNs>MGNs	5371	16.55			3046	22.98			-27.99		
	SUM	32457	100	100	100	13254	100	100	100			

Supplementary Table S3

neuron class	connection motif	VA1v	rel syn strength (%)	rel out classes (%)	rel in classes (%)	DA2	rel syn streng th (%)	rel out classes (%)	rel in classes (%)	rel difference (%)	rel out difference (%)	rel in difference (%)
OSNs	OSNs>uPNs	7226	22.26	59.84	15.51	2365	19.99	49.48	7.37	11.40	20.92	110.48
	OSNs>MGNs	10295	31,.2			3186	26.92			17.82		
	OSNs>OSNs	1901	5.86			305	2.58			127.25		
uPNs	uPNs>OSNs	117	0.36	6.83	30.67	16	0.14	10.92	32.62	166.60	-37.41	-5.96
	uPNs>MGNs	1801	5.55			1205	10.18			-45.51		
	uPNs>uPNs	300	0.92			71	0.60			54.06		
MGNs	MGNs>OSNs	3016	9.29	33.33	53.82	551	4.66	39.60	60.01	99.57	-15.84	-10.33
	MGNs>uPNs	2430	7.49			1424	12.03			-37.78		
	MGNs>MGNs	5371	16.55			2711	22.91			-27.76		
	SUM	32457	100	100	100	11833	100	100	100			

color code	rel syn strength (%)	<5	5-10	10-15	15-20	>20
	rel difference (%)	<10	10-20	20-50	50-100	>100

Supplementary Table S4

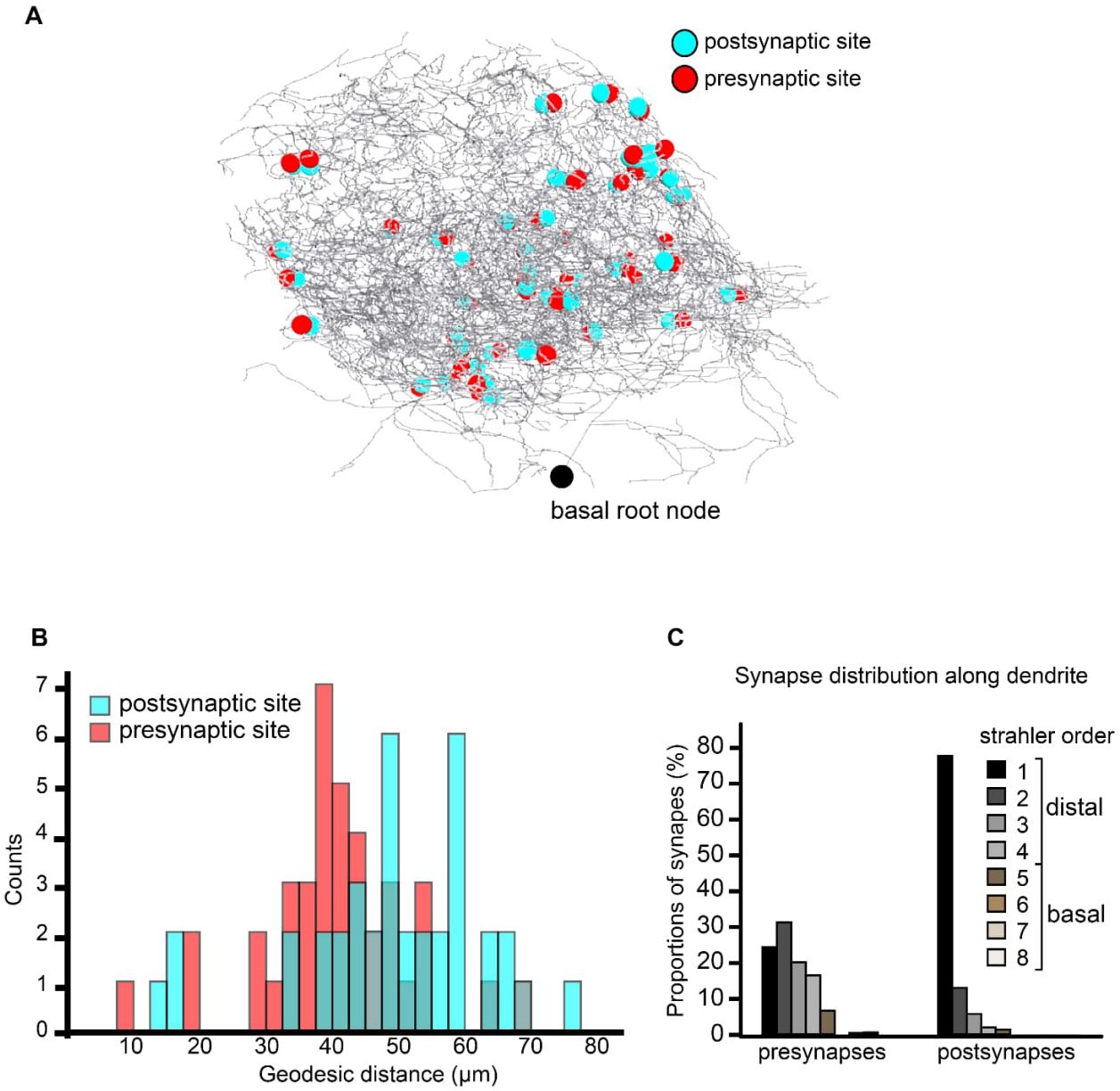

Figure 7 – figure supplement 1

CHAPTER 2

Synaptic Spinules in the Olfactory Circuit of *Drosophila melanogaster*

Lydia Gruber, Jürgen Rybak , Bill S. Hansson and Rafael Cantera

Frontiers in Cellular Neuroscience

Published online on March 27, 2018

FORM 1

Manuscript No. Manuscript II

Manuscript title:

Synaptic Spinules in the Olfactory Circuit of Drosophila melanogaster

Authors: Lydia Gruber, Jürgen Rybak, Bill S. Hansson and Rafael Cantera

Bibliographic information:

Gruber, L., Rybak, J., Hansson, B. S., & Cantera, R. (2018). Synaptic Spinules in the Olfactory Circuit of Drosophila melanogaster. *Front Cell Neurosci, 12*(86), 86. doi:10.3389/fncel.2018.00086

The candidate is (Please tick the appropriate box.)

☒ First author, ☐ Co-first author, ☐ Corresponding author, ☐ Co-author.

Status: published

Authors' contributions (in %) to the given categories of the publication

Author	Conceptual	Data analysis	Experimental	Writing the manuscript	Provision of material
Gruber, L.	**70%**	**90%**	**100%**	**60%**	-
Rybak, J.	10%	10%	-	5%	-
Hansson, B.S.	-	-	-	5%	100%
Cantera, R.	20%	-	-	30%	-
Others					
Total:	100%	100%	100%	100%	100%

_____ _____

Signature candidate Signature supervisor (member of the Faculty)

frontiers in Cellular Neuroscience

PERSPECTIVE
published: 27 March 2018
doi: 10.3389/fncel.2018.00086

Synaptic Spinules in the Olfactory Circuit of *Drosophila melanogaster*

Lydia Gruber[1], *Jürgen Rybak*[1], *Bill S. Hansson*[1] *and Rafael Cantera*[2,3]*

[1]Department of Evolutionary Neuroethology, Max Planck Institute for Chemical Ecology (MPG), Jena, Germany, [2]Departamento de Biología del Neurodesarrollo, Instituto de Investigaciones Biológicas Clemente Estable (IIBCE), Montevideo, Uruguay, [3]Zoology Department, Stockholm University, Stockholm, Sweden

Here we report on ultrastructural features of brain synapses in the fly *Drosophila melanogaster* and outline a perspective for the study of their functional significance. Images taken with the aid of focused ion beam-scanning electron microscopy (EM) at 20 nm intervals across olfactory glomerulus DA2 revealed that some synaptic boutons are penetrated by protrusions emanating from other neurons. Similar structures in the brain of mammals are known as synaptic spinules. A survey with transmission EM (TEM) disclosed that these structures are frequent throughout the antennal lobe. Detailed neuronal tracings revealed that spinules are formed by all three major types of neurons innervating glomerulus DA2 but the olfactory sensory neurons (OSNs) receive significantly more spinules than other olfactory neurons. Double-membrane vesicles (DMVs) that appear to represent material that has pinched-off from spinules are also most abundant in presynaptic boutons of OSNs. Inside the host neuron, a close association was observed between spinules, the endoplasmic reticulum (ER) and mitochondria. We propose that by releasing material into the host neuron, through a process triggered by synaptic activity and analogous to axonal pruning, synaptic spinules could function as a mechanism for synapse tagging, synaptic remodeling and neural plasticity. Future directions of experimental work to investigate this theory are proposed.

Keywords: olfactory circuitry, *Drosophila melanogaster*, synaptic spinules, FIB-SEM, synaptic plasticity

OPEN ACCESS

Edited by:
Frédéric Marion-Poll, AgroParisTech Institut des Sciences et Industries du Vivant et de l'Environnement, France

Reviewed by:
Ronald Sebastian Petralia, National Institute on Deafness and Other Communication Disorders (NIH), United States
Michael Fox, Virginia Tech Carilion Research Institute, United States

***Correspondence:**
Rafael Cantera
rafael.cantera@zoologi.su.se

Received: *16 January 2018*
Accepted: *12 March 2018*
Published: *27 March 2018*

Citation:
Gruber L, Rybak J, Hansson BS and Cantera R (2018) Synaptic Spinules in the Olfactory Circuit of Drosophila melanogaster. Front. Cell. Neurosci. 12:86. doi: 10.3389/fncel.2018.00086

INTRODUCTION

Research conducted in evolutionarily distant animals has contributed to our current understanding of olfactory synaptic circuits (Hildebrand and Shepherd, 1997; Ache and Young, 2005). The olfactory neuronal circuitry of the fly *Drosophila melanogaster* has been investigated successfully with anatomical, physiological, genetic and behavioral approaches and good models have been proposed to understand how chemosensory information is processed and how olfactory circuits contribute to learning and memory (Davis, 2004; Keene and Waddell, 2005; Fiala, 2007; Wilson, 2013; Guven-Ozkan and Davis, 2014; Hige, 2017).

This bounty of knowledge stood until recently in bright contrast to our insufficient understanding of the synaptic connections formed between the different cellular components of the olfactory neuronal network. Because of the small size of synapses and the need to map them in 3D across relatively large volumes of brain tissue, electron microscopy (EM) is necessary to map all synapses of the olfactory circuit. Progress in volume-based EM, image analysis, and automatic 3D reconstruction facilitates this challenging task and makes it possible to image

and analyze all synaptic sites in the volume spanning the region of interest (Helmstaedter, 2013; Schneider-Mizell et al., 2016; Zheng et al., 2017). These recent advances have already resulted in several publications reporting detailed information on olfactory microcircuits in *Drosophila* (Berck et al., 2016; Rybak et al., 2016; Takemura et al., 2017; Tobin et al., 2017).

We used focused ion beam-scanning EM (FIB-SEM; Knott et al., 2008) to acquire complete series of images taken at 20 nm intervals across the entire olfactory DA2 glomerulus in adult *Drosophila* females (Gruber et al., unpublished data). The ultimate goal is to obtain a complete connectome of this glomerulus, which plays an important ecological role since it senses the odorant geosmin, emitted by mold growing in rotten fruits, and mediates a life-saving escape in the fly (Stensmyr et al., 2012). In the course of our studies we observed that olfactory neurons form deep invaginations of their plasma membrane nearby synaptic sites, occupied by protrusions from other neurons, similar to what has been referred to as synaptic spinules in the mammalian brain and that had yet not been reported for *Drosophila*. Synaptic spinules are invaginating protrusions of variable size and morphology that penetrate presynaptic terminals and, less frequently, postsynaptic profiles, axons and even glia in the brain of mammals and other vertebrates (reviewed in Petralia et al., 2015). Synaptic spinules are dynamic structures that grow and proliferate following synaptic activity (Richards et al., 2005; Tao-Cheng et al., 2009) and have been suggested to contribute to membrane plasticity as well as to cell-to-cell communication and material exchange between neurons in an activity-dependent fashion (Petralia et al., 2015).

Our knowledge of these synapse-associated structures is still very limited. Here we present a viewpoint on this subject. We predict that spinules mediate localized synaptic plasticity mainly among olfactory sensory neurons (OSNs). Thus the finding of synaptic spinules in *Drosophila melanogaster* opens an avenue for an experimental investigation of their contribution and relevance for synapse plasticity, benefiting from the exceptional advantages offered by this organism.

RESULTS AND DISCUSSION

The observations reported here were done in the antennal lobe of female adults of *Drosophila melanogaster* studied with transmission electron microscopy (TEM, five specimens) and FIB-SEM (two specimens) across the entire DA2 glomerulus (see Supplementary Material). To achieve serial sections of this particular region with FIB-SEM it was marked previously by fiducial laser marks (see Supplementary Material). Images revealed that olfactory neurons make an interdigitating system of invaginating protrusions 20–500 nm in diameter close to active sites. Protrusions, emanating from one synaptic partner (the "protruding cell, PC"), penetrate the narrow funnels formed by deep invaginations of the plasma membrane of another synaptic partner (the "host cell, HC"; **Figures 1A,B**). The protrusions are therefore covered by two membranes: the evaginated membrane of the PC tightly covered by the invaginated membrane of the HC, which receives the protrusion (**Figure 1A**). FIB-SEM-based dense reconstructions (done with the TrakEM2 plugin for ImageJ Fiji[1]; see Supplementary Material) make it possible to study invaginating protrusions in different types of olfactory neurons, which were distinguished according to their morphology (branching pattern and diameter of single branches), their total volume inside one glomerulus and ultrastructural details (as for example their synaptic inventory of input and output synapses) and other criteria described previously (Rybak et al., 2016; Tobin et al., 2017). These criteria allow a clear identification of uniglomerular projection neurons (PNs) and olfactory receptor neurons (OSNs) whereas the remaining cell types were more difficult to distinguish and are described here with the generic term "multigomerular neurons" (MGs). Individual presynaptic boutons of olfactory neurons might receive protrusions from more than one neuron or cell type, most prominently seen in OSNs (**Figure 1B**), and mutually invaginating protrusions between two neurons were also observed (not shown) as reported previously for other olfactory glomeruli (Rybak et al., 2016; in Figures 5C,D). Many of invaginating protrusions traced to their fiber of origin were found to originate from other OSNs, whereas the remaining ones emanated either from MGs, which includes local interneurons and multiglomerular PNs (**Figure 1B**), or PNs (see Figures 5C,D in Rybak et al., 2016). The synaptic boutons of PNs were mostly devoid of protrusions (**Figures 1C,E**).

By size, shape and location these invaginating protrusions are interpreted here to be the type of structures which in mammalian brain have been designated as synaptic spinules (Petralia et al., 2015). They appear to be identical or very similar to invaginated profiles illustrated in images of *Drosophila* synapses in other brain neurons published by other authors, who did not name them explicitly (see for example Figures 4A,B in Leiss et al., 2009; Figure 3 in Butcher et al., 2012; Figure 1 in Berck et al., 2016; Figures 6D and Supplementary Figure S1A in Zheng et al., 2017). Our survey of several *Drosophila* brains with the aid of TEM confirmed that spinules are frequent throughout the antennal lobe (data not shown).

The spinules reported here contained cytoplasm and in many cases also clear and dark vesicles (**Figures 1A,D**, **2A,B**). The size of the spinules and that of their host boutons imply that spinules are in close vicinity with other organelles. Practically all spinules were observed in the proximity of presynaptic sites (**Figures 1**, **2**), mitochondria and what appeared to be cisternae of the endoplasmic reticulum (ER) of the HC (**Figures 1A,C,D**). In many cases spinules appeared to be in physical contact with mitochondria and ER. Therefore, spinules might be part of a recently well described neuronal ER network that includes contacts with the plasma membrane, mitochondria as well as lysosomes and multivesicular bodies (Wu et al., 2017). Similar connections between ER tubules and synaptic invaginations have been observed previously in presynaptic regions of visual receptor cells (Lovas, 1971). The close association between spinules, active sites and two major sources of Ca^{2+} might have functional consequences.

A quantification of every single spinule penetrating each randomly selected HC of each neuronal type (in one brain) inside

[1]https://imagej.net/TrakEM2

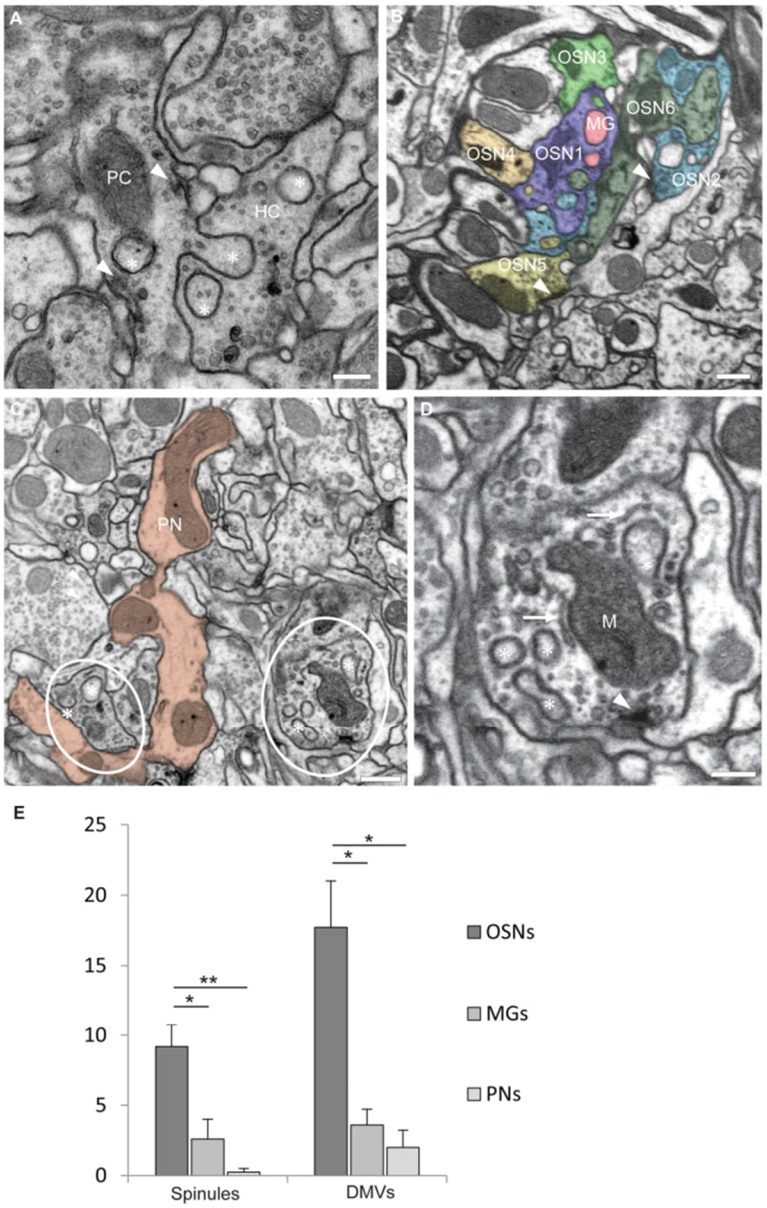

FIGURE 1 | Olfactory neurons in glomerulus DA2 contain invaginating protrusions. **(A)** Transmission electron microscopy (TEM) image of a 50 nm section showing examples of invaginating protrusions, or spinules (asterisks), enclosed by two plasma membranes and close to presynaptic sites (arrowheads). Notice that the evaginating membrane of the protruding cell (PC) is tightly adjoined by the invaginating membrane of the host cell (HC). Scale bar = 200 nm. **(B)** A synaptic bouton can receive invaginating protrusions from more than one neuron. This image from a focused ion beam-scanning EM (FIB-SEM) serial reconstruction of glomerulus DA2 depicts invaginating protrusions in presynaptic boutons of two different olfactory sensory neurons (OSN1 and OSN2) penetrated by protrusions from several neighboring cells. The PCs in this particular example are either a multiglomerular neuron (MG) or other OSNs (OSN3, 4, 5 and 6). Synaptic sites are indicated by an arrowhead and the reconstructed neurons are color-coded to assign the origin of the invaginated protrusions inside HCs. Scale bar = 500 nm. **(C)** Invaginating protrusions are not equally abundant among different types of olfactory neurons. This image (FIB-SEM) shows for example several boutons (red) of a uniglomerular projection neuron (PN), devoid of protrusions. In contrast, nearby OSN boutons (encircled) contain several protrusions (asterisks; see quantification in **E**).

(*Continued*)

FIGURE 1 | Continued
Scale bar = 500 nm. **(D)** FIB-SEM image showing invaginating protrusions (asterisks) close to mitochondria (M), putative endoplasmic reticulum (ER) cisternae (arrow) and a presynaptic site (arrowhead). For 3D surface view of spinules see **Figure 2B**. Scale bar = 200 nm. **(E)** Quantification of spinules and double-membrane vesicles (DMVs) found inside reconstructed OSNs ($n = 11$), Projection neurons (PNs) ($n = 4$) and MGs ($n = 5$). OSNs receive a larger number of spinules and DMVs compared to MGs and PNs. Quantification was done in one brain. Mean values with standard error of the mean are depicted. $^{*}p < 0.1$; $^{**}p < 0.01$, one-way ANOVA, Tukey *post hoc* test.

glomerulus DA2 indicated that OSNs receive spinules most frequently, MGs less frequently and PNs only rarely (**Figure 1E**). On the other hand, based on EM images published by others (Leiss et al., 2009; Butcher et al., 2012) we propose that PN presynaptic boutons, located in the calyx of the mushroom body, host abundant spinules protruding from their postsynaptic partners, the Kenyon cells.

The shape of spinules appeared to be variable. They were often relatively short and bulbous (**Figure 2A**) but sometimes more elongated, filopodium-like (**Figure 2B**) or varicose (**Figure 2C**) and even branched (**Figure 2C**). Inside their HCs synaptic spinules were closely associated with cellular entrapments of similar appearance and size, but not connected to other neurons and thus entirely embedded in the cytoplasm of the HC (**Figure 2A**). Similar to what is reported above for spinules, the two membranes in these "disconnected" profiles enclosed a cytosolic content with vesicles (**Figure 2A**). At synapses in the vertebrate brain, profiles of this type are called "double-membrane vesicles" (DMVs) and are considered to pinch-off from spinules (see for example Spacek and Harris, 2004; reviewed in Petralia et al., 2015). A quantification of DMVs in randomly selected host neurons (same as for spinule quantification) among the DA2 in one *Drosophila* brain (see Supplementary Material) revealed that, just like spinules, these structures are most abundant inside OSNs (**Figure 1E**), thus reinforcing the idea that they are derived from spinules. These vesicles appear to us to be clearly distinct from exosomes and other types of extracellular vesicles used by a variety of cell types and tissues to communicate at a distance through exchange of protein and RNA (Cocucci and Meldolesi, 2015; Budnik et al., 2016) secreted into the extracellular space with consequences for synaptic maintenance, plasticity and homeostasis (Korkut et al., 2009; Budnik et al., 2016; Ashley et al., 2018). A major difference between exosomes and the DMVs reported here is that the latter are delivered directly into the cytoplasm of the HC, enabling modification of the function of individual synapses, without affecting the function of other synapses of the same neuron.

The observation that some of the spinules observed in our reconstructed volume of glomerulus DA2 had a varicose shape might be relevant for a speculative interpretation of their functions. In *Drosophila*, during its metamorphosis from larva to adult, axonal and dendritic fibers become first varicose and subsequently subdivide into fragments in a process known as pruning, which is controlled by the steroid hormone ecdysone and triggered by Ca^{2+} (Yaniv and Schuldiner, 2016). We propose that in adult olfactory circuits synaptic-activity induced release of Ca^{2+} from mitochondria and ER, observed here to be in close proximity and contact to spinules at synaptic sites, could induce not only spinule growth and proliferation as previously proposed (Richards et al., 2005; Tao-Cheng et al., 2009; Ueda and Hayashi, 2013) but also spinule fragmentation inside the host neuron through a process analogous to the pruning of axonal terminals and dendritic branches during metamorphosis, with the difference that in this case the fragments are generated intracellularly and become DMVs in the HC.

It has been suggested that synaptic spinules mediate trans-synaptic exchange of material (reviewed in Petralia et al., 2015). Hence, activity-triggered spinule fragmentation mainly in OSNs could be the basis for localized synaptic plasticity, mediated by transference between synaptic partners of microRNA, proteins or other material (Edelstein and Smythies, 2014; Smalheiser, 2014; Busto et al., 2017) and affecting only one synaptic bouton of dozens present among the branches of a given neuron. This localized transference of material between OSNs and other neurons, at individual synaptic boutons that receive spinules and DMVs, could also mediate propagation of epigenetic changes and other modifications. It has been shown that spinules formation is induced by artificial generation of LTP (Toni et al., 1999; Stewart et al., 2005; Ueda and Hayashi, 2013). Concurrent synaptic activity dependent fragmentation of spinules could therefore be involved in synapse tagging and capture (Frey and Morris, 1997; Redondo and Morris, 2011) and would have functional consequences for future synaptic activity, including olfactory learning and memory processes.

Drosophila melanogaster, as a model organism, opens an avenue for future experimental investigations of the ideas outlined here. In a short perspective, experiments should be designed to demonstrate in a more conclusive way that the DMVs reported here are derived from the spinules and that this involves fragmentation of the spinules. Appropriate combinations of genetic labeling of pre- and postsynaptic neurons with different fluorophores and super resolution microscopy can be used for this aim. Screens of genetically tagged marker proteins or RNA, synthetized exclusively by one neuronal type and that ends up inside neurons which do not express the marker, would prove the exchange of material. Furthermore, decrease in activity-dependent spinule formation and fragmentation after blockage of mitochondrial Ca^{2+} release would prove our suggestion of this interplay.

Exchange of material via DMVs might serve synaptic tagging, which is a prerequisite for remodeling and plasticity of individual synapses within a dendritic tree. In the fly visual system it was shown that synaptogenesis correlates with the appearance of mutual invaginations in photoreceptor terminals within a short time window (Rybak and Meinertzhagen, 1997). Using fluorescent markers for pre- and postsynaptic partners in a genetically controlled system (Chen et al., 2014), in combination with the visualization of spinules, correlated cellular activity of spinules and synaptic turnover could be demonstrated. In a longer perspective, using transgenic flies to block spinule fragmentation after synaptic activity, complemented by behavioral assays, will help us understand

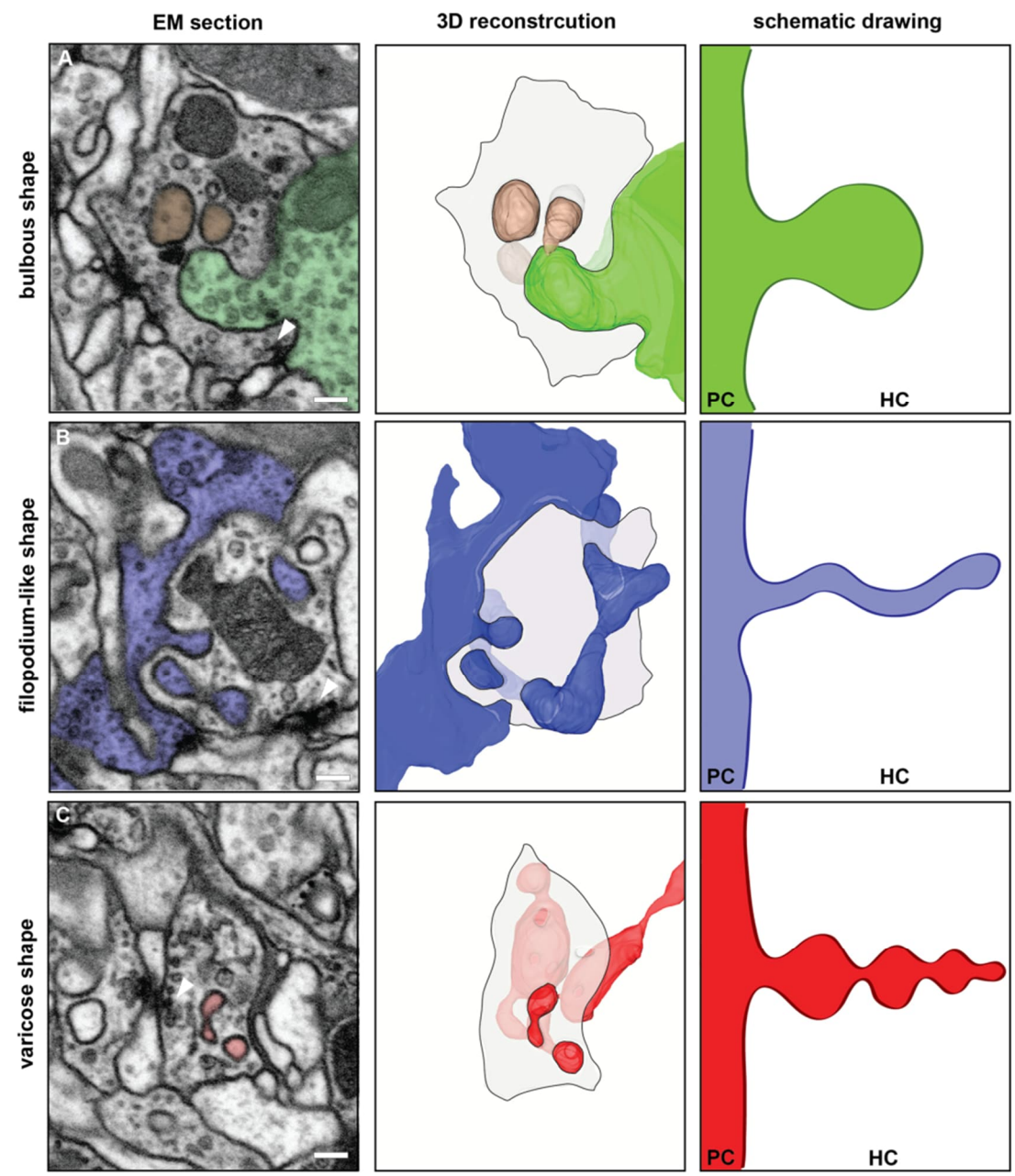

FIGURE 2 | FIB-SEM based 3D reconstructions of synaptic spinules disclosed their morphological diversity. The left column shows single images from the FIB-SEM-series used for the 3D reconstructions illustrated in the middle column. The reconstructed spinules and their cells of origin are colored in green **(A)**, blue **(B)** or red **(C)** DMVs are shown in brown **(A)**. Spinules and DMVs are close to presynaptic sites (arrowheads). Scale bar = 200 nm. The middle column shows surface views of the 3D reconstructions with the same color code. The HC is illustrated by a transparent shaded area, representing one section plane of the HC neurite, outlined with a black line. The right column shows schematic drawings of the different morphological types of spinules, emanating from the PC and growing into the HC, to illustrate the morphological diversity of synaptic spinules found here in glomerulus DA2. **(A)** The HC is an OSN containing a bulbous spinule (green) and two DMVs (brown) most likely pinched-off from the spinule. **(B)** shows an example of a filopodium-like spinule (blue) and **(C)** a varicose spinule (red).

whether the trans-synaptic exchange of material through this novel mechanism has consequences for learning and memory.

AUTHOR CONTRIBUTIONS

RC, LG and JR conceived and designed the study and the outline for this perspective. Experiments and analyses were planned by JR and LG and performed by LG. LG, JR and RC interpreted and evaluated the data. Figures of this article were prepared by LG. LG, RC, JR and BSH wrote and discussed the manuscript. All authors critically revised the article.

FUNDING

This project was funded by the Max-Planck-Society, Aura Optik (Jena) and the Agencia Nacional de Investigación e Innovación (Uruguay).

ACKNOWLEDGMENTS

We would like to thank Michael Steinert and Thomas Pertsch from the Abbe Center of Photonics, Jena, for their expert assistance with FIB-SEM. We are grateful to Katrin Buder (Leibniz Institute of Aging, Fritz-Lipmann Institute, Jena) for cooperative work in developing the EM protocol. For support and fruitful discussions we are grateful to Roland Kilper (Aura Optik, Jena), Sandor Nietzsche (Electron Microscopic Centrum, Jena), Katrin Buder (Leibniz Institute of Aging, Fritz-Lipmann Institute, Jena) and Veit Grabe (Max Planck Institute for Chemical Ecology).

SUPPLEMENTARY MATERIAL

The Supplementary Material for this article can be found online at: https://www.frontiersin.org/articles/10.3389/fncel.2018.00086/full#supplementary-material

REFERENCES

Ache, B. W., and Young, J. M. (2005). Olfaction: diverse species, conserved principles. *Neuron* 48, 417–430. doi: 10.1016/j.neuron.2005.10.022

Ashley, J., Cordy, B., Lucia, D., Fradkin, L. G., Budnik, V., and Thomson, T. (2018). Retrovirus-like gag protein Arc1 binds RNA and traffics across synaptic boutons. *Cell* 172, 262.e11–274.e11. doi: 10.1016/j.cell.2017.12.022

Berck, M. E., Khandelwal, A., Claus, L., Hernandez-Nunez, L., Si, G., Tabone, C. J., et al. (2016). The wiring diagram of a glomerular olfactory system. *Elife* 5:e14859. doi: 10.7554/eLife.14859

Budnik, V., Ruiz-Cañada, C., and Wendler, F. (2016). Extracellular vesicles round off communication in the nervous system. *Nat. Rev. Neurosci.* 17, 160–172. doi: 10.1038/nrn.2015.29

Busto, G. U., Guven-Ozkan, T., and Davis, R. L. (2017). MicroRNA function in *Drosophila* memory formation. *Curr. Opin. Neurobiol.* 43, 15–24. doi: 10.1016/j.conb.2016.10.002

Butcher, N. J., Friedrich, A. B., Lu, Z., Tanimoto, H., and Meinertzhagen, I. A. (2012). Different classes of input and output neurons reveal new features in microglomeruli of the adult *Drosophila* mushroom body calyx. *J. Comp. Neurol.* 520, 2185–2201. doi: 10.1002/cne.23037

Chen, Y., Akin, O., Nern, A., Tsui, C. Y. K., Pecot, M. Y., and Zipursky, S. L. (2014). Cell-type-specific labeling of synapses *in vivo* through synaptic tagging with recombination. *Neuron* 81, 280–293. doi: 10.1016/j.neuron.2013.12.021

Cocucci, E., and Meldolesi, J. (2015). Ectosomes and exosomes: shedding the confusion between extracellular vesicles. *Trends Cell Biol.* 25, 364–372. doi: 10.1016/j.tcb.2015.01.004

Davis, R. L. (2004). Olfactory learning. *Neuron* 44, 31–48. doi: 10.1016/j.neuron.2004.09.008

Edelstein, L., and Smythies, J. (2014). The role of epigenetic-related codes in neurocomputation: dynamic hardware in the brain. *Philos. Trans. R. Soc. Lond. B Biol. Sci.* 369:20130519. doi: 10.1098/rstb.2013.0519

Fiala, A. (2007). Olfaction and olfactory learning in *Drosophila*: recent progress. *Curr. Opin. Neurobiol.* 17, 720–726. doi: 10.1016/j.conb.2007.11.009

Frey, U., and Morris, R. G. (1997). Synaptic tagging and long-term potentiation. *Nature* 385, 533–536. doi: 10.1038/385533a0

Guven-Ozkan, T., and Davis, R. L. (2014). Functional neuroanatomy of *Drosophila* olfactory memory formation. *Learn. Mem.* 21, 519–526. doi: 10.1101/lm.034363.114

Helmstaedter, M. (2013). Cellular-resolution connectomics: challenges of dense neural circuit reconstruction. *Nat. Methods* 10, 501–507. doi: 10.1038/nmeth.2476

Hige, T. (2017). What can tiny mushrooms in fruit flies tell us about learning and memory? *Neurosci. Res.* doi: 10.1016/j.neures.2017.05.002 [Epub ahead of print].

Hildebrand, J. G., and Shepherd, G. M. (1997). Mechanisms of olfactory discrimination: converging evidence for common principles across phyla. *Annu. Rev. Neurosci.* 20, 595–631. doi: 10.1146/annurev.neuro.20.1.595

Keene, A. C., and Waddell, S. (2005). *Drosophila* memory: dopamine signals punishment? *Curr. Biol.* 15, R932–R934. doi: 10.1016/j.cub.2005.10.058

Knott, G., Marchman, H., Wall, D., and Lich, B. (2008). Serial section scanning electron microscopy of adult brain tissue using focused ion beam milling. *J. Neurosci.* 28, 2959–2964. doi: 10.1523/JNEUROSCI.3189-07.2008

Korkut, C., Ataman, B., Ramachandran, P., Ashley, J., Barria, R., Gherbesi, N., et al. (2009). Trans-synaptic transmission of vesicular Wnt signals through Evi/Wntless. *Cell* 139, 393–404. doi: 10.1016/j.cell.2009.07.051

Leiss, F., Groh, C., Butcher, N. J., Meinertzhagen, I. A., and Tavosanis, G. (2009). Synaptic organization in the adult *Drosophila* mushroom body calyx. *J. Comp. Neurol.* 517, 808–824. doi: 10.1002/cne.22184

Lovas, B. (1971). Tubular networks in the terminal endings of the visual receptor cells in the human, the monkey, the cat and the dog. *Z. Zellforsch. Mikrosk. Anat.* 121, 341–357. doi: 10.1007/bf00337638

Petralia, R. S., Wang, Y. X., Mattson, M. P., and Yao, P. J. (2015). Structure, distribution, and function of neuronal/synaptic spinules and related invaginating projections. *Neuromolecular Med.* 17, 211–240. doi: 10.1007/s12017-015-8358-6

Redondo, R. L., and Morris, R. G. (2011). Making memories last: the synaptic tagging and capture hypothesis. *Nat. Rev. Neurosci.* 12, 17–30. doi: 10.1038/nrn2963

Richards, D. A., Mateos, J. M., Hugel, S., de Paola, V., Caroni, P., Gähwiler, B. H., et al. (2005). Glutamate induces the rapid formation of spine head protrusions in hippocampal slice cultures. *Proc. Natl. Acad. Sci. U S A* 102, 6166–6171. doi: 10.1073/pnas.0501881102

Rybak, J., and Meinertzhagen, I. A. (1997). The effects of light reversals on photoreceptor synaptogenesis in the fly *Musca domestica*. *Eur. J. Neurosci.* 9, 319–333. doi: 10.1111/j.1460-9568.1997.tb01402.x

Rybak, J., Talarico, G., Ruiz, S., Arnold, C., Cantera, R., and Hansson, B. S. (2016). Synaptic circuitry of identified neurons in the antennal lobe of *Drosophila melanogaster*. *J. Comp. Neurol.* 524, 1920–1956. doi: 10.1002/cne.23966

Schneider-Mizell, C. M., Gerhard, S., Longair, M., Kazimiers, T., Li, F., Zwart, M. F., et al. (2016). Quantitative neuroanatomy for connectomics in *Drosophila*. *Elife* 5:e12059. doi: 10.7554/eLife.12059

Smalheiser, N. R. (2014). The RNA-centred view of the synapse: non-coding RNAs and synaptic plasticity. *Philos. Trans. R. Soc. Lond. B Biol. Sci.* 369:20130504. doi: 10.1098/rstb.2013.0504

Spacek, J., and Harris, K. M. (2004). Trans-endocytosis via spinules in adult rat hippocampus. *J. Neurosci.* 24, 4233–4241. doi: 10.1523/JNEUROSCI.0287-04.2004

Stensmyr, M. C., Dweck, H. K., Farhan, A., Ibba, I., Strutz, A., Mukunda, L., et al. (2012). A conserved dedicated olfactory circuit for detecting harmful microbes in *Drosophila*. *Cell* 151, 1345–1357. doi: 10.1016/j.cell.2012.09.046

Stewart, M. G., Medvedev, N. I., Popov, V. I., Schoepfer, R., Davies, H. A., Murphy, K., et al. (2005). Chemically induced long-term potentiation increases the number of perforated and complex postsynaptic densities but does not alter dendritic spine volume in CA1 of adult mouse hippocampal slices. *Eur. J. Neurosci.* 21, 3368–3378. doi: 10.1111/j.1460-9568.2005.04174.x

Takemura, S. Y., Aso, Y., Hige, T., Wong, A., Lu, Z., Xu, C. S., et al. (2017). A connectome of a learning and memory center in the adult *Drosophila* brain. *Elife* 6:e26975. doi: 10.7554/eLife.26975

Tao-Cheng, J. H., Dosemeci, A., Gallant, P. E., Miller, S., Galbraith, J. A., Winters, C. A., et al. (2009). Rapid turnover of spinules at synaptic terminals. *Neuroscience* 160, 42–50. doi: 10.1016/j.neuroscience.2009.02.031

Tobin, W. F., Wilson, R. I., and Lee, W. A. (2017). Wiring variations that enable and constrain neural computation in a sensory microcircuit. *Elife* 6:e24838. doi: 10.7554/eLife.24838

Toni, N., Buchs, P. A., Nikonenko, I., Bron, C. R., and Muller, D. (1999). LTP promotes formation of multiple spine synapses between a single axon terminal and a dendrite. *Nature* 402, 421–425. doi: 10.1038/46574

Ueda, Y., and Hayashi, Y. (2013). PIP_3 regulates spinule formation in dendritic spines during structural long-term potentiation. *J. Neurosci.* 33, 11040–11047. doi: 10.1523/JNEUROSCI.3122-12.2013

Wilson, R. I. (2013). Early olfactory processing in *Drosophila*: mechanisms and principles. *Annu. Rev. Neurosci.* 36, 217–241. doi: 10.1146/annurev-neuro-062111-150533

Wu, Y., Whiteus, C., Xu, C. S., Hayworth, K. J., Weinberg, R. J., Hess, H. F., et al. (2017). Contacts between the endoplasmic reticulum and other membranes in neurons. *Proc. Natl. Acad. Sci. U S A* 114, E4859–E4867. doi: 10.1073/pnas.1701078114

Yaniv, S. P., and Schuldiner, O. (2016). A fly's view of neuronal remodeling. *Wiley Interdiscip. Rev. Dev. Biol.* 5, 618–635. doi: 10.1002/wdev.241

Zheng, Z., Lauritzen, J. S., Perlman, E., Robinson, C. G., Nichols, M., Milkie, D., et al. (2017). A complete electron microscopy volume of the brain of adult *Drosophila Melanogaster*. *bioRxiv* 140905. doi: 10.1101/140905

Conflict of Interest Statement: The authors declare that the research was conducted in the absence of any commercial or financial relationships that could be construed as a potential conflict of interest.

CHAPTER 3

Inverse resource allocation between vision and olfaction across the genus *Drosophila*

Ian W. Keesey, Veit Grabe, Lydia Gruber, Sarah Koerte, George F. Obiero, Grant Bolton, Mohammed A. Khallaf, Grit Kunert, Sofia Lavista-Llanos, Dario Riccardo Valenzano, Jürgen Rybak, Bruce A. Barrett, Markus Knaden and Bill S. Hansson

Nature Communication

Published online on March 11, 2019

FORM 1

Manuscript No. Manuscript III

Manuscript title:

Inverse resource allocation between vision and olfaction across the genus *Drosophila*

Authors:

Ian W. Keesey, Veit Grabe, Lydia Gruber, Sarah Koerte, George F. Obiero, Grant Bolton, Mohammed A. Khallaf, Grit Kunert, Sofia Lavista-Llanos, Dario Riccardo Valenzano, Jürgen Rybak, Bruce A. Barrett, Markus Knaden1 & Bill S. Hansson

Bibliographic information:

Keesey, I. W., Grabe, V., Gruber, L., Koerte, S., Obiero, G. F., Bolton, G., . . . Hansson, B. S. (2019). Inverse resource allocation between vision and olfaction across the genus Drosophila. *Nature Communications, 10*(1), 1162. doi:10.1038/s41467-019-09087-z

The candidate is (Please tick the appropriate box.)

☐ First author, ☐ Co-first author, ☐ Corresponding author, ☒ Co-author.

Status: published

Authors' contributions (in %) to the given categories of the publication

Author	Conceptual	Data analysis	Experimental	Writing the manuscript	Provision of material
Keesey, I.W.	50%	60%	30%	80%	-
Grabe, V.	20%	10%	20%	-	-
Gruber, L.	**10%**	**10%**	**15%**	-	-
Koerte, S.	5%	5%	10%	5%	-
Obiero, G.F.	-	-	5%	-	-
Bolton, G.	-	-	5%	-	-
Khallaf, M.A.	-	-	5%	-	-
Kunert, G.	-	2.5%	-	-	-
Lavista-Llanos, S.	-	-	2.5%	-	-
Valenzano, D.R.	-	2.5%	-	-	-
Rybak, J.	5%	-	2.5%	-	-
Barrett, B.A.	-	-	5%	-	-
Hansson, B.S.	5%	-	-	5%	100%
Knaden, M.	5%	-	-	10%	-
Total:	100%	100%	100%	100%	100%

_____ _____

Signature candidate Signature supervisor (member of the Faculty)

nature COMMUNICATIONS

ARTICLE

https://doi.org/10.1038/s41467-019-09087-z OPEN

Inverse resource allocation between vision and olfaction across the genus *Drosophila*

Ian W. Keesey[1], Veit Grabe[1], Lydia Gruber[1], Sarah Koerte[1], George F. Obiero[1,2], Grant Bolton[3], Mohammed A. Khallaf[1], Grit Kunert[4], Sofia Lavista-Llanos[1], Dario Riccardo Valenzano[5], Jürgen Rybak[1], Bruce A. Barrett[3], Markus Knaden[1] & Bill S. Hansson[1]

Divergent populations across different environments are exposed to critical sensory information related to locating a host or mate, as well as avoiding predators and pathogens. These sensory signals generate evolutionary changes in neuroanatomy and behavior; however, few studies have investigated patterns of neural architecture that occur between sensory systems, or that occur within large groups of closely-related organisms. Here we examine 62 species within the genus *Drosophila* and describe an inverse resource allocation between vision and olfaction, which we consistently observe at the periphery, within the brain, as well as during larval development. This sensory variation was noted across the entire genus and appears to represent repeated, independent evolutionary events, where one sensory modality is consistently selected for at the expense of the other. Moreover, we provide evidence of a developmental genetic constraint through the sharing of a single larval structure, the eye-antennal imaginal disc. In addition, we examine the ecological implications of visual or olfactory bias, including the potential impact on host-navigation and courtship.

[1] Max Planck Institute for Chemical Ecology, Department of Evolutionary Neuroethology, Hans-Knöll-Straße 8, D-07745 Jena, Germany. [2] Department of Biochemistry and Biotechnology, Technical University of Kenya, Haille-Sellasie Avenue, Workshop Road, 0200 Nairobi, Kenya. [3] University of Missouri, Division of Plant Sciences, 3-22I Agriculture Building, Columbia, Missouri 65211, USA. [4] Max Planck Institute for Chemical Ecology, Department of Biochemistry, Hans-Knöll-Straße 8, D-07745 Jena, Germany. [5] Max Planck Institute for Biology of Ageing and CECAD at University of Cologne, Joseph-Stelzmann-Str 9b and 26, Cologne 50931, Germany. These authors jointly supervised this work: Markus Knaden, Bill S. Hansson. Correspondence and requests for materials should be addressed to M.K. (email: mknaden@ice.mpg.de) or to B.S.H. (email: hansson@ice.mpg.de)

A pivotal question in neuroscience focuses on how the morphology and structure of the brain relates to its function and thereby its behavioral relevance. Neuroscience in general utilizes a wide array of techniques, including both genetics and neuroanatomical imaging, in order to unravel neural mechanisms underlying animal behavior and to understand how these circuits translate into the natural behaviors that are associated with an animal's specific ecological niche, for example, in regard to decisions concerning host navigation or mate selection[1].

One of the ultimate goals of neuroethology is to understand the principles organizing and defining these complex neural circuits, both from an ecological as well as an evolutionary perspective, and to decipher how the brain processes information while guiding behavioral responses toward naturally occurring stimuli. Previous research has supported the notion that structural size in a sensory phenotype correlates with its functional significance, for example, the reduction of sight in cave fish[2,3], the enlarged ears of echolocating bats[4–6], or the enlarged eyes of predatory birds[7]. Moreover, neuroanatomical studies have also shown that the size of each brain region corresponds to the organism's morphological specialization, thus for example, the smaller the eyes, the less importance of visual stimuli, and the smaller the brain region dedicated toward vision[2,3]. Other studies have also sought to associate sensory size with behavioral or ecological importance, such as the enlarged male-specific macroglomerular complex (MGC) in the Lepidoptera[8,9], the enlarged DM2 glomerulus in *Drosophila sechellia*[10], or an enlarged glomerulus based on the number of OSNs or synapses[11,12]. In each of these cases, the enlarged structure is indicative of the importance of a particular ecological stimulus, and moreover, that the relative morphological size of a sensory structure relates to its importance. However, just as studying a single neuron will not be sufficient to understand the function of the whole brain, the study of a single animal species will not be sufficient to address overarching ecological and evolutionary questions. Consequently, as the field of neuroethology moves in the direction of understanding and incorporating the roles of multimodal signals for behavioral decision-making (i.e., visual, olfactory, gustatory, mechanosensory, and auditory cues), similarly, neuroethology is also beginning to examine a multitude of closely related animal species for evolutionary comparisons of morphology, behavior, and adaptation[13–15], which can help identify the selective pressures that drive these changes in sensory systems and neural development or neural plasticity.

One of the original genetic model organisms, the vinegar fly, *Drosophila melanogaster*, has been a workhorse of advanced genetics for the last several decades. The advantage of this invertebrate model is attributed to its short generation time, ease of colony establishment in the laboratory, the huge diversity of available molecular and genetic tools, as well as the immense efforts toward the complete mapping of neural circuits for both the adult and the larvae of this one species[16–18]. However, the genus *Drosophila* also provides between 1200 and 1500 individual species, with an ecology spanning nearly every imaginable environment and host choice, from deserts to forests, from islands to mountains, and across incredibly unique or specialized food resources, such as the gills of land crabs, protein sources within bat guano, or otherwise toxic fruits;[10,15,19–21] therefore, the potential to transform an already powerful model organism from a singular species into an entire genus is now possible due to the recent advances in cellular and genetic tools for examining the complex neurological mechanisms of natural behavior in novel, non-model species. Moreover, the expansion from a single species into an entire genus affords scientists the opportunity to address larger ecological, developmental, and evolutionary questions using the full gamut of molecular and genetic tools that have already been generated for *D. melanogaster*. Research into non-*melanogaster* species is already well underway, with researchers beginning to highlight individual species, often selecting those based on economic impact or behavioral specialization[22–27], with studies now also including CRISPR-cas9, the powerful gene editing tool, such as the studies in *D. suzukii*, *D. subobscura*, *D. simulans*, and *D. pseudoobscura*[28–31].

An emerging integrative field of the biological study, called ecological evolutionary developmental biology, or more commonly known as eco-evo-devo, focuses on the underlying interactions between an organism's environment, its genes, as well as its development in regard to how these three factors shape evolutionary trends and help create a map or framework for better understanding and predicting speciation[32–35]. The field of eco-evo-devo is built on the premise that evolution is animal development controlled by ecological and environmental forces. Thus with the above-mentioned factors in mind, one of the goals of the present study is to encourage the expansion of the *D. melanogaster* model to become the *Drosophila* system, and thereby encompass a broader array of species within this genus for comparative, ecological research into what drives the evolution of the nervous system.

Based on the many examples from the animal kingdom as well as our previous observations from a number of Drosophilid species[27,36], we set out to test the hypothesis that sensory systems occupy a restricted niche in the nervous system of these flies, where relative size and energy allocation prevents one sense from expanding without having an effect on another. Also, as an entry to creating a larger ecological and evolutionary framework for this genus of flies, our study samples a wide, phylogenetic array of 62 different species within the genus *Drosophila*, and begins to analyze both host navigation and mate selection or courtship with regard specifically toward visual and olfactory sensory modalities. This study includes investigation at the periphery, such as morphometrics of the antenna and compound eye, as well as measurements within the antennal lobe (AL), optic lobe (OL), and the central brain for each selected species. This phylogenetic comparative approach allows for a more precise study of adaptation, and making these interspecific comparisons allows us to assess the general rules governing evolutionary phenomena via observations of repeated, independent evolutionary events within a group of organisms.

In our study, we identify a consistent, inverse resource allocation between vision and olfaction across these 62 species, and we use a combination of phylogenetic, phenotypic as well as developmental data in order to examine the evolutionary pressures and constraints underlying this potential tradeoff between two critically important sensory structures in regard to both host navigation and mate selection.

Results

Phylogeny, species selection, and general morphometrics. An array of 62 species within the Dipteran family Drosophilidae were selected to span the diversity contained within the genus *Drosophila* (Fig. 1a, b). This genus of flies covers a multitude of hosts and host ranges, including examples such as rotten fruits, cacti, flowers, tree sap, and mushrooms. Each species was measured for a number of physical metrics, including body size, head size, eye surface area, and the surface area of the third antennal segment (the funiculus) (Supplementary Figure 1A). In general, there was a huge variety of physical sizes noted within this single genus of flies, providing much more variability in absolute or overall size between species than we initially anticipated. Not surprisingly, as fly species increased in either body or head size, eye surface area and funiculus surface area

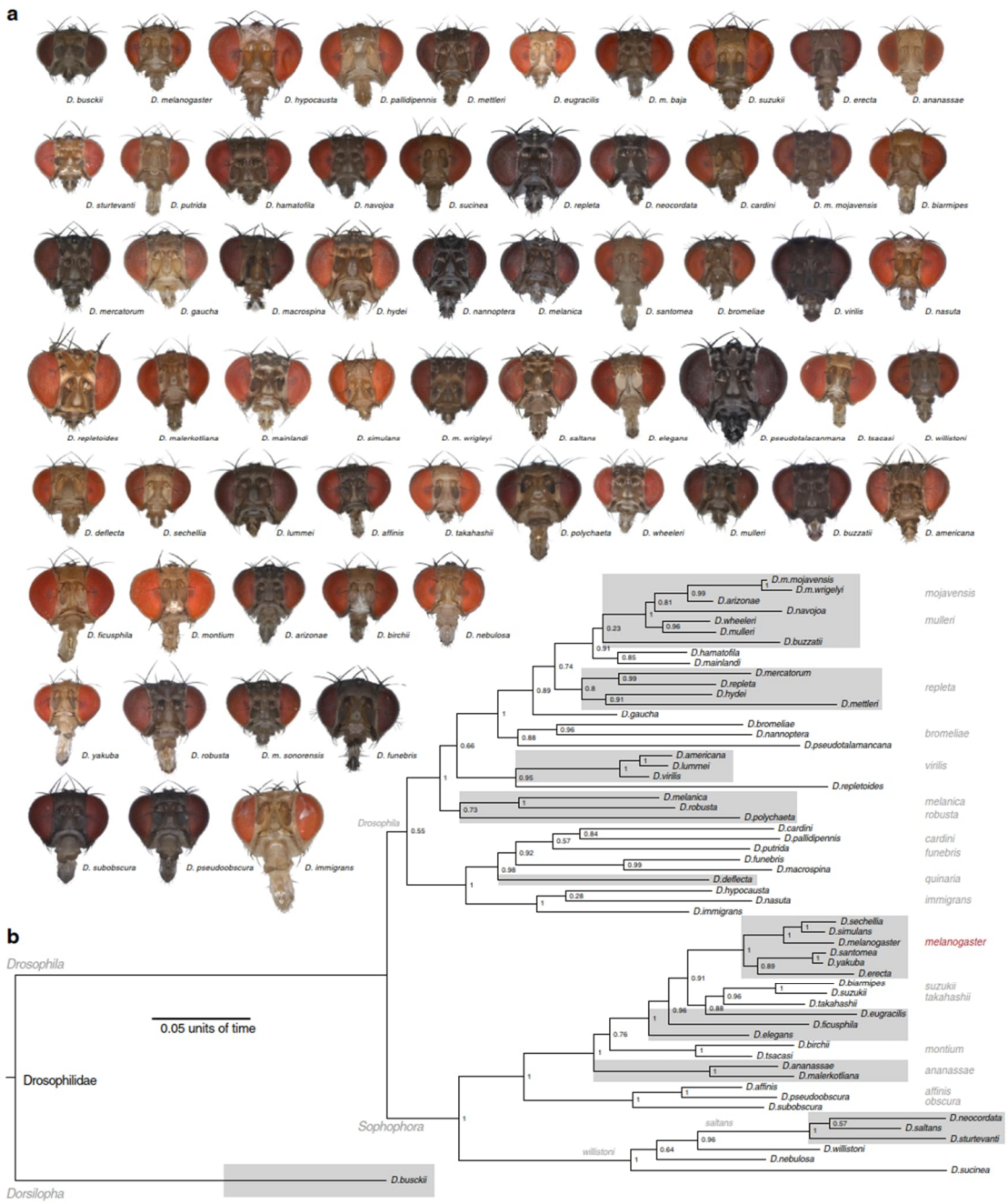

Fig. 1 Frontal head images of all tested *Drosophila* species and their associated phylogeny. **a** Frontal view of the head of all 62 species, illustrating the diversity in overall size, as well as in the variance of the visual and olfactory sensory systems across this genus. Also worth noting is the disparity in pigmentation that extends across the whole head, including the antenna and the compound eye. **b** Phylogeny of 59 species of *Drosophila* where genetic material was available for use in this study (*D. montium* and two subspecies of *D. mojavensis* are missing). Species were selected to span the width of subgroups and represent the genetic diversity within this genus of insect. Some species are denoted with gray boxes to provide more visual separation between subgroups. (Data are provided at https://doi.org/10.17617/3.1D)

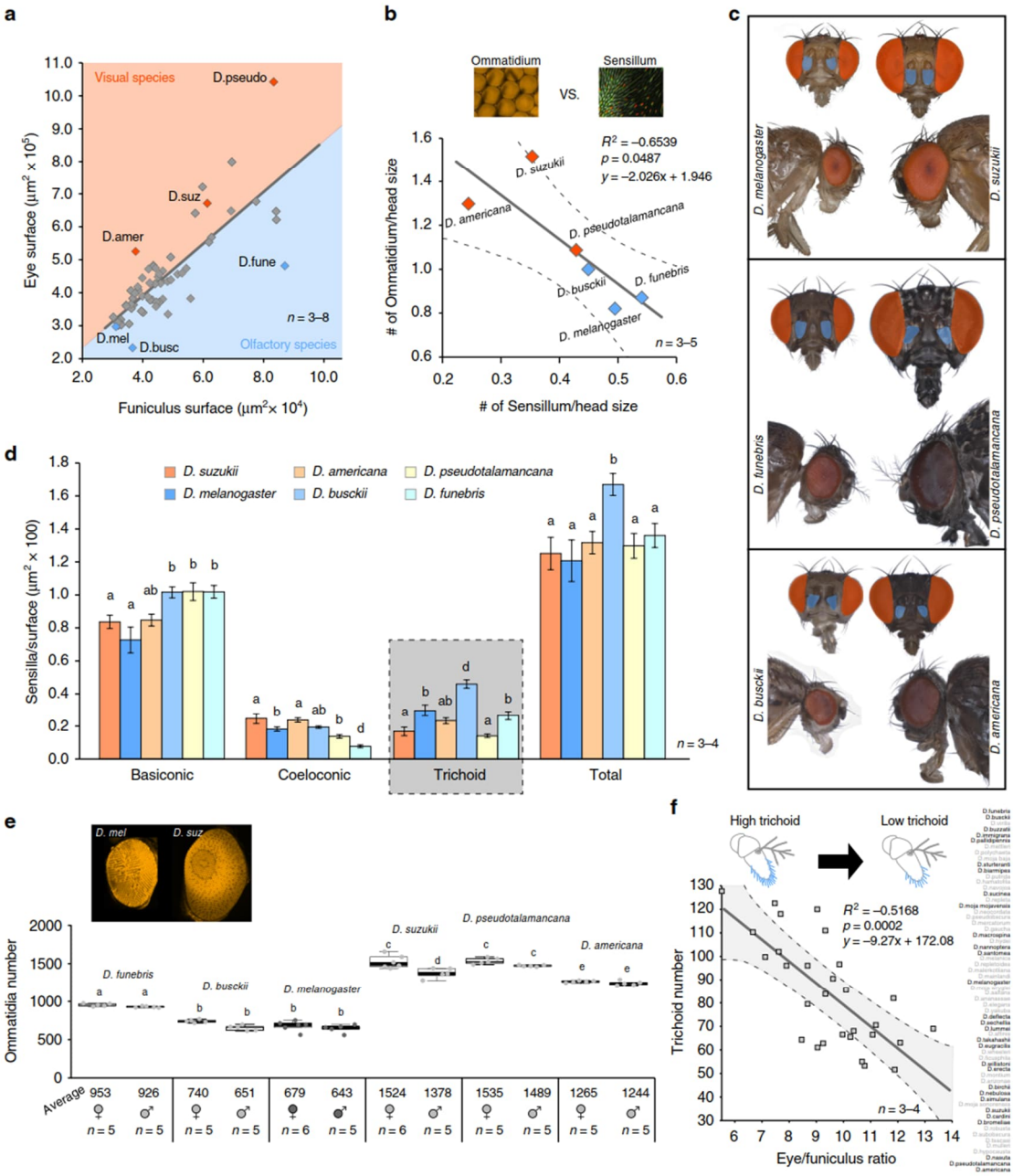

both increased as well, with head size always having a tighter positive correlation than body size for both eye and antennal metrics (Supplementary Figure 1). However, there was also quite a bit of variability in these sensory structures, both among similar body sizes and between flies with similar eye or funiculus sizes (Supplementary Figure 1). Here, we found that the eye and funiculus surface area scale isometrically with respect to both the body and head measurements (Supplementary Figure 1H); moreover, that the variance in these two sensory systems could not be explained by the absolute size of a species.

Ommatidium and sensillum comparisons among main species. For more in-depth comparison, we next sought to compare the sensory regions associated with visual and olfactory stimuli (Fig. 2a), and while again there was a general trend across the 62 species that larger insects had both larger eye surface area and larger funiculus surface area, there was still significant variability between these two sensory systems that was not explained by body or head size alone (Supplementary Figure 1H, I). From our robust array of species, we selected six Drosophilids for a more in-depth analysis of their sensory structures (Fig. 2a). These six

Fig. 2 External comparison of visual and olfactory system. Red color signifies vision or predicted visual bias, while blue indicates olfaction or potential olfactory bias. **a** All 62 species measured for eye and funiculus surface area, where six species were selected for additional measurements. These flies were selected to compare species with similar antennal surface area but contrasting eye sizes (e.g., *D. pseudotalamancana* and *D. funebris*, or *D. americana* and *D. busckii*) or species with similar eye size but contrasting antennal sizes (e.g., *D. americana* and *D. funebris*). We also selected two well-established species, *D. melanogaster* and *D. suzukii*, for an additional comparison and points of reference. **b** Inverse correlation between ommatidium number and sensillum number when corrected for head size from six species of *Drosophila*, suggesting a possible tradeoff between these sensory systems at the periphery. **c** All species were photographed for more detailed measurements of eye and antennal features across several frontal and lateral views. Highlighted in blue are the antennal surface area, and in red, the eye surface area. **d** Shown are the sensillum density metrics taken from stacked lambda mode scans (maximum intensity projections) of the anterior portion of the antenna for all six species examined, identifying strong differences for example in trichoid sensillum density, where potentially olfactory biased species (in blue) showed the significantly larger trichoid densities. Error bars represent standard deviation. **e** Ommatidium counts from each species, which illustrates the large differences in visual capabilities across this genus of fly, with some species having 2–3 times larger eyes. Boxplots represent the median (bold black line), quartiles (boxes), as well as the confidence intervals (whiskers). **d**, **e** Means with the same letter are not significantly different from each other (ANOVA with Tukey–Kramer multiple comparison test). **f** Expanded study to include additional species (that were selected using stratified random sampling), where we show that trichoids are consistently and inversely correlated with increasing eye-to funiculus ratio across the entire genus. (Data are provided at https://doi.org/10.17617/3.1D)

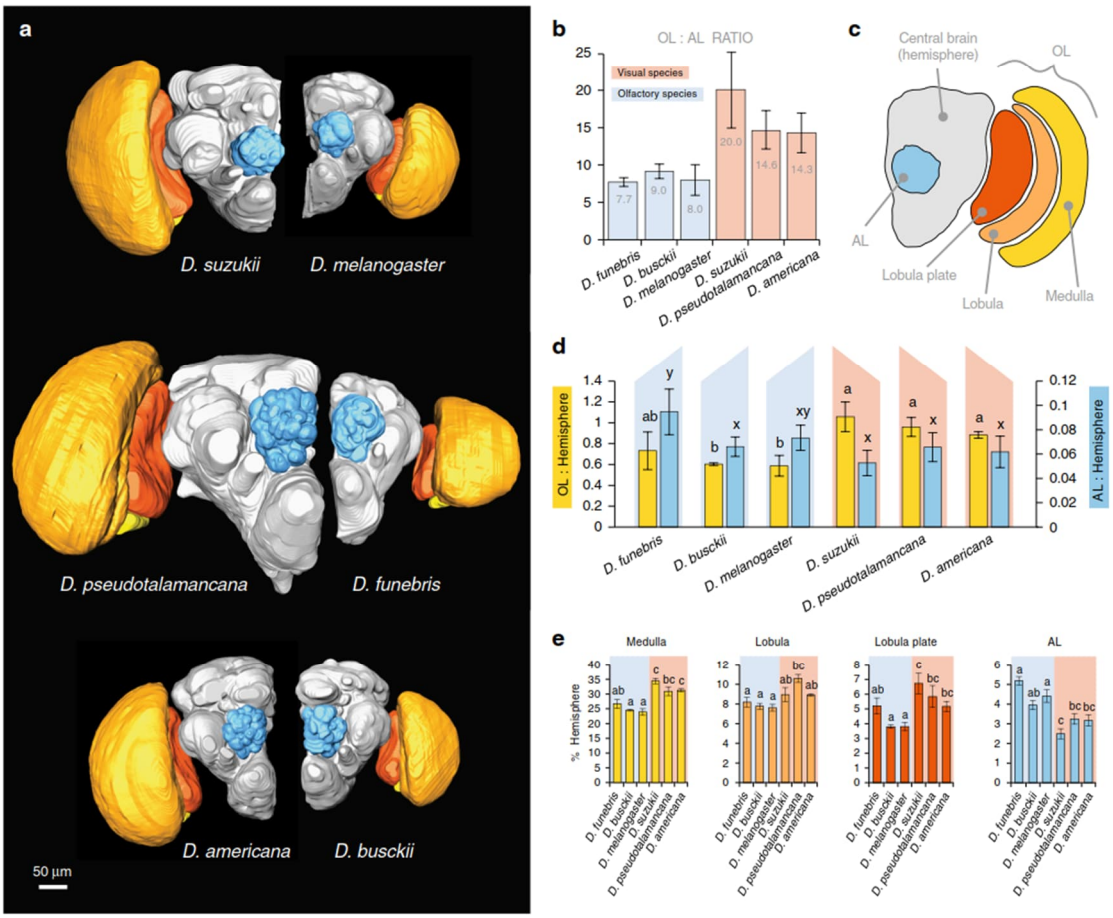

Fig. 3 Three-dimensional reconstructions of the visual and olfactory neuropils in six *Drosophila*. Red to yellow (warm) color signifies vision or visual bias, while blue indicates olfaction or olfactory species. **a** Whole brain reconstructions, highlighting visual (yellow to red) and olfactory (blue) regions, with central brain in gray. **b** The optic lobe (OL) to antennal lobe (AL) ratio for each species, showing the division between olfactory and visual bias among species. **c** Diagram of all measured volumes for comparison between species. **d** Relative sizes of OL (yellow) and AL (blue) as compared to the central brain, where the data show an inverse correlation between visual or olfactory investment. **e** Separate regions of OL and AL that were measured as a percentage of the central brain to provide a comparable value between insects of differing absolute size, again highlighting that brain regions mirror external measurements of visual or olfactory size bias. **d**, **e** Means with the same letter are not significantly different from each other (ANOVA with Tukey–Kramer multiple comparison test). Error bars represent standard deviation. (Data are provided at https://doi.org/10.17617/3.1D)

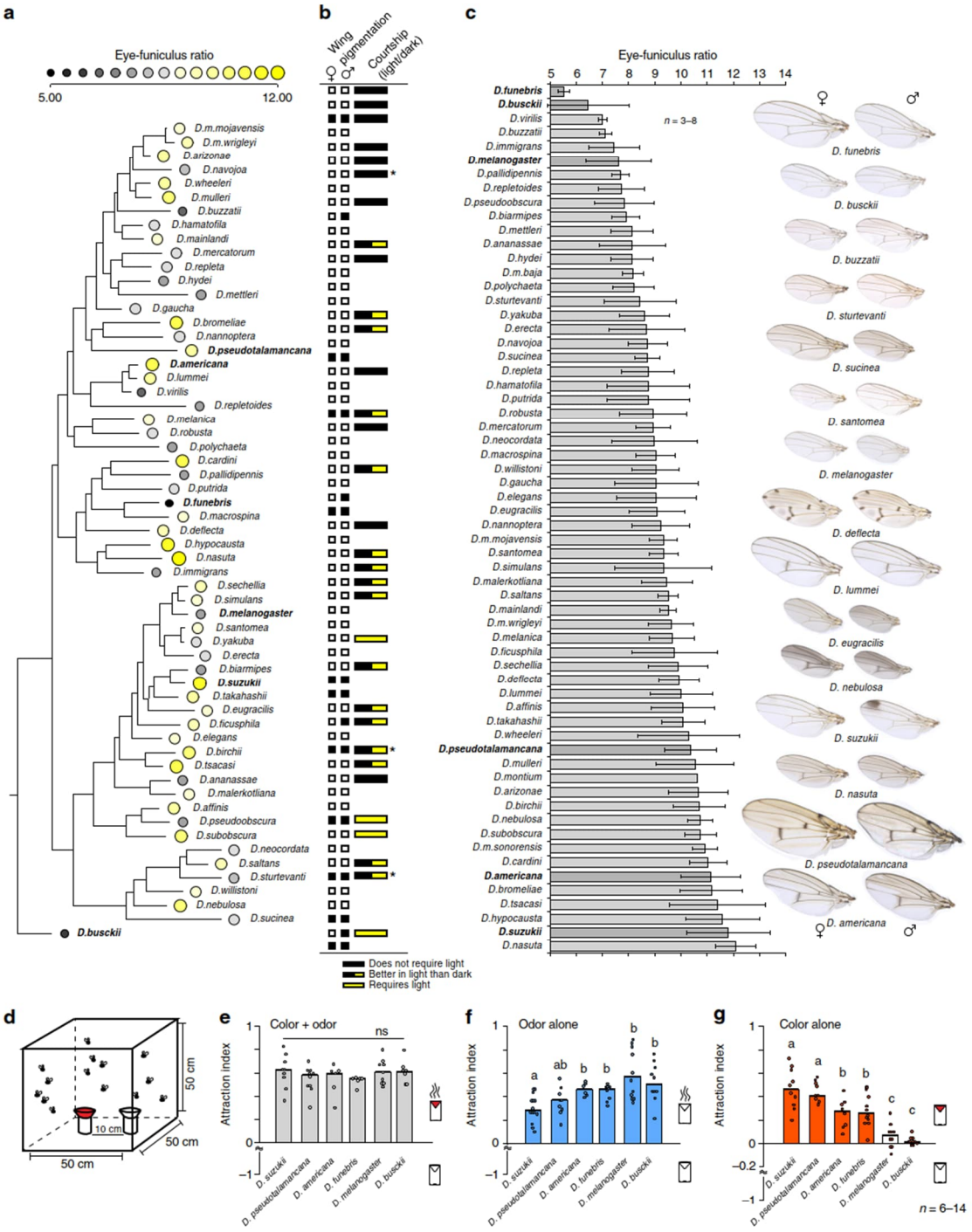

species were selected as either having similar funiculus size, but disparate eye size (i.e., *D. americana* and *D. busckii*; *D. pseudotalamancana*, and *D. funebris*), or vice versa (e.g., *D. americana* and *D. funebris*) (Fig. 2a). We also included *D. melanogaster*, given its prevalence in this genus as a model organism, and we included *D. suzukii*, as it has risen to become both an important invasive species for agricultural research as well as an important model for evolutionary neuroethology.

We were interested in documenting any drastic differences in sensory structures beyond surface area (Fig. 2a, c), and we next

Fig. 4 Host navigation and courtship differences across *Drosophila*. **a** Molecular phylogeny for 59 species that includes the eye-to-funiculus trait (EF ratio), which is visualized by both dot size and color. Two statistical tests (Blomberg K and Pagel's lambda) reveal that this sensory trait is not strongly supported by the phylogeny ($K = 0.478$, $p = 0.041$; $\lambda = 7.102e^{-05}$, $p = 1$). We note large variance within subgroups, and across habitat or ecological niche. **b** There was a significant correlation between both male/female wing pigmentation and EF ratio after phylogenetic correction ($p = 0.043$ and $p = 0.026$, respectively), suggesting that larger eyes correlate with pigmentation, which is not explained by phylogeny. Also shown are courtship values for mating pairs within light/dark environments, where light-based courtship is strongly correlated with larger EF ratio after phylogenetic correction ($p = 2.406e\text{-}07$), suggesting larger eye ratios correlate with visual mating. Asterisk indicates new data from this study. All other data from refs. [81–92]. **c** All 62 species arranged according to EF ratio, with wing pigmentation examples (standard deviation shown). **d** Diagram of behavioral assay used to test navigation of each species towards visual and olfactory objects. **e**–**g** Attraction indices for each species when stimuli were presented **e** together, **f** with odor alone, or **g** with visual target alone. While all species perform equally well when both odor and visual object are presented together, we observe a trend in behavioral preference where larger-eyed species perform more poorly in navigation towards odor objects when presented alone, but better towards visual objects, and vice versa for relative antennal size. (Data are provided at https://doi.org/10.17617/3.1D)

pursued additional metrics for visual and olfactory signal reception by quantifying sensillum and ommatidium number. Interestingly, the trend between visual and olfactory sensory structures was inversed among these six flies when we corrected for absolute head size (Fig. 2b), where large ommatidium counts in a fly species seemed to correspond with reduced sensillum counts, and vice versa. We also examined whether antennal surface area alone was a predictor of specific sensillum types, but surface area did not always predict the number of sensilla (Supplementary Figure 2G). In regard to olfaction, while these six species differed greatly in their absolute size, we discovered striking similarities in the density of sensilla found on either the anterior surface or the whole antennae (Fig. 2d; Supplementary Figure 2E, F). While both basiconic and coeloconic counts were roughly similar in their density, the largest difference between the species was in the number of trichoid sensilla (which have been shown to house sensory neurons detecting pheromone compounds[26,37,38]) (Fig. 2d). These trichoid differences were also apparent when we compared the absolute sensillum counts between species (Supplementary Figure 2D–F). Trichoids also varied in length and curvature. In addition to olfaction, we examined visual capabilities of each of these six species by counting the visual receptors or ommatidia (Fig. 2e; Supplementary Figure 2A–C, H), and again we noted large differences between these selected species, where ommatidia number was proportional to our previous measures of eye surface area. In order to further test the hypothesis that a tradeoff occurs between visual and olfactory sensory systems, we expanded our evolutionary comparison beyond these six examples to include additional species across the phylogeny (which were selected using stratified random sampling in order to represent as many subgroups as possible). Here, as before, we observed a significant inverse correlation between trichoid number and the eye-to-funiculus ratio (EF ratio) (Fig. 2f), where again, trichoid numbers were not correlated with antennal surface area or antennal size (Supplementary Figure 2G).

Neuroanatomy of visual and olfactory sensory circuitry. Given the disparity in external sensory morphology between our six species, we next sought to compare neuroanatomical metrics for the primary visual and olfactory processing centers within the brain (Fig. 3; Supplementary Figure 3). The species with the enlarged compound eyes also had a much larger OL relative to the AL, while the species with enlarged antenna had a relatively smaller OL (Fig. 3a, b). This matched our metrics related to external anatomy, suggesting as we predicted for example, that larger eyes correlates with larger OL volume. In order to account for differences in absolute size between each species, we used the central brain as a means to generate a weighed value for both OL and AL comparison (Fig. 3c–e). While it was not surprising that larger eyes or larger antennae matched with a larger brain region associated with these sensory structures, we started to see a pattern where an increase or an exaggeration of one sensory structure correlated with a relative reduction in the other. For example, that while *D. suzukii* has a much larger (OL:AL) ratio or (OL:central brain) ratio when compared with *D. melanogaster* (Fig. 3b, d), at the same time *D. suzukii* also had a significantly smaller (AL:central brain) ratio by comparison (Fig. 3d). This trend is true for each of the other reconstructions and species comparisons. We also assessed the selected six *Drosophila* species in regard to subunits of the OL, including the medulla, lobula, and lobula plate, where again we saw a similar pattern of a significant increase in size for each subunit of the OL in larger-eyed species; moreover, that the medulla represented the largest increase relative to central brain volume (Fig. 3e; Supplementary Figure 3G). Here, we also documented again that the AL of the larger-eyed species was relatively smaller when compared with larger antennal species, as expressed by a ratio to central brain volume (Fig. 3e). While these six species varied in their absolute sizes (Supplementary Figure 3A–G), we noted that the central brain relative to the whole brain was consistent in size across all tested species (Supplementary Figure 3E), thus a relative comparison of OL or AL to the central brain within each species gave a consistent measure or weighted value for comparison.

Phylogenetic correction of traits of interest. To examine whether the phylogeny of our species could account for the variations, that we measured in the eye and antenna, we compared the EF ratio trait to all relatives within the genus (Fig. 4a). Here, we utilized two independent statistical tests of phylogenetic signal, including the Blomberg K value and Pagel's lambda ($K = 0.478$; $p = 0.041$; $\lambda = 7.102e^{-05}$; $p = 1$), where we assess phylogenetic signal to indicate the tendency for closely related species to resemble each other more than a random species selected from the tree. Here, we found that both statistical measures agree that this phenotypic trait (EF ratio) is not strongly supported by the phylogeny, where a K value less than one indicates that variation is larger within subgroups than between subgroups (Fig. 4a). Thus, while we considered phylogenetic associations as a driver of trait variation, we did not find a relationship between phylogeny and trait variation. In addition, we noted that eye and antennal size diverge repeatedly throughout the genus and were not predicted by known ecology or shared habitats (e.g., EF ratio was not correlated with cactus-feeding or desert-living species; Fig. 4a); however, more ecological data are still needed for a multitude of species to discern the role ecology plays in the observed sensory variation.

Behavioral effects of sensory bias between species. Given the trends and correlations we observed in our in-depth analyses of six species, and in order to assess potential behavioral courtship

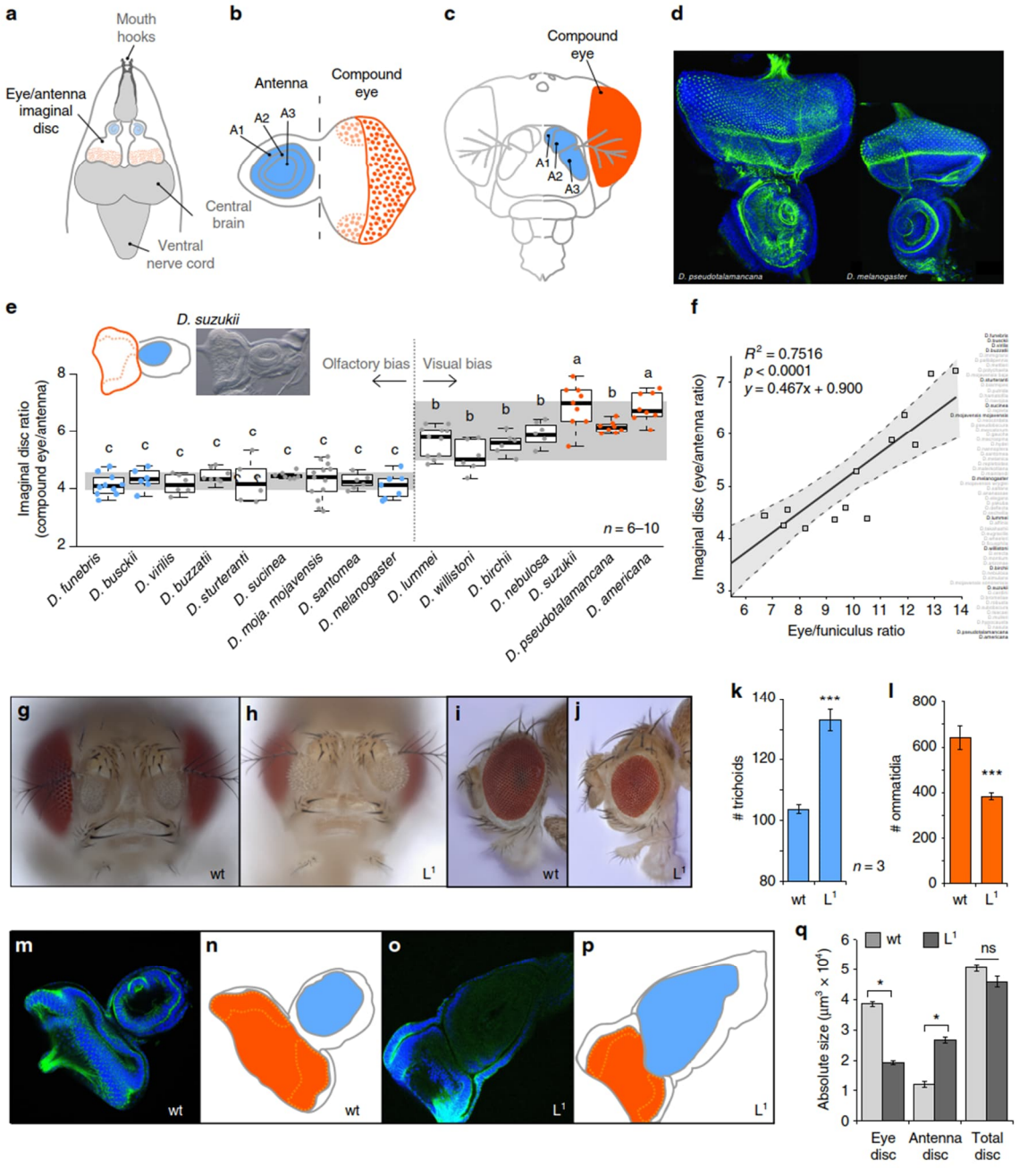

implications from the size variance of visual and olfactory sensory systems, we wanted to expand our comparative model to include all 62 species in our study (Fig. 4b, c). Here, we arranged all 62 species in regard to their EF ratio, as provided by measures of the surface area of each sensory structure, with smaller values indicating relatively large antennae, and bigger EF ratio values indicating a larger compound eye relative to the antenna (Fig. 4c). Photographs of wings from males and females were taken and used to provide information about wing spots or pigmentation for each species that was tested (Fig. 4b, c), and we also used previous literature to assess whether each species is influenced by light (lux intensity) during courtship or whether light is required for successful mating to occur (Fig. 4b). There was a significant correlation between female wing pigmentation and EF ratio after phylogenetic correction ($p = 0.0429$) (Supplementary Figure 3H, I). In addition, there was a significant correlation between male pigmentation and EF ratio after phylogenetic correction ($p = 0.0256$); therefore, because there was a correlation between wing

Fig. 5 Tradeoffs and developmental constraints. Red color signifies vision or visual bias, while blue indicates olfaction or olfactory species. **a**–**c** Diagrams of a single imaginal disc from larval development that gives rise to two separate adult structures, namely the eye and the antenna. **d** Two part staining (Hoechst & Phalloidin) of *Drosophila* species to visualize differences in absolute size of imaginal discs, highlighting the need for a ratio of eye to antenna for comparisons between species. **e** Imaginal disc ratios (eye to antenna) across each tested species where two groups were noted, olfactory biased and visually biased. Means with the same letter are not significantly different from each other (ANOVA with Tukey–Kramer multiple comparison test). Boxplots represent the median (bold black line), quartiles (boxes), as well as the confidence intervals (whiskers). **f** The significant correlation between larval imaginal disc measurements per species and the EF ratio from adult flies. **g**–**j** Eye and antennal mutants were compared to wild-type flies for both ommatidium and trichoid numbers. **k**, **l** From the mutants we screened, a single mutant, Lobe[1], displays increased trichoids and decreased ommatidia compared the the wild-type. An asterisk denotes statistical significance between two groups ($^{*}p \leq 0.05$, $^{***}p \leq 0.001$; T test). **m**–**p** Eye–antennal imaginal disc comparisons between wild-type and Lobe[1] mutant, visualizing the tradeoff between visual (red) and olfactory (blue) development. **q** Measurements show that while the total size of the imaginal disc is the same between wild-type and mutant, that the proportion of eye and antenna are inversely correlated, suggesting a developmental constraint between these two sensory systems. ($^{*}p \leq 0.05$, $^{***}p \leq 0.001$; *T* test) (Data are provided at https://doi.org/10.17617/3.1D)

pigmentation and EF ratio when we include the phylogenetic correction, the correlation between these two traits has no phylogenetic signal (i.e., the covariance of the residuals for the EF ratio and wing pigmentation regression do not follow phylogenetic signal). From the analyses of the light/dark courtship data in regard to EF ratio, we found these traits were strongly correlated both before phylogenetic correction ($p < 0.0001$) as well as after the correction based on relatedness of the species ($p = 2.406e\text{-}07$) (Supplementary Figure 3H, I). Thus in summary, it appears that proportionally larger eye size provides a potential visual bias in courtship that is associated with light-enhanced mating success. Moreover, we show that species with larger EF ratios (and thus those species with relatively larger eye size) were significantly more likely to possess wing pigmentation, and have significantly more successful copulation in light conditions (or display light-dependent courtship), perhaps as part of a successful visual display. However, due to the paucity of natural history for most species, additional work is needed to address all species-specific mating behaviors within this genus, including for example, pheromone-related courtship (or pheromone-related olfaction) in larger antennal species that display light-independent courtship.

As we had established a consistent difference between the visual and olfactory senses of the six species in regard to external and internal neuroanatomy as well as courtship, we wanted to next test if there was also any behavioral relevance to these sensory structure differences in regard to host navigation (Fig. 4d–g; Supplementary Figure 4A–D). When we combined visual and olfactory stimuli, all six species performed equally well in trap assays, including tests with several different olfactory cues, such as vinegar, blueberry, and strawberry (Fig. 4e; Supplementary Figure 4A). However, when we tested the olfactory stimuli alone, without any visual target, we observed a biased trend in that larger-eyed species navigated more poorly than larger-antennal flies (Fig. 4f), suggesting an olfactory advantage to large antennal species toward the odor object alone. The opposite phenomenon occurred when we tested visual stimuli in the absence of an odor source, where larger-eyed species performed significantly better than those species with enlarged antennae (Fig. 4g); moreover, we caught almost no flies from the larger antennal species using color alone. We also tested for species differences in their preference toward specific colors, with red and black being the most consistently attractive to all species, regardless of behavioral assay, but with *D. suzukii* also being attracted to green (Supplementary Figure 4A, B). However, this may be in part due to differences in contrast detection. Interestingly, *D. suzukii* was also more attracted to the combination of blue when presented with odor from blueberry, which may be linked to this species being reared for dozens of generations on this food source in our laboratory, and additional work will be required to test this combinatorial bias (Supplementary Figure 4A). In order to compare visible qualities of each color used, we generated a diffuse reflection gradient for each visual stimulus, to confirm the primary visible wavelength associated with each color we used in this study (Supplementary Figure 4C). We also confirmed the reliance on visual stimulus for host navigation by repeating a trial in either full light and complete darkness (Supplementary Figure 4D). Here, for example, *D. melanogaster*, a large antenna, olfactory-driven species, navigated equally well toward an odor source regardless of light conditions (Supplementary Figure 4D). However, in the same experimental design, *D. suzukii*, a large eye, potentially more visual species, performed as well as *D. melanogaster* toward an odor source in the dark, but roughly split capture with the visual stimulus and the odor source when in light conditions. In this case, as all species were still able to locate a host source successfully using a single-stimulus type (i.e., odor object in the dark), it would appear that the difference in size of a sensory structure indicates an innate preference or behavioral bias for certain navigational cues, but that both sensory systems still work well. Although again, visual and olfactory stimuli worked optimally in tandem, or when the two stimuli were in agreement in regard to the location of the host (Fig. 4e). Future work should examine the behavioral response of each species when the visual and olfactory objects are not in spatial congruence in regard to the location of the host or food source.

Evolutionary development of visual and olfactory structures. Although insect development is a complicated and delicate process under strict genetic control, the process by which *D. melanogaster* undergoes development has been relatively well elucidated. In general, there are 19 imaginal discs from the *Drosophila* larvae, each of which gives rise to a different adult structure (Supplementary Figure 6A); however, there is only one disc that gives rise to several separate adult structures, namely the eye–antennal imaginal disc (Fig. 5a–d). Here, a single larval developmental structure generates primarily both the eye and the antenna for the adult fly (Fig. 5b, c). With this in mind, we next examined the relative ratio of the two sides of this imaginal disc, including both the eye and antennal portions across a multitude of species (Fig. 5e). Although species varied in egg to pupal developmental time, by dissecting the tissues from late third instar larvae (wandering phase; Supplementary Figure 7), we could generate consistent ratios for each species during the same time window of development (Supplementary Figure 6B, C). To confirm these measurements, we used two stains (Hoechst & Phalloidin) in order to more closely monitor areas separating these two portions of the same developmental disc in each new non-*melanogaster* species (Fig. 5d). By using a ratio between the two parts of the same imaginal disc, we could account for any issues during the comparison of species that differed drastically in absolute size, for example between *D. pseudotalamancana* and *D.*

melanogaster (Fig. 5d). Using the data taken from a multitude of *Drosophila* species, we could identify essentially two main groups or two common ratios, either antennal biased or visually biased (Fig. 5e). This developmental data matched very well with the previously established external metrics taken from the compound eye and antennal surface areas, and thus further support the theory that there is a tight link between the imaginal disc size for the eye and antenna in comparison with the corresponding adult structures (Fig. 5f). This data again provide evidence for an inverse resource allocation between the eye and the antenna during development, as these two sensory structures would essentially be competing for the same resources within a single disc (Supplementary Figure 6D).

Genetic constraints on vision and olfaction. While we could not further examine the role development plays in non-*melanogaster* species of Drosophilidae, we could in fact, examine established genetic lines within *D. melanogaster* for either eye or antennal mutations (Fig. 5g–q). In these experiments, we used previously identified mutations for either eye or antennal development in *D. melanogaster*, and analyzed both of these adult sensory structures in order to test our hypothesis that there is a tradeoff or inverse resource allocation (Fig. 5g–q; Supplementary Figure 6E–G). Here, we counted trichoid sensilla and individual ommatidia from each mutant line in order to assess any potential candidate genes that match the phenotype we observed in the wild-type species (Fig. 5g–l; Supplementary Figure 6E–G)). Although some fly mutants have been previously published for either visual or olfactory abnormalities, most lines have not to our knowledge ever been examined for both sensory structures within a single mutant. While not an exhaustive screen of all possible gene candidates in *Drosophila* development, we did uncover a single-mutant allele in our screen that appeared to have a similar tradeoff between visual and olfactory sensory structures to that observed across the genus, more specifically, Lobe[1] (L^1), which has a significant reduction in the number of ommatidia while possessing a significant increase in the number of trichoid sensilla present on the funiculus (Fig. 5k, l), something that was consistent with the observations from wild types. This mutant has a reduced eye size, which has been previously published;[39–41] however, the alteration leading to increased antennal size (enlargement of all three segments) and the increase in trichoid sensillum number has not been previously described for this mutant (Fig. 5g–l).

In order to further test our hypothesis that the imaginal disc provides the framework for an inverse resource allocation based on the sharing of a single disc for two adult sensory structures, we next sought to examine the imaginal disc of this L^1 mutant in regard to eye and antennal ratio (Fig. 5m–p). Here, we observed that the Lobe[1] mutant has a marked reduction in the portion of this developmental disc that gives rise to the compound eye (Fig. 5o, p), while also showing a marked increase in the portion that gives rise to the antennal segments. When we measured the two portions of the developmental disc for both wild-type and mutant, we discovered that there was no significant difference in the total size of these imaginal discs (Fig. 5q), but rather that the proportion of the disc dedicated to each sensory structure had shifted in the mutant from the eye to the antenna (Fig. 5q). Thus, this new data lends additional support to our previous observation that a tradeoff might occur between visual and olfactory sensory systems, in this case during development, and that this inverse resource allocation is perhaps necessitated by the sharing of a single larval structure. Thus, for example, in order for the antennal region to increase in Lobe[1], there is necessarily a decrease in eye size to compensate. Recently, a preprint[31] has addressed this same developmental mechanism, and has proposed a similar tradeoff hypothesis by comparing two *Drosophila* species using CRISPR mutants, where they conclude that a single amino-acid shift can alter the functional timing of a gene, and explain the natural variation between eye and antenna during larval development. However, more research is needed to address whether this same developmental constraint can dictate the inverse correlation between visual and olfactory sensory systems that we have observed in all tested *Drosophila* species.

Discussion

In this study, we provide large-scale evidence for an inverse relationship between visual and olfactory anatomical investment across this genus of Drosophilid flies. The potential tradeoff seems to stem from a theoretically restricted resource allocation between the eye and antenna during larval development, which is linked to a single shared structure giving rise to both adult sensory systems (Fig. 5d–i). It remains to be seen whether this push–pull between the eye and antennal region of the imaginal disc is under similar genetic control in all non-*melanogaster* species; however, our study and a recent preprint[31] provide evidence that a simple mutation can mirror inverse variation in ommatidia and sensilla numbers for *D. melanogaster*, something which is consistent with our observations of repeated, independent evolutionary events across this genus of fly in regard to visual and olfactory divergence.

Investment in an exaggerated sensory structure might be costly[42], thus prominent structures often result in a tradeoff with another trait to minimize energetic costs[43–47]. Tradeoffs can occur across populations or between species within a single subfamily or genus, and each different sensory structure often has differing ecological and environmental pressures acting upon it[48,49]. An example from vertebrates of a similar tradeoff hypothesis examines trichromatic color vision in primates[50], where researchers found that primates with heightened color vision also had a higher number of olfactory pseudogenes or non-functional gene mutations. In order to test this pseudogene argument, we also examined the olfactory genes from many *Drosophila* species using previously published data on OR, GR, IR genes, and their associated pseudogenes across 14 members of Drosophilidae (Supplementary Figure 1J)[51], but we did not find any meaningful correlation between olfactory pseudogenes and eye size or visual enhancement. However, it is possible that gene expression levels differ between *Drosophila* species, either across rhodopsin types or other visual pigmentation genes, or perhaps across olfactory-related genes. For example, while the most-studied *Drosophila* species have roughly the same diversity of chemosensory genes and ommatidium types[51,52], different olfactory receptor ratios exist across basiconic or trichoid sensillum types, where variation in olfactory receptor expression is often associated with specialization[10,25,26]. This was the case in *D. sechellia*, where this species has similar olfactory gene diversity (or number of chemosensory genes) when compared with *D. melanogaster*, but vastly different expression levels of a few specific receptors. Additional research is required to assess this type of expression-level comparison for visual and olfactory genes between a wider array of *Drosophila* species, as it is not clear if fly species with increases in ommatidia or sensilla numbers represent a uniform increase across receptor types. It is also important to mention that there are some limitations in our extrapolation to true wild-type insects due to the usage of stock center or laboratory flies, but we anticipate that our findings will extend to natural populations as well.

From an ecological point of view, we considered mate-finding and host navigation when examining sensory systems in *Drosophila*. Both of these behaviors have been shown to rely heavily on visual and olfactory inputs in several species that have previously been investigated. For example, wing pigmentation has been extensively studied in *Drosophila*[53–56], although never before in correlation with olfactory function such as pheromone detection (Fig. 4b, c). The removal of pigmentation heavily influences sexual selection and courtship, thus further confirming the importance of visual cues during courtship in spotted wing *Drosophila* as well as in the visual courtship of other animals[57,58]. In addition, it was recently shown that *D. subobscura*, which requires light for courtship success[59,60], has enhanced fruitless-labeled gene expression and circuitry that maps to the OL, unlike *D. melanogaster*, where courtship is light-independent[29]. Moreover, that study also highlighted fruitless-labeled visual enhancement into the lobula and lobula plate of *D. subobscura*, a specific increase in brain volume which we also show in all three of our visually biased species examples (Fig. 3e). Another well-studied example of courtship and incipient speciation is the diverging populations of *D. mojavensis*[22–24], where our data again show that the largest divergence is found between the closest relatives and geographically overlapping subspecies, suggesting character displacement as an additional driving force for the observed differences in visual and olfactory investment (Fig. 4a, c). In fact, the vast majority of *Drosophila* species we tested show the largest differences within a species clade or subgroup (e.g., *D. virilis* vs. *D. americana*; *D. biarmpies* vs. *D. suzukii*; *D. pseudoobscura* vs. *D. subobscura*), where courtship, mate selection, and host competition pressures are potentially highest, and perhaps driving repeated speciation events that favor either visual or olfactory bias to differentiate the species' niche (Fig. 4a, c). Although recent work has examined differences in the visual and olfactory systems of *D. melanogaster* and *D. pseudoobscura*[31], we do not feel this is a good direct comparison, given the poor phylogenetic connection between these more distantly related species (17–30 million years apart), and that other pairings would perhaps better tackle the genetic, ecological, and evolutionary pressures that underpin this sensory tradeoff (e.g., that *D. subobscura* or *D. affinis* would be a better comparison for *D. pseudoobscura*, while *D. simulans* or *D. sechellia* would be a better comparison for *D. melanogaster*). Thus, we conclude that the correlations and model provided by our study, including eye size and wing pigmentation as well as light-dependent courtship, match with previous publications from the *Drosophila* genus and our study provides a large dataset for further testing. In addition, our data continue to strongly support the theory that visual investment and OL increases mirror the behavioral priority of vision for courtship and/or host navigation in those species with larger EF ratios and wing pigmentation (Fig. 4b, c; Supplementary Figure 3H, I).

Although additional work is required to confirm any differences in pheromone production or increased olfactory courtship reliance in species with larger antennal ratios, our data already support the inverse investment between the eye and antenna in regard to copulation based on the number of trichoid sensilla versus ommatidia (Fig. 2b, d, f; Supplementary Figure 2 E–G). Moreover, within the suzukii subgroup, it has been well established that *D. suzukii* produces very low amounts of the male pheromone known as cis-vaccenyl acetate (cVA; detected by trichoid at1, and Or67d) and that this species has a greatly reduced glomerular volume within the AL for this odor[26]. The previous research matches our findings here that *D. suzukii* flies have a reduced total number of trichoids, and in addition, that these flies instead possess an enlarged compound eye that is 2.5 times larger than in *D. melanogaster*. Similarly, *D. biarmipes*, the closest relative of *D. suzukii*, has also been previously studied and shown to have a large amount of cVA production, which is opposite to *D. suzukii*[36]. In the present study, we also found a correspondingly higher number of trichoid sensilla for *D. biarmipes* when compared with *D. suzukii*, even given the smaller overall size of *D. biarmipes*, matching a potential tradeoff between olfactory and visual investment between close relatives for courtship, again suggesting character displacement as a potential means of speciation or divergence (Fig. 4a, c).

Resource allocations have been well documented within other insects, such as in courting scarab beetles, where there is an inverse correlation of investment between physical horn size for fighting and sperm production for increasing the likelihood of paternity[61]. Examples of visual and olfactory variation have also been recently documented in other insects, such as in Lepidoptera, where nocturnal and diurnal species within the Sphingidae family of hawk moths vary widely in morphological investment toward either eye or antennal structures, as well as in their relative OL and AL sizes;[62] however, while a tradeoff between these sensory systems has not been previously proposed, these studies have shown by comparing two hawk moth species that relative brain structure increases match behavioral preferences, with diurnal species having enlarged visual centers and visual preferences, and nocturnal species having enlarged olfactory centers with olfactory behavioral preferences. Moreover, that these sensory brain measurements can be used to explain and predict differences in the importance or priority of these two senses (vision and olfaction) for host navigation. In these studies of Lepidopteran neuropils, it can be inferred from the data that investment in vision is perhaps associated with a relative decrease in olfactory processing centers, and vice versa, both for host-finding and migration, suggesting that perhaps an insect species cannot increase both sensory systems[62–64]. It has also been shown recently that a potential tradeoff might also occur between diurnal and nocturnal dung beetle species[65], where there was a difference across the two examined species between visual and olfactory brain regions based on circadian rhythm or daily activity patterns. Here, the diurnal species have a larger OL and are more visual, while the nocturnal species relies more on olfaction as well as possessing an enlarged AL. Another insect example of visual variation exists across Formicidae, where different ant species, or even different castes members within a species, have differing investment in vision depending on their ecological roles within the colony or depending on the amount of time they spend underground[66,67]. In addition, more distant insect relatives have been compared across visual brain structures[68], where the visual centers from Mantodea, Blattodea and Orthoptera were addressed for their anatomical similarities and differences. Although some of these latter studies did not address olfactory centers for relative comparison between both vision and olfaction, each example lends support to the hypothesis that all insects potentially demonstrate a tradeoff in sensory systems. However, additional work is still required in more orders of insects to assess this tradeoff hypothesis and the evolutionary pressures that lead to these potential compromises between sensory structures.

In many insect examples, the differential investment in OL or AL was linked to differences in activity (diurnal and nocturnal). These differences in circadian rhythm are not as well studied in all non-*melanogaster* species, and the timing of both courtship and host-seeking behaviors are not known for all species. However, in the *Drosophila* species that have been examined, they all share a similar crepuscular activity cycle, thus it is unlikely that differences in visual and olfactory sensory systems in *Drosophila* arise from nocturnal versus diurnal activity[60,69]. Additionally, tradeoffs between visual and olfactory signaling have been long

recognized in plant species, especially between odorous nectar or visual floral displays that are used in order to attract insect pollinators[70]. The difference in plants is evident where you have a visually large and distinct floral petal arrangement, but with reduced smell or reward. In contrast, other plants have little in the way of visual attraction, but utilize sweet nectar rewards or strong, pungent odor plumes to draw in olfactory-driven pollinators[71–73]. These plants examples again highlight potential differences across insect pollinators, such as hymenopterans and dipterans, where the plant takes advantage of insects that favor either visual or olfactory stimuli for host navigation, but perhaps not both sensory modalities[73]. It is possible in these cases that vision could assist some Drosophild species in finding their preferred plant hosts (i.e., flowers, or fruit ripening within leaves or tree canopies), although the paucity of ecological information for most species within this genus has made this impossible to examine so far.

In summary, our assessment of the genus *Drosophila* supports the hypothesis that the visual sensory system expands consistently at the expense of structures related to olfaction, and vice versa. In addition, we provide robust evidence that the inverse correlation observed between visual and olfactory sensory systems occurs repeatedly within the family Drosophilidae, and we conclude that our theory of a tradeoff is consistent with all observed patterns, and perhaps is necessitated by a developmental constraint. Moreover, while additional research is required to address the specific molecular genetic mechanism(s) that control this observed phenomenon across the entire genus, the data provided herein generate a solid foundation to continue to test this sensory tradeoff hypothesis in the future. By using a large subset of close relatives within one genus of Dipterans and creating an extensive overview of their visual and olfactory systems, including a robust molecular phylogeny, we were able to generate a finely tuned evolutionary framework, and we provide the first step in establishing a larger model system to encompass dozens of *Drosophila* species for additional study beyond *D. melanogaster* and its subgroup. In the end, we have also started to build evidence about the pressures and general rules governing developmental, ecological, and evolutionary phenomena related to differences in neuroanatomy and behavior across all insects, where the data provided support previous research as well as encourages new ideas and new avenues for the study of speciation, specialization, and the evolution of the nervous system.

Methods

Fly stocks. All wild-type species, stock numbers, and rearing diets are in Supplementary Table 1. Unless otherwise noted, all fly stocks were maintained on standard diet (normal food) at 25 °C with a 12 h light/dark cycle in 70% humidity. Stock population density was controlled by using 20–25 females per vial. Mutants lines included oc^1 (ocelliless; Bloomington #2291), ar^1 (arista-less; Bloomington #210), Antp (antennapedia; Bloomington #2235), Dll (distal-less; Bloomington #3306), $Diap^1$ (thread; Bloomington #618), L^1 (lobe; Bloomington #318), gl^1 (glass; Bloomington #506), and gla^1 (glazed; Bloomington #1951). Stocks were maintained according to previous publications[74], and for all behavioral experiments we used 2–7 -day-old flies of both sexes.

External morphometrics from head and body. For each fly species or mutant line, 3–8 females were photographed using a Zeiss AXIO microscope, including lateral, dorsal, and frontal views. Flies of the 62 wild-types were dispatched using pure ethyl acetate (MERCK, Germany, Darmstadt). Lateral body (40×), dissected frontal head (128×), and dissected antenna views (180×) were acquired as focal stacks on an AXIO Zoom V.16 (ZEISS, Germany, Oberkochen) with a 0.5x PlanApo Z objective (ZEISS, Germany, Oberkochen). The resulting stacks were compiled to extended focus images in Helicon Focus 6 (Helicon Soft, Dominica) using the pyramid method. Based on the extended focus images, we measured body length (abdominal tip to antennal tip), head width (between eye margins), eye width, and eye height, as well as funiculus width and length, all measurements are in µm (Supplementary Figure 1A). Assuming the eye as a full ellipsoid, we calculated the 3D surface based on the average eye width and half eye height as the ellipsoid radius (r), and used the formula $[4 \times (\pi) \times r^2]$ for the area of a sphere, then dividing the result by 2 to generate the eye surface area as a half-ellipsoid for each species. Calculations for the funiculus surface used its half-length and half-width as radius for the 3D ellipsoid surface area. Accounting for the proximal connection between funiculus and pedicel, we subtracted the circular base area, and then calculated with the funiculus width. In addition, we compared these calculations with previous publications for available species[52,75] in order to confirm that our metrics were similar, and while some of our estimates were low relative to other publications, they were consistent across replicates within each species. All raw measurements are available with the online library, as are the stock photos for all replicates (https://doi.org/10.17617/3.1D; 01 Species Images; Excel tables).

In order to test the validity of the usage of ratios for our comparisons made between visual and olfaction sensory systems, we have provided a statistical assessment of allometry (including a multiple regression analysis). First, we found that the eye and funiculus surface area measurements scale isometrically with respect to the measurements taken from the body and the head. Thus, we feel it continues to make sense to use the EF ratio as our primary trait, given that there is no real allometry in our data. Moreover, we show that neither body size ($p = 0.294$) nor head size ($p = 0.590$) significantly correlate with this EF ratio trait (Supplementary Figure 1H), and we have plotted the analyses of the residual variance (Supplementary Figure 1H). Last, we have also conducted a multiple regression analysis (using the EF ratio, eye, funiculus, body, and head measurements from all 62 species), and indeed again, the EF ratio does not correlate with body or head size in this multiple regression ($p = 0.354$ and $p = 0.295$, respectively). Overall, we continue to feel that we can safely maintain the usage of ratios, as the EF trait does not simply scale allometrically with body or head size, and these statistical tests again strengthen and further support our interpretations of the data that an inverse correlation exists between these sensory modalities that is not reflective of absolute body size. In addition, an online copy of the curated R scripts is available, including all measurements used to test allometry and to perform the multiple regressions (https://doi.org/10.17617/3.1D; 12Allometry).

Ommatidium measurements. In order to count ommatidia, the compound eye of each species was dissected and mounted on slides in water using a coverslip, and then photographed using a confocal microscope (Fig. 2e). A total of 5–6 individuals per species were used, and counts were done manually using ImageJ (Fiji) software tools (Supplementary Figure 2A). Diameters of single ommatidia were also assessed (Supplementary Figure 2B, C), with most species having roughly similar size.

Sensillum counts. Three different individuals from each species were anesthetized with CO_2, and their antennae were dissected. After removal, antennae were dipped into phosphate buffer (0.1 M pH, 7.3) with 5% Triton-X (Sigma-Aldrich) and they were washed in phosphate buffer and embedded in VectaShield (Vector Laboratories) between two cover slips[11]. To visualize the anterior surface of the antennae, lambda scans were obtained via confocal laser scanning microscopy (Zeiss LSM 880; Carl Zeiss) using a 40x water immersion objective (W Plan-Apochromat 40×/1.0 DIC M27; Carl Zeiss) in combination with the internal Argon 488 -nm laser (LASOS) and the 405 -nm Laser diode (Carl Zeiss). The broad emission spectrum of the samples auto-fluorescence was detected with the quasar detector (Carl Zeiss). Thereby images with 32 separate channels (each with a range of 9.7 nm) are generated simultaneously (Supplementary Figure 2D). To visually support the following sensilla quantification, lambda scans were post processed using the linear un-mixing technique (Carl Zeiss; http://zeiss-campus.magnet.fsu.edu/articles/spectralimaging/introduction.html). This technique enables the determination and separation of spectral profiles for every pixel and assigns each pixel, according to its spectral profile, to a manually defined spectral group. Three spectral groups were defined by selecting reference points in each stack (diameter 5 pixels) using the ZEN software (Carl Zeiss). This technique enables reassignment of one color for each group to a region (or group of pixels) that would otherwise appear as mixed color, and therefore supports visual separation of olfactory sensilla from other structures as well as the characterization of different sensillum types, due to structural differences (e.g., between trichoid, coeloconic, and basiconic shapes) that cause distinct emission spectra in their auto-fluorescence.

The sensillum quantification was done with the cell counting plugin (https://imagej.nih.gov/ij/plugins/cell-counter.html) in ImageJ (Fiji). Linear unmixed lambda stacks were visualized as a composite of all three channels and sensilla were manually counted by going through the stack. Each sensillum was assigned to one group (trichoid, basiconic, and coeloconic) and marked separately, and then each group was summed in the end.

Sensilla density of each anterior surface side was calculated as follows:

$$\text{Sensilla density} = \frac{\text{Sensilla number}}{\frac{1}{2}\,\text{funiculus surface}(\mu\text{m}^2)} \quad (1)$$

For trichoid sensillum counts of the other 24 species, counts were done manually for either the anterior or posterior or for both sides of the antennal surface. Counts were conducted with images from a Zeiss AXIO microscope under bright-field light, using arista up single sensillum recording preparations for each

insect that was examined (Supplementary Figure 5A, B), as this was the best preparation for viewing and counting trichoid sensilla[37]. A total of 3–6 individuals were counted per species, and where possible, these totals were compared with previous scanning electron microscopy (SEM) images, or lambda scans, or the previously published counts from the available species.

Phylogeny of *Drosophila* species. Species were initially selected, ordered, and arranged to include close relatives in pairs or triplicates for each major subgroup within the genus. Our initial molecular phylogeny search consisted of 16 mitochondrial and nuclear genes that were identified and used previously for studies of Drosophilidae[76,77]. However, many of these sequences were partial, or from older literature, while in addition, some genes had representation in only a few species. Therefore, we replaced much of the previously published data with the newer sequences that are currently available in public sources such as GenBank and Flybase repositories, with new sequences being either complete or longer in length than those that were previously published. In particular, no segments of the same gene in a species have been combined, as had been done in previous publications. We retrieved only the nucleotide coding sequence (CDS) regions of protein-coding genes, as well as the nucleotides for non-coding ribosomal RNA genes. In cases where mitochondrion genomes were available (bold after species names), then all the target mitochondrion genes sequences were retrieved from the same genome data. Moreover, in cases where the sourced data contained multiple genes, the specific region of the target gene sequence is given. After we assessed each individual gene, we generated trees for each gene individually, and ultimately narrowed our list from 16 down to 5 genes for concatenation (ADH-1, Amyrel, NADH-2, NADH4, and NADH4L). Raw molecular data, including sequences and accession numbers, are available at https://doi.org/10.17617/3.1D; 02 Molecular Phylogeny and in Supplementary Data 1.

For phylogenetic tree construction, we used available sequences from 59 Drosophila species drawn from the *Sophophora* and *Drosophila* clades, including *D. busckii* as an out group in the *Dorsilopha* clade of this genus. We assessed the dataset for each of the 16 gene families for quality in terms of representation or coverage across the sampled species, completeness of sequence length, the nucleotide multiple sequence alignment conservation, as well as the ability of each gene to reconstruct the phylogeny of the species represented (for individual phylogenetic trees see https://doi.org/10.17617/3.1D; 02 Molecular Phylogeny). This assessment enabled us to also determine the sequential order for concatenating the genes. Our final concatenated dataset were comprising two nuclear protein coding genes, amylase related (AmyRel) and alcohol dehydrogenase subunit 1 (ADH-1), as well as three mitochondrion genes, NADH: ubiquinone oxireductase subunit 2, −4, and −4L (NADH-2, NADH-4, and NADH-4L). We excluded non-coding mitochondrion genes for the reason that they individually failed to reconstruct the phylogenetic tree, as the sequences were often partial, had biased representation across the species, or failed to reproduce a consistent phylogeny, though we still include them for future reference in the online library (https://doi.org/10.17617/3.1D; 02 Molecular Phylogeny). The final dataset consisted of 229519 bp data points, in 59 concatenated sequences. The sequences were multiply aligned using a MAFFT tool with L-INS-I parameters, with 10000 bootstrap (Kato & Toh, 2008) and the final tree was reconstructed using maximum-likelihood approach with GTR+G+I model of nucleotide substitution and 1000 non-parametric bootstrapping, re-sampling of 10 initial random trees in Fasttree program. We did not partition the concatenated gene sets in this analysis. All emanating trees were visualized, and rendered using Figtree v.1.4.2.

Using this newly created phylogeny, we analyzed in two different ways the phylogenetic relationship for the eye–funiculus trait that we had generated for each species. First, we tested the Blomberg K value ($K = 0.478$; $p = 0.041$), where the K value being less than one suggests a lower phylogenetic signal than expected from Brownian motion; moreover, this low K value indicates that the variance is mostly within a given subgroup, and not between subgroup clades. Here, we determine phylogenetic signal to indicate the tendency for closely related species to resemble each other more than a random species selected from the tree. Second, we tested the Pagel's lambda value ($\lambda = 7.102e^{-05}$; $p = 1$), where again, a λ value that is not significantly different from zero indicates very little phylogenetic signal in this trait. Thus, given the consistency of these two different statistical measures, we determined that the eye–funiculus ratio is not strongly supported by the phylogenetic relationship of the species that we tested.

3D reconstructions and neuropil measurements. In order to assess neuroanatomy, the dissection of fly brains was carried out according to established practices[78]. The confocal scans were obtained using multiple photon confocal laser scanning microscopy (MPCLSM) (Zeiss laser scanning microscopy [LSM] 710 NLO confocal microscope; Carl Zeiss) using a 403 water immersion objective (W Plan-Apochromat 40×/1.0 DIC M27; Carl Zeiss) in combination with the internal Argon 488 (LASOS) and Helium-Neon 543 (Carl Zeiss) laser lines. Reconstruction of whole OLs and ALs was done using the segmentation software AMIRA version 5.5.0 (FEI Visualization Sciences Group). We analyzed scans of at least three specimens for each and reconstructed them in using the segmentation software AMIRA 5.5.0 (FEI Visualization Sciences Group). Using information on the voxel size from the laser scanning microscopy scans as well as the number of voxels labeled for each neuropil in AMIRA, we calculated the volume of the whole AL as well as the individual sections of the OL and the central brain (where central brain values exclude the AL volume).

Behavioral assays for visual and olfactory stimuli. Trap experiments were performed as previously described for individual odors[27,36], but using white or colored paper cones as an entrance to the trap (as non-*melanogaster* adults were too large to enter pipette tips). We also used an additional 200 µl of light mineral oil (Sigma-Aldrich, 330779-1L) that was added to capture and drown flies upon entering to the paper cone trap, and to ensure they did not escape over the 24 h testing window. Trials were conducted with 30 adult flies (15 males, 15 female), and each species was run separately. All behavioral cone traps consisted of 60 -ml plastic containers (Rotilabo sterile screw cap, Carl Roth GmbH, EA77.1), with one trap used as a white control and the other containing a colored cone entrance (red) (Fig. 4a–d, Supplementary Figure 4A, D). In experiments with whole fruit, each fruit was placed individually into traps that were presented simultaneously, where the sides of the container were opaque to avoid any extra visual stimuli, and as before, a large arena was used (BugDorm-44545 F) (Fig. 4a; Supplementary Figure 4A, D). For Petri dish behavioral traps (Supplementary Figure 4B), color paper circles were cut out and placed onto standard 10 -cm Petri dishes, either with or without an odor source, where mineral oil was again used to capture flies that landed on the paper disks. A total of 60 adults (30 males, 30 females) were used per trial, with a 16 L:8D photoperiod during testing. All odor dilutions were prepared in hexane or water, and all behavioral trials were conducted with odors diluted to 10^{-3} unless otherwise noted. Statistics were performed using GraphPad InStat version 3.10 at both $\alpha = 0.05$ and $\alpha = 0.01$ levels. No differences were noted between the sexes in regard to behavior, and thus, the data were pooled.

Color and wavelength measurements. The measurement of the backward light scattering with directed reflection took place using a Lambda 950 spectrometer (Perkin Elmer). This device is suitable for measurements in the UV/VIS/NIR range from about 200 nm to 2500 nm. The measurement of each colored paper was conducted at discrete wavelengths in this range with a distance of 1 nm (Supplementary Figure 4C), which allows for the more discrete characterization of each color used (i.e., green reflected light between 480 and 580 nm, and was well within the expected range for this color).

Wing pigmentation and light/dark courtship. The wings from male and female adults from each species were dissected and mounted with a slide and coverslip, with images generated using a Zeiss AXIO microscope under bright field and transmitted light (Fig. 4e, f). Wing pigmentation was noted for males and females from all species (https://doi.org/10.17617/3.1D; 08 Wings), with examples shown for most wings with any spots or pattern, where there was a significant trend of wing pigmentation being correlated with larger eye species relative to antennal size (Fig. 4c; Supplementary Figure 3H). Previously published data for courtship that required light, or where courtship was better under light conditions (yellow bars in Fig. 4e) or where courtship was possible in the absence of light (black bars in Fig. 4e) are shown (Supplementary References), with new data denoted by an asterisk. Light-dependent courtship, as well as mating better in light conditions, was also correlated with larger eye size relative to the antenna, suggesting a connection between vision and visually-mediated courtship signals such as wing pigmentation (Supplementary Figure 3 I). For statistical measurements, we used the package caper (Comparative Analyses of Phylogenetics and Evolution in R)[79] as well as the packages ape (Analyses of Phylogenetics and Evolution) and phytools (Phylogenetic Tools for Comparative Biology) to perform phylogenetic generalized least squares (pgls) and employed Pagel's lambda, Blomberg K, and the Brownian model of phylogenetic relatedness, with the R-script available online. We chose the caper package as we were most comfortable with the way it handles missing data, for example during the analyses of light/dark courtship, where published behavioral data are missing for several species. For all three phenotypes (female wing pigmentation, male wing pigmentation and courtship in light-dark), the estimates of Pagel's lambda for the branch length transformation significantly deviate from a strict Brownian motion process model of phylogenetic relatedness (i.e., deviate from lambda = 1; for more details, please see R-script at doi.org/10.17617/3.1D; 02 Molecular Phylogeny).

Staining of imaginal discs. Fly species were selected using stratified random sampling in order to represent as many subgroups as possible. Third instar larva were allowed to self-clean for several minutes in 1 M phosphate-buffered saline (PBS) and then dissected in fresh PBS. In a first dissection step, the imaginal discs were kept attached to mouth hooks and central brain to add structural stability. This coarse dissection product was transferred into 0.5 -mL reaction tubes with fresh, cold 300 µL of 1 M PBS. The PBS was exchanged against cold 400 µL of fixative, and the tissue was incubated in the paraformaldehyde solution on ice for 35 min. Next, tissue samples were washed in cold 400 µL of 1 M PBS five times for 5 min each. After removal of the PBS, the dissection products were incubated in the blocking solution on ice for 45 min. Then the blocking solution (1 M PBS plus 7% normal goat serum) was replaced with the staining solution (blocking solution with 0.07% Hoechst and 1% Phalloidin 488) and samples were incubated on a rotator at 4 °C for 2 h. Subsequently, the tissue was washed again in cold 400 µL of 1 M PBS

five times for 5 min each. In a fine dissection step, the imaginal discs were then freed from all other connected tissues, and then mounted on object slides using a drop of Entellan® (Merck, Darmstadt, Germany). Sections of the imaginal disc were measured in Fiji software, and ratios were generated of surface areas for the eye divided by the corresponding antennal surface area (Fig. 5h; Supplementary Figure 6C), with 6–14 replicates per species, always taken from third instar wandering phase larvae just prior to pupation (Supplementary Figure 7).

Statistics and figure preparation. Statistical analyses were conducted using GraphPad InStat 3 (https://www.graphpad.com/scientific-software/instat/) and R Project (https://www.r-project.org/), while figures were organized and prepared using R Studio, Microsoft Excel, and Adobe Illustrator CS5. Additional details concerning tests of allometry, multiple regression, and phylogenetic correction are contained within the publically available R scripts that are described below in the Code availability section.

Reporting summary. Further information on experimental design is available in the Nature Research Reporting Summary linked to this article.

Code availability. All scripts for R, including curation of what tests were conducted, as well as the raw data files used for each statistical analysis are available at DOI: 10.17617/3.1D [10.17617/3.1D] (see 02 Molecular Phylogeny; 12 Allometry)[80].

Data availability

All data supporting the findings of this study, including methodology examples, raw images and z-stack scans, molecular sequences, accession numbers, statistical assessments as well as species information are all available through Edmond, the Open Access Data Repository of the Max Planck Society, https://doi.org/10.17617/3.1D [10.17617/3.1D][80].

Received: 7 May 2018 Accepted: 14 February 2019
Published online: 11 March 2019

References

1. Hansson, B. S. & Stensmyr, M. C. Evolution of insect olfaction. *Neuron* **72**, 698–711 (2011).
2. Moran, D., Softley, R. & Warrant, E. J. The energetic cost of vision and the evolution of eyeless Mexican cavefish. *Sci. Adv.* **1**, e1500363 (2015).
3. McGaugh, S. E. et al. The cavefish genome reveals candidate genes for eye loss. *Nat. Commun.* **5**, 5307 (2014).
4. Jones, G. & Teeling, E. C. The evolution of echolocation in bats. *Trends Ecol. Evol.* **21**, 149–156 (2006).
5. Ulanovsky, N. & Moss, C. F. What the bat's voice tells the bat's brain. *Proc. Natl. Acad. Sci.* **105**, 8491–8498 (2008).
6. Thiagavel, J. et al. Auditory opportunity and visual constraint enabled the evolution of echolocation in bats. *Nat. Commun.* **9**, 98 (2018).
7. Burton, R. F. The scaling of eye size in adult birds: relationship to brain, head and body sizes. *Vision. Res.* **48**, 2345–2351 (2008).
8. Kazawa, T. et al. Constancy and variability of glomerular organization in the antennal lobe of the silkmoth. *Cell Tissue Res.* **336**, 119–136 (2009).
9. Namiki, S., Daimon, T., Iwatsuki, C., Shimada, T. & Kanzaki, R. Antennal lobe organization and pheromone usage in bombycid moths. *Biol. Lett.* **10**, 20140096 (2014).
10. Dekker, T., Ibba, I., Siju, K. P., Stensmyr, M. C. & Hansson, B. S. Olfactory shifts parallel superspecialism for toxic fruit in *Drosophila melanogaster* sibling, *D. sechellia*. *Curr. Biol.* **16**, 101–109 (2006).
11. Grabe, V. et al. Elucidating the neuronal architecture of olfactory glomeruli in the *Drosophila* antennal lobe. *Cell Rep.* **16**, 3401–3413 (2016).
12. Kondoh, Y., Kaneshiro, K. Y., Kimura, K. & Yamamoto, D. Evolution of sexual dimorphism in the olfactory brain of Hawaiian *Drosophila*. *Proc. R. Soc. B Biol. Sci.* **270**, 1005–1013 (2003).
13. Lamichhaney, S. et al. Evolution of Darwin's finches and their beaks revealed by genome sequencing. *Nature* **518**, 371–375 (2015).
14. Wernet, M. F., Perry, M. W. & Desplan, C. The evolutionary diversity of insect retinal mosaics: Common design principles and emerging molecular logic. *Trends Genet.* **31**, 316–328 (2015).
15. Jezovit, J. A., Levine, J. D. & Schneider, J. Phylogeny, environment and sexual communication across the *Drosophila* genus. *J. Exp. Biol.* **220**, 42–52 (2017).
16. Takemura, S. et al. A connectome of a learning and memory center in the adult *Drosophila* brain. *eLife* 1–43 (2017). https://doi.org/10.7554/eLife.26975
17. Schneider-mizell, C. M. et al. Quantitative neuroanatomy for connectomics in *Drosophila*. *eLife* 1–36 (2016). https://doi.org/10.7554/eLife.12059
18. Münch, D. & Galizia, C. G. DoOR 2.0 - comprehensive mapping of *Drosophila melanogaster* odorant responses. *Sci. Rep.* **6**, 1–14 (2016).
19. Markow, T. A. & Grady, P. M. O. Evolutionary genetics of reproductive behavior in *Drosophila*: connecting the dots. *Annu. Rev. Genet.* **39**, 263–293 (2005).
20. Stensmyr, M. C., Stieber, R. & Hansson, B. S. The Cayman crab fly revisited — phylogeny and biology of *Drosophila endobranchia*. *PLoS One* **3**, e1942 (2008).
21. Tosi, D., Martins, M., Vilela, C. R. & Pereira, M. A. Q. R. On a new cave-dwelling bat-guano-breeding *Drosophila* closely related to *D. repleta* Wollaston (Diptera, Drosophilidae). *Brazilian. J. Genet.* **13**, 19–31 (1990).
22. Reed, L. K., Nyboer, M. & Markow, T. A. Evolutionary relationships of *Drosophila mojavensis*geographic host races and their sister species *Drosophila arizonae*. *Mol. Ecol.* **16**, 1007–1022 (2006).
23. Etges, W. J., Oliveira, C. C., De, Noor, M. A. F. & Ritchie, G. Genetics of incipient speciation in *Drosophila mojavensis*. III. *Life-Hist. divergence allopatry Reprod. Isol. Evol. (N. Y).* **64**, 3549–3569 (2010).
24. Date, P., Dweck, H. K. M., Stensmyr, M. C., Shann, J. & Hansson, B. S. Divergence in olfactory host plant preference in *D. mojavensis* in response to cactus host use. *PLoS One* **8**, 1–10 (2013).
25. Linz, J. et al. Host plant-driven sensory specialization in *Drosophila erecta*. *Proc. R. Soc. B* **280**, 20130626 (2013).
26. Dekker, T. et al. Loss of *Drosophila* pheromone reverses its role in sexual communication in *Drosophila suzukii*. *Proc. R. Soc. B* **282**, 20143018 (2015).
27. Keesey, I. W., Knaden, M. & Hansson, B. S. Olfactory specialization in *Drosophila suzukii*supports an ecological shift in host preference from rotten to fresh fruit. *J. Chem. Ecol.* **41**, 121–128 (2015).
28. Karageorgi, M. et al. Evolution of multiple sensory systems drives novel egg-laying behavior in the fruit pest *Drosophila suzukii*. *Curr. Biol.* **27**, 847–853 (2017).
29. Tanaka, R., Higuchi, T., Kohatsu, S., Sato, K. & Yamamoto, D. Optogenetic activation of the fruitless-labeled circuitry in *Drosophila subobscura*males induces mating motor acts. *J. Neurosci.* **37**, 11662–11674 (2017).
30. Seeholzer, L. F., Seppo, M., Stern, D. L. & Ruta, V. Evolution of a central neural circuit underlies *Drosophila* mate preferences. *Nature*. https://doi.org/10.1038/s41586-018-0322-9 (2018).
31. Ramaekers, A., Weinberger, S., Claeys, A., Kapun, M. & Yan, J. Altering the temporal regulation of one transcription factor drives sensory trade-offs. *bioRxiv* 1–53 (2018). https://www.biorxiv.org/content/https://doi.org/10.1101/348375v1.
32. Gilbert, S. F., Bosch, T. C. G. & Ledón-rettig, C. Eco-evo-devo: developmental symbiosis and developmental plasticity as evolutionary agents. *Nat. Publ. Gr.* **16**, 611–622 (2015).
33. Sultan, S. E. Development in context: the timely emergence of eco-devo. *Trends Ecol. Evol.* **22**, 575–582 (2007).
34. Sultan S.E. Eco-Evo-Devo. In: Nuno de la Rosa L., Müller G. (*eds*) *Evolutionary Developmental Biology*. Springer, Cham, (2017).
35. Abouheif, E., Favé, M., Ibarrarán-viniegra, A. S., Lesoway, M. P. & Rafiqi, A. M. Eco-evo-devo: the time has come. *Adv. Exp. Med. Biol.* **781**, 107–125 (2014).
36. Keesey, I. W. et al. Adult frass provides a pheromone signature for *Drosophila* feeding and aggregation. *J. Chem. Ecol.* (2016). https://doi.org/10.1007/s10886-016-0737-4
37. Lin, C. & Potter, C. J. Re-classification of *Drosophila melanogaster* trichoid and intermediate sensilla using fluorescence-guided single sensillum recording. *PLoS One* 1–14 (2015). https://doi.org/10.1371/journal.pone.0139675
38. Dweck, H. K. M. et al. Pheromones mediating copulation and attraction in *Drosophila*. *PNAS* **112**, E2829–E2835 (2015).
39. Chern, J. J. & Choi, K. Lobe mediates Notch signaling to control domain-specific growth in the *Drosophila*eye disc. *Development* **129**, 4005–4013 (2002).
40. Singh, A., Shi, X. & Choi, K. Lobe and Serrate are required for cell survival during early eye development in *Drosophila*. *Development* **133**, 4771–4781 (2006).
41. Singh, A., Tare, M., Puli, O. R. & Kango-singh, M. A glimpse into dorso-ventral patterning of the *Drosophila* eye. *Dev. Dyn.* **241**, 69–84 (2012).
42. Andersson, M. B. *Sexual Selection*. (Princeton University Press, Princeton, 1994).
43. Reznick, D. Costs of reproduction: an evaluation of the empirical evidence. *Oikos* **44**, 257–267 (1985).
44. Bonduriansky, R. & Day, T. The evolution of static allometry in sexually selected traits. *Evol. (N. Y).* **57**, 2450–2458 (2003).
45. Tomkins, J. L., Kotiaho, J. S. & Lebas, N. R. Phenotypic plasticity in the developmental integration of morphological trade-offs and secondary sexual trait compensation. *Proc. R. Soc. B* **272**, 543–551 (2005). https://doi.org/10.1098/rspb.2004.2950
46. Niven, J. E. & Laughlin, S. B. Energy limitation as a selective pressure on the evolution of sensory systems. *J. Exp. Biol.* **211**, 1792–1804 (2008).

47. Weasner, B. M. & Kumar, J. P. Competition among gene regulatory networks imposes order within the eye-antennal disc of *Drosophila*. *Development* **140**, 205–215 (2013).
48. Nijhout, H. F. & Emlen, D. J. Competition among body parts in the development and evolution. *Proc. Natl. Acad. Sci.* **95**, 3685–3689 (1998).
49. Vollmer, J., Casares, F. & Iber, D. Growth and size control during development. *Open Biol.* **7**, 170190 (2017).
50. Gilad, Y., Wiebe, V., Przeworski, M., Lancet, D. & Pa, S. Loss of olfactory receptor genes coincides with the acquisition of full trichromatic vision in primates. *PLoS Biol.* **2**, 120–125 (2004).
51. Sanchez-Gracia A, Vieira F. G., Almeida F. C., Rozas J. 2011. Comparative genomics of the major chemosensory gene families in Arthropods. In: *Encyclopedia of Life Sciences*. Chichester (UK): John Wiley & Sons, Ltd. https://doi.org/10.1002/9780470015902.a0022848.
52. Posnien, N. et al. Evolution of eye morphology and rhodopsin expression in the *Drosophila melanogaster* species subgroup. *PLoS One* **7**, 1–11 (2012).
53. Gompel, N., Prud, B., Wittkopp, P. J., Kassner, V. A. & Carroll, S. B. Chance caught on the wing: cis-regulatory evolution and the origin of pigment patterns in *Drosophila*. *Nature* **433**, 481–487 (2005).
54. Edwards, K. A., Doescher, L. T., Kaneshiro, K. Y. & Yamamoto, D. A database of wing diversity in the Hawaiian *Drosophila*. *PLoS One* **2**, e487 (2007).
55. Yeh, S., Liou, S. & True, J. R. Genetics of divergence in male wing pigmentation and courtship behavior between *Drosophila elegans* and *D. gunungcola*. *Hered. (Edinb.)*. **96**, 383–395 (2006).
56. Prud'homme, B. et al. Repeated morphological evolution through cis-regulatory changes in a pleiotropic gene. *Nature* **440**, 1050–1054 (2006).
57. Kronforst, M. R. et al. Unraveling the thread of nature's tapestry: the genetics of diversity and convergence in animal pigmentation. *Pigment. Cell. Melanoma Res.* **25**, 411–433 (2012).
58. Hegde, S. N., Chethan, B. K. & Krishna, M. S. Mating success of males with and without wing patch in *Drosophila biarmipes*. *Indian J. Exp. Biol.* **43**, 902–909 (2005).
59. Aidinger-von Kleist, R. Genetic analysis of the light dependence of courtship in *Drosophila subobscura*. *Behav. Genet.* **15**, 123–134 (1985).
60. Noor, M. A. F. Diurnal activity patterns of *Drosophila subobscura* and *D. pseudoobscura* in sympatric populations. *Am. Midl. Nat.* **140**, 34–41 (1998).
61. Simmons, L. W. & Emlen, D. J. Evolutionary trade-off between weapons and testes. *PNAS* **103**, 16346–16351 (2006).
62. Stöckl, A. et al. Differential investment in visual and olfactory brain areas reflects behavioural choices in hawk moths. *Sci. Rep.* 1–10 (2016). https://doi.org/10.1038/srep26041
63. de Vries, L. et al. Comparison of navigation-related brain regions in migratory versus non-migratory noctuid moths. *Front. Behav. Neurosci.* **11**, 1–19 (2017).
64. Montgomery, S. H. & Merrill, R. M. Divergence in brain composition during the early stages of ecological specialization in *Heliconius* butterflies. *J. Evol. Biol.* **30**, 571–582 (2017).
65. Immonen, E., Dacke, M., Heinze, S. & Jundi, B. el. Anatomical organization of the brain of a diurnal and a nocturnal dung beetle. *J. Comp. Neurol.* **525**, 1879–1908 (2017). https://doi.org/10.1002/cne.24169
66. Bulova, S., Purce, K., Khodak, P., Sulger, E. & Donnell, S. O. Into the black and back: the ecology of brain investment in Neotropical army ants (Formicidae: Dorylinae). *Sci. Nat.* (2016). https://doi.org/10.1007/s00114-016-1353-4
67. Gronenberg, W. & Ho, B. Morphologic representation of visual and antennal information in the ant brain. *J. Comp. Neurol.* **240**, 229–240 (1999).
68. Rosner, R., Hadlen, J., von, Salden, T. & Homberg, U. Anatomy of the lobula complex in the brain of the praying mantis compared to the lobula complexes of the locust and cockroach. *J. Comp. Neurol.* **525**, 2343–2357 (2017).
69. Lin, A. Q. et al. Behavioral rhythms of *Drosophila suzukii* and *Drosophila melanogaster*. *Fla. Entomol.* **97**, 1424–1433 (2014).
70. Agrawal, A. A., Conner, J. K. & Rasmann, S. in Bell, M. A., Eanes, W. F., Futuyma, D. J., and Levinton, J. S. Tradeoffs and negative correlations in evolutionary ecology. in(*eds*) *Evolution after Darwin: the first 150 Years*. Sinauer Associates, Massachussetts, USA, (2010).
71. Wright, G. A. & Schiestl, F. P. The evolution of floral scent: the influence of olfactory learning by insect pollinators on the honest signalling of floral rewards. *Funct. Ecol.* **23**, 841–851 (2009).
72. Hirota, S. K. et al. Relative role of flower color and scent on pollinator attraction: experimental tests using F1 and F2 hybrids of daylily and nightlily. *PLoS One* **7**, e39010 (2012).
73. Valenta, K. et al. It's not easy being blue: are there olfactory and visual trade-offs in plant signalling? *PLoS One* **10**, 1–14 (2015).
74. Stökl, J. et al. A deceptive pollination system targeting drosophilids through olfactory mimicry of yeast. *Curr. Biol.* **20**, 1846–1852 (2010).
75. Arif, S. et al. Genetic and developmental analysis of differences in eye and face morphology between *Drosophila simulans* and *Drosophila mauritiana*. *Evol. Dev.* **267**, 257–267 (2013).
76. Da Lage, J. L. et al. A phylogeny of Drosophilidae using the Amyrel gene: questioning the *Drosophila melanogaster* species group boundaries. *J. Zool. Syst. Evol. Res.* **45**, 47–63 (2007).
77. O'Grady, P. & DeSalle, R. Out of Hawaii: the origin and biogeography of the genus *Scaptomyza* (Diptera: Drosophilidae). *Biol. Lett.* **4**, 195–199 (2008).
78. Silbering, A. F. et al. Complementary function and integrated wiring of the evolutionarily distinct *Drosophila* olfactory subsystems. *J. Neurosci.* **72**, 13357–13375 (2011).
79. Orme, D. et al. *The caper package: comparative analysis of phylogenetics and evolution in R. R package version 0.5*, 2 (2013) http://caper.r-forge.r-project.org.
80. Keesey et al. Inverse resource allocation between the evolution of vision and olfaction across the genus *Drosophila*. in Edmond. The open access data repository of the Max Planck Society, https://doi.org/10.17617/3.1D (2019).
81. Narda, R. D. Analysis of the stimuli involved in courtship and mating in *D. malerkotliana* (Sophophora, *Drosophila*). *Anim. Behav.* **14**, 378–383 (1966).
82. Colyott, K., Odu, C. & Gleason, J. M. Dissection of signalling modalities and courtship timing reveals a novel signal in *Drosophila saltans* courtship. *Anim. Behav.* **120**, 93–101 (2016).
83. Gleason, J. M., Pierce, A. A., Vezeau, A. L. & Goodman, S. F. Different sensory modalities are required for successful courtship in two species of the *Drosophila willistoni* group. *Anim. Behav.* **83**, 217–227 (2012).
84. Sakai, T., Isono, K., Tomaru, M. & Fukatami, A. Light wavelength dependency of mating activity in the *Drosophila melanogaster* species subgroup. *Genes. Genet. Syst.* **77**, 187–195 (2002).
85. Sakai, T., Isono, K., Tomaru, M. & Oguma, Y. Contribution by males to intraspecific variation of the light dependency of mating in the *Drosophila melanogaster* species subgroup. *Genes. Genet. Syst.* **72**, 269–274 (1997).
86. Bixler, A., Jenkins, J. B., Tompkins, L. & McRobert, S. P. Identification of acoustic stimuli that mediate sexual behavior in *Drosophila busckii* (Diptera: Drosophilidae). *J. Insect Behav.* **5**, 469–478 (1992).
87. Aidinger-von Kleist, R. Genetic analysis of the light dependence of courtship in *Drosophila subobscura*. *Behav. Genet.* **15**, 123–134 (1985).
88. Tompkins, L. Genetic analysis of sex appeal in *Drosophila*. *Behav. Genet.* **14**, 411–440 (1984).
89. Grossfield, J. O. E. Geographic distribution and light-dependent behavior in *Drosophila*. *PNAS* **68**, 2669–2673 (1971).
90. Spieth, H. T. & Hsu, T. C. The influence of light on the mating behavior of seven species of the *Drosophila melanogaster* species group. *Evol. (N. Y).* **4**, 316–325 (1950).
91. Croset, V. et al. Ancient protostome origin of chemosensory ionotropic glutamate receptors and the evolution of insect taste and olfaction. *PLoS Genet.* **6**, e1001064 (2010).
92. Wen, S.-Y. & Li, Y.-F. An evolutionary view on courtship behavior of *Drosophila*: from a comparative approach. *Low. Temp. Sci.* **69**, 87–100 (2011).

Acknowledgements

This research was supported through funding by the Max Planck Society. Genetic mutants used in this study were obtained from the Bloomington Drosophila Stock Center (NIH P40OD018537), and wild-type flies were obtained from the San Diego *Drosophila* Species Stock Center (now The National Drosophila Species Stock Center, Cornell University). We express our gratitude to S. Trautheim and her team for their technical support and guidance at MPI-CE. We thank Ibrahim Alali for his help with fly rearing and maintenance. Thank you to Dieter Gäbler from the Fraunhofer Institute for Applied Optics and Precision Engineering (IOF) for his support during the wavelength and reflectance measurements. We would also like to thank the research teams within the Department of Entomology at the University of Missouri, Division of Plant Sciences, and the scientists within the Department of Evolutionary Neuroethology, MPI-CE, in Jena, Germany, for their insights and comments.

Author contributions

This study was built on an idea conceived by I.W.K., while V.G., B.S.H., and M.K. all contributed to the design of this study. V.G. and I.W.K. completed the images and measurements associated with body morphometrics and ommatidium metrics. V.G. handled all neuroanatomy measures as well as the 3D reconstructions. L.G. and I.W.K. worked on the sensillum counts, while L.G. completed the lambda scans for antennal descriptions. I.W.K., G.B., and B.A.B. conducted the behavioral trials. I.W.K. and S.K. performed the imaginal disc experiments and metrics, including labeling, staining as well as confocal scans, with S.L.L. and J.R. providing their expertise. I.W.K. and D.R.V. worked on the courtship and wing images, as well as the data analyses. G.F.O., I.W.K., and M.A.K. assessed and built the molecular phylogeny, where D.R.V. and G.K. completed the statistical analyses for phylogenetic correction. M.A.K. and I.W.K. selected, ordered, and maintained fly species. I.W.K. prepared the original paper and all figures, while I.W.K., B.S.H., and M.K. all contributed to the final manuscript and subsequent revisions.

Additional information

Supplementary Information accompanies this paper at https://doi.org/10.1038/s41467-019-09087-z.

Competing interests: The authors declare no competing interests.

Reprints and permission information is available online at http://npg.nature.com/reprintsandpermissions/

Journal peer review information: *Nature Communications* thanks the anonymous reviewers for their contribution to the peer review of this work. Peer reviewer reports are available.

Publisher's note: Springer Nature remains neutral with regard to jurisdictional claims in published maps and institutional affiliations.

Supplementary Information

Inverse resource allocation between vision and olfaction across the genus *Drosophila*

Keesey et al.

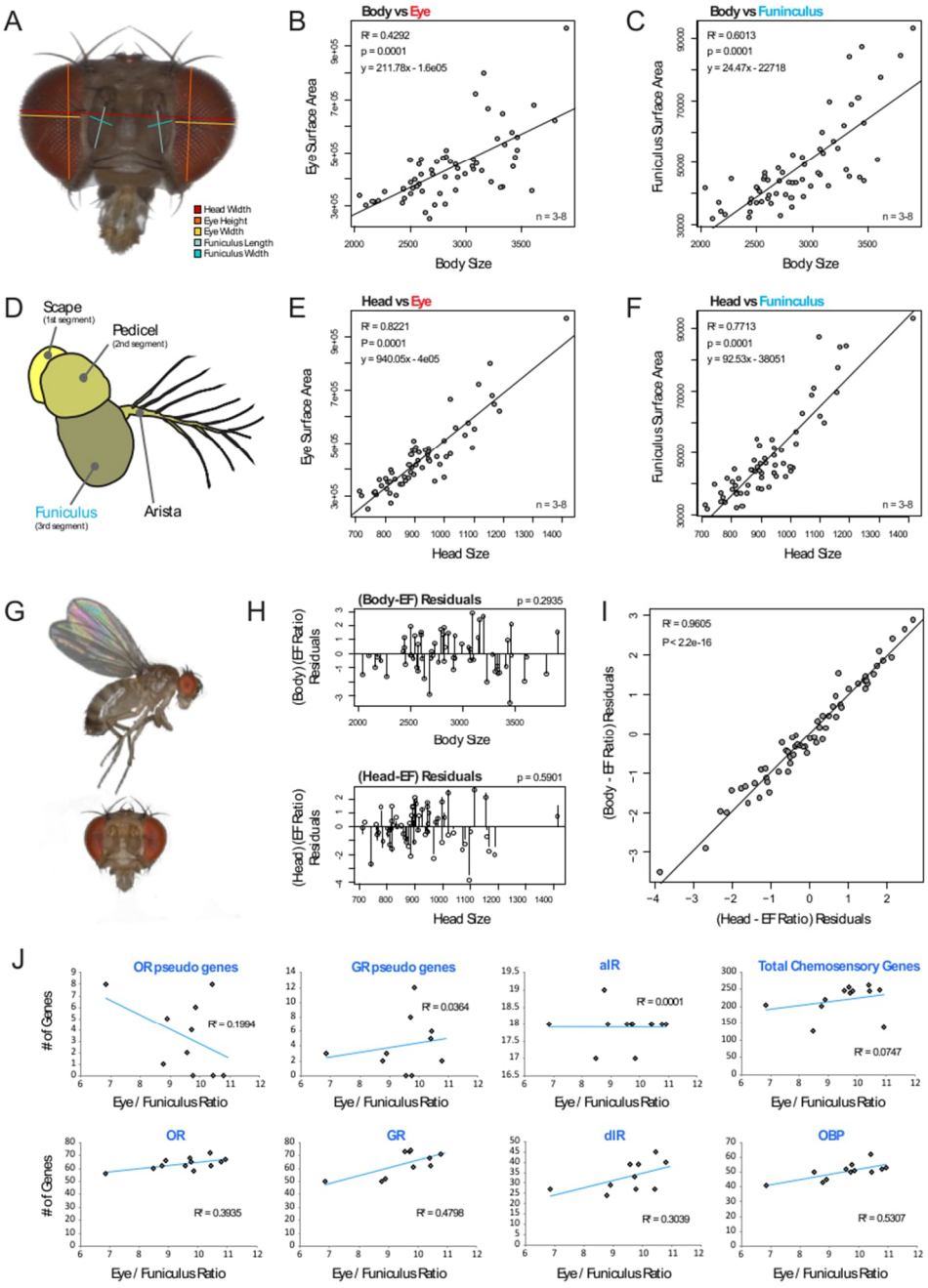

Supplementary Figure 1: External morphometrics from 62 species and functional chemoreceptor genes. (A) Example of measurements taken to calculate eye and funiculus surface area for each species. (B,C) Eye and funiculus surface area (μm^2) as compared to body size for each species. (D) Diagram of the *Drosophila* antenna, highlighting the 3rd antennal segment, also known as the funiculus (where the majority of chemosensory sensilla are located). (E,F) Eye and funiculus

surface area (μm^2) as compared to head size for each species. (G) Example of lateral and frontal views (*Drosophila melanogaster*), which were used to measure the body, head, eye and funiculus. (H) Plotting of the residuals, where neither body nor head size significantly correlate with the EF ratio trait, suggesting that this trait does not simply scale allometrically with respect to body and head size. (I) Residuals of head and body have highly similar deviations from EF-ratio, supporting that body and head size are highly correlated across all species. (J) Different chemosensory genes from 12-14 *Drosophila* species genomes and their correlation to the EF ratio [1], where number of olfactory pseudogenes, for example, does not suggest a sensory tradeoff. (Data are provided at doi.org/10.17617/3.1D).

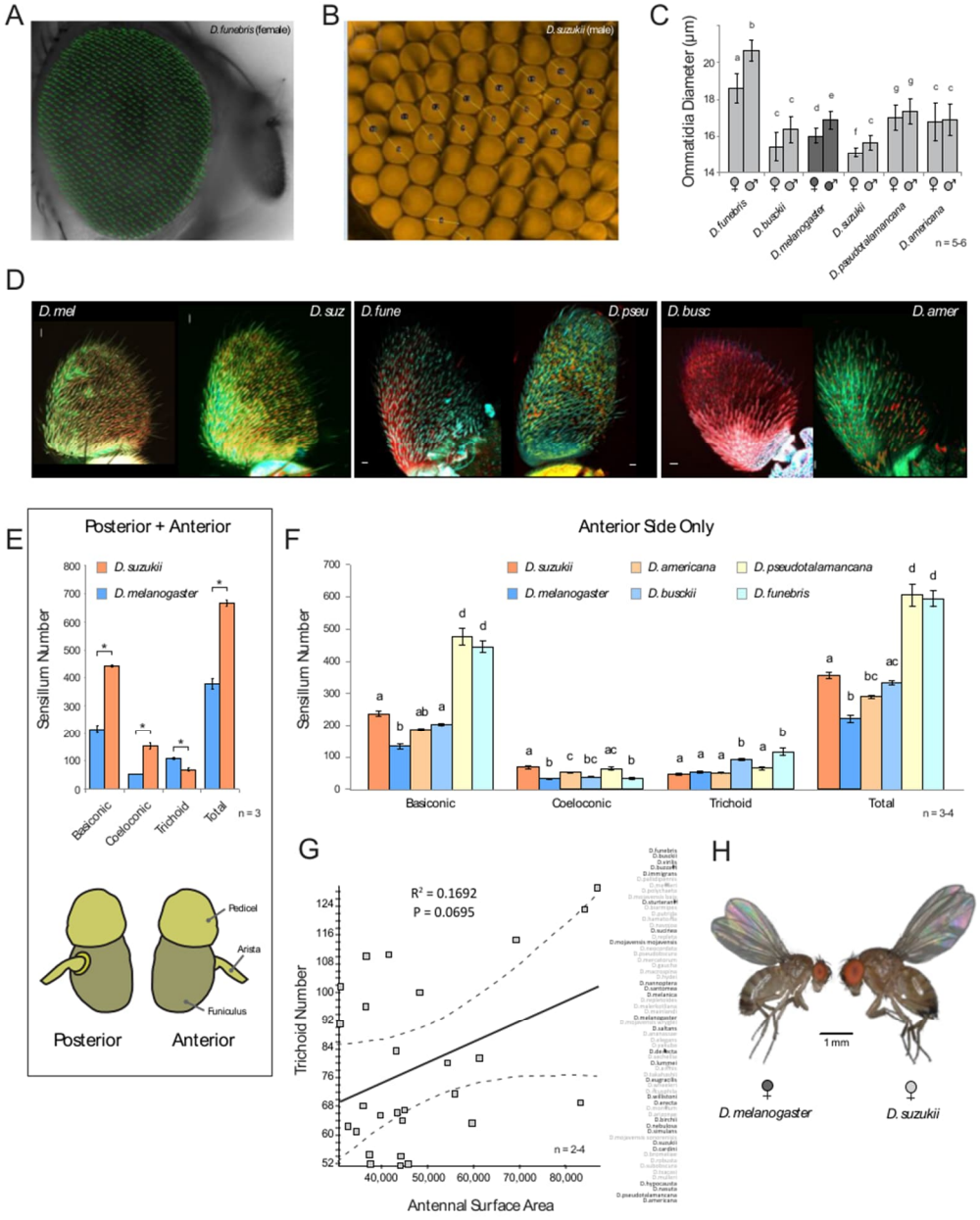

Supplementary Figure 2: Visual and olfactory sensory receptor measurements. (A) Example of ommatidium counts from photomontage of lateral view of *D. funebris* female head. (B) Examples of measurements taken to compare ommatidium diameters between species. (C) Ommatidia diameters. Means with the same letter are not significantly different from each other (ANOVA with Tukey-Kramer multiple comparison test). Error bars represent standard deviation. (D) Shown are examples of the images used for sensillum counts that were taken from stacked lambda mode scans (maximum intensity projections) of the anterior portion of the antenna for all 6 species examined. (E) Absolute sensillum counts from both sides of the antenna, as well as a diagram of anterior and posterior sides. Red to yellow color

signifies vision or visual bias, while blue indicates olfaction or olfactory species. An asterisk denotes statistical significance between two groups (*P ≤ 0.05, ***P ≤ 0.001; T-test). (F) Sensillum counts from lambda scans from only the anterior side of the antenna and the comparisons between all six species. Means with the same letter are not significantly different from each other (ANOVA with Tukey-Kramer multiple comparison test). Error bars represent standard deviation. (G) There is no correlation between trichoid number and antennal surface area, arguing against the idea that larger species necessarily have more trichoids. (H) Absolute size comparisons between two species, illustrating the differences in body, head, and eye morphology, where the body of the *D. suzukii* female is 1.5 times larger, but possesses a 2.5 times larger eye than the *D. melanogaster* female. (Data are provided at doi.org/10.17617/3.1D).

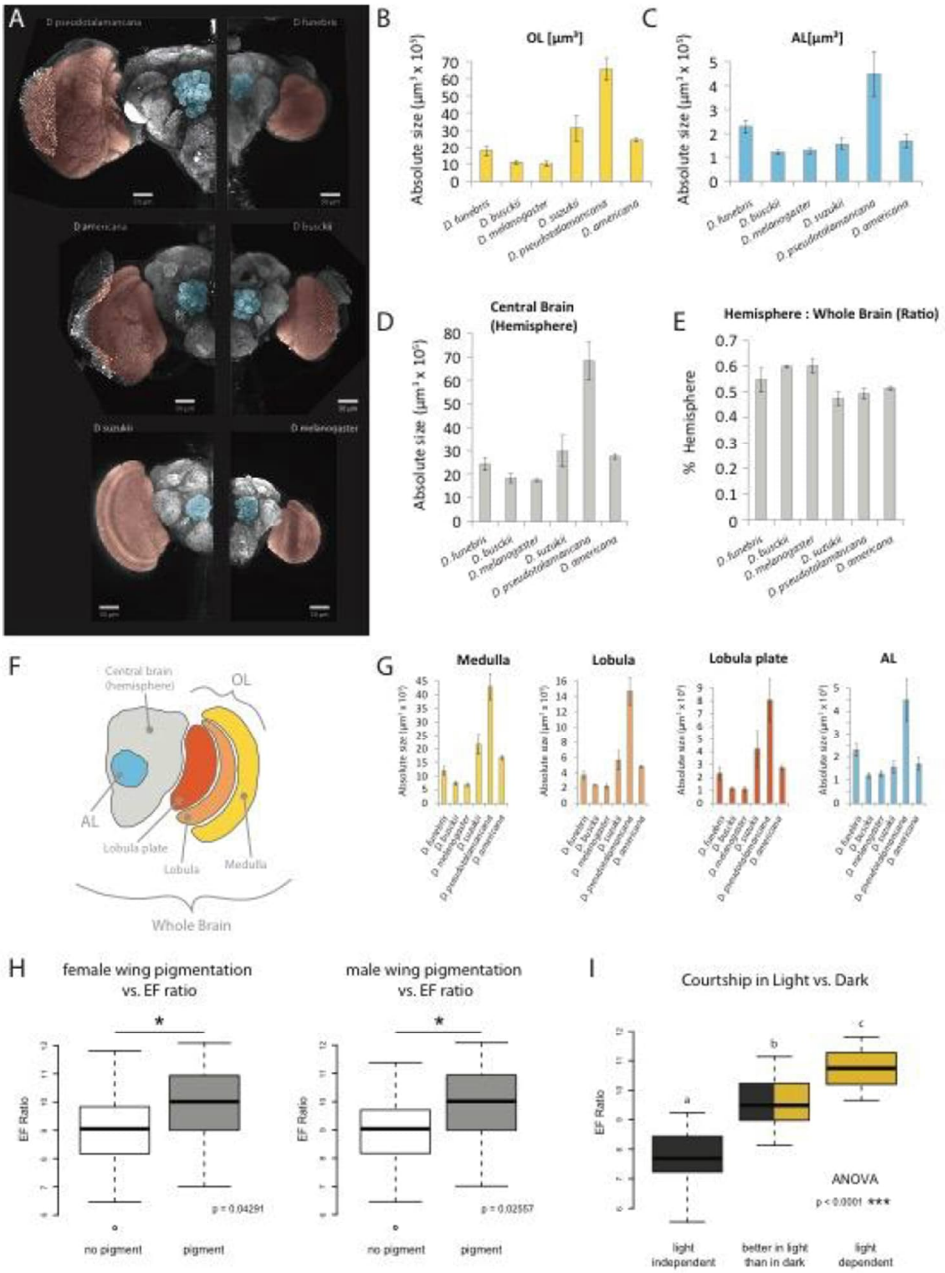

Supplementary Figure 3: Optic and antennal lobe measurements from 6 species. Red to yellow color signifies vision or visual bias, while blue indicates olfaction or olfactory species. (A) Confocal scans of each *Drosophila* species, with colored highlights for optic lobe (OL; red) and antennal lobe (AL; blue). Shown are the absolute measures of optic lobe (B), antennal lobe (C), and central brain volume (D), for each target species. (E) Although each species differed in absolute size, the ratio of central brain to total or whole brain (OL, AL, and central brain) for each species was roughly the same.

(F) Schematic of measurements taken from different species. (G) Absolute size of components of the OL and the AL from each species. (H) Female and male wing pigmentation plotted against EF ratio, where there is a correlation between relatively larger eyes and wing pigment across both sexes. An asterisk denotes statistical significance between two groups (*P ≤ 0.05, ***P ≤ 0.001; T-test). (I) Data from courtship in light or dark conditions as tested against EF ratio, where there is a highly significant difference in EF ratio across the three groups of courtship. Here again, relatively larger eyes correlate with better performance in light conditions, or with complete light-dependence for courtship. Means with the same letter are not significantly different from each other (ANOVA with Tukey-Kramer multiple comparison test). (Data are provided at doi.org/10.17617/3.1D).

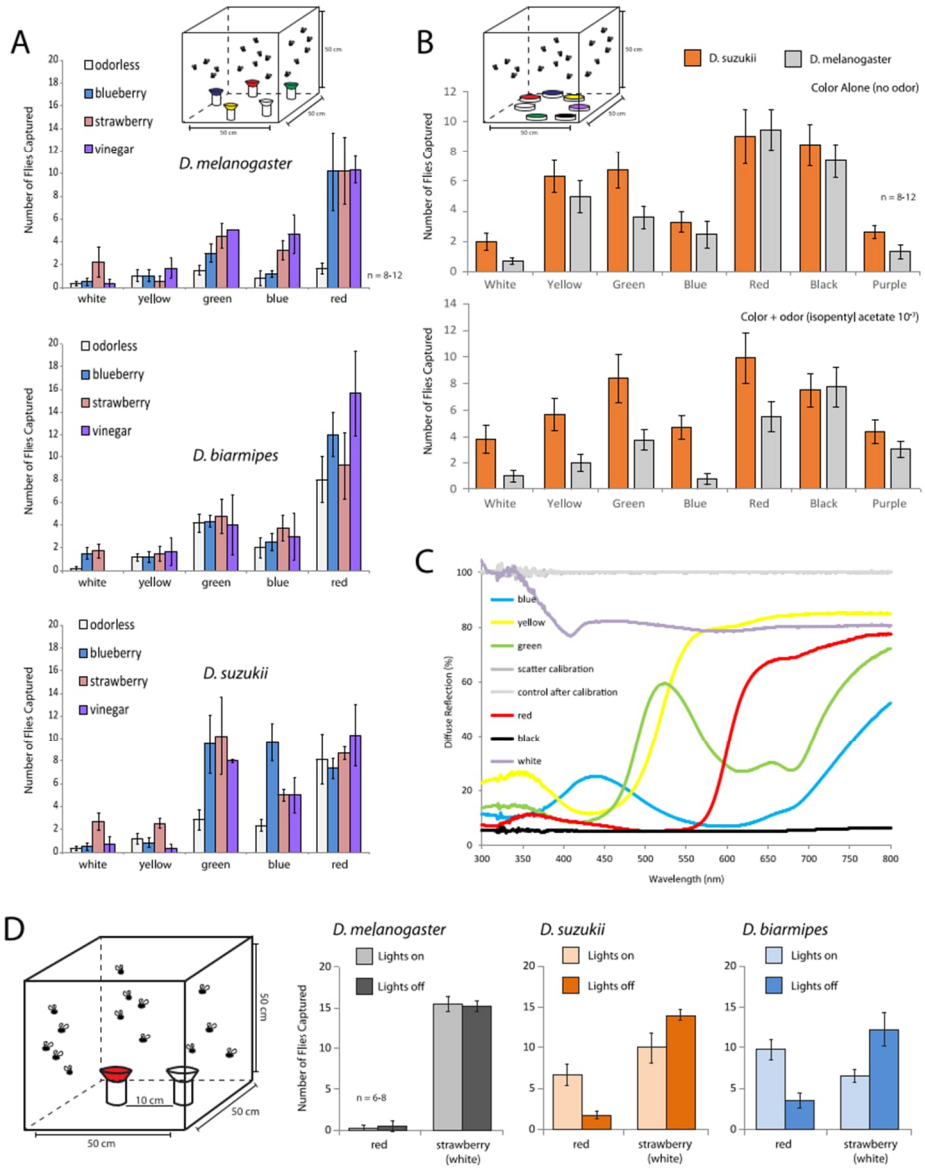

Supplementary Figure 4: Behavioral assays for visual and olfactory host navigation. (A) Design of trap assays using several visual and olfactory objects in testing attractive stimuli for each species. Red was the most attractive against the white background for all species regardless of the odor type, and even without odor, red was sufficient to capture spotted wing species. There was no significant difference in attraction to red when in combination with the three tested odors. The only color difference between species was noted to be an attraction to green for *D. suzukii*, as well as blue when in combination with blueberries, which they were reared upon. (B) Petri dish behavioral assay comparing *D. melanogaster* and *D. suzukii*, where both species showed similar color preference when presented without odor, although when with an odor, *D. suzukii* had a higher tendency towards white, yellow, green, blue and red than the other species. (C) Reflection index and wavelength for each color used in the behavioral assays. (D) Two-choice trap assay,

conducted in either full light, or full darkness. With lights off, all tested species were able to successfully navigate to the odor source; however, with lights on, the spotted wing species often mistakenly selected the visual object and not the odor object containing the fruit or food source, suggesting perhaps a visual bias or preference. In contrast, *D. melanogaster* always navigated to the odor source regardless of light condition or visual object, suggesting an olfactory bias or priority for this sensory cue. (Data are provided at doi.org/10.17617/3.1D).


A
D.funebris
D.erecta
D.eugracilis
D.nannoptera
D.immigrans
D.simulans
D.lummei
D.willistoni
D.hypocausta
D.moja moja
D.cardini
D.birchii
D.santomea
D.suzukii
D.deflecta
D.nebulosa
D.busckii
D.sucinea
D.sturtevanti
D.americana
D.melanogaster
D.virilis
D.nasuta
D.melanica
D.buzzatii
D.pseudotalamancana
D.neocordata
D.saltans
B
D.biarmipes
D.takahashii
D.suzukii

Supplementary Figure 5: Antennal preparations and trichoid counts from selected species. (A) Each *Drosophila* species was mounted using single-sensillum recording (SSR) preparation techniques, and a series of images was taken to generate a z-stack photomontage. Trichoid sensilla were counted from male individuals over the same region of the funiculus for each *Drosophila* species. Images were taken with the arista mounted upward for consistency and for the best viewing angle as previously described for this sensillum type [2]. (B) Example of *Drosophila* species from a single phylogenetic clade that show a decreasing number of trichoid sensillum (left to right), and differences in surface area containing these sensilla, as well as differing sensillum length.

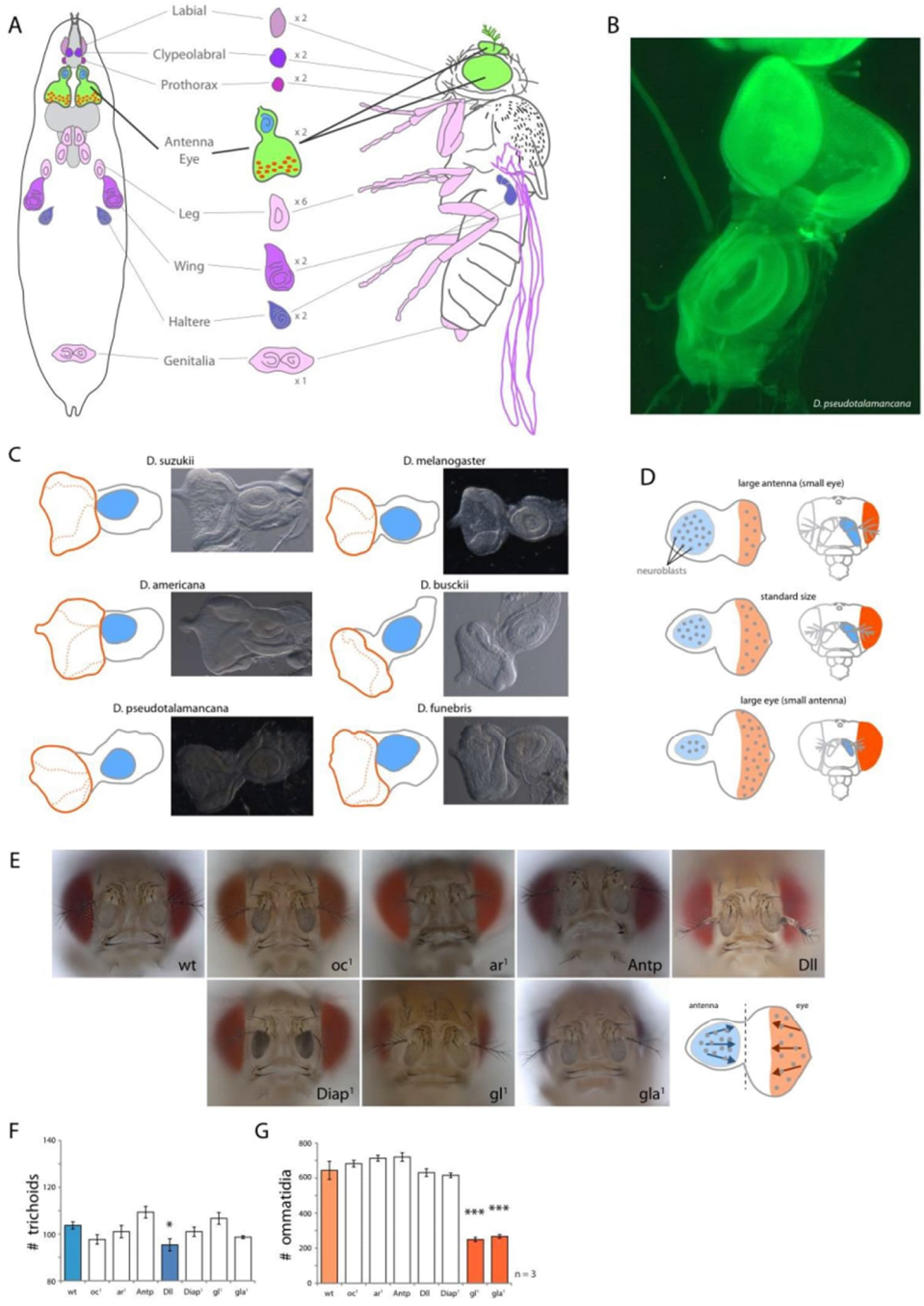

Supplementary Figure 6: The eye-antennal imaginal disc. (A) Diagram of the 19 total imaginal discs from *Drosophila* larvae and their corresponding location on the adult, highlighting that only one disc gives rise to two separate adult structures, namely the eye-antennal disc. (B) GFP labeling of *D. pseudotalamancana* imaginal disc, used to visualize the three-dimensional folding of the eye portion, as well as the shape and border of the antennal portion within the disc. (C)

Outlines and relative size measurements for eye and antenna from the imaginal discs of all 6 main species. Red color signifies vision or the visual system, while blue indicates olfaction. (D) Illustration of evo-devo theory of inverse resource allocation within one disc in order to generate a negative correlation between two adult sensory systems, the eye and antenna. (E) Wildtype and *melanogaster* mutants screened for either eye or antenna development, focusing on the ommatidium and trichoid numbers. (F) Trichoid number for each tested mutant, where only one was significantly different, Dll, which has an enlargement of the arista, and a decrease in each antennal segment size. Asterisk denotes significant difference from wildtype flies (T-test). (G) Ommatidium numbers from each mutant compared to the wildtype, where two lines showed marked reduction in ommatidia development. Asterisk denotes significant difference from wildtype flies (T-test). (Data are provided at doi.org/10.17617/3.1D).

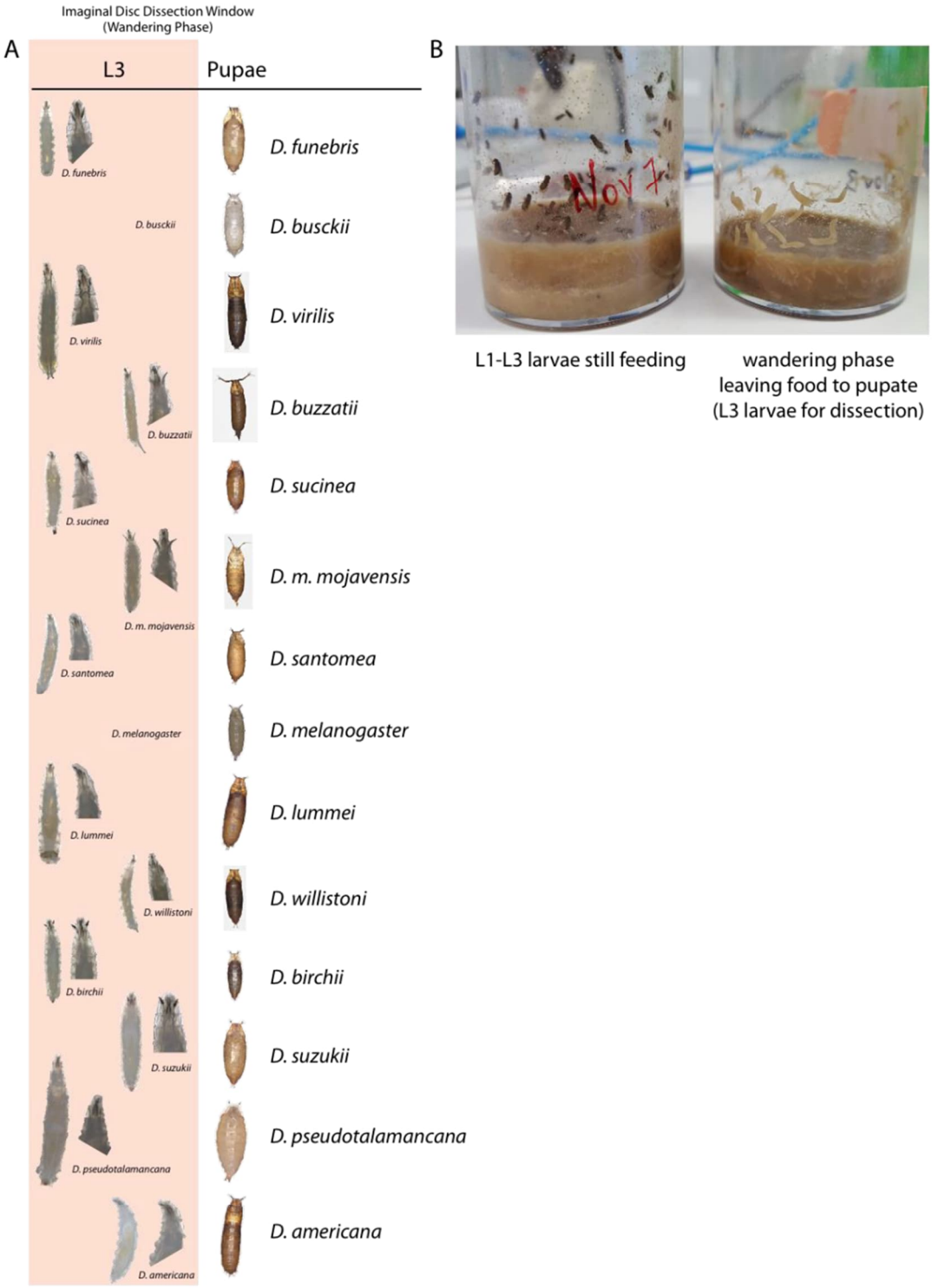

Supplementary Figure 7: Pupae and 3rd instar wandering phase larvae. (A) Given that each species had a different

developmental duration from egg to adult, we selected larvae for imaginal disc dissection during the same developmental window of time, namely the 3rd instar wandering phase larvae, which occurs just prior to the onset of pupation. (B) Example of 3rd instar larvae feeding on top layer of food (left) and 3rd instar wandering phase larvae (right) that have stopped feeding and are in search of a suitable pupation site. The latter of which were selected from each species for consistent dissection of the imaginal disc. (Data are provided at http://doi.org/10.17617/3.1D)

Supplementary Table 1: All scientific names, rearing media and stock numbers. (A) *Drosophila* species in alphabetical order, in conjunction with media used for rearing, as well as stock center identity. More information about each species is available through these stock numbers (e.g. site of insect collection, collection date, and reference specimens) (B-C) Recipe for diets used in this study. Green and blue colored diets were supplemented with either *Opuntia* cactus powder or fresh blueberries to enhance oviposition. Flies were maintained in a density-controlled manner, with 20-25 females per vial.

A

	Species Name	Diet/Media	UCSD/Cornell Stock #
1	*Drosophila affinis*	banana food	14012-0141.00
2	*Drosophila americana*	banana food	15010-0951.00
3	*Drosophila ananassae*	normal food	14024-0371.12
4	*Drosophila arizonae*	banana food	15081-1271.33
5	*Drosophila biarmipes*	normal food	14023-0361.10
6	*Drosophila birchii*	normal food	14028-0521.00
7	*Drosophila bromeliae*	banana food	15085-1682.00
8	*Drosophila busckii*	banana food	13000-0081.00
9	*Drosophila buzzatii*	normal food	15081-1291.02
10	*Drosophila cardini*	banana food	15181-2181.03
11	*Drosophila deflecta*	banana food	15130-2018.00
12	*Drosophila elegans*	normal food	14027-0461.00
13	*Drosophila erecta*	normal food	14021-0224.01
14	*Drosophila eugracilis*	normal food	14026-0451.02
15	*Drosophila ficusphila*	banana food	14025-0441.01
16	*Drosophila funebris*	normal food	15120-1911.05
17	*Drosophila gaucha*	banana food	15070-1231.03
18	*Drosophila hamatofila*	banana food	15081-1301.05
19	*Drosophila hydei*	normal food	15085-1641.03
20	*Drosophila hypocausta*	normal food	15115-1871.04
21	*Drosophila immigrans*	normal food	15111-1731.00
22	*Drosophila lummei*	wheat food	15010-1011.01
23	*Drosophila macrospina*	wheat food	15120-1931.00
24	*Drosophila mainlandi*	banana food	15081-1315.02
25	*Drosophila malerkotliana*	banana food	14024-0391.00
26	*Drosophila melanica*	normal food + blueberry	15030-1141.03
27	*Drosophila melanogaster Canton S*	normal food	Hansson Lab Strain
28	*Drosophila mercatorum*	normal food	15082-1521.00
29	*Drosophila mettleri*	banana food	15081-1502.11
30	*Drosophila mojavensis baja*	Banana-Opuntia	15081-1351.30
31	*Drosophila mojavensis mojavensis*	Banana-Opuntia	15081-1352.10
32	*Drosophila mojavensis sonorensis*	Banana-Opuntia	15081-1352.32
33	*Drosophila mojavensis wrigleyi*	Banana-Opuntia	15081-1352.30
34	*Drosophila montium*	banana food	14028-0701.00
35	*Drosophila mulleri*	Banana-Opuntia	15081-1371.01
36	*Drosophila nannoptera*	banana food	15090-1692.00
37	*Drosophila nasuta*	normal food	15112-1781.01
38	*Drosophila navojoa*	Banana-Opuntia	15081-1374.12
39	*Drosophila nebulosa*	normal food	14030-0761.00
40	*Drosophila neocordata*	banana food	14041-0831.00
41	*Drosophila pallidipennis*	banana food	15210-2331.01
42	*Drosophila polychaeta*	normal food	15100-1711.01
43	*Drosophila pseudoobscura*	banana food	14011-0121.00
44	*Drosophila pseudotalamancana*	normal food	15040-1191.00
45	*Drosophila putrida*	banana food	15150-2101.00
46	*Drosophila repleta*	banana food	15084-16611.02
47	*Drosophila repletoides*	banana food	15250-2451.01
48	*Drosophila robusta*	banana food	15020-1111.01
49	*Drosophila saltans*	banana food	14045-0911.00
50	*Drosophila santomea*	banana food	14021-0271.01
51	*Drosophila sechellia*	normal food + blueberry	14021-0248.07
52	*Drosophila simulans*	normal food	14021-0251.01
53	*Drosophila sturtevanti*	normal food	14043-0871.01
54	*Drosophila subobscura*	banana food	14011-0131.04
55	*Drosophila sucinea*	normal food	14030-0791.00
56	*Drosophila suzukii*	normal food + blueberry	14023-0311.01
57	*Drosophila takahashii*	normal food + blueberry	14022-0311.00
58	*Drosophila tsacasi*	banana food	14028-0701.00
59	*Drosophila virilis*	normal food	15010-1051.00
60	*Drosophila wheeleri*	banana food	15081-1501.04
61	*Drosophila willistoni*	normal food	14030-0811.24
62	*Drosophila yakuba*	normal food	14021-0261.38

B

Normal Food

		500ml
treacle	g	59
brewer`s yeast	g	5.4
hot water	ml	101
agar	g	2.1
cold water	ml	135
Polenta	g	47
fill up with hot water	ml	135
flush out with hot water	ml	34
cold water	ml	54
propionic acid	ml	1.2
Nipagin 30%	ml	1.65

C

Banana Food

agar	g	85
yeast	g	165
methylparaben	g	13.4
blended bananas	g	825
Karo syrup	g	570
liquid malt extract	g	180
100% ethanol	ml	134
water	L	6

D

Wheat Food

		1L
semolina (corn based)	g	50
wheatgerm	g	50
sugar	g	50
dry yeast	g	40
agarose	g	8
water	ml	1000
propionic acid	ml	5
methylparaben	ml	3.3

Supplementary References

1. Sanchez-Gracia, A., Vieira, F. G., Almeida, F. C. & Rozas, J. in : *Encyclopedia of Life Sciences (ELS)* (2011). doi:10.1002/9780470015902.a0022848
2. Lin, C. & Potter, C. J. Re-classification of *Drosophila melanogaster* trichoid and intermediate sensilla using fluorescence-guided single sensillum recording. *PLoS One* **10** e0139675 (2015). doi:10.1371/journal.pone.0139675

DISCUSSION

"*While a single neuron is the basic anatomical and processing unit of the brain, it is not capable of generating behavior or, ultimately, thinking. The true functional unit of the central nervous system is a population of neurons, or neuronal ensembles*." – Miguel Nicolelis

The aim of my thesis was to extend the knowledge about the neuronal architecture and synaptic circuitry of the olfactory system with the goal to get a better understanding how the olfactory system is organized in order to implement the computation of olfactory information and how it evolved in distinct species for adaptations to specific environmental conditions. To address this, my thesis focused on three main questions:

(1) How do specialized olfactory glomerular circuits in the AL of *Drosophila melanogaster* that are tuned to single odorant of ecological importance differ in their synaptic circuitry to more abundant and broadly tuned glomeruli (**chapter I**)?

(2) What are specific cellular features in olfactory glomeruli (**chapter II**)?

(3) How did the olfactory system evolved differently across the genus *Drosophila* and how does it adapt to altering species-specific external conditions and lifestyle (**chapter III**)?

To follow up this task, I used state of the art microscopy techniques. I developed a novel approach to perform targeted and volume-based electron microscopy of identified regions (**chapter I and II**). By using the spectral-based lambda scan and the un-mixing technique[6] at the confocal laser scanning microscopy, I separated auto-fluorescent spectral profiles of olfactory sensilla for a fast sensilla classification and quantification in diverse *Drosophilid* species (**chapter III**).

Circuit features of specialized narrowly tuned glomerular circuits

The **chapter I** accomplishes a more comprehensive understanding of the detailed neural architecture and microcircuits in the antennal lobe (AL) at the ultramicroscopic level of olfactory glomeruli in *Drosophila melanogaster* and I will discuss how synaptic circuit organization correlates with distinct signal processing demands in distinct glomerular circuits.

[6] http://zeiss-campus.magnet.fsu.edu/articles/spectralimaging/introduction.html

Inspired by fast-innovating high-resolution electron-microscopy techniques, such as Focused Ion Beam Scanning Electron Microscopy (FIB-SEM) (Xu *et al.*, 2020; Zheng *et al.*, 2017; Zheng *et al.*, 2020) and digital reconstruction tools, such as CATMAID[7] (Li, P. H. *et al.*, 2020; Saalfeld *et al.*, 2009; Schneider-Mizell *et al.*, 2016), this study aimed to investigate the dense connectomes of selected and previously morphologically and functionally described olfactory glomeruli: the DA2 and the DL5 (Grabe *et al.*, 2016; Knaden *et al.*, 2012; Stensmyr *et al.*, 2012). To accomplish this in an appropriate time scale, I developed a correlative workflow that combines transgenic neuron labeling to identify glomeruli of interest with near-infrared-laser-branding for precise volume targeting (Bishop *et al.*, 2011). Targeted glomerular volumes were subsequently scanned with FIB-SEM, an electron microscopy technique that images at the synaptic resolution level the full volume of the target glomeruli (Briggman *et al.*, 2012; Xu *et al.*, 2017). All neuronal fibers and their synapses were manually reconstructed in the two olfactory glomerular neuropils to untangle the dense neuropil and its microcircuits using CATMAID software (**Figure 5**). An advantage of this approach is that it facilitates localization of the volume of interest with high precision and consequently limits the image volume to a minimum and thus reduces scanning time. At the same time, the limitation in volume is a drawback of this workflow, as it was impossible to reconstruct neurons back to their soma. This is important to define neuronal lineages to identify neuron types, as performed in recent connectome studies (Bates *et al.*, 2020; Berck *et al.*, 2016; Eichler *et al.*, 2017; Horne *et al.*, 2018; Scheffer *et al.*, 2020; Schlegel *et al.*, 2021; Zheng *et al.*, 2018). In this study, we used ultrastructural criteria for neuron classification.

[7] http://www.catmaid.org

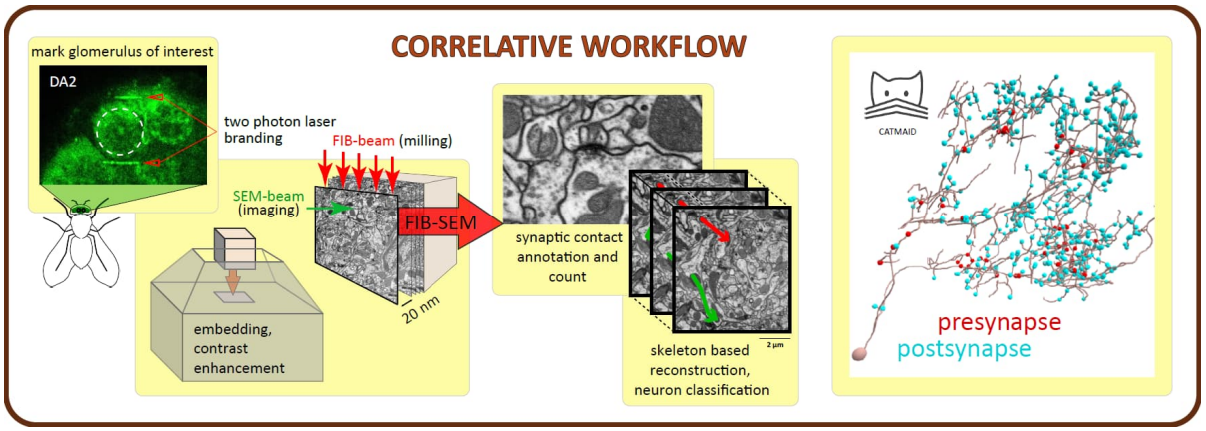

Figure 5 Correlative workflow to achieve a dense connectome of selected glomeruli. The scheme depicts the correlative workflow used to image previously marked olfactory glomeruli with high resolution volume targeting Focused Ion Beam Electron Microscopy (FIB-SEM) and to reconstruct the neuronal network. Transgenic neuron labeling combined with near-infrared-laser-branding with a two-photon laser enables glomerulus identification and marking. With the aid of subsequent FIB-SEM imaging and the software CATMAID, neurons, with their synaptic contacts, were reconstructed. The produced dense connectome of the glomerulus DA2 and DL5 provided important circuit information.

This approach helped to untangle the microarchitecture in the two glomeruli DA2 and DL5 (**manuscript I**). Recent publications gave clear evidence of the diversity in olfactory glomerular neuronal composition and its synaptic connections (Schlegel *et al.*, 2021) and that neuronal composition correlates with glomerular size and response profile (Grabe *et al.*, 2016), contradicting the assumed uniformity of glomerular neuronal composition (Ramaekers *et al.*, 2005; Vosshall *et al.*, 2000).

DA2 and DL5 circuits both contribute to an aversive behavior but have different response profiles, being highly dedicated either to single odorants (DA2) or activated by many odorants (DL5) (Knaden *et al.*, 2012; Mohamed *et al.*, 2019b; Münch *et al.*, 2016; Seki *et al.*, 2017; Stensmyr *et al.*, 2012). Narrowly tuned glomeruli, like the DA2, are often part of a specialized olfactory pathway, processing odorants of ecological importance for reproduction or in anticipation of hazards (Haverkamp *et al.*, 2018; Keesey *et al.*, 2021; Kurtovic *et al.*, 2007; Stensmyr *et al.*, 2012).

The dense connectome analysis adds up to missing information on the ultramicroscopic scale, by analyzing neuron arborizations, synaptic composition and local circuit motifs in olfactory glomeruli and how these differ from each other in correlation to the known glomerular response dynamics (Grabe *et al.*, 2016) (Figure 4). We compared all findings with the dense connectome of a second dedicated glomerular pheromone coding circuit, VA1v

(that has a positive valence) (Horne *et al.*, 2018). Five prominent features were disclosed as adaptations specific to narrowly tuned glomerular circuits that participate in a dedicated coding pathway, and which distinguish them from broadly tuned glomerular circuits participating in multi-glomerular coding (summarized in Figure 6). While narrowly tuned glomerular circuits, such as DA2 and VA1v show already high specificity to their odorant, due to the receptor tuning, the five features, disclosed in this study, are contributing to the maintenance of signal amplification, coding accuracy and integration speed in higher brain centers in "one-glomerular odorant coding pathways" as discussed in the following paragraphs.

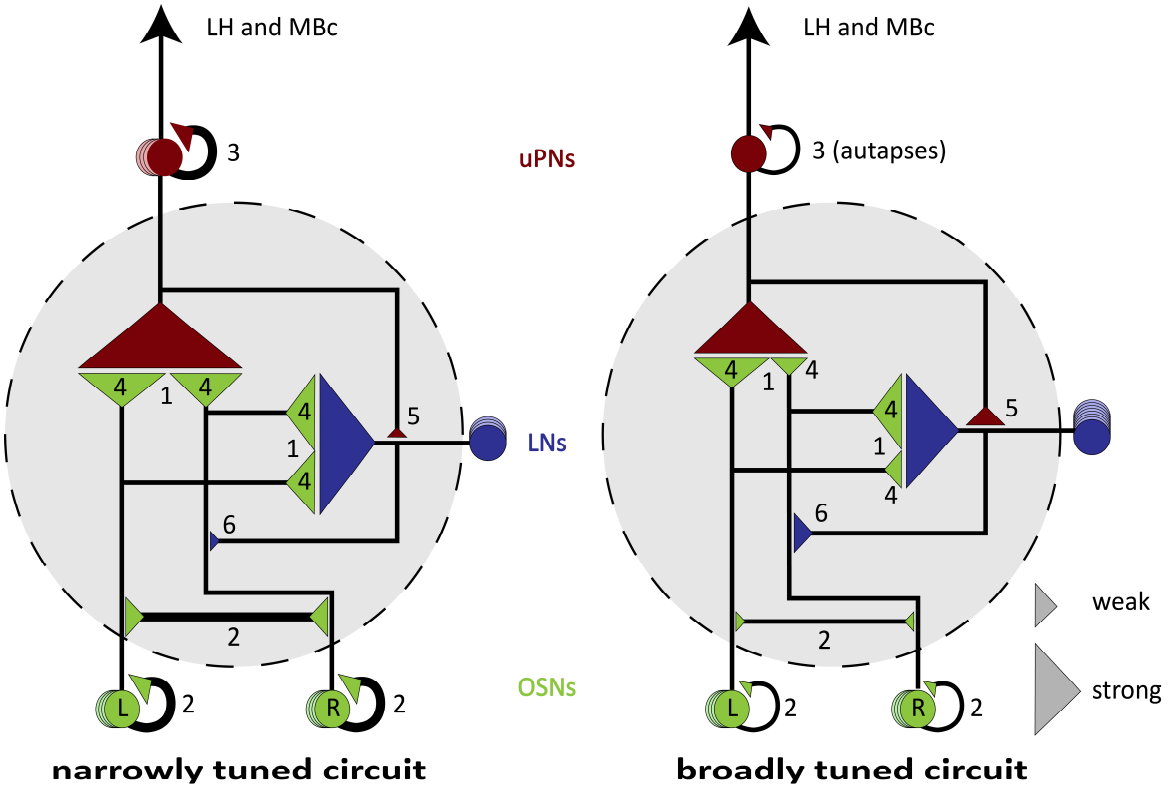

Figure 6 Special features in narrowly tuned glomerular circuits. Narrowly tuned glomerular circuits reveal five specific circuit features that differentiate them from broadly tuned ones. These features are illustrated in the scheme of the two types of glomeruli (grey circles). The different number of colored circles illustrate similar or distinct numbers of neurons in these two types of glomerular circuits (known from Grabe *et al*. (2016). Different sizes of triangles illustrate the strength of the connection between two classes of neurons (see legend on the right) with respect to the relative number of synapses in relation to the total number of synapses in the circuit. Narrowly tuned glomerular circuits have a stronger olfactory sensory neuron (OSNs; green) output (1), more reciprocal axo-axonic connections between OSNs (2) and dendro-dendritic connections between uniglomerular projection neurons (uPNs; red) (3), which transmit signals further to the lateral horn (LH) and the mushroom body calyx (MBc). OSNs are less lateralized in their connectivity (4), modulatory local interneurons (LNs; blue) receive less feedback from uPNs (5) and provide less feedback to OSNs (6). In the broadly tuned circuit, the uPN forms autaptic connections onto itself (3).

In the narrowly tuned circuits (DA2, VA1v) the synaptic output of OSNs was stronger (with respect to the number of synaptic contacts) than in the broadly tuned one (DL5), while maintaining the high convergences of OSN input at the level of the 5-7 second-order projection or AL output neurons (uPNs), i.e. each OSN synapses onto each of the 5-7 uPNs. This was in agreement with reports on the narrowly tuned glomerulus DA1 (Agarwal *et al.*, 2011; Jeanne *et al.*, 2015). The increased number of sensory input sites at the uPN level accompanied by the maintained high OSN input convergence putatively drives signal amplification at weak odorant concentrations (Acebes *et al.*, 2001) and supports the synchronization of uPN spiking events and improves the speed of signal integration (Kazama *et al.*, 2009; Rospars *et al.*, 2014).

Furthermore, the reciprocal excitatory axo-axonic connections between sister OSNs in the narrowly tuned glomeruli are more abundant in the narrowly tuned DA2 than in DL5. This confirms observations in the narrowly tuned pheromone coding circuits of the VA1v, DA1 and DL3 (Dweck, H. K. *et al.*, 2015; Ebrahim *et al.*, 2015; Horne *et al.*, 2018; Schlegel *et al.*, 2021; Suh *et al.*, 2004). Axo-axonic synapses have also been reported between gustatory and mechanosensory neurons in *Drosophila* larvae (Miroschnikow *et al.*, 2018) and in the olfactory epithelium and the olfactory bulb of vertebrates (Hirata, 1964; Nagayama *et al.*, 2014; Shepherd *et al.*, 2021). In vertebrates, axo-axonic synapses between excitatory sensory neurons are involved in a synchronized transmitter release (Cover *et al.*, 2021), reminiscent of the synchronized uPN spiking due to reciprocal synaptic and electric coupling in the *Drosophila* AL and LH (Huoviala *et al.*, 2020; Kazama *et al.*, 2009). Strong OSN-OSN connectivity has the potential to increase the correlation of OSN spiking events and therefore facilitate a robust OSN signal (de la Rocha *et al.*, 2007).

In addition, the narrowly tuned glomerulus DA2 has a substantial amount of excitatory dendro-dendritic uPN-uPN synapses as reported for the VA1v or other glomeruli with more than one uPN (Horne *et al.*, 2018; Jeanne *et al.*, 2015; Kazama *et al.*, 2009; Tobin *et al.*, 2017). Dendro-dendritic connections are also reported for mitral and tufted cells of the vertebrate olfactory bulb (Christie *et al.*, 2005; McTavish *et al.*, 2012; Shepherd *et al.*, 2021).

The reciprocal excitatory connectivity between sister OSNs and uPNs drives, in addition to the high convergence of the OSN-uPN connection, facilitates the synchronization of spike trains in uPNs (Chen *et al.*, 2005; Jeanne *et al.*, 2015; Kazama *et al.*, 2009). In the narrowly

tuned olfactory pathway a synchronized uPN activity between many uPNs, as reported for these circuits (Grabe *et al.*, 2016), improves intensively the signal-to-noise ratio (accuracy) of induced spikes. It increases furthermore processing speed, by reducing the latency of spike initiation in third-order neurons in the lateral horn (Jeanne *et al.*, 2018; Jeanne *et al.*, 2015).

Glomeruli participating in a dedicated olfactory pathway and processing ecologically important odorants, such as pheromones or host odorants are often described as macro-glomerular complexes innervated by an increased number of OSNs (Auer *et al.*, 2020; Boeckh *et al.*, 1993; Dekker *et al.*, 2006; Galizia *et al.*, 1999; Hansson *et al.*, 1992; Linz *et al.*, 2013; Nishino *et al.*, 2015). The DA2, however, by coding geosmin, is an important alarm signal of potentially toxic microorganisms (Gerber *et al.*, 1965; Jüttner *et al.*, 2007; Mattheis *et al.*, 1992), is rather small and has a moderate number of OSNs (~22 OSNs) (Grabe *et al.*, 2016; Grabe *et al.*, 2015). However, our study showed, a higher synaptic density in the DA2, in particular of OSNs (**manuscript I**), that stands in contradiction to previous descriptions depicting a uniform OSN synapse density throughout the AL (Mosca *et al.*, 2014). This increase in synapse number could be a way for the small DA2 glomerulus to improve signal sensitivity without an increased number of OSNs (Acebes *et al.*, 2001; Liu *et al.*, 2022).

OSNs project bilaterally to the left and right AL (Gaudry *et al.*, 2013; Schlegel *et al.*, 2021; Stocker *et al.*, 1990; Tanaka *et al.*, 2012). This is exceptional in the periphery of insects. In the mammalian olfactory system, for example, bilateral comparison of olfactory input occurs in higher brain centers (Dalal *et al.*, 2020). In flies, bilateral sensory input enables them to discriminate odor sources of different spatial origins through asymmetric OSN connection in the AL and a bilateral comparison of olfactory stimulation (Agarwal *et al.*, 2011; Borst *et al.*, 1982; Duistermars *et al.*, 2009; Gaudry *et al.*, 2013; Taisz *et al.*, 2022; Tobin *et al.*, 2017). In the narrowly tuned glomeruli, DA2 and VA1v, however, this asymmetry was weak (**manuscript I**) suggesting a weak left-right-contrast in the uPN response after methyl laurate (pheromone) or geosmin (alarm signal), respectively, stimulation. Both odorants act at short distances, while the fly is walking and not flying, influencing either aggregation or oviposition in females (investigated in this study). Perhaps, for the decision between avoiding and staying at a location at short distances the detection system needs to be less precise in location coding, as it is needed while flying and foraging (Demir *et al.*, 2020; Thoma *et al.*, 2015).

Last but not least, we found evidence in the narrowly tuned glomeruli, DA2 and VA1v for less presynaptic inhibition at OSNs (Root et al., 2008; Olsen et al., 2008), confirming

physiological observations in the AL (Hong *et al.*, 2015). Presynaptic inhibition is the main driver of gain and dynamic range control and regulates the duration and magnitude of incoming excitatory signals throughout the AL (Alon, 2007; Luo, 2021; Milo *et al.*, 2002). It plays, therefore, an important role in the combinatorial coding of olfactory cues in the AL (Galizia, 2014; Sachse *et al.*, 2021; Szyszka *et al.*, 2015). We found furthermore less uPN feedback onto modulatory LNs. The uPN feedback is described in the *Drosophila* larvae to synapse mainly onto pan-glomerular LNs, involved in lateral inhibition and gain control (Berck *et al.*, 2016). The OSN input that the LNs received and the LN output onto PNs in these circuits was still high, at least for DA2. So instead of inter-glomerular modulation, LNs in narrowly tuned glomeruli are likely to perform a stronger intra-glomerular modulation, which is important for PN fine-tuning and response adjustment (Assisi *et al.*, 2012; Ng *et al.*, 2002; Olsen *et al.*, 2010; Root *et al.*, 2007).

The circuit analysis in DA2 and DL5 in combination with the study from Horne *et al.* (2018) on the VA1v thus completes important knowledge on local circuit motifs and ultrastructural organization in these glomerular neuropils. It thus contributes to the large-scale connectome analysis of the *Drosophila* brain that includes the AL (Schlegel *et al.*, 2021) and sparse reconstructions in different glomeruli (Rybak *et al.*, 2016).

Autapses – short excitatory feedback loops within dendrites of olfactory neurons

Autapses are synapses that form feedback loops from a neuron onto itself, (Bekkers, 1998; Tamás *et al.*, 1997; Van der Loos *et al.*, 1972). They are reported at different frequencies in different types of neurons in the mammalian brain (Bekkers, 1998; Ikeda *et al.*, 2006; Saada *et al.*, 2009), acting either inhibitory (Bacci *et al.*, 2006; Saada *et al.*, 2009; Tamás *et al.*, 1997) or as excitatory feedback (Guo *et al.*, 2016; Wiles *et al.*, 2017; Yin *et al.*, 2018).

In the *Drosophila* AL, we found a substantial amount of autapses in the large dendrites of the DL5 uPN. So far, sparsely distributed autapses were briefly mentioned in the *Drosophila* brain in the medulla of the optic lobe (Takemura *et al.*, 2015) as well as in the glomerulus VA1v (Horne (Horne *et al.*, 2018). Our detailed analysis reports autapses, that form feedback loops from the basal dendritic tree of the DL5-uPN close to the entrance of the dendrite at the glomerulus border) to the distal branches and provide, to our knowledge, the first evidence of autapses within the dendritic tree of an insect neuron. These autapses have an inhomogeneous distribution, connecting more frequently rather distant than close sub-

regions of the dendritic tree and in addition form two clustered regions of autaptic input sites (**manuscript 1**). Recent studies in vertebrates show that excitatory autapses enhance neuron bursting and excitability (Guo *et al.*, 2016; Wiles *et al.*, 2017; Yin *et al.*, 2018). We hypothesize that the autapses in the DL5 uPN dendrite are also excitatory since the neurotransmitter of uPNs are acetylcholine (Yasuyama *et al.*, 2003). We suggest therefore an important role of the dendro-dendritic autapses in such large compartmentalized dendrites, as it is the case for the DL5 uPN, to enhance synchronized depolarization events of distinct dendritic subtrees, supporting a synchronized signal propagation along the dendrite to the axon initiation site situated at the AL border (Graubard *et al.*, 1980; Tran-Van-Minh *et al.*, 2015). In addition, clustered autaptic input can be important to set additional clustered depolarization events at dendritic subunits to the OSN-induced postsynaptic depolarization events (Kumar *et al.*, 2018; Liu *et al.*, 2022). A temporal summation of spatially close graded depolarization events induced by OSNs and autaptic excitatory feedback could thus be important to drive the polarization of the dendrite close to the threshold and therefore increases uPNs spiking probability of the uPN during OSN-induced activation (Stuart *et al.*, 2007)(Springer et al., in preparation).

Spinules – a generic feature in olfactory glomeruli

In **chapter II** we describe ultrastructural features in the olfactory glomeruli, reminiscent of synaptic spinules in the mammalian brain (reviewed in (Petralia *et al.*, 2015) that are not yet reported in the *Drosophila* brain. Synaptic spinules are deep invaginations nearby presynaptic sites formed by protrusions from neighboring neurons, as shown in our study of olfactory glomeruli. We observed most abundantly spinules innervating OSN presynaptic boutons (the latter are membrane swelling of the OSN axonal terminals) formed by protrusions from postsynaptic neurons (either branching off from PNs, OSNs or LNs). Similar invagination profiles are illustrated in images of *Drosophila* synapses in other brain neurons published by other authors, who did not name them explicitly (Berck *et al.*, 2016; Butcher *et al.*, 2012; Leiss *et al.*, 2009; Zheng *et al.*, 2018).

The spinules, as seen in the vertebrate brain (Spacek *et al.*, 2004), were also associated with double membrane vesicles (DMVs), which are considered to pinch-off from spinules, housing cytosolic content and vesicles. Moreover, we observed DMVs and spinules associated with mitochondria and with cisternae of the endoplasmic reticulum, two major sources of CA^{2+}

sources. Therefore, spinules and DMVs might be part of a recently well described neuronal ER network that includes contacts with the plasma membrane or mitochondria (Wu *et al.*, 2017) and might be involved in an activity-dependent growth and proliferation of spinules (Richards *et al.*, 2005; Tao-Cheng *et al.*, 2009; Ueda *et al.*, 2013).

The function of spinules remains elusive. However, they are discussed to play a role in synapse tagging, synaptic remodeling and neural plasticity by releasing material, such as microRNA or proteins, into the host neuron, triggered by synaptic activity and analogous to axonal pruning. Thus, they contribute to synaptic plasticity and synaptic tagging (Frey *et al.*, 1997; Redondo *et al.*, 2010), mediated by material transfer (Busto *et al.*, 2017; Cocucci *et al.*, 2015; Smalheiser, 2014). This might have therefore functional consequences for olfactory learning (Davis, 2004; Fiala, 2007; Hige, 2017; Keene *et al.*, 2007). Synaptic invaginations are also reported as sites of emphatic communication, a cellular non-synaptic communication referring to a coupling of adjusted cells, e.g. found in the vertebrate retina. Spinule-like invaginations provide thereby segregated regions inside the cell for ephaptic feedback (Vroman *et al.*, 2013). In the olfactory glomeruli, these invaginations could be also sites of ephaptic communication and therefore provide cell-to-cell communication in addition to chemical transmission via neurotransmitters, or neuropeptides (Carlsson *et al.*, 2010; Distler, 1990; Ignell *et al.*, 2009; Root *et al.*, 2011).

Evolutionary adaptation of the olfactory system across closely related species

In the last chapter, **chapter III**, I contributed to a large-scale study that focused on the evolution of the olfactory and the visual system across the genus of *Drosophila*. We provide a large-scale analysis of 62 Drosophila species and evidence for an inverse relationship between visual and olfactory neuropils and its investment of neural tissue, i.e. one sensory modality is consistently selected for investment in neuronal tissue at the expense of the other. This is associated with foraging behavior, in which one sensory modality performed more efficiently than the other one. The competition between those two traits (optic versus olfactory neuropil size), might be caused by a developmental constraint. A single imaginal disc, which gives rise to both the eye and antenna, might allow one system to grow at the expense of the other one. The sensory divergent variation was noted across the entire genus and appeared to represent repeated and independent evolutionary events. In sympatric species, sharing the same habitat, where courtship and host competition are strong, differences between vision and

olfaction investment were the highest and relaxed competition likely to drive opposing development of these two sensory systems (Keesey *et al.*, 2020). It remains an open question whether the developmental constraints, we investigated in *Drosophila melanogaster* is under similar constraints in non-melanogaster species. However, there is evidence of a single mutation that causes an inverse variation in ommatidia and sensilla numbers (Ramaekers *et al.*, 2019). A similar tradeoff has been reported in another group of flies (miltogrammine flies) and also in primates (Polidori *et al.*, 2022). This sensory specialization to different sensory inputs could be important, not only in foraging but also to evolve divergent courtship behavior and therefore for sexual isolation (Keesey *et al.*, 2020; Khallaf *et al.*, 2020).

Interestingly, species that exhibit a pronounced olfactory system had an increased number of trichoid sensilla. It would be of high interest for future studies to investigate the correlation of olfactory investment with evolutionary changes in glomerular number and size, OSN receptor specialization and changes in the olfactory networks (Keesey *et al.*, 2022; Seeholzer *et al.*, 2018). In fact, while most *Drosophila* species have roughly the same diversity of chemosensory genes and ommatidium types (Posnien *et al.*, 2012; Sánchez-Gracia *et al.*), across basiconic and trichoid sensilla different receptor ratios exist, where this variation is often associated with specialization (Auer *et al.*, 2020; Dekker *et al.*, 2006; Dekker *et al.*, 2015; Linz *et al.*, 2013). On the other hand, species with enlarged eyes and optic lobes exhibited a low number of trichoid sensilla and a greater degree of body pigmentation. Some of these species, such as *Drosophila suzukii* are known to produce a very low amount of a specific pheromone, that is detected by OSNs in trichoid sensilla (Keesey *et al.*, 2016). These examples demonstrate how the tight interplay between environmental conditions, species competition and developmental predisposition influences brain evolution.

Conclusion and future perspective

This thesis provided important insights into the complexity of the neural ultrastructure, synaptic connectivity and subcellular features of the olfactory nervous system and how this correlates with computational demands or, on a lower scale of resolution, how sensory neuropils change dependent upon species-specific external conditions and lifestyle. This work contributes therefore to a better understanding of how sensory systems implement specific computational tasks and how certain circuitry motifs dictate certain behaviors. During the last decades, a great effort has been done to comprehend the correlation between neuronal

network structure in the olfactory system and its function (reviewed in (Luo, 2021; Scheffer *et al.*, 2021). This thesis contributes to an expansion of this knowledge in the field of sensory neuroscience. Although still an unfinished picture, we provide data on ultrastructural features and network motifs that are important to improve the sensory performance in the insect's olfactory system. Our data provide also a solid base for modeling studies in order to better understand how the nervous system builds up and performs its computation on neural processing.

"*Design in nature is but a concatenation of accidents, culled by natural selection until the result is so beautiful or effective as to seem a miracle of purpose*." – Michael Pollan

It has always been amazing what we can learn from nature if we take the time to learn from it. What can we learn from insect brains? These tiny insects, despite their limited body and brain size, have evolved over a million years well-adapted sensory systems and achieve maximum efficiency in sensory tasks (miniaturization of brain size) (Polilov, 2016; Rybak *et al.*, 2016). Investigating their sensory system in more detail can find important technical applications (Marshall *et al.*, 2010), such as in the "artificial nose" to detect odorants that we as humans cannot detect and/or discriminate (Nowotny *et al.*, 2012).

SUMMARY

The perception of the olfactory world is not an easy task. Odor plumes are dynamic blends of diverse and mixed olfactory signals. Insects have evolved, in over millions of years, sophisticated sensory systems to perceive the olfactory environment and extract valuable information to induce an appropriate behavior, which ensures their survival and successful reproduction.

This thesis aimed to understand the details of the neural architecture of the olfactory system in flies of the genus *Drosophila* and its evolutionary adaptation to diverse species-specific environmental conditions. In the insect olfactory first relay station, the antennal lobe, olfactory sensory neurons (OSNs) relay odorant previously induced signals to segregated coding units, the olfactory glomeruli. At this level, the system already extracts and encodes valuable information, such as odor identity, concentration, or odor location. To cope with the almost infinite amount of olfactory chemicals, most insect's volatile odorants are encoded in a combinatorial manner, i.e. one odorant activates many distinct glomerular coding units, which in turn are activated by several odorants. Selected odorants with particular ecological importance for the fly's survival or reproduction are encoded in single and distinct glomerular circuitries.

In the first part of the thesis, I show in a dense connectome analysis in the fruit fly, *Drosophila melanogaster*, that these dedicated glomerular coding units have evolved specific circuit features that might be important to ensure improved accuracy and signal amplification. Furthermore, this study provides evidence that these glomeruli have fewer synapses involved in inter-glomerular modulation and rather more synapses involved in intra-glomerular modulation. The OSNs bilateral connection in these glomeruli displays a weak degree of asymmetry, which is important to induce a bilateral contrast and therefore to encode odor source location. This thesis discovered furthermore a substantial amount of autapses, self-activating feedback synapses, along the large dendrite of a uniglomerular projection neuron, which is a target neuron of OSNs further conveying the olfactory signal to following brain areas. The autapses are likely to play a role in the induction of fast action potentials during weak odor stimulation. In the second part, I discovered deep invaginations nearby presynaptic sites of mainly OSNs formed by protrusions from neighboring neurons. The so-called "synaptic spinules" play a role in neuronal communication and/ or modulation.

In the last part of my thesis, I contributed to a large-scale analysis, in which we investigated more than 60 species of the genus *Drosophila* with respect to their phenotypic properties, behavior, and their olfactory and visual systems. We identified an inverse resource allocation between vision and olfaction, consistently favoring one sensory modality over the other one in repeated evolutionary events across the genus *Drosophila*.

This work provides important information on synaptic circuits and architecture and on the question, of how the system might has evolved in the best possible way to adapt to species-specific environmental conditions and lifestyles.

ZUSAMMENFASSUNG

Die Wahrnehmung der olfaktorischen Welt ist keine leichte Aufgabe. Duftwolken sind eine Mischung aus vielfältigen olfaktorischen Informationen. Insekten haben über einen Zeitraum von Millionen von Jahren ihrer Evolution ausgefeilte sensorische Systeme entwickelt um die Düfte ihrer Umgebung wahrzunehmen und die wertvollen Informationen zu extrahieren um wiederum ein präzises angepasstes Verhalten auszulösen was ihr Überleben sowie auch eine erfolgreiche Vermehrung sicherstellt.

Das Ziel dieser Doktorarbeit war es die Details der neuronalen Architektur des olfaktorischen sensorischen Systems der Fliege, der Gattung *Drosophila*, besser zu verstehen und dessen evolutionäre Anpassung an die vielseitigen artenspezifischen Umgebungsbedingungen. In der ersten Schaltzentrale des olfaktorischen Systems der Insekten, im Antennallobus, leiten olfaktorische sensorische Neurone (OSNs) zuvor induzierte Signale an abgegrenzte Kodierungseinheiten, die olfaktorischen Glomeruli weiter. Auf dieser Ebene extrahiert und codiert das System wertvolle Informationen, wie zum Beispiele die Duftidentität, dessen Konzentration und Lokalisation. Um die fast unendliche Zahl an Duftstoffen zu verarbeiten hat das olfaktorische System der Insekten eine kombinatorische Strategie entwickelt dies zu tun, das heißt ein Duftstoff aktiviert viele glomeruläre Kodierungseinheiten, welche wiederum von vielen Duftstoffen aktiviert werden. Bestimmte Düfte mit besonderer ökologischer Bedeutung für das Überleben der Fliege und dessen Fortpflanzung werden jedoch innerhalb eines einzigen glomerulären Schaltkreises verarbeitet.

Im ersten Teil meiner Doktorarbeit zeige ich in einer Konnektomanalyse in der Fruchtfliege, *Drosophila melanogaster*, dass diese spezialisierten glomerulären Kodierungseinheiten spezifische Merkmale in ihren Schaltkreisen entwickelt haben, welche in der Sicherstellung einer genaueren Signalverarbeitung und Signalverstärkung eine Rolle spielen. Diese Arbeit liefert außerdem Beweise dafür, dass diese spezialisierten Glomeruli weniger Synapsen besitzen, die in der interglomerulären Verarbeitung von Duftsignalen beteiligt sind und mehr die in der intraglomerulären Verbreitung involviert sind. Die bilaterale Verschaltung der OSNs in diesen Glomeruli zeigen einen sehr geringen Grad an Asymmetrie, was eine wichtige Rolle in der Lokalisation der Duftstoffquelle spielt. Eine wesentliche Anzahl an Autapsen, welche selbst-aktivierende Rückverschaltungen des Neurons auf sich selbst darstellen, wurden entlang eines großen Dendriten eines uniglomerulären

Projektionsneurons entdeckt. Die Projektionsneurone sind Zielneurone der OSNs welches das olfaktorische Signal an nachgeschaltete Gehirnregionen weiterleitet. Die Autapsen spielen demzufolge wahrscheinlich eine wichtige Rolle in der schnellen Induzierung von Aktionspotentialen während einer schwachen Duftstimulierung. Im zweiten Teil der Arbeit beschreibe ich Einstülpungen in der Nähe der Präsynapsen der OSNs welche von Ausstülpungen der benachbarten Neuronen geformt werden. Diese sogenannten „synaptischen Spinules“ spielen eine Rolle in der neuronalen Kommunikation und Modulation. Im letzten Teil der Doktorarbeit habe ich an einer groß angelegten Studie teilgenommen, welche mehr als 60 *Drosophila*-Arten bezüglich deren phänotypischen Eigenschaften, Verhalten und ihrer olfaktorischen und visuellen Systeme untersucht hat. Wir haben eine entgegengesetzt gerichtete Ressourcenvergabe zwischen dem visuellen und olfaktorischen System beobachtet, bei der sich ein System immer auf Kosten des andern Systems entwickelt, was als wiederholte evolutionäre Ereignisse innerhalb der Gattung *Drosophila* zu beobachten war.

Diese Doktorarbeit liefert essentielle Informationen zur neuronalen Architektur und zu synaptischen Schaltkreisen im olfaktorischen System und zu der Frage wie olfaktorische Systeme sich im Laufe der Evolution bestmöglich und die artspezifische Umwelt und Lebensweise angepasst haben.

REFERENCES

Acebes, A., & Ferrus, A. (2001). Increasing the Number of Synapses Modifies Olfactory Perception in Drosophila. *Journal of Neuroscience, 21*(16), 6264–6273.

Ache, B. W., & Young, J. M. (2005). Olfaction: Diverse Species, Conserved Principles. *Neuron, 48*, 417-430. doi:10.1016/j.neuron.2005.10.022

Adams, M. D. (2000). The Genome Sequence of *Drosophila melanogaster*. *Science, 287*(5461), 2185-2195. doi:10.1126/science.287.5461.2185

Agarwal, G., & Isacoff, E. (2011). Specializations of a pheromonal glomerulus in the Drosophila olfactory system. *Journal of Neurophysiology, 105*(4), 1711-1721. doi:10.1152/jn.00591.2010

Alon, U. (2007). Network motifs: theory and experimental approaches. *Nature Reviews: Genetics, 8*(6), 450-461.

Andersson, M. N., Löfstedt, C., & Newcomb, R. D. (2015). Insect olfaction and the evolution of receptor tuning. *Frontiers in Ecology and Evolution, 3*. doi:10.3389/fevo.2015.00053

Asahina, K., Louis, M., Piccinotti, S., & Vosshall, L. B. (2009). A circuit supporting concentration-invariant odor perception in Drosophila. *Journal of Biology, 8*(1), 9. doi:10.1186/jbiol108

Aso, Y., Grubel, K., Busch, S., Friedrich, A. B., Siwanowicz, I., & Tanimoto, H. (2009). The mushroom body of adult Drosophila characterized by gal4 drivers. *Journal of Neurogenetics, 23*. doi:10.1080/01677060802471718

Assisi, C., Stopfer, M., & Bazhenov, M. (2012). Excitatory Local Interneurons Enhance Tuning of Sensory Information. *PLoS Computational Biology, 8*(7), e1002563. doi:10.1371/journal.pcbi.1002563

Auer, T. O., Khallaf, M. A., Silbering, A. F., Zappia, G., Ellis, K., Álvarez-Ocaña, R., . . . Benton, R. (2020). Olfactory receptor and circuit evolution promote host specialization. *Nature*. doi:10.1038/s41586-020-2073-7

Bacci, A., & Huguenard, J. R. (2006). Enhancement of spike-timing precision by autaptic transmission in neocortical inhibitory interneurons. *Neuron, 49*(1), 119-130. doi:10.1016/j.neuron.2005.12.014

Badel, L., Ohta, K., Tsuchimoto, Y., & Kazama, H. (2016). Decoding of Context-Dependent Olfactory Behavior in Drosophila. *Neuron, 91*(1), 155-167. doi:10.1016/j.neuron.2016.05.022

Barth, M., & Heisenberg, M. (1997). Vision affects mushroom bodies and central complex in *Drosophila melanogaster*. *Learning & Memory, 4*(2), 219-229. doi:10.1101/lm.4.2.219

Bates, A. S., Schlegel, P., Roberts, R. J. V., Drummond, N., Tamimi, I. F. M., Turnbull, R., . . . Jefferis, G. (2020). Complete Connectomic Reconstruction of Olfactory Projection Neurons in the Fly Brain. *Current Biology, 30*(16), 3183-3199 e3186. doi:10.1016/j.cub.2020.06.042

Becher, P. G., Verschut, V., Bibb, M. J., Bush, M. J., Molnár, B. P., Barane, E., . . . Flärdh, K. (2020). Developmentally regulated volatiles geosmin and 2-methylisoborneol attract a soil arthropod to Streptomyces bacteria promoting spore dispersal. *Nat Microbiol, 5*(6), 821-829. doi:10.1038/s41564-020-0697-x

Bekkers, J. M. (1998). Neurophysiology: are autapses prodigal synapses? *Current Biology, 8*(2), R52-55. doi:10.1016/s0960-9822(98)70033-8

Bell, J. S., & Wilson, R. I. (2016). Behavior Reveals Selective Summation and Max Pooling among Olfactory Processing Channels. *Neuron, 91*(2), 425-438. doi:10.1016/j.neuron.2016.06.011

Bellen, H. J., Tong, C., & Tsuda, H. (2010). 100 years of Drosophila research and its impact on vertebrate neuroscience: a history lesson for the future. *Nature Reviews: Neuroscience, 11*(7), 514-522. doi:10.1038/nrn2839

Benton, R., Sachse, S., Michnick, S. W., & Vosshall, L. B. (2006). Atypical Membrane Topology and Heteromeric Function of *Drosophila* Odorant Receptors In Vivo. *PLoS Biology, 4*(2), 240-257. doi:10.1371/journal.pbio.0040020

Benton, R., Vannice, K. S., Gomez-Diaz, C., & Vosshall, L. B. (2009). Variant ionotropic glutamate receptors as chemosensory receptors in Drosophila. *Cell, 136*(1), 149-162.

doi:10.1016/j.cell.2008.12.001

Benton, R., Vannice, K. S., & Vosshall, L. B. (2007). An essential role for a CD36-related receptor in pheromone detection in Drosophila. *Nature, 450*(7167), 289-293. doi:10.1038/nature06328

Berck, M. E., Khandelwal, A., Claus, L., Hernandez-Nunez, L., Si, G., Tabone, C. J., . . . Cardona, A. (2016). The wiring diagram of a glomerular olfactory system. *Elife, 5*, e14859. doi:10.7554/eLife.14859

Betzig, E., Patterson, G. H., Sougrat, R., Lindwasser, O. W., Olenych, S., Bonifacino, J. S., . . . Hess, H. F. (2006). Imaging Intracellular Fluorescent Proteins at Nanometer Resolution. *Science, 313*(5793), 1642-1645. doi:doi:10.1126/science.1127344

Bhandawat, V., Maimon, G., Dickinson, M. H., & Wilson, R. I. (2010). Olfactory modulation of flight in Drosophila is sensitive, selective and rapid. *Journal of Experimental Biology, 213*(Pt 21), 3625-3635. doi:10.1242/jeb.040402

Bhandawat, V., Olsen, S. R., Gouwens, N. W., Schlief, M. L., & Wilson, R. I. (2007). Sensory processing in the *Drosophila* antennal lobe increases reliability and separability of ensemble odor representations. *Nature Neuroscience, 10*(11), 1474-1482. doi:10.1038/nn1976

Bishop, D., Nikic, I., Brinkoetter, M., Knecht, S., Potz, S., Kerschensteiner, M., & Misgeld, T. (2011). Near-infrared branding efficiently correlates light and electron microscopy. *Nat Meth, 8*(7), 568-570. doi:10.1038/nmeth.1622

Boeckh, J., & Tolbert, L. P. (1993). Synaptic organization and development of the antennal lobe in insects. *Microscopy Research and Technique, 24*(3), 260-280. doi:10.1002/jemt.1070240305

Bokil, H., Laaris, N., Blinder, K., Ennis, M., & Keller, A. (2001). Ephaptic Interactions in the Mammalian Olfactory System. *The Journal of Neuroscience, 21*(20), RC173-RC173. doi:10.1523/JNEUROSCI.21-20-j0004.2001

Borst, A., & Heisenberg, M. (1982). Osmotropotaxis inDrosophila melanogaster. *Journal of comparative Physiology, 147*(4), 479-484. doi:10.1007/BF00612013

Breer, H., Fleischer, J., Pregitzer, P., & Krieger, J. (2019). Molecular Mechanism of Insect Olfaction: Olfactory Receptors. In J.-F. Picimbon (Ed.), *Olfactory Concepts of Insect Control - Alternative to insecticides: Volume 2* (pp. 93-114). Cham: Springer International Publishing.

Briggman, K. L., & Bock, D. D. (2012). Volume electron microscopy for neuronal circuit reconstruction. *Current Opinion in Neurobiology, 22*(1), 154-161. doi:http://dx.doi.org/10.1016/j.conb.2011.10.022

Busto, G. U., Cervantes-Sandoval, I., & Davis, R. L. (2010). Olfactory Learning in Drosophila. *Physiology, 25*(6), 338-346. doi:10.1152/physiol.00026.2010

Busto, G. U., Guven-Ozkan, T., & Davis, R. L. (2017). MicroRNA function in Drosophila memory formation. *Current Opinion in Neurobiology, 43*, 15-24. doi:10.1016/j.conb.2016.10.002

Butcher, N. J., Friedrich, A. B., Lu, Z., Tanimoto, H., & Meinertzhagen, I. A. (2012). Different classes of input and output neurons reveal new features in microglomeruli of the adult *Drosophila* mushroom body calyx. *Journal of Comparative Neurology, 520*(10), 2185-2201. doi:10.1002/cne.23037

Butterwick, J. A., Del Mármol, J., Kim, K. H., Kahlson, M. A., Rogow, J. A., Walz, T., & Ruta, V. (2018). Cryo-EM structure of the insect olfactory receptor Orco. *Nature, 560*(7719), 447-452. doi:10.1038/s41586-018-0420-8

Cajal, S. R. (1894). *Die Retina der Wirbelthiere*: Bergmann.

Cardona, A., Saalfeld, S., Preibisch, S., Schmid, B., Cheng, A., Pulokas, J., . . . Hartenstein, V. (2010). An integrated micro- and macroarchitectural analysis of the *Drosophila* brain by computer-assisted serial section electron microscopy. *PLoS Biology, 8*(10), 1-17. doi:10.1371/journal.pbio.1000502

Carlson, J. (1991). Olfaction in *Drosophila*: genetic and molecular analysis. *Trends in Neurosciences, 14(12)*, 520-524.

Carlsson, M. A., Diesner, M., Schachtner, J., & Nässel, D. R. (2010). Multiple neuropeptides in the Drosophila antennal lobe suggest complex modulatory circuits. *The Journal of Comparative Neurology, 518*(16), 3359-3380. doi:10.1002/cne.22405

Caron, S. J., Ruta, V., Abbott, L. F., & Axel, R. (2013). Random convergence of olfactory inputs in the

Drosophila mushroom body. *Nature, 497*(7447), 113-117. doi:10.1038/nature12063

Chalfie, M., Tu, Y., Euskirchen, G., Ward, W. W., & Prasher, D. C. (1994). Green fluorescent protein as a marker for gene expression. *Science, 263*(5148), 802-805. doi:10.1126/science.8303295

Chatterjee, A., Roman, G., & Hardin, P. E. (2009). Go contributes to olfactory reception in Drosophila melanogaster. *BMC Physiology, 9*, 22. doi:10.1186/1472-6793-9-22

Chen, W. R., & Shepherd, G. M. (2005). The olfactory glomerulus: A cortical module with specific functions. *Journal of Neurocytology, 34*, 353–360.

Chou, Y. H., Spletter, M. L., Yaksi, E., Leong, J. C., Wilson, R. I., & Luo, L. (2010). Diversity and wiring variability of olfactory local interneurons in the *Drosophila* antennal lobe. *Nature Neuroscience, 13*(4), 439-449. doi:10.1038/nn.2489

Christie, J. M., Bark, C., Hormuzdi, S. G., Helbig, I., Monyer, H., & Westbrook, G. L. (2005). Connexin36 mediates spike synchrony in olfactory bulb glomeruli. *Neuron, 46*(5), 761-772. doi:10.1016/j.neuron.2005.04.030

Clyne, P. J., Warr, C. G., Freeman, M. R., Lessing, D., Kim, J., & Carlson, J. R. (1999). A novel family of divergent seven-transmembrane proteins: candidate odorant receptors in Drosophila. *Neuron, 22*(2), 327-338. doi:10.1016/s0896-6273(00)81093-4

Coates, K. E., Calle-Schuler, S. A., Helmick, L. M., Knotts, V. L., Martik, B. N., Salman, F., . . . Dacks, A. M. (2020). The Wiring Logic of an Identified Serotonergic Neuron That Spans Sensory Networks. *The Journal of Neuroscience, 40*(33), 6309-6327. doi:10.1523/jneurosci.0552-20.2020

Cocucci, E., & Meldolesi, J. (2015). Ectosomes and exosomes: shedding the confusion between extracellular vesicles. *Trends in Cell Biology, 25*(6), 364-372. doi:10.1016/j.tcb.2015.01.004

Collmann, C., Carlsson, M. A., Hansson, B. S., & Nighorn, A. (2004). Odorant-Evoked Nitric Oxide Signals in the Antennal Lobe of Manduca sexta. *The Journal of Neuroscience, 24*(27), 6070-6077. doi:10.1523/jneurosci.0710-04.2004

Couto, A., Alenius, M., & Dickson, B. J. (2005). Molecular, anatomical, and functional organization of the *Drosophila* olfactory system. *Current Biology, 15*(17), 1535-1547. doi:10.1016/j.cub.2005.07.034

Cover, K. K., & Mathur, B. N. (2021). Axo-axonic synapses: Diversity in neural circuit function. *Journal of Comparative Neurology, 529*(9), 2391-2401. doi:10.1002/cne.25087

Croset, V., Treiber, C. D., & Waddell, S. (2018). Cellular diversity in the Drosophila midbrain revealed by single-cell transcriptomics. *eLife, 7*. doi:10.7554/eLife.34550

Dacks, A. M., Christensen, T. A., Agricola, H. J., Wollweber, L., & Hildebrand, J. G. (2005). Octopamine-immunoreactive neurons in the brain and subesophageal ganglion of the hawkmoth Manduca sexta. *Journal of Comparative Neurology, 488*(3), 255-268.

Dacks, A. M., Green, D. S., Root, C. M., Nighorn, A. J., & Wang, J. W. (2009). Serotonin modulates olfactory processing in the antennal lobe of Drosophila. *Journal of Neurogenetics, 23*(4), 366-377. doi:10.3109/01677060903085722

Dalal, T., Gupta, N., & Haddad, R. (2020). Bilateral and unilateral odor processing and odor perception. *Commun Biol, 3*(1), 150. doi:10.1038/s42003-020-0876-6

Das Chakraborty, S., & Sachse, S. (2021). Olfactory processing in the lateral horn of Drosophila. *Cell and Tissue Research, 383*(1), 113-123. doi:10.1007/s00441-020-03392-6

Das, S., Trona, F., Khallaf, M. A., Schuh, E., Knaden, M., Hansson, B. S., & Sachse, S. (2017). Electrical synapses mediate synergism between pheromone and food odors in *Drosophila melanogaster*. *Proceedings of the National Academy of Sciences, 114*(46), E9962-E9971. doi:10.1073/pnas.1712706114

Datta, S. R., Vasconcelos, M. L., Ruta, V., Luo, S., Wong, A., Demir, E., . . . Axel, R. (2008). The *Drosophila* pheromone cVA activates a sexually dimorphic neural circuit. *Nature, 452*(7186), 473-477. doi:10.1038/nature06808

Davie, K., Janssens, J., Koldere, D., De Waegeneer, M., Pech, U., Kreft, Ł., . . . Aerts, S. (2018). A Single-Cell Transcriptome Atlas of the Aging Drosophila Brain. *Cell, 174*(4), 982-998.e920. doi:10.1016/j.cell.2018.05.057

Davis, R. L. (2004). Olfactory Learning. *Neuron, 44*(1), 31-48.

doi:http://dx.doi.org/10.1016/j.neuron.2004.09.008

de Belle, J. S., & Heisenberg, M. (1994). Associative odor learning in Drosophila abolished by chemical ablation of mushroom bodies. *Science, 263*(5147), 692-695. doi:10.1126/science.8303280

de Bruyne, M., Clyne, P. J., & Carlson, J. R. (1999). Odor coding in a model olfactory organ: the *Drosophila* maxillary palp. *Journal of Neuroscience, 19*(11), 4520-4532.

de Bruyne, M., Foster, K., & Carlson, J. R. (2001). Odor Coding in the *Drosophila* Antenna. *Neuron, 30*(2), 537-552. doi:10.1016/S0896-6273(01)00289-6

de la Rocha, J., Doiron, B., Shea-Brown, E., Josić, K., & Reyes, A. (2007). Correlation between neural spike trains increases with firing rate. *Nature, 448*(7155), 802-806. doi:10.1038/nature06028

DeFelipe, J. (2010). From the Connectome to the Synaptome: An Epic Love Story. *Science, 330*. doi:10.1126/science.1193378

Dekker, T., Ibba, I., Siju, K. P., Stensmyr, M. C., & Hansson, B. S. (2006). Olfactory shifts parallel superspecialism for toxic fruit in Drosophila melanogaster sibling, D. sechellia. *Current Biology, 16*(1), 101-109. doi:10.1016/j.cub.2005.11.075

Dekker, T., Revadi, S., Mansourian, S., Ramasamy, S., Lebreton, S., Becher, P. G., . . . Anfora, G. (2015). Loss of Drosophila pheromone reverses its role in sexual communication in Drosophila suzukii. *Proc Biol Sci, 282*(1804), 20143018. doi:10.1098/rspb.2014.3018

Demir, M., Kadakia, N., Anderson, H. D., Clark, D. A., & Emonet, T. (2020). Walking Drosophila navigate complex plumes using stochastic decisions biased by the timing of odor encounters. *Elife, 9*. doi:10.7554/eLife.57524

Deng, Y., Zhang, W., Farhat, K., Oberland, S., Gisselmann, G., & Neuhaus, E. M. (2011). The stimulatory Gα(s) protein is involved in olfactory signal transduction in Drosophila. *PLoS ONE, 6*(4), e18605. doi:10.1371/journal.pone.0018605

Denk, W., Briggman, K. L., & Helmstaedter, M. (2012). Structural neurobiology: missing link to a mechanistic understanding of neural computation. *Nature Reviews: Neuroscience, 13*(5), 351-358.

Denk, W., & Horstmann, H. (2004a). Scanning Electron Microscopy to Reconstruct Three-Dimensional Tissue Nanostructure. *PLoS Biology, 2*(11), 10. doi:10.1371/journal.pbio.0020329

Denk, W., & Horstmann, H. (2004b). Serial block-face scanning electron microscopy to reconstruct three-dimensional tissue nanostructure. *PLoS Biology, 2*(11), e329. doi:10.1371/journal.pbio.0020329

Distler, P. (1990). Synaptic connections of dopamine-immunoreactive neurons in the antennal lobes of Periplaneta americana. Colocalization with GABA-like immunoreactivity. *Histochemistry, 93*(4), 401-408.

Dolan, M.-J., Frechter, S., Bates, A. S., Dan, C., Huoviala, P., Roberts, R. J. V., . . . Jefferis, G. S. X. E. (2019). Neurogenetic dissection of the Drosophila lateral horn reveals major outputs, diverse behavioural functions, and interactions with the mushroom body. *Elife, 8*, e43079. doi:10.7554/eLife.43079

Dolan, M. J., Belliart-Guérin, G., Bates, A. S., Frechter, S., Lampin-Saint-Amaux, A., Aso, Y., . . . Jefferis, G. (2018). Communication from Learned to Innate Olfactory Processing Centers Is Required for Memory Retrieval in Drosophila. *Neuron, 100*(3), 651-668.e658. doi:10.1016/j.neuron.2018.08.037

Duffy, J. B. (2002). GAL4 system in drosophila: A fly geneticist's swiss army knife. *Genesis, 34*(1-2), 1-15. doi:10.1002/gene.10150

Duistermars, B. J., Chow, D. M., & Frye, M. A. (2009). Flies require bilateral sensory input to track odor gradients in flight. *Current Biology, 19*(15), 1301-1307.

Dweck, H. K., Ebrahim, S. A., Farhan, A., Hansson, B. S., & Stensmyr, M. C. (2015). Olfactory proxy detection of dietary antioxidants in Drosophila. *Current Biology, 25*(4), 455-466. doi:10.1016/j.cub.2014.11.062

Dweck, H. K. M., Ebrahim, S. A. M., Khallaf, M. A., Koenig, C., Farhan, A., Stieber, R., . . . Hansson, B. S. (2016). Olfactory channels associated with the Drosophila maxillary palp mediate short- and long-range attraction. *Elife, 5*, e14925. doi:10.7554/eLife.14925

Dweck, H. K. M., Ebrahim, S. A. M., Thoma, M., Mohamed, A. A. M., Keesey, I. W., Trona, F., . . . Hansson, B. S. (2015). Pheromones mediating copulation and attraction in *Drosophila*. *Proceedings of the National Academy of Sciences, 112*(21), E2829-E2835. doi:10.1073/pnas.1504527112

Ebrahim, S. A. M., Dweck, H. K. M., Stökl, J., Hofferberth, J. E., Trona, F., Weniger, K., . . . Knaden, M. (2015). *Drosophila* Avoids Parasitoids by Sensing Their Semiochemicals via a Dedicated Olfactory Circuit. *PLoS Biology, 13*(12), e1002318. doi:10.1371/journal.pbio.1002318

Eichler, K., Litwin-Kumar, A., Li, F., Park, Y., Andrade, I., Schneider-Mizell, C. M., . . . Cardona, A. (2017). The Complete Connectome Of A Learning And Memory Center In An Insect Brain. *bioRxiv*. doi:10.1101/141762

Elliott, D. A., & Brand, A. H. (2008). The GAL4 system: a versatile system for the expression of genes *Methods in Molecular Biology* (Vol. 420, pp. 79–95): Humana Press Inc.

Emmons, S. W. (2015). The beginning of connectomics: a commentary on White et al. (1986) 'The structure of the nervous system of the nematode Caenorhabditis elegans'. *Philos Trans R Soc Lond B Biol Sci, 370*(1666). doi:10.1098/rstb.2014.0309

Ernst, K. D., Boeckh, J., & Boeckh, V. (1977). A neuroanatomical study on the organization of the central antennal pathways in insects. *Cell and Tissue Research, 176*(3), 285-308. doi:10.1007/bf00221789

Erö, C., Gewaltig, M.-O., Keller, D., & Markram, H. (2018). A Cell Atlas for the Mouse Brain. *Frontiers in Neuroinformatics, 12*. doi:10.3389/fninf.2018.00084

Fan, J., Francis, F., Liu, Y., Chen, J. L., & Cheng, D. F. (2011). An overview of odorant-binding protein functions in insect peripheral olfactory reception. *Genet Mol Res, 10*(4), 3056-3069. doi:10.4238/2011.December.8.2

Fandino, R. A., Haverkamp, A., Bisch-Knaden, S., Zhang, J., Bucks, S., Nguyen, T. A. T., . . . Große-Wilde, E. (2019). Mutagenesis of odorant coreceptor Orco fully disrupts foraging but not oviposition behaviors in the hawkmoth *Manduca sexta*. *Proceedings of the National Academy of Sciences*, 201902089. doi:10.1073/pnas.1902089116 %J Proceedings of the National Academy of Sciences

Feinberg, E. H., VanHoven, M. K., Bendesky, A., Wang, G., Fetter, R. D., Shen, K., & Bargmann, C. I. (2008). GFP Reconstitution Across Synaptic Partners (GRASP) Defines Cell Contacts and Synapses in Living Nervous Systems. *Neuron, 57*(3), 353-363.

Fiala, A. (2007). Olfaction and olfactory learning in Drosophila: recent progress. *Current Opinion in Neurobiology, 17*(6), 720-726. doi:10.1016/j.conb.2007.11.009

Fisek, M., & Wilson, R. I. (2014). Stereotyped connectivity and computations in higher-order olfactory neurons. *Nature Neuroscience, 17*(2), 280-288. doi:10.1038/nn.3613

Frechter, S., Bates, A. S., Tootoonian, S., Dolan, M. J., Manton, J., Jamasb, A. R., . . . Jefferis, G. (2019). Functional and anatomical specificity in a higher olfactory centre. *eLife, 8*. doi:10.7554/eLife.44590

French, A. S., Torkkeli, P. H., & Schuckel, J. (2011). Dynamic characterization of Drosophila antennal olfactory neurons indicates multiple opponent signaling pathways in odor discrimination. *Journal of Neuroscience, 31*(3), 861-869. doi:10.1523/jneurosci.5243-10.2011

Frey, U., & Morris, R. G. M. (1997). Synaptic tagging and long-term potentiation. *Nature, 385*(6616), 533-536. doi:10.1038/385533a0

Fusca, D., & Kloppenburg, P. (2021). Task-specific roles of local interneurons for inter- and intraglomerular signaling in the insect antennal lobe. *Elife, 10*. doi:10.7554/eLife.65217

Galizia, C. G. (2014). Olfactory coding in the insect brain: data and conjectures. *European Journal of Neuroscience, 39*(11), n/a-n/a. doi:10.1111/ejn.12558

Galizia, C. G., McIlwrath, S. L., & Menzel, R. (1999). A digital three-dimensional atlas of the honeybee antennal lobe based on optical sections acquired by confocal microscopy. *Cell and Tissue Research, 295*(3), 383-394.

Galizia, C. G., & Menzel, R. (2001). The role of glomeruli in the neural representation of odours: results from optical recording studies. *Journal of Insect Physiology, 47*(2), 115-130.

Gao, Q., Yuan, B., & Chess, A. (2000). Convergent projections of Drosophila olfactory neurons to

specific glomeruli in the antennal lobe. *Nature*.

Gao, X. J., Clandinin, T. R., & Luo, L. (2015). Extremely Sparse Olfactory Inputs Are Sufficient to Mediate Innate Aversion in *Drosophila PLoS ONE, 10*(4), e0125986. doi:10.1371/journal.pone.0125986

Gaudry, Q., Hong, E. J., Kain, J., de Bivort, B. L., & Wilson, R. I. (2013). Asymmetric neurotransmitter release enables rapid odour lateralization in *Drosophila*. *Nature, 493*(7432), 424-428. doi:10.1038/nature11747

Gerber, N. N., & Lechevalier, H. A. (1965). Geosmin, an earthly-smelling substance isolated from actinomycetes. *Appl Microbiol, 13*(6), 935-938. doi:10.1128/am.13.6.935-938.1965

Getahun, M. N., Olsson, S. B., Lavista-Llanos, S., Hansson, B. S., & Wicher, D. (2013). Insect odorant response sensitivity is tuned by metabotropically autoregulated olfactory receptors. *PLoS ONE, 8*(3), e58889.

Getahun, M. N., Wicher, D., Hansson, B. S., & Olsson, S. B. (2012). Temporal response dynamics of Drosophila olfactory sensory neurons depends on receptor type and response polarity. *Front Cell Neurosci, 6*, 54. doi:10.3389/fncel.2012.00054

Gomez-Diaz, C., Bargeton, B., Abuin, L., Bukar, N., Reina, J. H., Bartoi, T., . . . Benton, R. (2016). A CD36 ectodomain mediates insect pheromone detection via a putative tunnelling mechanism. *Nat Commun, 7*, 11866. doi:10.1038/ncomms11866

Grabe, V., Baschwitz, A., Dweck, Hany K. M., Lavista-Llanos, S., Hansson, Bill S., & Sachse, S. (2016). Elucidating the Neuronal Architecture of Olfactory Glomeruli in the *Drosophila* Antennal Lobe. *Cell Reports, 16*(12), 3401-3413. doi:10.1016/j.celrep.2016.08.063

Grabe, V., & Sachse, S. (2018). Fundamental principles of the olfactory code. *BioSystems, 164*, 94-101. doi:10.1016/j.biosystems.2017.10.010

Grabe, V., Schubert, M., Strube-Bloss, M., Reinert, A., Trautheim, S., Lavista-Llanos, S., . . . Sachse, S. (2020). Odor-Induced Multi-Level Inhibitory Maps in Drosophila. *eNeuro, 7*(1). doi:10.1523/eneuro.0213-19.2019

Grabe, V., Strutz, A., Baschwitz, A., Hansson, B. S., & Sachse, S. (2015). Digital in vivo 3D atlas of the antennal lobe of *Drosophila melanogaster*. *Journal of Comparative Neurology, 523*(3), 530-544. doi:10.1002/cne.23697

Graubard, K., Raper, J. A., & Hartline, D. K. (1980). Graded synaptic transmission between spiking neurons. *Proc Natl Acad Sci U S A, 77*(6), 3733-3735. doi:10.1073/pnas.77.6.3733

Gruntman, E., & Turner, G. C. (2013). Integration of the olfactory code across dendritic claws of single mushroom body neurons. *Nature Neuroscience, 16*(12), 1821-1829. doi:10.1038/nn.3547

Guo, D., Wu, S., Chen, M., Perc, M., Zhang, Y., Ma, J., . . . Yao, D. (2016). Regulation of Irregular Neuronal Firing by Autaptic Transmission. *Sci Rep, 6*, 26096. doi:10.1038/srep26096

Hallem, E. A., & Carlson, J. R. (2006). Coding of odors by a receptor repertoire. *Cell, 125*(1), 143-160. doi:10.1016/j.cell.2006.01.050

Halty-deLeon, L., Hansson, B. S., & Wicher, D. (2018). The Drosophila melanogaster Na(+)/Ca(2+) Exchanger CALX Controls the Ca(2+) Level in Olfactory Sensory Neurons at Rest and After Odorant Receptor Activation. *Front Cell Neurosci, 12*, 186. doi:10.3389/fncel.2018.00186

Halty-deLeon, L., Pal Mahadevan, V., Hansson, B. S., & Wicher, D. (2021). Response plasticity of *Drosophila* olfactory sensory neurons. *bioRxiv*, 2021.2012.2006.471362. doi:10.1101/2021.12.06.471362

Hanslovsky, P., Bogovic, J. A., & Saalfeld, S. (2017). Image-based correction of continuous and discontinuous non-planar axial distortion in serial section microscopy. *Bioinformatics, 33*(9), 1379-1386. doi:10.1093/bioinformatics/btw794

Hansson, B. S., Ljungberg, H., Hallberg, E., & Löfstedt, C. (1992). Functional specialization of olfactory glomeruli in a moth. *Science, 256*, 1313-1315.

Hansson, B. S., & Stensmyr, M. C. (2011). Evolution of Insect Olfaction. *Neuron, 72*(5), 698–711. doi:10.1016/j.neuron.2011.11.003

Harzsch, S., & Krieger, J. (2018). Crustacean olfactory systems: A comparative review and a crustacean perspective on olfaction in insects. *Progress in Neurobiology, 161*, 23-60. doi:10.1016/j.pneurobio.2017.11.005

Haverkamp, A., Hansson, B. S., & Knaden, M. (2018). Combinatorial Codes and Labeled Lines: How Insects Use Olfactory Cues to Find and Judge Food, Mates, and Oviposition Sites in Complex Environments. *Front Physiol, 9*, 49. doi:10.3389/fphys.2018.00049

Heimbeck, G., Bugnon, V., Gendre, N., Keller, A., & Stocker, R. F. (2001). A central neural circuit for experience-independent olfactory and courtship behavior in Drosophila melanogaster. *Proceedings of the National Academy of Sciences, 98*(26), 15336-15341. doi:10.1073/pnas.011314898

Heisenberg, M. (2003). Mushroom body memoir: from maps to models. *Nature Reviews: Neuroscience, 4*(4), 266-275.

Hell, S. W., & Wichmann, J. (1994). Breaking the diffraction resolution limit by stimulated emission: stimulated-emission-depletion fluorescence microscopy. *Opt. Lett., 19*(11), 780-782.

Herculano-Houzel, S. (2009). The human brain in numbers: a linearly scaled-up primate brain. *Front Hum Neurosci, 3*. doi:10.3389/neuro.09.031.2009

Herculano-Houzel, S., Mota, B., & Lent, R. (2006). Cellular scaling rules for rodent brains. *Proceedings of the National Academy of Sciences, 103*(32), 12138-12143.

Hige, T. (2017). What can tiny mushrooms in fruit flies tell us about learning and memory? *Neuroscience Research*. doi:https://doi.org/10.1016/j.neures.2017.05.002

Hirata, Y. (1964). Some observations on the fine structure of the synapses in the olfactory bulb of the mouse, with particular reference to the atypical synaptic configurations. *Archivum histologicum japonicum, 24*(3), 293-302.

Homberg, U., Christensen, T. A., & Hildebrand, J. G. (1989). Structure and function of the deutocerebrum in insects. *Annual Review of Entomology, 34*, 477-501. doi:10.1146/annurev.en.34.010189.002401

Hong, E. J., & Wilson, R. I. (2015). Simultaneous encoding of odors by channels with diverse sensitivity to inhibition. *Neuron, 85*(3), 573-589. doi:10.1016/j.neuron.2014.12.040

Horne, J. A., Langille, C., McLin, S., Wiederman, M., Lu, Z., Xu, C. S., . . . Meinertzhagen, I. A. (2018). A resource for the *Drosophila* antennal lobe provided by the connectome of glomerulus VA1v. *Elife, 7*, e37550. doi:10.7554/eLife.37550

Huang, J., Zhang, W., Qiao, W., Hu, A., & Wang, Z. (2010). Functional Connectivity and Selective Odor Responses of Excitatory Local Interneurons in *Drosophila* Antennal Lobe. *Neuron, 67*(6), 1021-1033. doi:10.1016/j.neuron.2010.08.025

Huoviala, P., Dolan, M.-J., Love, F. M., Myers, P., Frechter, S., Namiki, S., . . . Jefferis, G. S. X. E. (2020). Neural circuit basis of aversive odour processing in *Drosophila* from sensory input to descending output. 394403. doi:10.1101/394403 %J bioRxiv

Ignell, R., Root, C. M., Birse, R. T., Wang, J. W., Nassel, D. R., & Winther, A. M. (2009). Presynaptic peptidergic modulation of olfactory receptor neurons in *Drosophila*. *Proceedings of the National Academy of Sciences, 106*(31), 13070-13075. doi:10.1073/pnas.0813004106

Ikeda, K., & Bekkers, J. M. (2006). Autapses. *Current Biology, 16*(9), R308. doi:10.1016/j.cub.2006.03.085

Ito, K., Awano, W., Suzuki, K., Hiromi, Y., & Yamamoto, D. (1997). The Drosophila mushroom body is a quadruple structure of clonal units each of which contains a virtually identical set of neurones and glial cells. *Development, 124*(4), 761-771.

Jeanne, J. M., Fişek, M., & Wilson, R. I. (2018). The Organization of Projections from Olfactory Glomeruli onto Higher-Order Neurons. *Neuron, 98*(6), 1198-1213.e1196. doi:10.1016/j.neuron.2018.05.011

Jeanne, James M., & Wilson, Rachel I. (2015). Convergence, Divergence, and Reconvergence in a Feedforward Network Improves Neural Speed and Accuracy. *Neuron, 88*(5), 1014-1026. doi:10.1016/j.neuron.2015.10.018

Jefferis, G. S., Potter, C. J., Chan, A. M., Marin, E. C., Rohlfing, T., Maurer, C. R., Jr., & Luo, L. (2007). Comprehensive maps of *Drosophila* higher olfactory centers: spatially segregated fruit and pheromone representation. *Cell, 128*(6), 1187-1203. doi:10.1016/j.cell.2007.01.040

Jennings, B. H. (2011). Drosophila – a versatile model in biology & medicine. *Materials Today, 14*(5),

190-195. doi:https://doi.org/10.1016/S1369-7021(11)70113-4

Jezovit, J. A., Levine, J. D., & Schneider, J. (2017). Phylogeny, environment and sexual communication across the Drosophila genus. *Journal of Experimental Biology, 220*(Pt 1), 42-52. doi:10.1242/jeb.143008

Jones, E. G. (2006). The impossible interview with the man of the neuron doctrine. *Journal of the History of the Neurosciences, 15*(4), 326-340. doi:10.1080/09647040600649319

Jones, W. D., Cayirlioglu, P., Kadow, I. G., & Vosshall, L. B. (2007). Two chemosensory receptors together mediate carbon dioxide detection in Drosophila. *Nature, 445*(7123), 86-90. doi:10.1038/nature05466

Jüttner, F., & Watson, S. B. (2007). Biochemical and ecological control of geosmin and 2-methylisoborneol in source waters. *Applied and Environmental Microbiology, 73*(14), 4395-4406. doi:10.1128/aem.02250-06

Kain, P., Chakraborty, T. S., Sundaram, S., Siddiqi, O., Rodrigues, V., & Hasan, G. (2008). Reduced odor responses from antennal neurons of G(q)alpha, phospholipase Cbeta, and rdgA mutants in Drosophila support a role for a phospholipid intermediate in insect olfactory transduction. *Journal of Neuroscience, 28*(18), 4745-4755. doi:10.1523/jneurosci.5306-07.2008

Kazama, H., & Wilson, R. I. (2008). Homeostatic Matching and Nonlinear Amplification at Identified Central Synapses. *Neuron, 58*(3), 401-413. doi:http://dx.doi.org/10.1016/j.neuron.2008.02.030

Kazama, H., & Wilson, R. I. (2009). Origins of correlated activity in an olfactory circuit. *Nature Neuroscience, 12*(9), 1136-1144. doi:10.1038/nn.2376

Keene, A. C., & Waddell, S. (2007). Drosophila olfactory memory: single genes to complex neural circuits. *Nature Reviews: Neuroscience, 8*(5), 341-354.

Keesey, I. W., Grabe, V., Knaden, M., & Hansson, B. S. (2020). Divergent sensory investment mirrors potential speciation via niche partitioning across Drosophila. *Elife, 9*, e57008. doi:10.7554/eLife.57008

Keesey, I. W., & Hansson, B. S. (2021). 10 - The neuroethology of labeled lines in insect olfactory systems. In G. J. Blomquist & R. G. Vogt (Eds.), *Insect Pheromone Biochemistry and Molecular Biology (Second Edition)* (pp. 285-327). London: Academic Press.

Keesey, I. W., Koerte, S., Retzke, T., Haverkamp, A., Hansson, B. S., & Knaden, M. (2016). Adult Frass Provides a Pheromone Signature for Drosophila Feeding and Aggregation. *Journal of Chemical Ecology, 42*(8), 739-747. doi:10.1007/s10886-016-0737-4

Keesey, I. W., Zhang, J., Depetris-Chauvin, A., Obiero, G. F., Gupta, A., Gupta, N., . . . Hansson, B. S. (2022). Functional olfactory evolution in Drosophila suzukii and the subgenus Sophophora. *iScience, 25*(5), 104212. doi:https://doi.org/10.1016/j.isci.2022.104212

Keil, T. (1999). Morphology and Development of the Peripheral Olfactory Organs. In B. S. Hansson (Ed.), *Insect Olfaction*. Berlin, Heidelberg, New York: Springer Verlag.

Khallaf, M. A., Auer, T. O., Grabe, V., Depetris-Chauvin, A., Ammagarahalli, B., Zhang, D.-D., . . . Knaden, M. (2020). Mate discrimination among subspecies through a conserved olfactory pathway. *Science Advances, 6*(25), eaba5279. doi:doi:10.1126/sciadv.aba5279

Kim, A. J., Lazar, A. A., & Slutskiy, Y. B. (2011). System identification of Drosophila olfactory sensory neurons. *Journal of Computational Neuroscience, 30*(1), 143-161. doi:10.1007/s10827-010-0265-0

Kim, A. J., Lazar, A. A., & Slutskiy, Y. B. (2015). Projection neurons in Drosophila antennal lobes signal the acceleration of odor concentrations. *Elife, 4*. doi:10.7554/eLife.06651

Knaden, M., & Hansson, B. S. (2014). Mapping odor valence in the brain of flies and mice. *Current Opinion in Neurobiology, 24*(1), 34-38. doi:10.1016/j.conb.2013.08.010

Knaden, M., Strutz, A., Ahsan, J., Sachse, S., & Hansson, B. S. (2012). Spatial representation of odorant valence in an insect brain. *Cell Reports, 1*, 392-399. doi:10.1016/j.celrep.2012.03.002

Knott, G., Marchman, H., & Lich, B. (2008). Serial Section Scanning Electron Microscopy of Adult Brain Tissue Using Focused Ion Beam Milling. *Journal of Neuroscience, 28*(12), 2964-2959. doi:10.1523/JNEUROSCI.3189-07.2008

Kohl, J., Huoviala, P., & Jefferis, G. S. (2015). Pheromone processing in Drosophila. *Current Opinion in Neurobiology, 34*, 149-157. doi:10.1016/j.conb.2015.06.009

Kumar, A., Schiff, O., Barkai, E., Mel, B. W., Poleg-Polsky, A., & Schiller, J. (2018). NMDA spikes mediate amplification of inputs in the rat piriform cortex. *Elife, 7*, e38446. doi:10.7554/eLife.38446

Kurtovic, A., Widmer, A., & Dickson, B. J. (2007). A single class of olfactory neurons mediates behavioural responses to a Drosophila sex pheromone. *Nature, 446*(7135), 542-546. doi:10.1038/nature05672

Kwon, J. Y., Dahanukar, A., Weiss, L. A., & Carlson, J. R. (2007). The molecular basis of CO2 reception in Drosophila. *Proc Natl Acad Sci U S A, 104*(9), 3574-3578. doi:10.1073/pnas.0700079104

Lai, S.-L., & Lee, T. (2006). Genetic mosaic with dual binary transcriptional systems in *Drosophila*. *Nature Neurosci., 9*(5). doi:10.1038/nn1681

Laissue, P. P., Reiter, C., Hiesinger, P. R., Halter, S., Fischbach, K. F., & Stocker, R. F. (1999). Three-dimensional reconstruction of the antennal lobe in *Drosophila melanogaster*. *The Journal of Comparative Neurology, 405*(4), 543-552. doi:10.1002/(sici)1096-9861(19990322)405:4<543::aid-cne7>3.0.co;2-a

Laissue, P. P., & Vosshall, L. B. (2008). The Olfactory Sensory Map in *Drosophila*. In G. M. Technau (Ed.), *Brain Development in Drosophila melanogaster* (pp. 102-114). New York: Springer.

Larsson, M. C., Domingos, A. I., Jones, W. D., Chiappe, M. E., Amrein, H., & Vosshall, L. B. (2004). Or83b encodes a broadly expressed odorant receptor essential for Drosophila olfaction. *Neuron, 43*(5), 703-714. doi:10.1016/j.neuron.2004.08.019

Laurent, G. (2002). Olfactory network dynamics and the coding of multidimensional signals. *Nature Reviews Neuroscience, 3*(11), 884-895.

Lee, T., & Luo, L. Q. (1999). Mosaic analysis with a repressible cell marker for studies of gene function in neuronal morphogenesis. *Neuron, 22*(3), 451-461.

Leiss, F., Groh, C., Butcher, N. J., Meinertzhagen, I. A., & Tavosanis, G. (2009). Synaptic organization in the adult *Drosophila* mushroom body calyx. *Journal of Comparative Neurology, 517*(6), 808-824. doi:10.1002/cne.22184

Li, F., Lindsey, J. W., Marin, E. C., Otto, N., Dreher, M., Dempsey, G., . . . Rubin, G. M. (2020). The connectome of the adult Drosophila mushroom body provides insights into function. *Elife, 9*. doi:10.7554/eLife.62576

Li, J., Mahoney, B. D., Jacob, M. S., & Caron, S. J. C. (2020). Visual Input into the Drosophila melanogaster Mushroom Body. *Cell Rep, 32*(11), 108138. doi:10.1016/j.celrep.2020.108138

Li, P. H., Lindsey, L. F., Januszewski, M., Zheng, Z., Bates, A. S., Taisz, I., . . . Jain, V. (2020). Automated Reconstruction of a Serial-Section EM *Drosophila* Brain with Flood-Filling Networks and Local Realignment. *bioRxiv*, 605634. doi:10.1101/605634

Liang, L., Li, Y., Potter, Christopher J., Yizhar, O., Deisseroth, K., Tsien, Richard W., & Luo, L. (2013). GABAergic Projection Neurons Route Selective Olfactory Inputs to Specific Higher-Order Neurons. *Neuron, 79*(5), 917-931. doi:http://dx.doi.org/10.1016/j.neuron.2013.06.014

Liang, L., & Luo, L. (2010). The olfactory circuit of the fruit fly *Drosophila melanogaster*. *Sci China Life Sci, 53*(4), 472-484. doi:10.1007/s11427-010-0099-z

Liato, V., & Aïder, M. (2017). Geosmin as a source of the earthy-musty smell in fruits, vegetables and water: Origins, impact on foods and water, and review of the removing techniques. *Chemosphere, 181*, 9-18.

Lichtman, J. W., Livet, J., & Sanes, J. R. (2008). A technicolour approach to the connectome. *Nature Reviews: Neuroscience, 9*(6), 417-422.

Linz, J., Baschwitz, A., Strutz, A., Dweck, H. K., Sachse, S., Hansson, B. S., & Stensmyr, M. C. (2013). Host plant-driven sensory specialization in Drosophila erecta. *Proc Biol Sci, 280*(1760), 20130626. doi:10.1098/rspb.2013.0626

Liu, T. X., Davoudian, P. A., Lizbinski, K. M., & Jeanne, J. M. (2022). Connectomic features underlying diverse synaptic connection strengths and subcellular computation. *Current Biology, 32*(3), 559-569.e555. doi:https://doi.org/10.1016/j.cub.2021.11.056

Liu, W. W., & Wilson, R. I. (2013). Glutamate is an inhibitory neurotransmitter in the *Drosophila*

olfactory system. *Proceedings of the National Academy of Sciences, 110*(25), 10294–10299. doi:10.1073/pnas.1220560110

Lizbinski, K. M., & Dacks, A. M. (2018). Intrinsic and Extrinsic Neuromodulation of Olfactory Processing. *Frontiers in Cellular Neuroscience, 11*(424). doi:10.3389/fncel.2017.00424

Luo, L. (2021). Architectures of neuronal circuits. *Science, 373*(6559), eabg7285. doi:doi:10.1126/science.abg7285

Malnic, B., Hirono, J., Sato, T., & Buck, L. B. (1999). Combinatorial receptor codes for odors. *Cell, 96*(5), 713-723. doi:10.1016/s0092-8674(00)80581-4

Maresh, A., Rodriguez Gil, D., Whitman, M. C., & Greer, C. A. (2008). Principles of glomerular organization in the human olfactory bulb--implications for odor processing. *PLoS ONE, 3*(7), e2640. doi:10.1371/journal.pone.0002640

Marin, E. C., Jefferis, G. S., Komiyama, T., Zhu, H., & Luo, L. (2002). Representation of the glomerular olfactory map in the Drosophila brain. *Cell, 109*(2), 243-255.

Markow, T. A., & O'Grady, P. M. (2005). Evolutionary genetics of reproductive behavior in Drosophila: connecting the dots. *Annual Review of Genetics, 39*, 263-291. doi:10.1146/annurev.genet.39.073003.112454

Marshall, B., Warr, C. G., & de Bruyne, M. (2010). Detection of volatile indicators of illicit substances by the olfactory receptors of Drosophila melanogaster. *Chemical Senses, 35*(7), 613-625. doi:10.1093/chemse/bjq050

Martin, J. P., Beyerlein, A., Dacks, A. M., Reisenman, C. E., Riffell, J. A., Lei, H., & Hildebrand, J. G. (2011). The neurobiology of insect olfaction: sensory processing in a comparative context. *Progress in Neurobiology, 95*(3), 427-447. doi:10.1016/j.pneurobio.2011.09.007

Masse, N. Y., Turner, G. C., & Jefferis, G. S. (2009). Olfactory information processing in Drosophila. *Current Biology, 19*(16), R700-713. doi:10.1016/j.cub.2009.06.026

Mattheis, J. P., & Roberts, R. G. (1992). Identification of geosmin as a volatile metabolite of Penicillium expansum. *Applied and Environmental Microbiology, 58*(9), 3170-3172. doi:10.1128/aem.58.9.3170-3172.1992

Matthews, K. A., Kaufman, T. C., & Gelbart, W. M. (2005). Research resources for Drosophila: the expanding universe. *Nature Reviews Genetics, 6*(3), 179-193. doi:10.1038/nrg1554

McTavish, T., Migliore, M., Shepherd, G., & Hines, M. (2012). Mitral cell spike synchrony modulated by dendrodendritic synapse location. *Frontiers in Computational Neuroscience, 6*. doi:10.3389/fncom.2012.00003

Meinertzhagen, I. A. (2016). Connectome studies on Drosophila: a short perspective on a tiny brain. *Journal of Neurogenetics, 30*(2), 62-68. doi:10.3109/01677063.2016.1166224

Meinertzhagen, I. A. (2018). Of what use is connectomics? A personal perspective on the *Drosophila* connectome. *Journal of Experimental Biology, 221*(10), jeb164954. doi:10.1242/jeb.164954 %J The Journal of Experimental Biology

Melo, N., Wolff, G. H., Costa-da-Silva, A. L., Arribas, R., Triana, M. F., Gugger, M., . . . Stensmyr, M. C. (2020). Geosmin attracts Aedes aegypti mosquitoes to oviposition sites. *Current Biology, 30*(1), 127-134. e125.

Menini, A. (2010). *The Neurobiology of Olfaction*.

Miazzi, F., Hansson, B. S., & Wicher, D. (2016). Odor-induced cAMP production in Drosophila melanogaster olfactory sensory neurons. *Journal of Experimental Biology, 219*(Pt 12), 1798-1803. doi:10.1242/jeb.137901

Milo, R., Shen-Orr, S., Itzkovitz, S., Kashtan, N., Chklovskii, D., & Alon, U. (2002). Network Motifs: Simple Building Blocks of Complex Networks. *Science, 298*(5594), 824-827. doi:10.1126/science.298.5594.824

Minsky, L. (2018). Inside the Invisible but Influential World of Scent Branding. *Harvard business review*.

Miroschnikow, A., Schlegel, P., Schoofs, A., Hueckesfeld, S., Li, F., Schneider-Mizell, C. M., . . . Pankratz, M. J. (2018). Convergence of monosynaptic and polysynaptic sensory paths onto common motor outputs in a Drosophila feeding connectome. *Elife, 7*, e40247. doi:10.7554/eLife.40247

Mishchenko, Y. (2011). Reconstruction of complete connectivity matrix for connectomics by sampling

neural connectivity with fluorescent synaptic markers. *Journal of Neuroscience Methods, 196*(2), 289-302. doi:10.1016/j.jneumeth.2011.01.021

Missbach, C., Dweck, H. K., Vogel, H., Vilcinskas, A., Stensmyr, M. C., Hansson, B. S., & Grosse-Wilde, E. (2014). Evolution of insect olfactory receptors. *Elife, 3*, e02115.

Mohamed, A. A. M., Hansson, B. S., & Sachse, S. (2019a). Third-Order Neurons in the Lateral Horn Enhance Bilateral Contrast of Odor Inputs Through Contralateral Inhibition in Drosophila. *Front Physiol, 10*, 851. doi:10.3389/fphys.2019.00851

Mohamed, A. A. M., Retzke, T., Das Chakraborty, S., Fabian, B., Hansson, B. S., Knaden, M., & Sachse, S. (2019b). Odor mixtures of opposing valence unveil inter-glomerular crosstalk in the Drosophila antennal lobe. *Nat Commun, 10*(1), 1201. doi:10.1038/s41467-019-09069-1

Morgan, T. H. (1910). SEX LIMITED INHERITANCE IN DROSOPHILA. *Science, 32*(812), 120-122. doi:10.1126/science.32.812.120

Mori, K. (2014). *The Olfactory System*.

Mosca, T. J., & Luo, L. (2014). Synaptic organization of the *Drosophila* antennal lobe and its regulation by the Teneurins. *Elife, 3*(3), e03726. doi:10.7554/eLife.03726

Münch, D., & Galizia, C. G. (2016). DoOR 2.0 - Comprehensive Mapping of Drosophila melanogaster Odorant Responses. *Scientific Reports, 6*, 21841. doi:10.1038/srep21841

Murlis J, Elkinton J S, a., & T, C. R. (1992). Odor Plumes and How Insects Use Them. *Annual Review of Entomology, 37*(1), 505-532. doi:10.1146/annurev.en.37.010192.002445

Myers, E. W., Sutton, G. G., Delcher, A. L., Dew, I. M., Fasulo, D. P., Flanigan, M. J., . . . Venter, J. C. (2000). A Whole-Genome Assembly of *Drosophila*. *Science, 287*(5461), 2196-2204. doi:doi:10.1126/science.287.5461.2196

Nagayama, S., Homma, R., & Imamura, F. (2014). Neuronal organization of olfactory bulb circuits. *Frontiers in Neural Circuits, 8*. doi:10.3389/fncir.2014.00098

Nagel, K. I., Hong, E. J., & Wilson, R. I. (2015). Synaptic and circuit mechanisms promoting broadband transmission of olfactory stimulus dynamics. *Nature Neuroscience, 18*(1), 56-65. doi:10.1038/nn.3895

Nagel, K. I., & Wilson, R. I. (2011). Biophysical mechanisms underlying olfactory receptor neuron dynamics. *Nature Neuroscience, 14*(2), 208-216. doi:10.1038/nn.2725

Nässel, D. R., & Homberg, U. (2006). Neuropeptides in interneurons of the insect brain. *Cell and Tissue Research, 326*(1), 1-24. doi:10.1007/s00441-006-0210-8

Nava Gonzales, C., McKaughan, Q., Bushong, E. A., Cauwenberghs, K., Ng, R., Madany, M., . . . Su, C.-Y. (2021). Systematic morphological and morphometric analysis of identified olfactory receptor neurons in Drosophila melanogaster. *eLife, 10*, e69896. doi:10.7554/eLife.69896

Ng, M., Roorda, R. D., Lima, S. Q., Zemelman, B. V., Morcillo, P., & Miesenböck, G. (2002). Transmission of Olfactory Information between Three Populations of Neurons in the Antennal Lobe of the Fly. *Neuron, 36*(3), 463-474. doi:10.1016/s0896-6273(02)00975-3

Nishino, H., Watanabe, H., Kamimura, I., Yokohari, F., & Mizunami, M. (2015). Coarse topographic organization of pheromone-sensitive afferents from different antennal surfaces in the American cockroach. *Neuroscience Letters, 595*, 35-40. doi:https://doi.org/10.1016/j.neulet.2015.04.006

Nowotny, T., Trowell, S., & de Bruyne, M. (2012). Benchmarking Drosophilareceptor neurons for technical applications. *BMC Neuroscience, 13*(1), P155. doi:10.1186/1471-2202-13-S1-P155

Okada, R., Awasaki, T., & Ito, K. (2009). Gamma-aminobutyric acid (GABA)-mediated neural connections in the *Drosophila* antennal lobe. *Journal of Comparative Neurology, 514*(1), 74-91. doi:10.1002/cne.21971

Olsen, S. R., Bhandawat, V., & Wilson, R. I. (2010). Divisive normalization in olfactory population codes. *Neuron, 66*(2), 287-299. doi:10.1016/j.neuron.2010.04.009

Olsen, S. R., & Wilson, R. I. (2008). Lateral presynaptic inhibition mediates gain control in an olfactory circuit. *Nature, 452*(7190), 956-960. doi:10.1038/nature06864

Owald, D., & Waddell, S. (2015). Olfactory learning skews mushroom body output pathways to steer behavioral choice in Drosophila. *Current Opinion in Neurobiology, 35*, 178-184.

doi:10.1016/j.conb.2015.10.002

Pannunzi, M., & Nowotny, T. (2019). Odor Stimuli: Not Just Chemical Identity. *Front Physiol, 10*, 1428. doi:10.3389/fphys.2019.01428

Parnas, M., Lin, Andrew C., Huetteroth, W., & Miesenböck, G. (2013). Odor Discrimination in Drosophila: From Neural Population Codes to Behavior. *Neuron, 79*(5), 932-944. doi:10.1016/j.neuron.2013.08.006

Pech, U., Pooryasin, A., Birman, S., & Fiala, A. (2013). Localization of the Contacts Between Kenyon Cells and Aminergic Neurons in the Drosophila melanogaster Brain Using SplitGFP Reconstitution. *Journal of Comparative Neurology, 521*(17), 3992-4026. doi:10.1002/cne.23388

Pelz, D., Roeske, T., Syed, Z., Bruyne, M. d., & Galizia, C. G. (2006). The molecular receptive range of an olfactory receptor in vivo (*Drosophila melanogaste*r Or22a). *Journal of Neurobiology, 66*(14), 1544-1563. doi:10.1002/neu.20333

Petralia, R. S., Wang, Y. X., Mattson, M. P., & Yao, P. J. (2015). Structure, Distribution, and Function of Neuronal/Synaptic Spinules and Related Invaginating Projections. *Neuromolecular Medicine, 17*(3), 211-240. doi:10.1007/s12017-015-8358-6

Polidori, C., Piwczynski, M., Ronchetti, F., Johnston, N. P., & Szpila, K. (2022). Host-trailing satellite flight behaviour is associated with greater investment in peripheral visual sensory system in miltogrammine flies. *Scientific Reports, 12*(1), 2773. doi:10.1038/s41598-022-06704-8

Polilov, A. A. (2016). *At the Size Limit - Effects of Miniaturization in Insects*: Springer.

Posnien, N., Hopfen, C., Hilbrant, M., Ramos-Womack, M., Murat, S., Schönauer, A., . . . McGregor, A. P. (2012). Evolution of Eye Morphology and Rhodopsin Expression in the Drosophila melanogaster Species Subgroup. *PLoS ONE, 7*(5), e37346. doi:10.1371/journal.pone.0037346

Potter, C. J., Tasic, B., Russler, E., Liang, L., & Luo, L. (2010). The Q System: A Repressible Binary System for Transgene Expression, Lineage Tracing, and Mosaic Analysis. *Cell, 141*, 536–548. doi:10.1016/j.cell.2010.02.025

Prelic, S., Pal Mahadevan, V., Venkateswaran, V., Lavista-Llanos, S., Hansson, B. S., & Wicher, D. (2021). Functional Interaction Between Drosophila Olfactory Sensory Neurons and Their Support Cells. *Front Cell Neurosci, 15*, 789086. doi:10.3389/fncel.2021.789086

Prieto-Godino, L. L., Rytz, R., Cruchet, S., Bargeton, B., Abuin, L., Silbering, A. F., . . . Benton, R. (2017). Evolution of Acid-Sensing Olfactory Circuits in Drosophilids. *Neuron, 93*(3), 661-676.e666. doi:https://doi.org/10.1016/j.neuron.2016.12.024

Raji, J. I., & Potter, C. J. (2021). The number of neurons in Drosophila and mosquito brains. *PLoS One, 16*(5), e0250381. doi:10.1371/journal.pone.0250381

Ramaekers, A., Claeys, A., Kapun, M., Mouchel-Vielh, E., Potier, D., Weinberger, S., . . . Hassan, B. A. (2019). Altering the Temporal Regulation of One Transcription Factor Drives Evolutionary Trade-Offs between Head Sensory Organs. *Developmental Cell, 50*(6), 780-792.e787. doi:10.1016/j.devcel.2019.07.027

Ramaekers, A., Magnenat, E., Marin, E. C., Gendre, N., Jefferis, G. S., Luo, J. L., & Stocker, B. (2005). Glomerular Maps without Cellular Redundancy at Successive Levels of the *Drosophila* Larval Olfactory Circuit. *Current Biology, 15*, 982–992. doi:10.1016/j.cub.2005.04.032

Redondo, R. L., & Morris, R. G. M. (2010). Making memories last: the synaptic tagging and capture hypothesis. *Nature Reviews Neuroscience, 12*, 17. doi:10.1038/nrn2963

Richards, D. A., Mateos, J. M., Hugel, S., de Paola, V., Caroni, P., Gähwiler, B. H., & McKinney, R. A. (2005). Glutamate induces the rapid formation of spine head protrusions in hippocampal slice cultures. *Proceedings of the National Academy of Sciences, 102*(17), 6166-6171. doi:doi:10.1073/pnas.0501881102

Rihani, K., Ferveur, J.-F., & Briand, L. (2021). The 40-Year Mystery of Insect Odorant-Binding Proteins. *Biomolecules, 11*(4), 509.

Rodrigues, V. (1988). Spatial coding of olfactory information in the antennal lobe of Drosophila melanogaster. *Brain Research, 453*(1), 299-307. doi:https://doi.org/10.1016/0006-8993(88)90170-9

Root, C. M., Ko, K. I., Jafari, A., & Wang, J. W. (2011). Presynaptic facilitation by neuropeptide signaling mediates odor-driven food search. *Cell, 145*(1), 133-144. doi:10.1016/j.cell.2011.02.008

Root, C. M., Masuyama, K., Green, D. S., Enell, L. E., Nassel, D. R., Lee, C. H., & Wang, J. W. (2008). A presynaptic gain control mechanism fine-tunes olfactory behavior. *Neuron, 59*(2), 311-321. doi:10.1016/j.neuron.2008.07.003

Root, C. M., Semmelhack, J. L., Wong, A. M., Flores, J., & Wang, J. W. (2007). Propagation of olfactory information in Drosophila. *Proc Natl Acad Sci U S A, 104*(28), 11826-11831. doi:10.1073/pnas.0704523104

Rospars, J.-P., Grémiaux, A., Jarriault, D., Chaffiol, A., Monsempes, C., Deisig, N., . . . Martinez, D. (2014). Heterogeneity and Convergence of Olfactory First-Order Neurons Account for the High Speed and Sensitivity of Second-Order Neurons. *PLoS Computational Biology, 10*(12), e1003975. doi:10.1371/journal.pcbi.1003975

Rybak, J. (2013). Exploring Brain Connectivity in Insect Model Systems of Learning and Memory. In R. Menzel & P. Benjamin (Eds.), *Invertebrate Learning and Memory* (pp. 26-40). San Diego: Academic Press.

Rybak, J., & Hansson, B. S. (2018). Olfactory Microcircuits in *Drosophila Melanogaster*. In G. M. Shepherd & S. Grillner (Eds.), *Handbook of Brain Microcircuits* (2nd ed., pp. 361-367). Oxford, UK: Oxford University Press.

Rybak, J., Talarico, G., Ruiz, S., Arnold, C., Cantera, R., & Hansson, B. S. (2016). Synaptic circuitry of identified neurons in the antennal lobe of *Drosophila melanogaster*. *Journal of Comparative Neurology, 524*(9), 1920-1956. doi:10.1002/cne.23966

Saada, R., Miller, N., Hurwitz, I., & Susswein, A. J. (2009). Autaptic excitation elicits persistent activity and a plateau potential in a neuron of known behavioral function. *Current Biology, 19*(6), 479-484. doi:10.1016/j.cub.2009.01.060

Saalfeld, S. (2012). Elastic volume
reconstruction from series of ultra-thin microscopy sections. *Nat Meth, 9*(7). doi:10.1038/NMETH.2072

Saalfeld, S., Cardona, A., Hartenstein, V., & Tomančák, P. (2009). CATMAID: collaborative annotation toolkit for massive amounts of image data. *Bioinformatics, 25*(15), 1984-1986. doi:10.1093/bioinformatics/btp266

Sachse, S., & Beshel, J. (2016). The good, the bad, and the hungry: how the central brain codes odor valence to facilitate food approach in *Drosophila*. *Current Opinion in Neurobiology, 40*, 53-58. doi:http://doi.org/10.1016/j.conb.2016.06.012

Sachse, S., & Hansson, B. S. (2016). Research spotlight: Olfactory coding in *Drosophila melanogaster*. In A. Schmidt-Rhaesa, S. Harzsch, & G. Purschke (Eds.), *Structure and Evolution of Invertebrate Nervous Systems* (pp. 640-645). Oxford: Oxford University Press.

Sachse, S., & Manzini, I. (2021). Editorial for the special issue "Olfactory Coding and Circuitries". *Cell and Tissue Research, 383*(1), 1-6. doi:10.1007/s00441-020-03389-1

Sánchez-Gracia, A., Vieira, F. G., Almeida, F. C., & Rozas, J. Comparative Genomics of the Major Chemosensory Gene Families in Arthropods *eLS*.

Sass, H. (1976). Zur nervösen Codierung von Geruchsreizen bei Periplaneta americana. *J.Comp.Physiol.A., 107*, 49-65.

Sato, K., Pellegrino, M., Nakagawa, T., Nakagawa, T., Vosshall, L. B., & Touhara, K. (2008). Insect olfactory receptors are heteromeric ligand-gated ion channels. *Nature, 452*(7190), 1002-1006. doi:10.1038/nature06850

Scarano, F., Suresh, M. D., Tiraboschi, E., Cabirol, A., Nouvian, M., Nowotny, T., & Haase, A. (2021). Geosmin suppresses defensive behaviour and elicits unusual neural responses in honey bees. *bioRxiv*, 2021.2010.2006.463314. doi:10.1101/2021.10.06.463314

Scheffer, L. K., & Meinertzhagen, I. A. (2021). A connectome is not enough – what is still needed to understand the brain of Drosophila? *Journal of Experimental Biology, 224*(21). doi:10.1242/jeb.242740

Scheffer, L. K., Xu, C. S., Januszewski, M., Lu, Z., Takemura, S.-y., Hayworth, K. J., . . . Plaza, S. M. (2020).

A connectome and analysis of the adult Drosophila central brain. *Elife, 9*, e57443. doi:10.7554/eLife.57443

Schermelleh, L., Heintzmann, R., & Leonhardt, H. (2010). A guide to super-resolution fluorescence microscopy. *Journal of Cell Biology, 190*(2), 165-175. doi:10.1083/jcb.201002018

Schlegel, P., Bates, A. S., Stürner, T., Jagannathan, S. R., Drummond, N., Hsu, J., . . . Jefferis, G. S. X. E. (2021). Information flow, cell types and stereotypy in a full olfactory connectome. *Elife, 10*, e66018. doi:10.7554/eLife.66018

Schneider-Mizell, C. M., Gerhard, S., Longair, M., Kazimiers, T., Li, F., Zwart, M. F., . . . Cardona, A. (2016). Quantitative neuroanatomy for connectomics in *Drosophila*. *Elife, 5*, e12059. doi:10.7554/eLife.12059

Schuckel, J., Meisner, S., Torkkeli, P. H., & French, A. S. (2008). Dynamic properties of Drosophila olfactory electroantennograms. *J Comp Physiol A Neuroethol Sens Neural Behav Physiol, 194*(5), 483-489. doi:10.1007/s00359-008-0322-6

Schultzhaus, J. N., Saleem, S., Iftikhar, H., & Carney, G. E. (2017). The role of the Drosophila lateral horn in olfactory information processing and behavioral response. *Journal of Insect Physiology, 98*, 29-37. doi:10.1016/j.jinsphys.2016.11.007

Seeholzer, L. F., Seppo, M., Stern, D. L., & Ruta, V. (2018). Evolution of a central neural circuit underlies Drosophila mate preferences. *Nature, 559*(7715), 564-569.

Seki, Y., Dweck, H. K. M., Rybak, J., Wicher, D., Sachse, S., & Hansson, B. S. (2017). Olfactory coding from the periphery to higher brain centers in the Drosophila brain. *BMC Biology, 15*(1), 56. doi:10.1186/s12915-017-0389-z

Seki, Y., Rybak, J., Wicher, D., Sachse, S., & Hansson, B. S. (2010). Physiological and morphological characterization of local interneurons in the *Drosophila* antennal lobe. *Journal of Neurophysiology, 104*(2), 1007-1019. doi:jn.00249.2010 [pii]

10.1152/jn.00249.2010

Serizawa, S., Ishii, T., Nakatani, H., Tsuboi, A., Nagawa, F., Asano, M., . . . Sakano, H. (2000). Mutually exclusive expression of odorant receptor transgenes. *Nature Neuroscience, 3*(7), 687-693. doi:10.1038/76641

Shanbhag, S. R., Muller, B., & Steinbrecht, R. A. (1999). Atlas of olfactory organs of *Drosophila melanogaster* - 1. Types, external organization, innervation and distribution of olfactory sensilla. *International Journal of Insect Morphology & Embryology, 28*(4), 377-397. doi:Doi 10.1016/S0020-7322(99)00039-2

Shanbhag, S. R., Müller, B., & Steinbrecht, R. A. (2000). Atlas of olfactory organs of Drosophila melanogaster 2. Internal organization and cellular architecture of olfactory sensilla. *Arthropod Structure and Development, 29*(3), 211-229. doi:10.1016/s1467-8039(00)00028-1

Shanbhag, S. R., Singh, K., & Singh, R. N. (1995). Fine structure and primary sensory projections of sensilla located in the sacculus of the antenna of Drosophila melanogaster. *Cell and Tissue Research, 282*(2), 237-249. doi:10.1007/bf00319115

Shang, Y., Claridge-Chang, A., Sjulson, L., Pypaert, M., & Miesenböck, G. (2007). Excitatory Local Circuits and Their Implications for Olfactory Processing in the Fly Antennal Lobe. *Cell, 128*, 601-612. doi:10.1016/j.cell.2006.12.034

Shepherd, G. M. (2011). The Olfactory Bulb: A Simple System in the Mammalian Brain *Comprehensive Physiology*: John Wiley & Sons, Inc.

Shepherd, G. M., Rowe, T. B., & Greer, C. A. (2021). An Evolutionary Microcircuit Approach to the Neural Basis of High Dimensional Sensory Processing in Olfaction. *Frontiers in Cellular Neuroscience, 15*. doi:10.3389/fncel.2021.658480

Silbering, A. F., & Galizia, C. G. (2007). Processing of odor mixtures in the Drosophila antennal lobe reveals both global inhibition and glomerulus-specific interactions. *Journal of Neuroscience, 27*(44), 11966-11977. doi:10.1523/jneurosci.3099-07.2007

Silbering, A. F., Okada, R., Ito, K., & Galizia, C. G. (2008). Olfactory information processing in the *Drosophila* antennal lobe: anything goes? *Journal of Neuroscience, 28*(49), 13075-13087. doi:10.1523/JNEUROSCI.2973-08.2008

Singh, R. N., & Nayak, S. V. (1985). Fine structure and primary sensory projections of sensilla on the maxillary palp of Drosophila melanogaster Meigen (Diptera: Drosophilidae). *International Journal of Insect Morphology and Embryology, 14*(5), 291-306.

Singh, S., & Joseph, J. (2019). Evolutionarily conserved anatomical and physiological properties of olfactory pathway through fourth-order neurons in a species of grasshopper (Hieroglyphus banian). *Journal of Comparative Physiology A, 205*(6), 813-838. doi:10.1007/s00359-019-01369-7

Smalheiser, N. R. (2014). The RNA-centred view of the synapse: non-coding RNAs and synaptic plasticity. *Philosophical Transactions of the Royal Society B: Biological Sciences, 369*(1652). doi:10.1098/rstb.2013.0504

Soudry, Y., Lemogne, C., Malinvaud, D., Consoli, S. M., & Bonfils, P. (2011). Olfactory system and emotion: Common substrates. *European Annals of Otorhinolaryngology, Head and Neck Diseases, 128*(1), 18-23. doi:https://doi.org/10.1016/j.anorl.2010.09.007

Spacek, J., & Harris, K. M. (2004). Trans-Endocytosis via Spinules in Adult Rat Hippocampus. *The Journal of Neuroscience, 24*(17), 4233-4241. doi:10.1523/jneurosci.0287-04.2004

Sporns, O., Tononi, G., & Kötter, R. (2005). The Human Connectome: A Structural Description of the Human Brain. *PLoS Computational Biology, 1*(4), e42. doi:10.1371/journal.pcbi.0010042

Stensmyr, M. C., Dweck, H. K., Farhan, A., Ibba, I., Strutz, A., Mukunda, L., . . . Hansson, B. S. (2012). A conserved dedicated olfactory circuit for detecting harmful microbes in *Drosophila*. *Cell, 151*(6), 1345-1357. doi:10.1016/j.cell.2012.09.046

Stensmyr, M. C., Stieber, R., & Hansson, B. S. (2008). The Cayman crab fly revisited--phylogeny and biology of Drosophila endobranchia. *PLoS ONE, 3*(4), e1942. doi:10.1371/journal.pone.0001942

Stieb, S. M., Kelber, C., Wehner, R., & Rössler, W. (2011). Antennal-Lobe Organization in Desert Ants of the Genus *Cataglyphis*. *Brain, Behavior and Evolution, 77*(3), 136-146.

Stocker, R. F. (1994). The organization of the chemosensory system in Drosophila melanogaster: a review. *Cell and Tissue Research, 275*(1), 3-26.

Stocker, R. F. (2001). *Drosophila* as a focus in olfactory research: mapping of olfactory sensilla by fine structure, odor specificity, odorant receptor expression, and central connectivity. *Microscopy Research and Technique, 55*(5), 284-296. doi:10.1002/jemt.1178

Stocker, R. F., Lienhard, M. C., Borst, A., & Fischbach, K. F. (1990). Neuronal architecture of the antennal lobe in Drosophila melanogaster. *Cell and Tissue Research, 262*(1), 9-34.

Stocker, R. F., Singh, R. N., Schorderet, M., & Siddiqi, O. (1983). Projection patterns of different types of antennal sensilla in the antennal glomeruli of Drosophila melanogaster. *Cell and Tissue Research, 232*(2), 237-248. doi:10.1007/bf00213783

Stork, N. E. (2018). How Many Species of Insects and Other Terrestrial Arthropods Are There on Earth? *Annual Review of Entomology, 63*(1), 31-45. doi:10.1146/annurev-ento-020117-043348

Strutz, A., Soelter, J., Baschwitz, A., Farhan, A., Grabe, V., Rybak, J., . . . Sachse, S. (2014). Decoding odor quality and intensity in the *Drosophila* brain. *Elife, 3*, e04147. doi:10.7554/eLife.04147

Stuart, G., Spruston, N., & Häusser, M. (2007). *Dendrites*: Oxford University Press.

Su, C.-Y., Menuz, K., & Carlson, J. R. (2009). Olfactory Perception: Receptors, Cells, and Circuits. *Cell, 139*(1), 45-59. doi:10.1016/j.cell.2009.09.015

Su, C.-Y., Menuz, K., Reisert, J., & Carlson, J. R. (2012). Non-synaptic inhibition between grouped neurons in an olfactory circuit. *Nature, 492*(7427), 66–71. doi:http://www.nature.com/nature/journal/vaop/ncurrent/abs/nature11712.html#supplementary-information

Suh, G. S. B., Wong, A. M., Hergarden, A. C., Wang, J. W., Simon, A. F., Benzer, S., . . . Anderson, D. J. (2004). A single population of olfactory sensory neurons mediates an innate avoidance behaviour in *Drosophila*. *Nature, 431*(7010), 854-859. doi:http://www.nature.com/nature/journal/v431/n7010/suppinfo/nature02980_S1.html

Szyszka, P., & Galizia, C. G. (2015). Olfaction in Insects. In R. L. Doty (Ed.), *Handbook of Olfaction and Gustation* (3 ed., pp. 531-546): John Wiley & Sons, Inc.

Taisz, I., Donà, E., Münch, D., Bailey, S. N., Morris, W. J., Meechan, K. I., . . . Galili, D. S. (2022). Generating parallel representations of position and identity in the olfactory system. *bioRxiv*, 2022.2005.2013.491877. doi:10.1101/2022.05.13.491877

Takemura, S.-Y., Lu, Z., & Meinertzhagen, I. A. (2008). Synaptic circuits of the *Drosophila* optic lobe: The input terminals to the medulla. *Journal of Comparative Neurology, 509*(5), 493-513. doi:10.1002/cne.21757

Takemura, S.-y., Xu, C. S., Lu, Z., Rivlin, P. K., Parag, T., Olbris, D. J., . . . Scheffer, L. K. (2015). Synaptic circuits and their variations within different columns in the visual system of Drosophila. *Proceedings of the National Academy of Sciences, 112*(44), 13711-13716. doi:10.1073/pnas.1509820112

Tamás, G., Buhl, E. H., & Somogyi, P. (1997). Massive Autaptic Self-Innervation of GABAergic Neurons in Cat Visual Cortex. *The Journal of Neuroscience, 17*(16), 6352-6364. doi:10.1523/jneurosci.17-16-06352.1997

Tanaka, N. K., Endo, K., & Ito, K. (2012). The organization of antennal lobe-associated neurons in the adult *Drosophila* melanogaster brain. *Journal of Comparative Neurology, 520*(18), 4067-4130. doi:10.1002/cne.23142

Tao-Cheng, J.-H., Dosemeci, A., Gallant, P. E., Miller, S., Galbraith, J. A., Winters, C. A., . . . Reese, T. S. (2009). Rapid Turnover of Spinules at Synaptic Terminals. *Neuroscience, 160*(1), 42-50. doi:10.1016/j.neuroscience.2009.02.031

Task, D., Lin, C.-C., Vulpe, A., Afify, A., Ballou, S., Brbic, M., . . . Potter, C. J. (2022). Chemoreceptor co-expression in Drosophila melanogaster olfactory neurons. *Elife, 11*, e72599. doi:10.7554/eLife.72599

Thoma, M., Hansson, B. S., & Knaden, M. (2015). High-resolution Quantification of Odor-guided Behavior in Drosophila melanogaster Using the Flywalk Paradigm. *J Vis Exp*(106), e53394. doi:10.3791/53394

Tobin, W. F., Wilson, R. I., & Lee, W.-C. A. (2017). Wiring variations that enable and constrain neural computation in a sensory microcircuit. *Elife, 6*, e24838. doi:10.7554/eLife.24838

Tran-Van-Minh, A., Cazé, R. D., Abrahamsson, T., Cathala, L., Gutkin, B. S., & DiGregorio, D. A. (2015). Contribution of sublinear and supralinear dendritic integration to neuronal computations. *Frontiers in Cellular Neuroscience, 9*. doi:10.3389/fncel.2015.00067

Ueda, Y., & Hayashi, Y. (2013). PIP3 Regulates Spinule Formation in Dendritic Spines during Structural Long-Term Potentiation. *The Journal of Neuroscience, 33*(27), 11040-11047. doi:10.1523/jneurosci.3122-12.2013

Ugur, B., Chen, K., & Bellen, H. J. (2016). Drosophila tools and assays for the study of human diseases. *Disease models & mechanisms, 9*(3), 235-244.

Van der Loos, H., & Glaser, E. M. (1972). Autapses in neocortex cerebri: synapses between a pyramidal cell's axon and its own dendrites. *Brain Research, 48*, 355-360. doi:10.1016/0006-8993(72)90189-8

Vareschi, E. (1971). Odor discrimination in the Honey bee - single cell and behavioural response. *Zeitschrift f r vergleichende Physiologie, 75*, 143-173.

Venken, K. J. T., & Bellen, H. J. (2005). Emerging technologies for gene manipulation in Drosophila melanogaster. *Nature Reviews Genetics, 6*(3), 167-178. doi:10.1038/nrg1553

Vogt, K., Aso, Y., Hige, T., Knapek, S., Ichinose, T., Friedrich, A. B., . . . Tanimoto, H. (2016). Direct neural pathways convey distinct visual information to Drosophila mushroom bodies. *Elife, 5*, e14009. doi:10.7554/eLife.14009

Vogt, K., Schnaitmann, C., Dylla, K. V., Knapek, S., Aso, Y., Rubin, G. M., & Tanimoto, H. (2014). Shared mushroom body circuits underlie visual and olfactory memories in Drosophila. *Elife, 3*, e02395. doi:10.7554/eLife.02395

Vosshall, L. B., Amrein, H., Morozov, P. S., Rzhetsky, A., & Axel, R. (1999). A spatial map of olfactory receptor expression in the Drosophila antenna. *Cell, 96*(5), 725-736. doi:10.1016/s0092-8674(00)80582-6

Vosshall, L. B., & Hansson, B. S. (2011). A unified nomenclature system for the insect olfactory

coreceptor. *Chemical Senses, 36*(6), 497-498. doi:10.1093/chemse/bjr022

Vosshall, L. B., Wong, A. M., & Axel, R. (2000). An olfactory sensory map in the fly brain. *Cell, 102*(2), 147-159. doi:10.1016/S0092-8674(00)00021-0

Vroman, R., Klaassen, L. J., & Kamermans, M. (2013). Ephaptic communication in the vertebrate retina. *Front Hum Neurosci, 7*, 612. doi:10.3389/fnhum.2013.00612

White, J. G., Southgate, E., Thomson, J. N., & Brenner, S. (1986). The structure of the nervous system of the nematode Caenorhabditis elegans. *Phil Transact R Soc Lond B, 314*(1-340).

White, J. G., Southgate, E., Thomson, J. N., & Brenner, S. (1986). The structure of the nervous system of the nematode Caenorhabditis elegans. *Philos Trans R Soc Lond B Biol Sci, 314*(1165), 1-340. doi:10.1098/rstb.1986.0056

Wicher, D. (2010). Design principles of sensory receptors. *Frontiers in Cellular Neuroscience, 4*. doi:10.3389/fncel.2010.00025

Wicher, D. (2018). Tuning Insect Odorant Receptors. *Front Cell Neurosci, 12*, 94. doi:10.3389/fncel.2018.00094

Wicher, D., & Miazzi, F. (2021). Functional properties of insect olfactory receptors: ionotropic receptors and odorant receptors.*Cell and Tissue Research, 383*(1),7-19. doi:10.1007/s00441-020-03363-x

Wiles, L., Gu, S., Pasqualetti, F., Parvesse, B., Gabrieli, D., Bassett, D. S., & Meaney, D. F. (2017). Autaptic Connections Shift Network Excitability and Bursting. *Sci Rep, 7*, 44006. doi:10.1038/srep44006

Willig, K. I., Harke, B., Medda, R., & Hell, S. W. (2007). STED microscopy with continuous wave beams. *Nature Methods, 4*(11), 915-918. doi:10.1038/nmeth1108

Wilson, R. I. (2013). Early Olfactory Processing in Drosophila: Mechanisms and Principles. *Annual Review of Neuroscience, 36*, 217-241. doi:10.1146/annurev-neuro-062111-150533

Wilson, R. I., & Laurent, G. (2005). Role of GABAergic Inhibition in Shaping Odor-Evoked Spatiotemporal Patterns in the Drosophila Antennal Lobe. *Journal of Neuroscience, 25*(40), 9069-9079. doi:10.1523/jneurosci.2070-05.2005

Wilson, R. I., & Mainen, Z. F. (2006). Early events in olfactory processing. *Annual Review of Neuroscience, 29*, 163-201. doi:10.1146/annurev.neuro.29.051605.112950

Wong, A. M., Wang, J. W., & Axel, R. (2002). Spatial Representation of the Glomerular Map in the Drosophila Protocerebrum. *Cell, 109*(2), 229-241. doi:10.1016/s0092-8674(02)00707-9

Wu, Y., Whiteus, C., Xu, C. S., Hayworth, K. J., Weinberg, R. J., Hess, H. F., & De Camilli, P. (2017). Contacts between the endoplasmic reticulum and other membranes in neurons. *Proceedings of the National Academy of Sciences, 114*(24), E4859-E4867. doi:doi:10.1073/pnas.1701078114

Xu, C. S., Hayworth, K. J., Lu, Z., Grob, P., Hassan, A. M., García-Cerdán, J. G., . . . Hess, H. F. (2017). Enhanced FIB-SEM systems for large-volume 3D imaging. *Elife, 6*, e25916. doi:10.7554/eLife.25916

Xu, C. S., Januszewski, M., Lu, Z., Takemura, S.-y., Hayworth, K. J., Huang, G., . . . Plaza, S. M. (2020). A Connectome of the Adult *Drosophila* Central Brain. 2020.2001.2021.911859. doi:10.1101/2020.01.21.911859 %J bioRxiv

Yaksi, E., & Wilson, R. I. (2010). Electrical coupling between olfactory glomeruli. *Neuron, 67*(6), 1034-1047. doi:10.1016/j.neuron.2010.08.041

Yamaguchi, M., & Yoshida, H. (2018). Drosophila as a Model Organism. *Advances in Experimental Medicine and Biology, 1076*, 1-10. doi:10.1007/978-981-13-0529-0_1

Yasuyama, K., Meinertzhagen, I. A., & Schurmann, F. W. (2003). Synaptic connections of cholinergic antennal lobe relay neurons innervating the lateral horn neuropile in the brain of *Drosophila melanogaster*. *Journal of Comparative Neurology, 466*(3), 299-315. doi:10.1002/cne.10867

Yin, L., Zheng, R., Ke, W., He, Q., Zhang, Y., Li, J., . . . Shu, Y. (2018). Autapses enhance bursting and coincidence detection in neocortical pyramidal cells. *Nature Communications, 9*(1), 4890. doi:10.1038/s41467-018-07317-4

Younger, M. A., Herre, M., Goldman, O. V., Lu, T.-C., Caballero-Vidal, G., Qi, Y., . . . Vosshall, L. B. (2022). Non-Canonical Odor Coding in the Mosquito. *bioRxiv*, 2020.2011.2007.368720.

doi:10.1101/2020.11.07.368720

Yu, D., Ponomarev, A., & Davis, R. L. (2004). Altered Representation of the Spatial Code for Odors after Olfactory Classical Conditioning: Memory Trace Formation by Synaptic Recruitment. *Neuron, 42*(3), 437-449. doi:10.1016/s0896-6273(04)00217-x

Yu, H.-H., Kao, C.-F., He, Y., Ding, P., Kao, J.-C., & Lee, T. (2010). A Complete Developmental Sequence of a Drosophila Neuronal Lineage as Revealed by Twin-Spot MARCM. *PLoS Biology, 8*(8), e1000461. doi:10.1371/journal.pbio.1000461

Zaroubi, L., Ozugergin, I., Mastronardi, K., Imfeld, A., Law, C., Gélinas, Y., . . . Findlay, B. L. (2022). The Ubiquitous Soil Terpene Geosmin Acts as a Warning Chemical. *Applied and Environmental Microbiology, 88*(7), e0009322. doi:10.1128/aem.00093-22

Zhang, Y., Tsang, T. K., Bushong, E. A., Chu, L. A., Chiang, A. S., Ellisman, M. H., . . . Su, C. Y. (2019). Asymmetric ephaptic inhibition between compartmentalized olfactory receptor neurons. *Nat Commun, 10*(1), 1560. doi:10.1038/s41467-019-09346-z

Zhao, Z., & McBride, C. S. (2020). Evolution of olfactory circuits in insects. *Journal of Comparative Physiology A, 206*(3), 353-367. doi:10.1007/s00359-020-01399-6

Zheng, Z., Lauritzen, J. S., Perlman, E., Robinson, C. G., Nichols, M., Milkie, D., . . . Bock, D. D. (2017). A Complete Electron Microscopy Volume Of The Brain Of Adult Drosophila melanogaster. *bioRxiv*. doi:10.1101/140905

Zheng, Z., Lauritzen, J. S., Perlman, E., Robinson, C. G., Nichols, M., Milkie, D., . . . Bock, D. D. (2018). A Complete Electron Microscopy Volume of the Brain of Adult Drosophila melanogaster. *Cell, 174*(3), 730-743.e722. doi:https://doi.org/10.1016/j.cell.2018.06.019

Zheng, Z., Li, F., Fisher, C., Ali, I. J., Sharifi, N., Calle-Schuler, S., . . . Bock, D. (2020). Structured sampling of olfactory input by the fly mushroom body. *bioRxiv*, 2020.2004.2017.047167. doi:10.1101/2020.04.17.047167 %J bioRxiv

Zou, D.-J., Chesler, A., & Firestein, S. (2009). How the olfactory bulb got its glomeruli: a just so story? *Nature Reviews: Neuroscience, 10*(8), 611-618.

DECLARATION OF INDEPENDENT ASSIGNMENT

I, the author of this thesis, am aware of the applicable doctoral examination regulations. I declare in accordance with the conferral of the degree of doctor from the Faculty of Biological Science of the Friedrich-Schiller University Jena that the submitted thesis was written by me with only the assistance and literature cited in the text. People who assisted in experiments, data analysis and writing of manuscripts are listed as co-authors of the respective manuscript. I was not assisted by a consultant for doctorate theses. Third parties have neither directly nor indirectly received monetary benefits from me for work related to the content of the submitted dissertation. The thesis has not been previously submitted whether to the Friedrich-Schiller University Jena or to any other University.

---------- ----------

Place, Date Lydia Gruber

ACKNOWLEDGMENTS

It has been a long journey, and many people has been at my side during this adventure. It is very difficult to thank everybody, but I will give it a try.

First of all, thank you **Bill** for including me in the HAN family and for all the inspiring talks and thoughts that motivate us all to present our work in the best way. Thank you also for your effort to keep up, even in a scientific environment, a good work-life balance. This might be the key to our department's good communication and productivity. I will always think back to these inspiring times at the MPI-CE in Jena.

Jürgen, es war eine aufregende Zeit mit dir als Betreuer. Ich möchte mich insbesondere bei dir für die vielen interessanten wissenschaftlichen Diskussionen und deine intensive praxisnahe Betreuung aber auch die erheiternden und sehr interessanten persönlichen Gespräche bedanken. Ich hatte das Gefühle wir waren ein sehr gutes Team. Ich danke dir auch für die schöne aber auch aufregende Zeit während unserer wissenschaftlichen Reisen. Mit dir war es nie ein Problem mit den Menschen ins Gespräch zu kommen. Deine Gabe dein Wissen über die Neuroanatomie und die Insekten weiterzugeben ist fesselnd und inspirierend.

A kind and special thanks goes also to **Rafael**. I am very grateful that I had the opportunity to convince you to be my second supervisor. Your precise and critical eyes and your efficiency have been helpful. Your fruitful discussions and knowledge have supported this work a lot.

Liebste **Katrin**, ich danke dir für die Einarbeitung in die Elektronenmikroskopie und deine wertvollen Erfahrungen, die du mit mir geteilt hast. Ich danke dir auch für die schönen und interessanten Gespräche während stundenlanger Probenvorbereitungen und der Aufnahmen am Elektronenmikroskop. Wir beiden Naturliebhaber und Radfahrer waren sofort auf einer Wellenlänge.

Nicht vergessen möchte ich, dir, **Sandor**, einen Dank auszusprechen. Ohne dich hätte ich die Faszination für die Ultrastruktur des Nervensystems und der Elektronenmikroskopie nie entdecken können.

Ich danke **Thomas Pertsch** und **Michael Steinert** für die Zusammenarbeit am Beutenberg Campus in Jena und die Möglichkeit das FIB-SEM nutzen zu können. Vielen Dank Michael für deine Zeit, dein Wissen und konstruktive Umsetzung der bis dato für dich neuartigen Bildgebung einer biologischen Probe, d.h. der neuronalen Netzwerke im Gehirn der Fliege am FIB-SEM.

Thank you, **Albert Cardona** and **Tom Kazimiers**, for the support and collaboration with the software CATMAID. I thank also Albert for the invitation to the Janelia research campus in Ashburn. It was a special experience for me.

A special thanks to **Eckard**, **Dami** and **Michael**, and the rest of the tracing team. Without your keenness and preciseness we would have never traced all these neurons.

I thank **Katharina Eichler** (Cambridge) for the contact with Markus Pleijzier. Special thanks go to **Markus Pleijzier** and your informatic expertise that helped to extract neuronal and synaptic data from CATMAID and the buildup of dendrograms.

Vielen Dank an **Roland** und **Ute**. Auch ohne euch wäre diese Arbeit nicht entstanden. Ich danke euch zu aller erst für die Organisation meines Firmenstipendiums in den ersten drei Jahren, aber auch für die Gespräche über eure wissenschaftlichen Projekte, die ihr mit der Firma aura optik begleitet, unterstützt und ermöglicht.

Martin, ohne deine EDV- Hilfe wäre diese Studie nicht umsetzbar gewesen. Danke, für die Hilfe bei der Verwaltung meiner Bilddatensätze, Metadaten und bei CATMAID. Außerdem, danke für die konstante Hilfe bei IT-Fragen jeglicher Art.

Veit, unser Mann mit den Lösungen für fast jedes Problem. Vielen Dank für deine Zeit, deinen Rat und dein geteiltes Wissen zu so vielen anatomischen und mikroskopischen Fragen. Es war mir eine Ehre mit dir das Büro teilen zu dürfen.

Silke Sachse, danke, dass ich die Möglichkeit hatte ein Teil des Imaging-Teams gewesen zu sein. Das regelmäßige Meetings und Paper Diskussionen waren sehr informativ. Danke auch für Diskussionen und Vorschläge bezüglich meines Projektes

Danke dir, **Silke Trautheim**, in erster Linie für hingebungsvolle Aufzucht der Fliegen und dein stetiges Engagement den hohen Standard einer sehr gut funktionierenden Aufzucht aufrechtzuerhalten. An zweiter Stelle danke ich dir für die schnelle Einweisung in die Präparation der Fliegengehirne.

Regina … wo soll ich anfangen? Vielleicht fange ich einfach damit an dir für deine Begrüßung in der neuen Arbeitsgruppe zu Danken und dass ich, Dank deiner Hilfe, mich in den ersten Tage schnell in unseren Laboren zurechtfand. Deine motivierende, energiegeladene und engagieret Art und Weise ist immer wieder erfrischend und sorgt für neue Motivation und Inspiration im oftmals von Niederlagen geprägten wissenschaftlichen Alltag. Es ist eine pure Freude, wenn dein Lachen die Gänge erfüllt. Es war mir eine Ehre mit dir zusammen jedes Jahr das Drachenbootrennen zu organisieren und daran teilzunehmen. Ich freu mich dich auch als Freundin gewonnen zu haben.

Angi … auch da kann ich nur sagen, wo soll ich anfangen? Du gibst unserer Arbeitsgruppe so viel Wärme, Menschlichkeit, Kreativität, und immer ein lockeres Liedchen was über die Gänge schwingt. Auch ohne dich würde im Labor nichts so laufen wie es soll. Ich liebe deine ehrliche und vor allem hilfsbereite Art. Deine Liebe zum Detail hat mir so manch süße Überraschung beschert. Du kannst so stolz auf das sein, was du geschafft hast. Danke, dir für dein offenes Ohr und dass du eine so gute Freundin bist.

Swetlana, ohne dich würden wir Doktoranden uns nur halb so gut auf die wissenschaftliche Arbeit konzentrieren können, denn nur mit dir sind die administrativen Aufgaben so schnell und effektiv erledigt. Danke dafür!

Daniel, vielen Dank für deine vielen technischen Hilfen und Konstruktionen. Danke, dass man immer auf dich zählen kann und für deine vielen technischen Tipps auch für den heimischen Gebrauch. Ohne dich würde hier so gut wie gar nichts funktionieren

Lorena, it all started with the organization of our retreat and it became a friendship that I would not like to miss. We shared so many moments, the good and the bad, and even our maternal leave. It was such a pleasure having you here as a colleague and as a friend. I will never forget our trip to Nairobi and I am looking forward to visiting you soon in Spain.

Benjamin, es ist ein Genuss dich als Büropartner zu haben. Ich liebe deine direkte Art und deinen, manchmal unbeabsichtigten, schwarzen Humor. Auch wenn ich liebend gern mit dir die negativen Aspekte der wissenschaftlichen Karrierewelt und unser Publikationssystem ausgewertet habe, bleibe positiv (deine Daten sind beeindruckend). Danke für deine Hilfe bei der Doktorarbeit und deinen kritischen Blick. Es war eine Freude mit dir das Interesse für die Geosmin-Kodierung zu teilen.

Nandita & Rolando, thanks for being great office mates! Rolando, I got used to your sick drum solos on the office desk and now I cannot work without it anymore.

Fabio, you were my hero and role model of good scientific practice.

Elisa, es ist mir eine Freude dich als Kollegin, Tanzkollegin und Freundin gewonnen zu haben. Deine Organisation von Familie und Arbeit hat mir immer Zuversicht gegeben.

Anna, auch dein Lachen war unvergesslich und hat mir immer wieder ein Lächeln entlockt.

Tom, ach Tom, deine netten Nachrichten, deine Gelassenheit und deine entspannte Arbeitsweise hat unser Büro gebraucht.

Ahmed, thanks for sharing Basketball on your screen with me ☺ and thanks for all your gustation papers you shared with us.

Mohammed, it was a pleasure to have you as a colleague. I will never forget our trip to Nairobi. I felt safe when you were around. Your talks were always inspiring and fascinating.

Karen, you are just an awesome person and an outstanding scientist with infinite energy and ideas. Thanks a lot for your last-minute help with this thesis. I love your extrovert personality and engagement. Our HAN family just needs people like you.

Eli, ich liebe deinen Humor und deine extrovertierte Frohnatur. Deine ehrlich und erfrischenden Art und Weise lockert jedes Gespräch auf. Danke dafür! Ich werde dein unvergessliches Lachen sehr vermissen.

Sudeshna, thank you also for your constant scientific input at all imaging meetings and our interesting discussions. It has been a pleasure to have you as a colleague.

Ana, thank you for your constant interesting input in all imaging meetings and your discussions about my data.

Sonja, danke, dass du dein Wissen in der Statistik mit uns teilst.

Sascha, danke für die vielen kleinen, nette Gespräche und dass du ein so umwerfender „Prinz“ warst ☺. Bleib positiv.

Dieter, dein Wissen in der Welt der Molekularbiologie ist von unschätzbarem Wert. Gepaart mit deiner scheinbar unendlichen Schatztruhe an interessantem Wissen über Geschichte, Kultur, Kunst, Musik und interessante Reiseziel, ist ein Gespräch mit dir immer eine wahre Freude.

Thanks to everyone else in the HAN family. It was a pleasure to work with you all. I enjoyed all the fruitful discussions, interesting breaks, and events with you.

IT-Team, vielen Dank für eure Arbeit an der Aufrechterhaltung unserer IT-Infrastruktur. Es erleichtert das Arbeiten ungemein.

Danke, liebes **Verwaltungsteam**. Ihr zieht die wichtigen unsichtbaren Strippen im Hintergrund. Es ist eine enorme Erleichterung eine so kompetente Hilfe bei den Verwaltungsarbeiten und dem „Papierkram“ zu haben.

Julz, mein chaotisches Genie für alles. Danke, dass du mir vor allem in den letzten Stunden meiner Arbeit so zur Seite standst! Das gab mir viel Kraft und Zuversicht. Ich liebe deine ungebremste Begeisterung für die Natur, Kunst, Musik und alles was dich umgibt und dein stetiges Bestreben alles wissenschaftlich erklären zu können. Meine Kinder lieben es auch. Bleib dran! Bald feiern wir auch deine Abgabe.

Marko, mein Mann an meiner Seite, tausend Dank dafür, dass du, trotz deiner völligen Auslastung durch deine Selbständigkeit, mich unterstützt hast. Die Zeit (ich erwähne nur Corona) hat es uns nicht einfach gemacht. Doch wir haben alles zusammen gemeistert und haben mittlerweile auch ein Diplom in „Management“ ;-)

Danke **Liesann** und **Matteo** (meine geliebten Kinder), die mir so viel Freude und den nötigen Ausgleich geben. Es ist so schön euch aufwachsen zu sehen. Danke Liesann, für deine immer wieder ernüchternde und witzige Sichtweise meiner Arbeit ☺.

Danke auch an meine **Brüder**. Ihr habt mich auch auf diesem Weg begleitet. Vor allem dir Thomas für dein informatisches Wissen, dass ich zu fast jeder Tages- und Nachtzeit abrufen darf.

Zu guter Letzt danke ich ganz besonders meinen **Eltern**, die mich bei jedem Schritt in meinem Leben begleitet und unterstützt habe, auch ohne euch stände ich jetzt nicht da wo ich jetzt bin.

APPENDIX

FORM 2

Manuscript No. Manuscript I

Short reference Gruber et al. (2022), bioRxiv

Contribution of the doctoral candidate

Contribution of the doctoral candidate to figures reflecting experimental data (only for original articles):

Figure(s) # 1-7	☒	100% (the data presented in this figure come entirely from experimental work carried out by the candidate)
	☐	0% (the data presented in this figure are based exclusively on the work of other co-authors)
	☐	Approximate contribution of the doctoral candidate to the figure: ___% Brief description of the contribution: *(e.g. "Figure parts a, d and f" or "Evaluation of the data" etc.)*

_____ _____

Signature candidate Signature supervisor (member of the Faculty)

FORM 2

Manuscript No. Manuscript II

Short reference Gruber et al. (2018), Front. Cell. Neurosci

Contribution of the doctoral candidate

Contribution of the doctoral candidate to figures reflecting experimental data (only for original articles):

Figure(s) # 1-2	☒	100% (the data presented in this figure come entirely from experimental work carried out by the candidate)
	☐	0% (the data presented in this figure are based exclusively on the work of other co-authors)
	☐	Approximate contribution of the doctoral candidate to the figure: _____% Brief description of the contribution: *(e.g. "Figure parts a, d and f" or "Evaluation of the data" etc.)*

_____ _____

Signature candidate Signature supervisor (member of the Faculty)

FORM 2

Manuscript No. Manuscript III

Short reference Keesey *et al*. (2019), Nature Communications

Contribution of the doctoral candidate

Contribution of the doctoral candidate to figures reflecting experimental data (only for original articles):

Figure(s) # 2	☐	100% (the data presented in this figure come entirely from experimental work carried out by the candidate)
	☐	0% (the data presented in this figure are based exclusively on the work of other co-authors)
	☒	Approximate contribution of the doctoral candidate to the figure: 30 % Brief description of the contribution: *(e.g. "Figure parts a, d and f" or "Evaluation of the data" etc.)*

_____ _____

Signature candidate Signature supervisor (member of the Faculty)